Role of brain-type Creatine Kinase in cytoskeletal dynamics

Jan W.P. Kuiper

Role of brain-type Creatine Kinase in cytoskeletal dynamics

Een wetenschappelijke proeve op het gebied

van de Medische Wetenschappen

PROEFSCHRIFT

ter verkrijging van de graad van doctor aan de Radboud Universiteit Nijmegen op

gezag van de rector magnificus prof. mr. S.C.J.J. Kortmann,

volgens besluit van het college van decanen in het openbaar te verdedigen

op donderdag **2 april 2009** om **13.00** uur precies

door

Johannes Wilhelmus Plechelmus Kuiper

geboren op 21 januari 1976

te Oldenzaal

Promotor:

prof. dr. B. Wieringa

Manuscriptcommissie:

prof. dr. J. Smeitink

dr. F.N. van Leeuwen

prof. dr. U. Schlattner (Université Joseph Fourier, Grenoble)

The research presented in this thesis was performed at the Department of Cell Biology, Nijmegen Centre for Molecular Life Sciences, Radboud University Nijmegen Medical Centre and was supported by NWO ZON-MW Program grant 901-01-191.

ISBN 978-90-9023988-0

Printed by PrintPartners Ipskamp, Enschede

"So now the sadness comes--the revelation. There is a depression after an answer is given. It was almost fun not knowing. Yes, now we know. At least we know what we sought in the beginning. But there is still the question: why?"

The Log Lady

TABLE OF CONTENTS

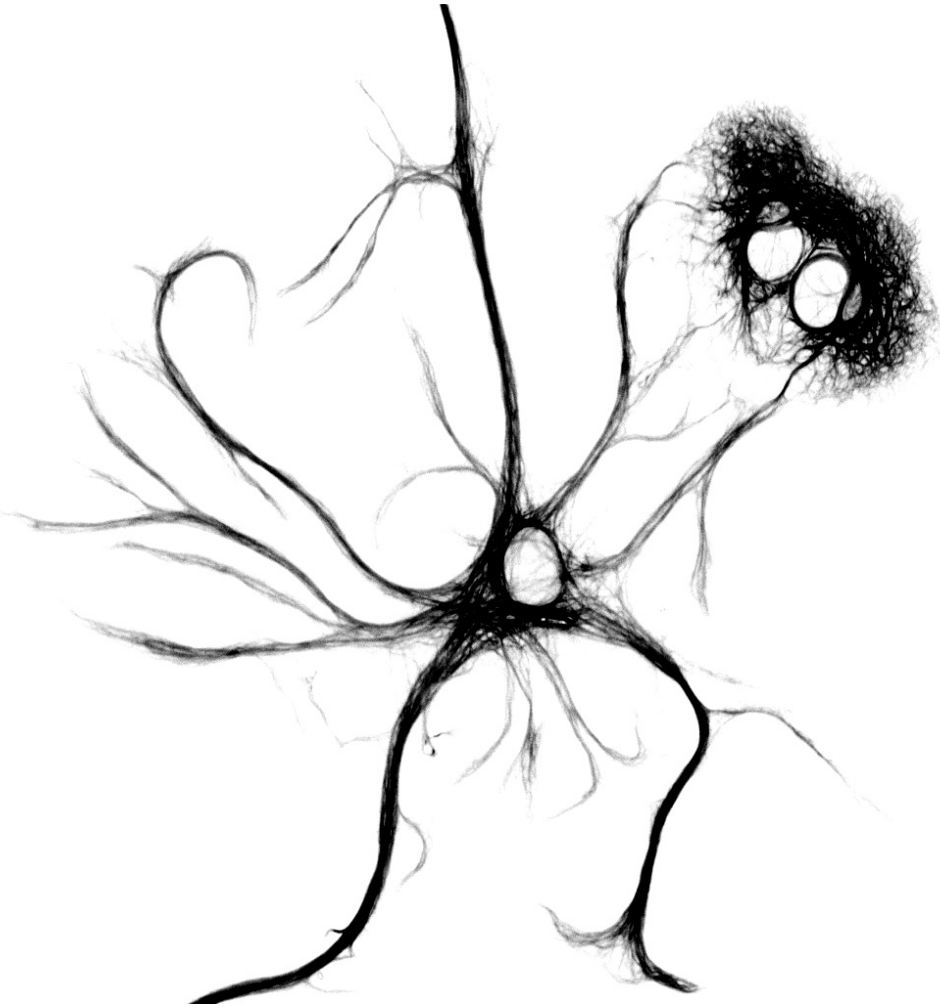

Chapter - 1 -

General Introduction

1.1 Cellular energy metabolism

Processes such as growth, tissue homeostasis (i.e. the maintenance of a constant internal environment), and reproduction are essential for life of multicellular organisms. All these qualities have a cellular basis and are highly dependent on macromolecular dynamics with a high energy-demand, driven by an intricate network of chemical reactions. Thus, ultimately, every organism lives at the expense of free energy provided by metabolic conversion of nutrients. By transferring free energy between spatially separated reactions (Stryer 1988) the hydrolysis of adenosine 5' tri-phosphate (ATP: $ATP^{4-} + H_2O \rightarrow ADP^{3-} + P_i^{2-} + H^+$) plays a central role. Metabolic generation of ATP occurs by cellular respiration and other catabolic pathways that unleash energy stored in carbohydrates, fatty acids and amino acids. In eukaryotes, these pathways feed ultimately into two principal reaction cascades: Glycolysis and oxidative phosphorylation (OXPHOS). Glycolysis consists of a sequence of reactions that take place in the cytoplasm of the cell. The initial substrate, glucose, is imported through glucose transporters present in the plasma membrane after which it is phosphorylated by hexokinase (Stryer 1988; Wood and Trayhurn 2003). Subsequent enzymatic steps convert glucose-6-phosphate into pyruvate, yielding 2 ATP and 2 NADH molecules ($Glucose + 2P_i^{2-} + 2\ ADP^{3-} + 2\ NAD^+ \rightarrow 2\ pyruvate^- + 2\ ATP^{4-} + 2\ NADH + 2\ H^+ + H_2O$). Under aerobic conditions pyruvate can be metabolized in the mitochondrion, where it enters the citric acid cycle (or tricarboxic acid cycle; TCA cycle) after conversion into acetyl-CoA. Alternatively, under anaerobic conditions (e.g. during extreme exercise) pyruvate can be converted into lactate to prevent glycolysis running out of NAD^+ ($Pyruvate^- + NADH + H^+ \rightarrow lactate^- + NAD^+$) (Stryer 1988).

The TCA cycle comprises a set of mitochondrial enzymes that metabolize substrates under aerobic conditions to yield guanosine 5' tri-phosphate (GTP) and the electron carriers NADH and $FADH_2$ (Stryer 1988). Several substrates can enter the TCA cycle at different points. The end-product of glycolysis, pyruvate, reacts with oxaloacetate and acetyl CoA to citrate. The amino acids glutamine and asparagine can be converted into glutamate and aspartate, which enter the cycle as α-

ketoglutarate and oxaloacetate, respectively. Another important pathway to generate TCA cycle substrates is the beta-oxidation of fatty acids. The stepwise breakdown of the fatty acid chains generates one molecule of acetyl-CoA and one molecule of $FADH_2$ and NADH each, per oxidation cycle. The electron carriers NADH and $FADH_2$ generated during glycolysis, beta-oxidation and the TCA cycle, supply reduction equivalents to the electron transport chain during OXPHOS. The electron chain consists of 4 multi-subunit protein complexes (complex I-V). Complex I, III, IV and V are partitioned in the inner membrane of mitochondria and complex II binds to the inner leaflet of the inner membrane. When electrons are being transported along the complexes I-IV with molecular oxygen serving as the final electron acceptor, protons are being released into the intermembrane space, building up a proton gradient, called the proton motive force (PMF) (Salway 2002). The energy stored in the PMF is a combination of a membrane potential and chemical gradient of protons, which can be used to channel protons back into the mitochondrial matrix through complex V. This is a membrane bound F_0F_1-ATPase that catalyzes the formation of ATP from ADP and inorganic phosphate (P_i). According to the classical view, the overall yield of OXPHOS is 2.5 moles and 1.5 moles of ATP per mole of NADH and $FADH_2$, respectively. Consequently, one molecule of glucose can yield up to 38 ATPs, of which 2 ATPs originate from glycolysis, 2 ATPs from the TCA cycle, 32 ATPs generated by OXPHOS from NADH and $FADH_2$ and 2 ATPs from glycolytically generated NADH, which is imported into the mitochondrion by the glycerol phosphate shuttle or the malate-aspartate shuttle (Stryer 1988; Eto, Tsubamoto et al. 1999). An additional extra ATP could be generated from TCA cycle derived GTP by nucleoside diphosphate kinases (NDPKs): GTP + ADP $\rightarrow$ GDP + ATP. However, a more modern view dictates that the number of ATP molecules produced per oxygen molecule (P/O) during OXPHOS cannot be expressed as a simple integer, but rather should be considered as a function of proton force formation (H^+/O) divided by proton consumption via ATP-synthetase (H^+/ATP) (Brand 2005). In addition, other reactions involving proton translocation during OXPHOS contribute to this equation. Using theoretical and experimental values for these components, the actual maximum number of ATPs that can be generated per molecule glucose should be estimated to be 28.9

instead of 38 (Brand 2005). Moreover, mechanisms such as molecular slipping of H^+-pumps, superoxide generation and (cell type dependent) mitochondrial uncoupling due to intrinsic leakage and uncoupling proteins will reduce the actual yield of ATP (Pietrobon, Zoratti et al. 1983; Kadenbach 2003; Rousset, Alves-Guerra et al. 2004; Andreyev, Kushnareva et al. 2005). Especially, proton leak (uncoupling) can dramatically lower P/O in skeletal muscle by accounting for almost 50% of the resting respiration rate (Rolfe and Brand 1996).

1.2 Phosphotransfer systems: the Creatine Kinase system

Proper cellular functioning relies on availability of ATP to fuel essential processes, such as the synthesis and breakdown of macromolecules (protein, DNA, RNA), the safeguarding of structural and funtional integrity, actin/myosin contraction involved in cell shape changes, transport and motility, ion homeostasis and electrogenic activity, and protein phosphorylation. Most of these processes are spatially confined within the cell, leading to a locally increased demand for ATP and simultaneous release of a local surplus of ADP. Some cell types (e.g. skeletal muscle, neurons) can drastically increase their activity during short time spans, resulting in highly fluctuating ATP demands. ATP generation by glycolysis and OXPHOS does not necessarily coincide temporally and spatially with these cellular energy requirements and simple diffusion of adenine nucleotides is considered too slow for efficient exchange between sites of ATP production and sites were ATP is hydrolyzed (Meyer, Sweeney et al. 1984). Consequently, ATPases would run out of ATP and simultaneously be inhibited by accumulating hydrolysis products, ADP and P_i. To counteract this effect, cells possess mechanisms to improve energy exchange between sites of ATP generation and ATP hydrolysis. By relocating metabolic enzymes or entire mitochondria to specific subcellular locales, the diffusion distance between ATP production and hydrolysis can be minimized. An illustration of such a process, providing subcellular ATP to membrane associated processes is given by the binding of glycolytic enzymes to Na^+/K^+-ATPases (Glitsch and Tappe 1993) or caveolines (Raikar, Vallejo et al. 2006). Interactions with cytoskeletal components, such as microtubules (Gitlits, Toh et al. 2000; Keller, Peltzer et al. 2007) or actin (Waingeh,

Gustafson et al. 2006) provide other examples of functional subcellular partitioning of glycolytic enzymes. Direct inter-association of enzymes involved in the glycolytic pathway has also been claimed (Campanella, Chu et al. 2005). Intriguingly, GAPDH and lactate dehydrogenase were even found to be part of a multicomponent transcriptional coactivator complex in the nucleus, possibly linking the redox-energy status of the cell with transcription regulation (Zheng, Roeder et al. 2003).

Besides subcellular partitioning of glycolytic enzymes, cells can use other strategies for energy distribution. For example, cells redirect OXPHOS to strategic subcellular sites by re-localizing mitochondria via active transport over microtubules and actin filaments (Hollenbeck and Saxton 2005; Boldogh and Pon 2007). Indeed, mitochondria are often found concentrated at subcellular sites with high ATP consumption, such as synapses (Chang, Honick et al. 2006) and at the base of dendritic spines (Li, Okamoto et al. 2004).

In addition to the ability to dynamically relocalize their glycolytic and OXPHOS pathways into the areas of highest need, cells also acquired a complicated network of highly specialized metabolic enzymes – and isoforms thereof - for the production, transportation, and utilization of energy. Among these, the phosphoryl transfer systems are of special interest, since they offer versatile ways to spatially and temporarily buffer subcellular pools of high-energy phosphoryls (~P). The three main ~P transfer systems are the creatine kinases (CKs), adenylate kinases (AKs) and nucleoside diphosphate kinases (NDPKs), which distribute and buffer the intracellular concentrations of mono-, di- and triphosphate nucleotides (Dzeja and Terzic 2003). This thesis will focus only on the CK system.

1.3 Enzymes of the Creatine Kinase – Creatine System

Vertebrates express 5 different CK isoforms that differ in their subunit composition, tissue distribution and subcellular localization. All CK enzymes catalyze the reversible transfer of ~P from ATP to creatine ($MgATP^{2-} + Cr \leftrightarrow MgADP^{-} + PCr^{2-} + H^{+}$). The two mitochondrial CKs, sarcomeric mitochondrial CK (ScCKmit) and ubiquitous mitochondrial CK (UbCKmit) are composed of subunits encoded by two different but related genes, a large ScCKmit gene and a compactly structured

UbCKmit gene (Steeghs, Peters et al. 1995; Pineda and Ellington 2001). In cells where these subunits are produced homo-dimeric or homo-octameric CKmit enzymes are formed that reside within the intermembrane space of mitochondria (Stachowiak, Schlattner et al. 1998). UbCKmit has – as indicated by its name - a ubiquitous tissue expression, whereas ScCKmit is mainly expressed in skeletal and cardiac muscle. Two other evolutionary related CK genes specify subunits of muscle-CK (CK-MM) and brain-type CK (CK-BB), occurring as homodimeric, cytosolic, proteins. In addition, CK-B and CK-M subunits can also heterodimerize into CK-MB, an isoform seen in cardiac muscle where the genes for both subunits are co-expressed (Wallimann, Wyss et al. 1992). Homodimeric CK-MM is by far the most abundant CK isoform in cardiac muscle, and in adult skeletal muscle is the only cytosolic CK. In addition, CK-MM was detected in discrete regions of human brain, though mRNA levels appeared rather low (Hamburg, Friedman et al. 1990). Low transcriptional activity of the mouse CK-M promotor in brain was also detected in a heterologous reporter system in Xenopus laevis during metamorphosis (Lim, Neff et al. 2004). In contrast, no muscle-type creatine kinase was detected in mouse brain tissue using zymogram analysis (van Deursen, Heerschap et al. 1993). Therefore, it remains possible that CK-M is expressed in brain, but it surely is present at very low levels, is restricted to only special cell types, and found in a species-specific and/or developmentally regulated manner. The tissue distribution of CK-BB is less restricted and high levels of this protein are found in astrocytes and inhibitory but not excitatory neurons throughout the brain (see Streijger et al, 2007 for details (Streijger, In 't Zandt et al. 2007)), smooth muscle, intestine, epithelium, kidney, macrophages and osteoclasts (Sistermans, de Kok et al. 1995). CK's substrate creatine is imported from circulation into cells by dedicated sodium-driven transporters (Guimbal and Kilimann 1993). Although most of the creatine in circulation is build up via oral intake, as it is a common nutrient found in meat and fish, it is also synthesized by mammals in a two-step process (Wyss and Kaddurah-Daouk 2000). In the kidneys guanidino acetate is formed from arginine and glycine by L-arginine:glycine amidinotransferase (AGAT). Via the blood stream, guanidino acetate enters the liver where it is subsequently methylated by S-adenosyl-L-methionine:N-guanidinoacetate methyltransferase (GAMT) to yield creatine (Wyss and Kaddurah-Daouk 2000). In

addition, certain cell types like astrocytes and neurons are able to synthesize creatine endogenously by co-expressing AGAT and GAMT (Braissant, Henry et al. 2001).

Human disease caused by genetic disruption of CK isoforms is rare. Two patients displaying myocardial symptoms were reported to be deficient for CK-M activity (Shibuya, Matsumoto et al. 1992; Yamamichi, Kasakura et al. 2001). In one case, the total CK-activity was determined to be 3% (compared to control) in cardiac muscle, due to a 50-fold decrease in gene expression (Yamamichi, Kasakura et al. 2001). In addition, this patient had a single point mutation leading to a functionally uncharacterized amino acid substitution (Asp-54 -> Gly-54). More frequent than CK deficiencies are inborn errors of creatine synthesis and import. Mutations have been found in AGAT (Item, Stockler-Ipsiroglu et al. 2001), GAMT (Stockler, Hanefeld et al. 1996) and the creatine transporter (Salomons, van Dooren et al. 2001). Defects in the creatine-synthesizing pathway cause a variety of symptoms and may include mild to severe mental retardation, extra-pyramidal symptoms, delayed (speech-) development and seizures (Stromberger, Bodamer et al. 2003). Although, oral supplementation of creatine improves most of the symptoms in patients with AGAT and GAMT deficiency, normal development is not fully restored (Schulze 2003). Oral intake is of course not of help in cases with Cr-import defects (Bizzi, Bugiani et al. 2002).

Genetic ablation of enzymes involved in creatine synthesis and CK isozymes, offers an excellent tool to unravel their tissue specific physiological functions. Mouse knock-out models of GAMT (Schmidt, Marescau et al. 2004) and all four isoforms (CK-M, CK-B, UbCKmit and scCKmit), and combinations of isoforms (CK-M/scCKmit and CK-B/UbCKmit) have been established and analyzed (van Deursen, Heerschap et al. 1993; Steeghs, Oerlemans et al. 1995; Steeghs, Benders et al. 1997; Steeghs, Heerschap et al. 1997; Jost, Van Der Zee et al. 2002; Streijger, Oerlemans et al. 2005). Important consequences of CK deficiency in these mouse models will be discussed in the next paragraph (1.4, CK and energy compartmentalization).

1.4 CK and energy compartmentalization

As mentioned in chapter 1.3, cells tend to minimize the distance between sites of ATP consumption and production by relocalizing mitochondria and glycolytic enzymes. Indeed, diffusional exchange of adenine nucleotides is a thermodynamically unfavorable process (Meyer, Sweeney et al. 1984), which could reduce ATPase activity. Inefficient on-site removal of hydrolysis end products, ADP, P_i and H^+ represents an additional factor that inhibits effective ATPase activity. Therefore, shuttling of high-energy phosphoryls (~P) through a network of tightly coupled phosphotransfer reactions, such as the CK-system, contributes to the efficiency of ATPase activity (Meyer, Sweeney et al. 1984; Wallimann, Wyss et al. 1992; Saks, Khuchua et al. 1994; Dzeja and Terzic 2003).

Data on specific subcellular localization of the different CK isoforms and metabolic modeling studies suggest the existence of unidirectional fluxes of ~P between cellular compartments (Joubert, Mazet et al. 2002). **Figure 1** provides a hypothetical model of how CK enzymes could connect sites of ATP production and utilization by conveying a unidirectional "transport" flux of ~P (Dzeja and Terzic 2003). Obviously, this model requires the presence of both the mitochondrial and cytosolic isoforms of CK.

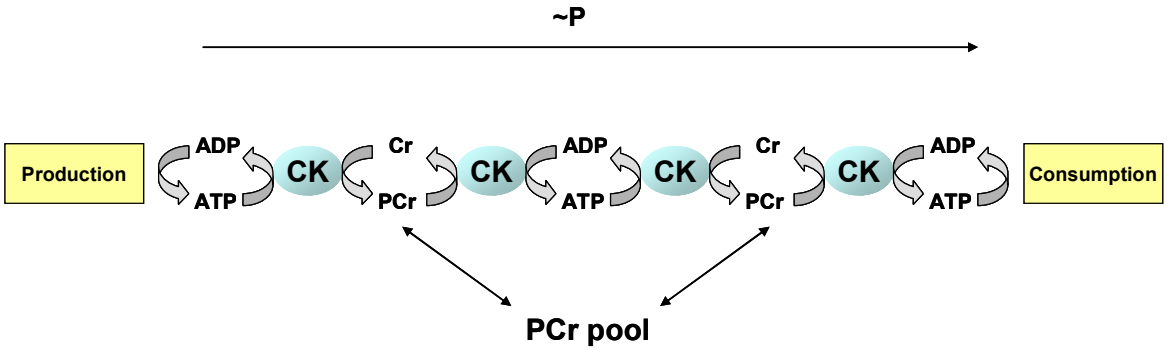

Figure 1. Schematic representation of spatio-temporal buffering by the CK shuttle: Regional distribution of CK enzymes provides cells with an interconnected "network" for local ATP regeneration from locally available PCr. Please note that this is a simplified model; a more elaborate description of phosphotransfer networks in cells can be found in Dzeja and Terzic (Dzeja and Terzic, 2003).

In addition, the phosphocreatine shuttle is able to temporally buffer local and global ATP/ADP levels. During periods of low energy expenditure ~P is stored in the PCr pool. When the demand for ATP suddenly rises, this storage of ~P provides a source of ATP through CK mediated conversion. Thus, CK mediated ~P transfer supplies cells with both an enhanced flux of ATP as well as temporal storage of ~P, which will assure almost steady access to "fuel" during transient periods of high ATP consumption.

The metabolically highly compartmentalized sea urchin sperm cell provides an example of the functional-mechanistic role of the phosphocreatine shuttle in energy compartmentalization. In the sperm cell, flagellar movement is the major energy drain, driven by ATP-fuelled dyneins located in the tail region. ATP needed for this activity is generated elsewhere, by mitochondria located in the sperm head, but diffusion of ATP into the flagellum is too slow to support efficient dynein activity. Here, CK-mediated ATP relay from mitochondria to the flagellum "rescues" this coupling and enables normal flagellum function (Tombes and Shapiro 1985).

In mammals, several tissues with high and fluctuating energy demand, such as cardiac muscle, skeletal muscle and brain tissue, are highly dependent on adequate ATP-supply. These tissues also display prominent expression of members of the CK isozyme family. Especially, the role of CK in skeletal and cardiac muscle has been investigated extensively. Nuclear magnetic resonance studies demonstrated the presence of a CK-shuttle in cardiac muscle and skeletal muscle (van Dorsten, Reese et al. 1997; Joubert, Mazet et al. 2002). Knockout mice were created that lack the muscle isoform, CK-M or ScCKmit or both enzymes (van Deursen, Heerschap et al. 1993; Steeghs, Benders et al. 1997; Steeghs, Heerschap et al. 1997). Phenotypical analysis demonstrated that ablation of the cytosolic isoform CK-M affected burst activity, without affecting absolute muscle force (van Deursen, Heerschap et al. 1993). Interestingly, CK-deficient muscles displayed adaptations to compensate for the loss of flux through the CK reaction, by increasing mitochondrial volume and glycolytic potential. The molecular basis for these adaptations involve upregulation of mitochondrial genes, such as cytochrome C oxidase, ARNT and inorganic phosphate carrier, as well as certain glycolytic enzymes (de Groof, Oerlemans et al. 2001; de Groof, Fransen et al. 2002).

The creation of CK-knockout mice offered also the possibility to examine the function of (ubiquitously) expressed CK isozymes in integral physiological processes, such as behavior and development. Indeed, these studies revealed that CK-B (-/-) mice exhibit disturbed exploration behavior and decreased spatial learning acquisition in a Morris water maze test (Jost, Van Der Zee et al. 2002). In addition, CK-B (-/-) mice have an increased intra- and infrapyramidal mossy fiber field size. Interestingly, this area in the hippocampus is associated with spatial learning and exploration behavior (Schwegler and Crusio 1995). Considering the relatively mild phenotype, CK-B's function could be (partially) compensated for by UbCKmit. Indeed, when mice were ablated for both CK-B and UbCKmit, additional effects of CK deficiency were observed. Notably, the weight of brain and overall body weight were decreased (Streijger, Oerlemans et al. 2005) and problems with thermogenesis were observed (Streijger 2007). In addition, some of the phenotypic features found in CK-B single knockout mice were aggravated, such as poor spatial learning acquisition.

Still, to resolve the precise mechanistic aspects behind the phenotypic changes in CK knockout mice, it will be necessary to study isolated cellular functions in distinct cell types in great detail. An example of such an approach is given by Shin et al., who recently identified CK-B to be abundantly expressed in hair bundle cells in the inner ear (Shin, Streijger et al. 2007). These cells possess elongated processes of 2-15 μm long called stereocilia, which constitute the mechano-transducers necessary for hearing. Within these stereocilia large amounts of ATP are being used for actin treadmilling, myosin ATPase activity and calcium homeostasis (Yamoah, Lumpkin et al. 1998; Schneider, Belyantseva et al. 2002; Gillespie and Cyr 2004). Because of the diffusion limitations of ATP into these highly elongated stereocilia, ATP consuming processes could depend on the CK phosphocreatine shuttle. Indeed, Shin et al. found that CK-B is required to adequately sustain calcium homeostasis, and perhaps other relevant ATP-requiring functions, within the hair bundle cells. High-sensitivity hearing was lost in CK-B deficient mice (Shin, Streijger et al. 2007). This finding is in analogy with data on the role of CK-M, which was implicated also in calcium pumping and in rapid fuelling of myosin ATPases in skeletal muscle (Steeghs, Benders et al. 1997; Rome and Klimov 2000; de Groof, Fransen et al. 2002)

1.5 Subcellular localization of CK isoforms

To fulfill their role in shuttling of ~P CK isozymes need to be localized at proper distance of subcellular sites where ATP is generated and consumed. Indeed, CK is spatially associated with mitochondria and sometimes also found clustered with glycolytic enzymes (Kraft, Hornemann et al. 2000). The two mitochondrial CK isoforms reside in the intermembrane space of mitochondria in close contact to the adenine nucleotide translocase (ANT) (Beutner, Ruck et al. 1998; Vendelin, Lemba et al. 2004), thus enabling a functional connection between the OXPHOS activity, the adenosine nucleotide translocator (ANT) and the CK-system. Likewise, molecular complex formation of CK-M with phosphofructokinase (PFK) and aldolase has been observed in skeletal muscle fibers (Kraft, Hornemann et al. 2000), suggesting a role in the distribution of glycolytically produced ATP.

In addition, interactions of CK with ATP consuming ATPases have been identified. A strong functional coupling between regulation of intracellular calcium levels and the CK system was found in skeletal muscle. Both the release and sequestration of Ca^{2+} in muscle fibers was affected when CK-M or both CK-M and ScCKmit were ablated, resulting in affected muscle performance (van Deursen, Heerschap et al. 1993; Korge and Campbell 1994; Steeghs, Benders et al. 1997; de Groof, Fransen et al. 2002). In addition, point-mutation studies with CK-M (but not CK-B) identified conserved lysine residues that mediate binding to myomesin and M-protein at the M-line in skeletal muscle (Hornemann, Stolz et al. 2000; Hornemann, Kempa et al. 2003). This interaction is functionally coupled with actin activated Mg^{2+}-ATPases (Wallimann, Schlosser et al. 1984).

The functional coupling between cellular processes and the non-muscle isoform, CK-B, is less well understood. This is in part due to the fact that in contrast to CK-M, no specific subcellular localization (other than cytosolic) has been found that could point to its function. Moreover, just a few physical and functional interactions have been described for CK-B, and only of two physical associations the functional significance has been examined in detail. Binding partners that have been identified to date, include Golgi matrix protein 130 (GM130) (Burklen, Hirschy et al. 2007), metallothionein-3 (Lahti, Hoekman et al. 2005), the SOCS box-containing

protein Asb-9 (Debrincat, Zhang et al. 2007), K^+-Cl^- co-transporter 2 (KCC2) (Inoue, Ueno et al. 2004) and the thrombin receptor, PAR-1 (Mahajan, Pai et al. 2000). To assess whether KCC2 requires CK-B for proper functioning, Inoue et al. inhibited CK-B by expressing dominant negative CK-B or utilizing pharmacological inhibition. A moderate decrease in the ability of KCC2 to maintain proper $[Cl^-]_i$ was observed. However, the precise regulatory mechanism by which CK-B affects KCC2 has not been identified (Inoue, Yamada et al. 2006). In a similar way the interaction of CK-B and the thrombin receptor, PAR-1, was analyzed. Pharmacological inhibition and expression of dominant negative CK-B dramatically reduced the thrombin-induced morphological changes in astrocytes (Mahajan, Pai et al. 2000). This effect was accompanied by a reduction in activated (GTP-loaded) RhoA, which is an important mediator of signaling to the actin cytoskeleton. The authors suggest that CK-B is important for local ATP supply during receptor signal transduction. However, no specific signaling event was pointed out to be directly and/or mechanistically regulated by CK-B. Although the mentioned studies may not precisely clarify the mechanistic contribution of CK-B in non-muscle cells, they demonstrate a wide variety of processes in which CK-B could be directly or indirectly involved. This thesis adds further to these studies.

1.6 Cytoskeletal remodeling and ATP

Actin polymerization

Actin filaments (F-actin) form the cell's cytoskeleton, together with microtubules and intermediate filaments. The filaments consist of actin monomers (G-actin) that possess the intrinsic capacity to polymerize and form F-actin. A hallmark of F-actin is its ability to form contractile filaments together with myosin proteins. Together, actins and myosins are crucial for numerous cellular processes such as maintenance of – and changes in - cell morphology, cellular motility and intracellular transport (Pollard and Borisy 2003; Vale 2003).

Actin remodeling can be considered as the combined outcome of actin treadmilling and myosin activity, which are both mechanisms mediated by the

hydrolysis of ATP (Le Clainche and Carlier 2008; Olson and Sahai 2008). Actin treadmilling is the result of a net addition of actin monomers (G-actin) to the barbed end of actin filaments and the dissociation of actin subunits at the pointed end (see **Figure 2**: Actin treadmilling, key proteins and ATP usage). The addition of actin subunits is a thermodynamically favorable process, which is dependent on the actual concentration of monomers (Pollard 1986). Since spontaneously nucleation is thermodynamically unfavorable, actin polymerization relies on the availability of free barbed ends or nucleator proteins, such as Arp2/3 (Goley and Welch 2006), Spir (Kerkhoff 2006), Cordon-Bleu (Ahuja, Pinyol et al. 2007) or formins (Evangelista, Zigmond et al. 2003). Once nucleated, ATP-loaded actin monomers (ATP-actin) are being added preferentially to the barbed end, since the cellular concentration of ATP-actin is higher than the critical concentration required for barbed-end polymerization (Pollard 1986; Fujiwara, Vavylonis et al. 2007). Moreover, binding of the ATP-actin sequestering-protein, profilin, promotes barbed-end addition of monomers (Pantaloni and Carlier 1993).

During filament polymerization, ATP is being hydrolyzed relatively quickly, which results in ADP+P_i bound actin subunits within the filament. Subsequent dissociation of P_i is rather slow and acts like a timer for filament age (Korn, Carlier et al. 1987). The severing and depolymerization of actin filaments requires the action of regulatory proteins, including ADF/cofilin and gelsolin (Bearer 1991; Kiuchi, Ohashi et al. 2007) Indeed, depolymerizing proteins can sense the nucleotide state of actin and thereby promote depolymerization of older filaments (Blanchoin and Pollard 1999). The net dissociation of ADP-actin at the pointed end requires monomers to be reloaded with ATP. The actin binding protein profilin is able to increase this exchange by 140-fold (Selden, Kinosian et al. 1999). Therefore, rapid actin assembly requires profilin mediated nucleotide exchange on actin, as clearly shown by in vivo data in yeast (Wolven, Belmont et al. 2000).

During fast (transient) elongation of filaments, large quantities of monomers need to be available. Concurrently, cytosolic concentrations of free actin monomers should be kept low to prevent uncontrolled polymerization Binding of a fraction of actin monomers to profilin keeps ATP-bound actin in an unpolymerized state till the molecules are recruited to the barbed ends of filaments. In vertebrates, the rest of the

monomers are stored in an unpolymerizable pool through binding of another actin sequestering protein, thymosin-β4. Interestingly, this interaction is strongly dependent on whether actin is in its ATP or ADP bound state (Cassimeris, Safer et al. 1992; Atkinson, Hosford et al. 2004). Exchange of thymosin-β4 with profilin will replenish the available pool of polymerizable actin when needed, since actin binds profilin with higher affinity (Pantaloni and Carlier 1993; Yarmola and Bubb 2004). Finally, the availability of actin monomers is warranted by the action of depolymerization and severing activities described above (Kiuchi, Ohashi et al. 2007).

Paradoxically, extreme ATP depletion causes an increase in the F-actin/G-actin ratio with disappearance of F-actin fibers and formation of unorganized F-actin patches (Atkinson, Hosford et al. 2004; Suurna, Ashworth et al. 2006). Strikingly, this increase in F-actin could not be inhibited by the (barbed-end) actin polymerization inhibitor cytochalasin D. Therefore, massive ATP depletion is likely to increase F-actin, or – better - its occurrence in abnormally rigid F-actin structures, by inhibiting depolymerization or increasing pointed-end polymerization (Ashworth, Southgate et al. 2003; Atkinson, Hosford et al. 2004). Perhaps, this reduction in actin turnover dynamics helps the cell in preventing further energy depletion. A contributing factor in this control might be the preference of thymosin for ATP-actin. When ATP-depletion simultaneously increases ADP-actin and decrease ATP-actin, less monomeric actin will be sequestered by thymosin. Consequently, raised levels of G-actin could spur spontaneous (pointed-end) actin polymerization (Atkinson, Hosford et al. 2004). Thus, under both physiological and extreme energy-depleting conditions there is a tight link between ATP/ADP ratio and control of actin polymerization.

Efficient actin polymerization and proper control of this process requires a constant supply of ATP-actin monomers and free barbed ends. Importantly, a surplus of free barbed ends could drain the pool of monomers and thus inhibit local polymerization. Capping proteins, such as CapZ and gelsolin, are able to bind barbed ends and thereby prevent addition of monomers (Isenberg, Aebi et al. 1980; Caldwell, Heiss et al. 1989). A consequence of capping is that the average size of filaments is shorter and makes them stiffer, which could render them more suitable for generating protrusive force at the leading edge (Kuhlman 2005). In addition, capping can modulate branching within the actin filament network required for switching

between lamellipodial or filopodial morphology (Mejillano, Kojima et al. 2004). In this way, blocking or de-blocking of barbed ends regulates local polymerization.

Myosins

Myosins are a family of motor proteins that move along actin filaments driven by repeated cycles of ATP hydrolysis. Although myosins share common features like actin binding and generation of movement by hydrolyzing ATP, there is a remarkable variety of family members (Sellers 2000). Phylogenetically, myosins can be classified into 15 subgroups, containing both muscle-specific and non-muscle forms (Sellers 2000).Whereas muscle myosins play a role in muscle contraction, several non-muscle myosins have been implicated in (local) cytoskeletal remodeling during phagocytosis, cell migration and adhesion. Class-II myosins are among the best-studied myosin members. They represent a group of conventional motor proteins that consist of two identical heavy subunits (Myosin heavy chains, MHC's), two essential light chains (ELC's) and 2 regulatory light chains (RLC's) (Trybus 1994; Landsverk and Epstein 2005). A variety of MHC and MLC isoforms are expressed in tissue and cell type specific manner. Non-muscle myosin-II is the major myosin involved in cell migration and is important for cell polarization, adhesion and tail retraction in migrating cells (Kolega 1998; Giannone, Dubin-Thaler et al. 2007; Vicente-Manzanares, Zareno et al. 2007). In addition, myosin-II is implicated in cup-formation during complement-mediated phagocytosis (Olazabal, Caron et al. 2002) and generation of contractile activity for phagocytic cup "sqeezing" during IgG-mediated phagocytosis (Araki, Hatae et al. 2003).

Another prominent myosin in non-muscle cells is the unconventional myosin-X. This widely expressed motor protein contains a FERM (band 4.1/ezrin/radixin/moesin) domain and interacts with regions of dynamic actin, such as lamellipodia and filopodia (Berg, Derfler et al. 2000). The FERM domain in myosin-X is important for its interaction with beta-integrins and the integrin-dependent formation of filopodia (Zhang, Berg et al. 2004). However, myosin-X mediated induction of filopodia is not uniquely dependent on the FERM domain. Dorsal filopodia formation is also facilitated by myosin-X that lacks the FERM

domain (Bohil, Robertson et al. 2006). Considering its association with cellular regions that are rich in dynamic actin, it is not surprising that myosin-X is implicated in cell adhesion, migration and phagocytis (Cox, Berg et al. 2002; Zhang, Berg et al. 2004; Pi, Ren et al. 2007).

Although the many diverse properties of myosins have been relatively well studied, still not much is known about their individual ATP requirements during activity in actomyosin based cell dynamics. Here, in this thesis we present findings that suggest that different CK isoenzymes may couple to these activities in a cell-type and process-type dependent manner.

1.7 Cell migration

Active cell migration is an important process in organisms. Single-cell organisms require cell locomotion to find suitable habitats, food sources and conjugation partners. Cells within multicellular organisms migrate during embryonic development, wound healing, immunological defense reactions, and tissue remodelling. Moreover, migration is a hallmark of malignant and invasive tumor cells, which makes the process an important target for clinical intervention. Cells use several molecular mechanisms for their mobility. For example, both spermatozoa and the unicellular algae Chlamydomonas reinhardtii use flagella for their propulsion. Another common mechanism for locomotion in multicellular eukaryotes is driven by activity of the actin cytoskeleton, often in combination with force generation by myosins.

Since the process of actin-driven cell motility is complex and knowledge is extensive, some essential features will be only briefly discussed here (see for more background on this topic reviews (Small, Stradal et al. 2002; Webb, Parsons et al. 2002; Pollard and Borisy 2003; Le Clainche and Carlier 2008; Olson and Sahai 2008). Cell migration can be divided into four discrete steps: 1) Protrusion of the leading edge, 2) Adhesion, 3) Retraction of the rear end of the cell, and 4) De-adhesion (**Figure 2**). The Arp2/3 complex is the main initiator (see chapter 1.5) for the formation of a branched network of filamentous actin that drives lamellipodial protrusion. Numerous accessory proteins are able to activate and modulate this branching

activity. Members of the WASP/Scar family of proteins are able to interact with - and activate - Arp2/3 through their VCA domains (Rohatgi, Ma et al. 1999; Takenawa and Miki 2001). The VCA domain is able to bind with an actin monomer through its WH2 motif (V) and simultaneously with the Arp2/3 complex through its acidic segment (A). The resulting complex may then act as a scaffold for further polymerization. The connecting sequence of the VCA domain (C) might also have a role during nucleation by recruitment of an actin monomer (Kelly, Kranitz et al. 2006). Furthermore, activation of Arp2/3 mediated actin nucleation by WASP is regulated by autoinhibiton and the subsequent release by Cdc42 and PIP2 (Kim, Kakalis et al. 2000; Prehoda, Scott et al. 2000).

Protrusive activity of actin polymerization in the leading edge requires simultaneous depolymerization activity to sustain the treadmilling process. It was observed that these opposing activities interchange in periodic cycles (Ponti, Matov et al. 2005) and depolymerization factors such as ADF/Cofilin are required for migration (Chen, Godt et al. 2001; Ghosh, Song et al. 2004).

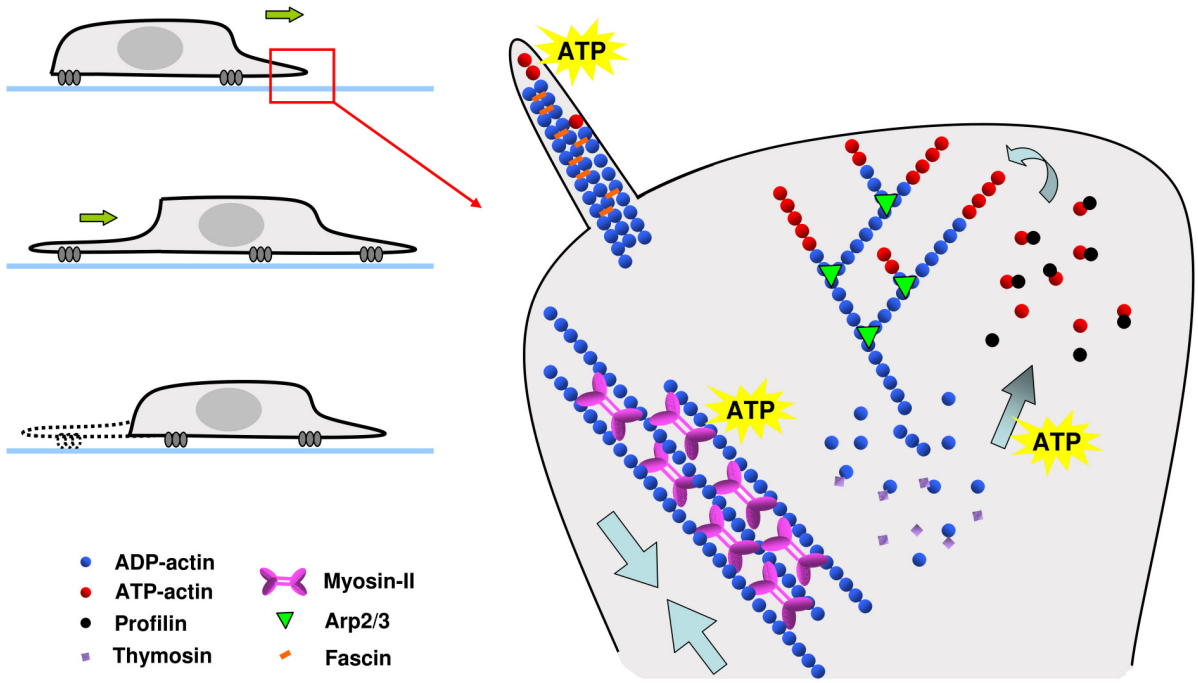

Figure 2. Cellular migration is driven by periodic phases of lamellipodial protrusion, adhesion and retraction. The right-hand panel shows a schematic representation of a lamellipodium and a filopodium at the leading edge of a migrating cell. Actin treadmilling and myosin contraction are associated with hydrolysis of ATP. Exchange of ADP on actin monomers by ATP is facilitated by the action of profilin.

After extension of the leading edge by actin polymerization the cell creates integrin-mediated adhesion sites to the extracellular matrix. Integrins are heterodimeric transmembrane receptors consisting of an α- and β-chain that bind to specific extracelullar matrix components (Humphries, Byron et al. 2006). Integrin-mediated adhesion is characterized by reciprocal communication between the "inside" and "outside" of the cell. Binding to specific ligands tranduces signals to the cytosol, whereas signals from within the cell can regulate integrin adhesion. Total adhesiveness ("avidity") is the sum of the density of integrins ("valency") and their individual affinity for the ligand (Carman and Springer 2003).

The family of small Rho GTPases fulfills a key role in coupling integrin signaling to dedicated activity in the actomyosin network (Heasman and Ridley 2008). GTPases act as on/off switches: Binding of GTP activates these proteins, while intrinsic GTPase activity switches them off. The activation state of GTPases is determined by other proteins, such as guanine exchange factors (GEFs), GTPase activating proteins (GAPs) and guanine nucleotide dissociation inhibitors (GDIs) (Moon and Zheng 2003; DerMardirossian and Bokoch 2005; Rossman, Der et al. 2005). Activity of the GTPase Rac is required for formation of new adhesions during protrusion of the leading edge, whereas RhoA mediates maturation (Rottner, Hall et al. 1999). In addition, RhoA regulates disassembly of focal adhesions at the trailing edge by decreasing integrin mediated adhesion and promoting retraction (Worthylake, Lemoine et al. 2001). During formation of focal complexes (the earliest adhesion event) several proteins like paxillin and alpha-actinin are serially being recruited. This ultimately can lead to the formation of stable, more organized, focal adhesions (Laukaitis, Webb et al. 2001). At the same time cells have to detach at the trailing edge. Actin-myosin contraction is the main force behind detachment of the trailing edge and it is now commonly accepted that detachment and protrusion are mechanically coupled (Gupton and Waterman-Storer 2006; Giannone, Dubin-Thaler et al. 2007).

Key elements of cell migration, such as integrin-mediated adhesion, actin polymerization and small Rho GTPase signaling, are equally important during cell spreading. In this process cells adhere to the extracellular matrix and extent lamellipodia to increase their surfaces, which is crucial for cellular functioning such as

thrombocyte activation (McCarty, Larson et al. 2005; Eto, Nishikii et al. 2007). Numerous other processes where adhesion and motility go hand in hand can also be mentioned here. For example, several cell types in brain require cell motility and adhesion during development and for normal physiological functioning in adults. Neuronal migration and neurite outgrowth are regulated by integrin-mediated adhesion and signaling (Lois, Garcia-Verdugo et al. 1996; Condic and Letourneau 1997). Also, astrocyte and microglia migrate extensively during brain development and pathological situations (Milner, Huang et al. 1999; Hama, Hara et al. 2004; Garden and Moller 2006). Likewise, other key processes in brain, such as neuronal-astrocyte interaction, synaptogensis and dendritic spine generation depend heavily on actin reorganization (Mattila and Lappalainen 2008). Recent work has demonstrated that the structural plasticity of dendritic spines is largely determined by the dynamics of actin fiber organisation (Honkura, Matsuzaki et al. 2008). The importance of ATP in these types of process is well illustrated by the fact that neurons spend up to 50% of their ATP for actin polymerization (Bernstein and Bamburg 2003).

1.8 Phagocytosis

Phagocytosis is yet another example of cell motility, but a very special process. Phagocytosis is critically dependent on local actin remodeling and is required to internalize particles that are larger than ~0.5 μm in size. Whereas unicellular eukaryotes employ phagocytosis mainly to acquire food from their extracellular environment, higher eukaryotes evolved additional specialized phagocytic functions, such as removing apoptotic cells during development (Penaloza, Lin et al. 2006). In addition, phagocytosis serves an important function within the innate immune defense, which constitutes the first line of protection against invading microorganisms. Innate immunity enforces cellular and humoral defense systems, such as cytokine production and phagocytosis (Medzhitov and Janeway 2000). Moreover, it activates the second major line of immune defense, adaptive immunity, which protects the organism against re-infection of pathogens.

Phagocytosis is initiated by the clustering and subsequent activation of dedicated receptors in the plasma membrane, followed by local actin polymerization at the membrane that drives membrane expansion to engulf the phagocytic target (**Figure 3**) (Swanson 2008). Once particles or foreign cells are internalized, intracellular pathways will orchestrate microbial killing, antigen expression and cytokine release (Vieira, Botelho et al. 2002; Blander and Medzhitov 2006). Phagocytic receptors specifically recognize a molecular signature present on the pathogen itself, or bind to an intermediate host molecule that recognizes the pathogen. The first category of reactions involves receptors that recognize a relatively small number of highly conserved molecular signatures on the particle/cell surface, such as mannose, lipopolysacharide (LPS) and β-glucan groups (Brown and Gordon

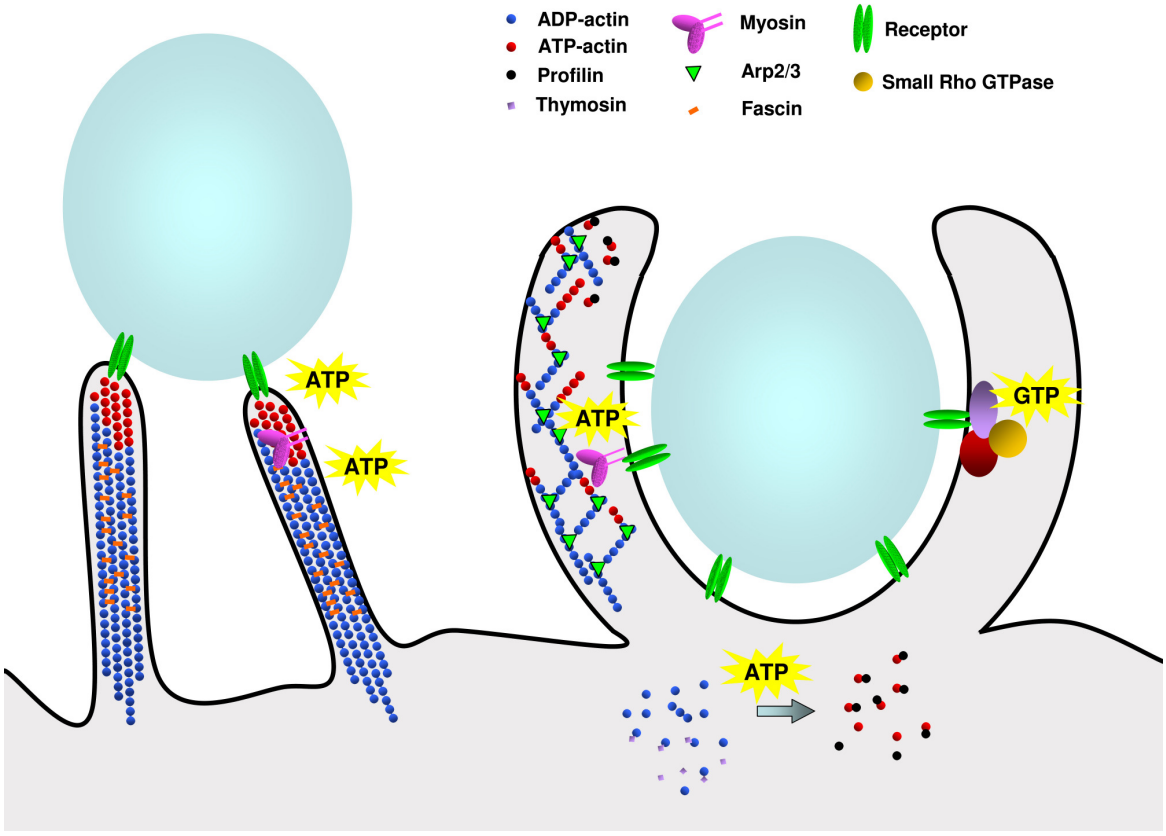

Figure 3. Phagocytosis is initiated by the "catching" of particles by filopodia and adhesion by dedicated receptors. Subsequently, engulfment op the particles is driven by the action of actin driven protrusion of cell membrane around the target. Myosins play a role in filopodial dynamics (Myosin-X) and organization and squeezing of the phagocytic cup (e.g. Myosin-II).

2001; McGreal, Miller et al. 2005). In the second mode of reactions, receptors such as complement and Fc-γ-receptors, recognize pathogens indirectly through host molecules that interact with pathogens. Because the type of receptor determines the signal transduction and functional outcome of phagocytosis, it is important to discuss the phagocytic process in the context of the (type of) receptor initiating it. The two archetypal phagocytic receptors are the Fc-γ-receptor (FcγR) and the complement receptor type 3 (CR3).

FcγRs are membrane receptors that bind the constant (Fc) portion of immunoglobulin G (IgG). Human and murine cells of the hematopoetic lineage, like monocytes and macrophages, express three types of phagocytic FcγRs: FcγRIa, FcγRIIa and FcγRIIIa. Binding to IgG opsonized targets trigger clustering and activation of these receptors (Sobota, Strzelecka-Kiliszek et al. 2005). Downstream signaling events will culminate in a highly localized remodeling of the actin cytoskeleton, whereby extending pseudopodia engulf the phagocytic target (Allen and Aderem 1996).

Clustering of FcγRs at the cell membrane triggers tyrosine phosphorylation of ITAMs (immunoreceptor tyrosine-based activation motives; $YxxLx_{5-12}Yx_{2-3}L/I$) present in the intracellular part of FcγRs, by tyrosine kinases of the Src family (Isakov 1997; Suzuki, Kono et al. 2000). The phosphorylated ITAM motifs serve as docking places for the SH2 (Src homology 2) domain containing tyrosine kinase, Syk, which is important for inducing local actin polymerization (Cox, Chang et al. 1996; Greenberg, Chang et al. 1996).

Complement receptor 3 (CR3, also: Mac-1) is a heterodimeric integrin and consists of a α_m and β_2 subunit. This receptor is expressed in phagocytic cells, such as macrophages, neutrophils and dendritic cells. Other than with binding to the FcγR, CR3 ligand binding is rather promiscuous. Consequently, CR3 is involved in a wide variety of leukocyte functions. CR3 mediates extracellular matrix adhesion and cell-cell interaction through binding partners, such as fibrinogen and intercellular adhesion molecule 1 (ICAM-1) (Wright, Weitz et al. 1988; Ross and Vetvicka 1993). These adhesive properties are crucial for leukocyte migration to sites of infection by diapedesis (Dejana 2006). In addition, complement-mediated phagocytosis is

principally mediated by CR3. The complement system of serum proteins is part of the innate immune system and governs opsonization and lysis of pathogens (Gasque 2004). C3bi, a potent opsonin that is produced during activation of the complement cascade, is a major ligand for CR3 and induces a phagocytic response. Also non-opsonic ligands have been observed to mediate phagocytosis via the lectin-binding properties of the CR3 receptor (Le Cabec, Cols et al. 2000). In contrast with FcγR-mediated phagocytosis, ultrastructural analysis demonstrates that complement-mediated phagocytosis does not employ pseudopodia for particle engulfment, but rather induces particles to "sink" into the cells (Kaplan 1977; Allen and Aderem 1996), although there are exceptions (Le Cabec, Carreno et al. 2002; Patel and Harrison 2008)

Importantly, the same Rho GTPases that are active in cell spreading and motility are also active in phagocytosis as signaling-organizers of the actin cytoskeleton. Numerous studies implicated the small Rho GTPases Rac1 and Cdc42 in FcγR mediated phagocytosis (Cox, Chang et al. 1997; Caron and Hall 1998; Cougoule, Hoshino et al. 2006; Hall, Gakidis et al. 2006). The dynamic recruitment of Rac1, Rac2 and Cdc42 was investigated in detail by fluorescence resonance energy transfer (FRET) based imaging techniques. Cdc42 preferentially localizes at the tips of pseudopodia during engulfment, whereas Rac1 displays a biphasic recruitment during initiation of phagocytosis and later during closure of the phagosome (Hoppe and Swanson 2004). Despite the rapid advancement of knowledge in this area, the role of RhoA in FcγR mediated phagocytosis remains somewhat obscure. Some studies implicate a essential role for RhoA in FcγR mediated phagocytosis, whereas other studies claim redundancy (Hackam, Rotstein et al. 1997; Caron and Hall 1998; Hall, Gakidis et al. 2006; Heasman and Ridley 2008).

Interestingly, CR3 mediated phagocytosis is strictly dependent on RhoA and Rap1, whereas Rac and Cdc42 are expendable (Caron and Hall 1998; Caron, Self et al. 2000). Moreover, several downstream targets that require activated RhoA have been specifically implicated in complement-mediated phagocytosis (Olazabal, Caron et al. 2002; Colucci-Guyon, Niedergang et al. 2005).

Actin nucleation during phagocytosis can be initiated by Arp2/3 during CR3 and FcγR mediated phagocytosis (May, Caron et al. 2000). Alternatively, CR3 mediated phagocytosis employs the nucleating activity of formins (Colucci-Guyon, Niedergang et al. 2005). Many other proteins involved in actin cytoskeletal rearrangements are also localized at the phagosome and/or functionally implicated in phagocytosis. For example, the Wiskott-Aldrich syndrome (WASP) and Ena/VASP family of proteins have been implicated in phagocytosis (Lorenzi, Brickell et al. 2000; Coppolino, Krause et al. 2001). These proteins interact with the small Rho GTPases and the Arp2/3 complex as already described for cell migration (Aspenstrom, Lindberg et al. 1996; Rohatgi, Ma et al. 1999).

Since actin remodeling involves both polymerization and myosin force generation, it not surprising that several studies report on the necessity of myosin activity during distinct phases of phagocytosis (**Figure 3**). In Dictyostelium discoideum myosin VII is required for the initial adhesion-step during phagocytosis in addition to cell-cell and cell-substratum adhesion, which are closely related processes (Tuxworth, Weber et al. 2001). In mammalian macrophages myosin-X enhances pseudopod extension during FcγR mediated phagocytosis, but myosin-X's role in complement-mediated phagocytosis is still not well studied. Myosin-II is involved in both FcγR mediated as well as complement-mediated phagocytosis. Decreasing myosin-II activity through inhibition of myosin light chain kinase (MLCK) affected the "squeezing" of phagocytic targets (Araki, Hatae et al. 2003). Also particle internalization required myosin-II activity (Olazabal, Caron et al. 2002). Both complement-mediated internalization, as well as phagocytic cup formation is dependent on myosin-II, whereas it was redundant for cup formation during FcγR mediated phagocytosis (Olazabal, Caron et al. 2002). In addition to the myosins mentioned above, several other myosins have been found localizing to the phagocytic cup, however the precise functional contributions of different myosin family members remain to be resolved (Diakonova, Bokoch et al. 2002).

In this thesis we propose on the basis of new findings that the high energy needs for actin dynamics and myosin activity during special steps in phagocytosis form a local ATP drain, a drain that can only be adequately filled by CK mediated ATP delivery.

1.9 Aim and outine of thesis

Transgenic mouse models with CK deficiencies have provided important insights into energy compartmentalization of cellular energy, i.e. ATP. Especially the connection between the CK system and ATP supply in skeletal muscle function has been well described. However, the function of CK in tissues other than muscle have been largely neglected or appeared difficult to study. The aim of this thesis was to elucidate how highly localized dynamic cellular processes in non-muscle cells depend on CK-B mediated ATP shuttling. To provide answers to many remaining questions we focused our research efforts on cells with high and fluctuating energy demands, such as neurons, astrocytes and macrophages, which resulted in four experimental chapters. In chapter 2 a functional relation between CK-B mediated phospotransfer and early adhesion events during phagocytosis is presented. It was found that CK-B transiently accumulates with F-actin during engulfment and inhibition of CK-B decreased actin accumulation in the phagocytic cup. The data presented in chapter 3 further explores the link between CK-B and the actin cytoskeleton during cell migration and cell spreading. Primary astrocytes that are deficient for CK-B exhibit slower cell spreading and motility as compared with their wildtype counterparts. In addition, these effects could be reproduced in a fibroblast model system, demonstrating the universality of the link between CK-B and the actin cytoskeleton. In chapter 4 the function of CK-B in fast intracellular transportation of amyloid precursor protein (APP) and mitochondria is investigated in cultured neurons from wildtype and CK-B deficient mice. Although, CK-B does not seem to influence the velocity of fast axonal transport, the total number of migratory mitochondria is increased in neurons deficient for CK-B. Finally, chapter 5 describes the derivation of conditionally immortalized neuronal and glial cell lines from CK-B deficient mice, which could provide valuable tools for further elucidation of CK-function in brain.

References

Ahuja, R., R. Pinyol, et al. (2007). "Cordon-bleu is an actin nucleation factor and controls neuronal morphology." Cell **131**(2): 337-50.

Allen, L. A. and A. Aderem (1996). "Molecular definition of distinct cytoskeletal structures involved in complement- and Fc receptor-mediated phagocytosis in macrophages." J Exp Med **184**(2): 627-37.

Andreyev, A. Y., Y. E. Kushnareva, et al. (2005). "Mitochondrial metabolism of reactive oxygen species." Biochemistry (Mosc) **70**(2): 200-14.
Araki, N., T. Hatae, et al. (2003). "Phosphoinositide-3-kinase-independent contractile activities associated with Fcgamma-receptor-mediated phagocytosis and macropinocytosis in macrophages." J Cell Sci **116**(Pt 2): 247-57.
Ashworth, S. L., E. L. Southgate, et al. (2003). "ADF/cofilin mediates actin cytoskeletal alterations in LLC-PK cells during ATP depletion." Am J Physiol Renal Physiol **284**(4): F852-62.
Aspenstrom, P., U. Lindberg, et al. (1996). "Two GTPases, Cdc42 and Rac, bind directly to a protein implicated in the immunodeficiency disorder Wiskott-Aldrich syndrome." Curr Biol **6**(1): 70-5.
Atkinson, S. J., M. A. Hosford, et al. (2004). "Mechanism of actin polymerization in cellular ATP depletion." J Biol Chem **279**(7): 5194-9.
Bearer, E. L. (1991). "Direct observation of actin filament severing by gelsolin and binding by gCap39 and CapZ." J Cell Biol **115**(6): 1629-38.
Berg, J. S., B. H. Derfler, et al. (2000). "Myosin-X, a novel myosin with pleckstrin homology domains, associates with regions of dynamic actin." J Cell Sci **113 Pt 19**: 3439-51.
Bernstein, B. W. and J. R. Bamburg (2003). "Actin-ATP hydrolysis is a major energy drain for neurons." J Neurosci **23**(1): 1-6.
Beutner, G., A. Ruck, et al. (1998). "Complexes between porin, hexokinase, mitochondrial creatine kinase and adenylate translocator display properties of the permeability transition pore. Implication for regulation of permeability transition by the kinases." Biochim Biophys Acta **1368**(1): 7-18.
Bizzi, A., M. Bugiani, et al. (2002). "X-linked creatine deficiency syndrome: a novel mutation in creatine transporter gene SLC6A8." Ann Neurol **52**(2): 227-31.
Blanchoin, L. and T. D. Pollard (1999). "Mechanism of interaction of Acanthamoeba actophorin (ADF/Cofilin) with actin filaments." J Biol Chem **274**(22): 15538-46.
Blander, J. M. and R. Medzhitov (2006). "On regulation of phagosome maturation and antigen presentation." Nat Immunol **7**(10): 1029-35.
Bohil, A. B., B. W. Robertson, et al. (2006). "Myosin-X is a molecular motor that functions in filopodia formation." Proc Natl Acad Sci U S A **103**(33): 12411-6.
Boldogh, I. R. and L. A. Pon (2007). "Mitochondria on the move." Trends Cell Biol.
Braissant, O., H. Henry, et al. (2001). "Endogenous synthesis and transport of creatine in the rat brain: an in situ hybridization study." Brain Res Mol Brain Res **86**(1-2): 193-201.
Brand, M. D. (2005). "The efficiency and plasticity of mitochondrial energy transduction." Biochem Soc Trans **33**(Pt 5): 897-904.
Brown, G. D. and S. Gordon (2001). "Immune recognition. A new receptor for beta-glucans." Nature **413**(6851): 36-7.
Burklen, T. S., A. Hirschy, et al. (2007). "Brain-type creatine kinase BB-CK interacts with the Golgi Matrix Protein GM130 in early prophase." Mol Cell Biochem **297**(1-2): 53-64.
Caldwell, J. E., S. G. Heiss, et al. (1989). "Effects of CapZ, an actin capping protein of muscle, on the polymerization of actin." Biochemistry **28**(21): 8506-14.
Campanella, M. E., H. Chu, et al. (2005). "Assembly and regulation of a glycolytic enzyme complex on the human erythrocyte membrane." Proc Natl Acad Sci U S A **102**(7): 2402-7.
Carman, C. V. and T. A. Springer (2003). "Integrin avidity regulation: are changes in affinity and conformation underemphasized?" Curr Opin Cell Biol **15**(5): 547-56.
Caron, E. and A. Hall (1998). "Identification of two distinct mechanisms of phagocytosis controlled by different Rho GTPases." Science **282**(5394): 1717-21.
Caron, E., A. J. Self, et al. (2000). "The GTPase Rap1 controls functional activation of macrophage integrin alphaMbeta2 by LPS and other inflammatory mediators." Curr Biol **10**(16): 974-8.
Cassimeris, L., D. Safer, et al. (1992). "Thymosin beta 4 sequesters the majority of G-actin in resting human polymorphonuclear leukocytes." J Cell Biol **119**(5): 1261-70.
Chang, D. T., A. S. Honick, et al. (2006). "Mitochondrial trafficking to synapses in cultured primary cortical neurons." J Neurosci **26**(26): 7035-45.
Chen, J., D. Godt, et al. (2001). "Cofilin/ADF is required for cell motility during Drosophila ovary development and oogenesis." Nat Cell Biol **3**(2): 204-9.
Colucci-Guyon, E., F. Niedergang, et al. (2005). "A role for mammalian diaphanous-related formins in complement receptor (CR3)-mediated phagocytosis in macrophages." Curr Biol **15**(22): 2007-12.

Condic, M. L. and P. C. Letourneau (1997). "Ligand-induced changes in integrin expression regulate neuronal adhesion and neurite outgrowth." Nature **389**(6653): 852-6.
Coppolino, M. G., M. Krause, et al. (2001). "Evidence for a molecular complex consisting of Fyb/SLAP, SLP-76, Nck, VASP and WASP that links the actin cytoskeleton to Fcgamma receptor signalling during phagocytosis." J Cell Sci **114**(Pt 23): 4307-18.
Cougoule, C., S. Hoshino, et al. (2006). "Dissociation of recruitment and activation of the small G-protein Rac during Fcgamma receptor-mediated phagocytosis." J Biol Chem **281**(13): 8756-64.
Cox, D., J. S. Berg, et al. (2002). "Myosin X is a downstream effector of PI(3)K during phagocytosis." Nat Cell Biol **4**(7): 469-77.
Cox, D., P. Chang, et al. (1996). "Syk tyrosine kinase is required for immunoreceptor tyrosine activation motif-dependent actin assembly." J Biol Chem **271**(28): 16597-602.
Cox, D., P. Chang, et al. (1997). "Requirements for both Rac1 and Cdc42 in membrane ruffling and phagocytosis in leukocytes." J Exp Med **186**(9): 1487-94.
de Groof, A. J., J. A. Fransen, et al. (2002). "The creatine kinase system is essential for optimal refill of the sarcoplasmic reticulum Ca2+ store in skeletal muscle." J Biol Chem **277**(7): 5275-84.
de Groof, A. J., F. T. Oerlemans, et al. (2001). "Changes in glycolytic network and mitochondrial design in creatine kinase-deficient muscles." Muscle Nerve **24**(9): 1188-96.
Debrincat, M. A., J. G. Zhang, et al. (2007). "Ankyrin repeat and suppressors of cytokine signaling box protein asb-9 targets creatine kinase B for degradation." J Biol Chem **282**(7): 4728-37.
Dejana, E. (2006). "The transcellular railway: insights into leukocyte diapedesis." Nat Cell Biol **8**(2): 105-7.
DerMardirossian, C. and G. M. Bokoch (2005). "GDIs: central regulatory molecules in Rho GTPase activation." Trends Cell Biol **15**(7): 356-63.
Diakonova, M., G. Bokoch, et al. (2002). "Dynamics of cytoskeletal proteins during Fcgamma receptor-mediated phagocytosis in macrophages." Mol Biol Cell **13**(2): 402-11.
Dzeja, P. P. and A. Terzic (2003). "Phosphotransfer networks and cellular energetics." J Exp Biol **206**(Pt 12): 2039-47.
Eto, K., H. Nishikii, et al. (2007). "The WAVE2/Abi1 complex differentially regulates megakaryocyte development and spreading: implications for platelet biogenesis and spreading machinery." Blood **110**(10): 3637-47.
Eto, K., Y. Tsubamoto, et al. (1999). "Role of NADH shuttle system in glucose-induced activation of mitochondrial metabolism and insulin secretion." Science **283**(5404): 981-5.
Evangelista, M., S. Zigmond, et al. (2003). "Formins: signaling effectors for assembly and polarization of actin filaments." J Cell Sci **116**(Pt 13): 2603-11.
Fujiwara, I., D. Vavylonis, et al. (2007). "Polymerization kinetics of ADP- and ADP-Pi-actin determined by fluorescence microscopy." Proc Natl Acad Sci U S A **104**(21): 8827-32.
Garden, G. A. and T. Moller (2006). "Microglia biology in health and disease." J Neuroimmune Pharmacol **1**(2): 127-37.
Gasque, P. (2004). "Complement: a unique innate immune sensor for danger signals." Mol Immunol **41**(11): 1089-98.
Ghosh, M., X. Song, et al. (2004). "Cofilin promotes actin polymerization and defines the direction of cell motility." Science **304**(5671): 743-6.
Giannone, G., B. J. Dubin-Thaler, et al. (2007). "Lamellipodial actin mechanically links myosin activity with adhesion-site formation." Cell **128**(3): 561-75.
Gillespie, P. G. and J. L. Cyr (2004). "Myosin-1c, the hair cell's adaptation motor." Annu Rev Physiol **66**: 521-45.
Gitlits, V. M., B. H. Toh, et al. (2000). "The glycolytic enzyme enolase is present in sperm tail and displays nucleotide-dependent association with microtubules." Eur J Cell Biol **79**(2): 104-11.
Glitsch, H. G. and A. Tappe (1993). "The Na+/K+ pump of cardiac Purkinje cells is preferentially fuelled by glycolytic ATP production." Pflugers Arch **422**(4): 380-5.
Goley, E. D. and M. D. Welch (2006). "The ARP2/3 complex: an actin nucleator comes of age." Nat Rev Mol Cell Biol **7**(10): 713-26.
Greenberg, S., P. Chang, et al. (1996). "Clustered syk tyrosine kinase domains trigger phagocytosis." Proc Natl Acad Sci U S A **93**(3): 1103-7.

Guimbal, C. and M. W. Kilimann (1993). "A Na(+)-dependent creatine transporter in rabbit brain, muscle, heart, and kidney. cDNA cloning and functional expression." J Biol Chem **268**(12): 8418-21.
Gupton, S. L. and C. M. Waterman-Storer (2006). "Spatiotemporal feedback between actomyosin and focal-adhesion systems optimizes rapid cell migration." Cell **125**(7): 1361-74.
Hackam, D. J., O. D. Rotstein, et al. (1997). "Rho is required for the initiation of calcium signaling and phagocytosis by Fcgamma receptors in macrophages." J Exp Med **186**(6): 955-66.
Hall, A. B., M. A. Gakidis, et al. (2006). "Requirements for Vav guanine nucleotide exchange factors and Rho GTPases in FcgammaR- and complement-mediated phagocytosis." Immunity **24**(3): 305-16.
Hama, H., C. Hara, et al. (2004). "PKC signaling mediates global enhancement of excitatory synaptogenesis in neurons triggered by local contact with astrocytes." Neuron **41**(3): 405-15.
Hamburg, R. J., D. L. Friedman, et al. (1990). "Muscle creatine kinase isoenzyme expression in adult human brain." J Biol Chem **265**(11): 6403-9.
Heasman, S. J. and A. J. Ridley (2008). "Mammalian Rho GTPases: new insights into their functions from in vivo studies." Nat Rev Mol Cell Biol **9**(9): 690-701.
Hollenbeck, P. J. and W. M. Saxton (2005). "The axonal transport of mitochondria." J Cell Sci **118**(Pt 23): 5411-9.
Honkura, N., M. Matsuzaki, et al. (2008). "The subspine organization of actin fibers regulates the structure and plasticity of dendritic spines." Neuron **57**(5): 719-29.
Hoppe, A. D. and J. A. Swanson (2004). "Cdc42, Rac1, and Rac2 display distinct patterns of activation during phagocytosis." Mol Biol Cell **15**(8): 3509-19.
Hornemann, T., S. Kempa, et al. (2003). "Muscle-type creatine kinase interacts with central domains of the M-band proteins myomesin and M-protein." J Mol Biol **332**(4): 877-87.
Hornemann, T., M. Stolz, et al. (2000). "Isoenzyme-specific interaction of muscle-type creatine kinase with the sarcomeric M-line is mediated by NH(2)-terminal lysine charge-clamps." J Cell Biol **149**(6): 1225-34.
Humphries, J. D., A. Byron, et al. (2006). "Integrin ligands at a glance." J Cell Sci **119**(Pt 19): 3901-3.
Inoue, K., S. Ueno, et al. (2004). "Interaction of neuron-specific K+-Cl- cotransporter, KCC2, with brain-type creatine kinase." FEBS Lett **564**(1-2): 131-5.
Inoue, K., J. Yamada, et al. (2006). "Brain-type creatine kinase activates neuron-specific K+-Cl- co-transporter KCC2." J Neurochem **96**(2): 598-608.
Isakov, N. (1997). "Immunoreceptor tyrosine-based activation motif (ITAM), a unique module linking antigen and Fc receptors to their signaling cascades." J Leukoc Biol **61**(1): 6-16.
Isenberg, G., U. Aebi, et al. (1980). "An actin-binding protein from Acanthamoeba regulates actin filament polymerization and interactions." Nature **288**(5790): 455-9.
Item, C. B., S. Stockler-Ipsiroglu, et al. (2001). "Arginine:glycine amidinotransferase deficiency: the third inborn error of creatine metabolism in humans." Am J Hum Genet **69**(5): 1127-33.
Jost, C. R., C. E. Van Der Zee, et al. (2002). "Creatine kinase B-driven energy transfer in the brain is important for habituation and spatial learning behaviour, mossy fibre field size and determination of seizure susceptibility." Eur J Neurosci **15**(10): 1692-706.
Joubert, F., J. L. Mazet, et al. (2002). "31P NMR detection of subcellular creatine kinase fluxes in the perfused rat heart: contractility modifies energy transfer pathways." J Biol Chem **277**(21): 18469-76.
Kadenbach, B. (2003). "Intrinsic and extrinsic uncoupling of oxidative phosphorylation." Biochim Biophys Acta **1604**(2): 77-94.
Kaplan, G. (1977). "Differences in the mode of phagocytosis with Fc and C3 receptors in macrophages." Scand J Immunol **6**(8): 797-807.
Keller, A., J. Peltzer, et al. (2007). "Interactions of enolase isoforms with tubulin and microtubules during myogenesis." Biochim Biophys Acta **1770**(6): 919-26.
Kelly, A. E., H. Kranitz, et al. (2006). "Actin binding to the central domain of WASP/Scar proteins plays a critical role in the activation of the Arp2/3 complex." J Biol Chem **281**(15): 10589-97.
Kerkhoff, E. (2006). "Cellular functions of the Spir actin-nucleation factors." Trends Cell Biol **16**(9): 477-83.
Kim, A. S., L. T. Kakalis, et al. (2000). "Autoinhibition and activation mechanisms of the Wiskott-Aldrich syndrome protein." Nature **404**(6774): 151-8.

Kiuchi, T., K. Ohashi, et al. (2007). "Cofilin promotes stimulus-induced lamellipodium formation by generating an abundant supply of actin monomers." J Cell Biol **177**(3): 465-76.
Kolega, J. (1998). "Cytoplasmic dynamics of myosin IIA and IIB: spatial 'sorting' of isoforms in locomoting cells." J Cell Sci **111 (Pt 15)**: 2085-95.
Korge, P. and K. B. Campbell (1994). "Local ATP regeneration is important for sarcoplasmic reticulum Ca2+ pump function." Am J Physiol **267**(2 Pt 1): C357-66.
Korn, E. D., M. F. Carlier, et al. (1987). "Actin polymerization and ATP hydrolysis." Science **238**(4827): 638-44.
Kraft, T., T. Hornemann, et al. (2000). "Coupling of creatine kinase to glycolytic enzymes at the sarcomeric I-band of skeletal muscle: a biochemical study in situ." J Muscle Res Cell Motil **21**(7): 691-703.
Kuhlman, P. A. (2005). "Dynamic changes in the length distribution of actin filaments during polymerization can be modulated by barbed end capping proteins." Cell Motil Cytoskeleton **61**(1): 1-8.
Lahti, D. W., J. D. Hoekman, et al. (2005). "Identification of mouse brain proteins associated with isoform 3 of metallothionein." Protein Sci **14**(5): 1151-7.
Landsverk, M. L. and H. F. Epstein (2005). "Genetic analysis of myosin II assembly and organization in model organisms." Cell Mol Life Sci **62**(19-20): 2270-82.
Laukaitis, C. M., D. J. Webb, et al. (2001). "Differential dynamics of alpha 5 integrin, paxillin, and alpha-actinin during formation and disassembly of adhesions in migrating cells." J Cell Biol **153**(7): 1427-40.
Le Cabec, V., S. Carreno, et al. (2002). "Complement receptor 3 (CD11b/CD18) mediates type I and type II phagocytosis during nonopsonic and opsonic phagocytosis, respectively." J Immunol **169**(4): 2003-9.
Le Cabec, V., C. Cols, et al. (2000). "Nonopsonic phagocytosis of zymosan and Mycobacterium kansasii by CR3 (CD11b/CD18) involves distinct molecular determinants and is or is not coupled with NADPH oxidase activation." Infect Immun **68**(8): 4736-45.
Le Clainche, C. and M. F. Carlier (2008). "Regulation of actin assembly associated with protrusion and adhesion in cell migration." Physiol Rev **88**(2): 489-513.
Li, Z., K. Okamoto, et al. (2004). "The importance of dendritic mitochondria in the morphogenesis and plasticity of spines and synapses." Cell **119**(6): 873-87.
Lim, W., E. S. Neff, et al. (2004). "The mouse muscle creatine kinase promoter faithfully drives reporter gene expression in transgenic Xenopus laevis." Physiol Genomics **18**(1): 79-86.
Lois, C., J. M. Garcia-Verdugo, et al. (1996). "Chain migration of neuronal precursors." Science **271**(5251): 978-81.
Lorenzi, R., P. M. Brickell, et al. (2000). "Wiskott-Aldrich syndrome protein is necessary for efficient IgG-mediated phagocytosis." Blood **95**(9): 2943-6.
Mahajan, V. B., K. S. Pai, et al. (2000). "Creatine kinase, an ATP-generating enzyme, is required for thrombin receptor signaling to the cytoskeleton." Proc Natl Acad Sci U S A **97**(22): 12062-7.
Mattila, P. K. and P. Lappalainen (2008). "Filopodia: molecular architecture and cellular functions." Nat Rev Mol Cell Biol **9**(6): 446-54.
May, R. C., E. Caron, et al. (2000). "Involvement of the Arp2/3 complex in phagocytosis mediated by FcgammaR or CR3." Nat Cell Biol **2**(4): 246-8.
McCarty, O. J., M. K. Larson, et al. (2005). "Rac1 is essential for platelet lamellipodia formation and aggregate stability under flow." J Biol Chem **280**(47): 39474-84.
McGreal, E. P., J. L. Miller, et al. (2005). "Ligand recognition by antigen-presenting cell C-type lectin receptors." Curr Opin Immunol **17**(1): 18-24.
Medzhitov, R. and C. Janeway, Jr. (2000). "Innate immunity." N Engl J Med **343**(5): 338-44.
Mejillano, M. R., S. Kojima, et al. (2004). "Lamellipodial versus filopodial mode of the actin nanomachinery: pivotal role of the filament barbed end." Cell **118**(3): 363-73.
Meyer, R. A., H. L. Sweeney, et al. (1984). "A simple analysis of the "phosphocreatine shuttle"." Am J Physiol **246**(5 Pt 1): C365-77.
Milner, R., X. Huang, et al. (1999). "Distinct roles for astrocyte alphavbeta5 and alphavbeta8 integrins in adhesion and migration." J Cell Sci **112 (Pt 23)**: 4271-9.
Moon, S. Y. and Y. Zheng (2003). "Rho GTPase-activating proteins in cell regulation." Trends Cell Biol **13**(1): 13-22.
Olazabal, I. M., E. Caron, et al. (2002). "Rho-kinase and myosin-II control phagocytic cup formation during CR, but not FcgammaR, phagocytosis." Curr Biol **12**(16): 1413-18.

Olson, M. F. and E. Sahai (2008). "The actin cytoskeleton in cancer cell motility." Clin Exp Metastasis.
Pantaloni, D. and M. F. Carlier (1993). "How profilin promotes actin filament assembly in the presence of thymosin beta 4." Cell **75**(5): 1007-14.
Patel, P. C. and R. E. Harrison (2008). "Membrane Ruffles Capture C3bi-opsonized Particles in Activated Macrophages." Mol Biol Cell.
Penaloza, C., L. Lin, et al. (2006). "Cell death in development: shaping the embryo." Histochem Cell Biol **126**(2): 149-58.
Pi, X., R. Ren, et al. (2007). "Sequential roles for myosin-X in BMP6-dependent filopodial extension, migration, and activation of BMP receptors." J Cell Biol **179**(7): 1569-82.
Pietrobon, D., M. Zoratti, et al. (1983). "Molecular slipping in redox and ATPase H+ pumps." Biochim Biophys Acta **723**(2): 317-21.
Pineda, A. O., Jr. and W. R. Ellington (2001). "Organization of the gene for an invertebrate mitochondrial creatine kinase: comparisons with genes of higher forms and correlation of exon boundaries with functional domains." Gene **265**(1-2): 115-21.
Pollard, T. D. (1986). "Rate constants for the reactions of ATP- and ADP-actin with the ends of actin filaments." J Cell Biol **103**(6 Pt 2): 2747-54.
Pollard, T. D. and G. G. Borisy (2003). "Cellular motility driven by assembly and disassembly of actin filaments." Cell **112**(4): 453-65.
Ponti, A., A. Matov, et al. (2005). "Periodic patterns of actin turnover in lamellipodia and lamellae of migrating epithelial cells analyzed by quantitative Fluorescent Speckle Microscopy." Biophys J **89**(5): 3456-69.
Prehoda, K. E., J. A. Scott, et al. (2000). "Integration of multiple signals through cooperative regulation of the N-WASP-Arp2/3 complex." Science **290**(5492): 801-6.
Raikar, L. S., J. Vallejo, et al. (2006). "Overexpression of caveolin-1 results in increased plasma membrane targeting of glycolytic enzymes: the structural basis for a membrane associated metabolic compartment." J Cell Biochem **98**(4): 861-71.
Rohatgi, R., L. Ma, et al. (1999). "The interaction between N-WASP and the Arp2/3 complex links Cdc42-dependent signals to actin assembly." Cell **97**(2): 221-31.
Rolfe, D. F. and M. D. Brand (1996). "Contribution of mitochondrial proton leak to skeletal muscle respiration and to standard metabolic rate." Am J Physiol **271**(4 Pt 1): C1380-9.
Rome, L. C. and A. A. Klimov (2000). "Superfast contractions without superfast energetics: ATP usage by SR-Ca2+ pumps and crossbridges in toadfish swimbladder muscle." J Physiol **526 Pt 2**: 279-86.
Ross, G. D. and V. Vetvicka (1993). "CR3 (CD11b, CD18): a phagocyte and NK cell membrane receptor with multiple ligand specificities and functions." Clin Exp Immunol **92**(2): 181-4.
Rossman, K. L., C. J. Der, et al. (2005). "GEF means go: turning on RHO GTPases with guanine nucleotide-exchange factors." Nat Rev Mol Cell Biol **6**(2): 167-80.
Rottner, K., A. Hall, et al. (1999). "Interplay between Rac and Rho in the control of substrate contact dynamics." Curr Biol **9**(12): 640-8.
Rousset, S., M. C. Alves-Guerra, et al. (2004). "The biology of mitochondrial uncoupling proteins." Diabetes **53 Suppl 1**: S130-5.
Saks, V. A., Z. A. Khuchua, et al. (1994). "Metabolic compartmentation and substrate channelling in muscle cells. Role of coupled creatine kinases in in vivo regulation of cellular respiration--a synthesis." Mol Cell Biochem **133-134**: 155-92.
Salomons, G. S., S. J. van Dooren, et al. (2001). "X-linked creatine-transporter gene (SLC6A8) defect: a new creatine-deficiency syndrome." Am J Hum Genet **68**(6): 1497-500.
Salway, J. (2002). Metabolism at a glance.
Schmidt, A., B. Marescau, et al. (2004). "Severely altered guanidino compound levels, disturbed body weight homeostasis and impaired fertility in a mouse model of guanidinoacetate N-methyltransferase (GAMT) deficiency." Hum Mol Genet **13**(9): 905-21.
Schneider, M. E., I. A. Belyantseva, et al. (2002). "Rapid renewal of auditory hair bundles." Nature **418**(6900): 837-8.
Schulze, A. (2003). "Creatine deficiency syndromes." Mol Cell Biochem **244**(1-2): 143-50.
Schwegler, H. and W. E. Crusio (1995). "Correlations between radial-maze learning and structural variations of septum and hippocampus in rodents." Behav Brain Res **67**(1): 29-41.
Selden, L. A., H. J. Kinosian, et al. (1999). "Impact of profilin on actin-bound nucleotide exchange and actin polymerization dynamics." Biochemistry **38**(9): 2769-78.
Sellers, J. R. (2000). "Myosins: a diverse superfamily." Biochim Biophys Acta **1496**(1): 3-22.

Shibuya, J., T. Matsumoto, et al. (1992). "The first report of a case with acute myocardial infarction showing familial deficiency of creatine kinase." Intern Med **31**(5): 611-6.
Shin, J. B., F. Streijger, et al. (2007). "Hair bundles are specialized for ATP delivery via creatine kinase." Neuron **53**(3): 371-86.
Sistermans, E. A., Y. J. de Kok, et al. (1995). "Tissue- and cell-specific distribution of creatine kinase B: a new and highly specific monoclonal antibody for use in immunohistochemistry." Cell Tissue Res **280**(2): 435-46.
Small, J. V., T. Stradal, et al. (2002). "The lamellipodium: where motility begins." Trends Cell Biol **12**(3): 112-20.
Sobota, A., A. Strzelecka-Kiliszek, et al. (2005). "Binding of IgG-opsonized particles to Fc gamma R is an active stage of phagocytosis that involves receptor clustering and phosphorylation." J Immunol **175**(7): 4450-7.
Stachowiak, O., U. Schlattner, et al. (1998). "Oligomeric state and membrane binding behaviour of creatine kinase isoenzymes: implications for cellular function and mitochondrial structure." Mol Cell Biochem **184**(1-2): 141-51.
Steeghs, K., A. Benders, et al. (1997). "Altered Ca2+ responses in muscles with combined mitochondrial and cytosolic creatine kinase deficiencies." Cell **89**(1): 93-103.
Steeghs, K., A. Heerschap, et al. (1997). "Use of gene targeting for compromising energy homeostasis in neuro-muscular tissues: the role of sarcomeric mitochondrial creatine kinase." J Neurosci Methods **71**(1): 29-41.
Steeghs, K., F. Oerlemans, et al. (1995). "Mice deficient in ubiquitous mitochondrial creatine kinase are viable and fertile." Biochim Biophys Acta **1230**(3): 130-8.
Steeghs, K., W. Peters, et al. (1995). "Mouse ubiquitous mitochondrial creatine kinase: gene organization and consequences from inactivation in mouse embryonic stem cells." DNA Cell Biol **14**(6): 539-53.
Stockler, S., F. Hanefeld, et al. (1996). "Creatine replacement therapy in guanidinoacetate methyltransferase deficiency, a novel inborn error of metabolism." Lancet **348**(9030): 789-90.
Streijger, F. (2007). "The biological role of the brain specific creatine kinase energy system in mice - a behavioral approach." 169-205.
Streijger, F., H. J. In 't Zandt, et al. (2007). Developmental and functional consequences of disturbed energetic communication in brain of creatine kinase-deficient mice: Understanding CK's role in the fuelling of behavior and learning. Molecular system bioenergetics. V. A. Saks. Weinheim, Wiley-VCH Verlag GmbH & Co. KGaA**:** 339-366.
Streijger, F., F. Oerlemans, et al. (2005). "Structural and behavioural consequences of double deficiency for creatine kinases BCK and UbCKmit." Behav Brain Res **157**(2): 219-34.
Stromberger, C., O. A. Bodamer, et al. (2003). "Clinical characteristics and diagnostic clues in inborn errors of creatine metabolism." J Inherit Metab Dis **26**(2-3): 299-308.
Stryer, L. (1988). Biochemistry. New York, W. H. Freeman and Company**:** 350-356, 374-424.
Suurna, M. V., S. L. Ashworth, et al. (2006). "Cofilin mediates ATP depletion-induced endothelial cell actin alterations." Am J Physiol Renal Physiol **290**(6): F1398-407.
Suzuki, T., H. Kono, et al. (2000). "Differential involvement of Src family kinases in Fc gamma receptor-mediated phagocytosis." J Immunol **165**(1): 473-82.
Swanson, J. A. (2008). "Shaping cups into phagosomes and macropinosomes." Nat Rev Mol Cell Biol **9**(8): 639-49.
Takenawa, T. and H. Miki (2001). "WASP and WAVE family proteins: key molecules for rapid rearrangement of cortical actin filaments and cell movement." J Cell Sci **114**(Pt 10): 1801-9.
Tombes, R. M. and B. M. Shapiro (1985). "Metabolite channeling: a phosphorylcreatine shuttle to mediate high energy phosphate transport between sperm mitochondrion and tail." Cell **41**(1): 325-34.
Trybus, K. M. (1994). "Role of myosin light chains." J Muscle Res Cell Motil **15**(6): 587-94.
Tuxworth, R. I., I. Weber, et al. (2001). "A role for myosin VII in dynamic cell adhesion." Curr Biol **11**(5): 318-29.
Vale, R. D. (2003). "The molecular motor toolbox for intracellular transport." Cell **112**(4): 467-80.
van Deursen, J., A. Heerschap, et al. (1993). "Skeletal muscles of mice deficient in muscle creatine kinase lack burst activity." Cell **74**(4): 621-31.
van Dorsten, F. A., T. Reese, et al. (1997). "Fluxes through cytosolic and mitochondrial creatine kinase, measured by P-31 NMR." Mol Cell Biochem **174**(1-2): 33-42.

Vendelin, M., M. Lemba, et al. (2004). "Analysis of functional coupling: mitochondrial creatine kinase and adenine nucleotide translocase." Biophys J **87**(1): 696-713.
Vicente-Manzanares, M., J. Zareno, et al. (2007). "Regulation of protrusion, adhesion dynamics, and polarity by myosins IIA and IIB in migrating cells." J Cell Biol **176**(5): 573-80.
Vieira, O. V., R. J. Botelho, et al. (2002). "Phagosome maturation: aging gracefully." Biochem J **366**(Pt 3): 689-704.
Waingeh, V. F., C. D. Gustafson, et al. (2006). "Glycolytic enzyme interactions with yeast and skeletal muscle F-actin." Biophys J **90**(4): 1371-84.
Wallimann, T., T. Schlosser, et al. (1984). "Function of M-line-bound creatine kinase as intramyofibrillar ATP regenerator at the receiving end of the phosphorylcreatine shuttle in muscle." J Biol Chem **259**(8): 5238-46.
Wallimann, T., M. Wyss, et al. (1992). "Intracellular compartmentation, structure and function of creatine kinase isoenzymes in tissues with high and fluctuating energy demands: the 'phosphocreatine circuit' for cellular energy homeostasis." Biochem J **281 (Pt 1)**: 21-40.
Webb, D. J., J. T. Parsons, et al. (2002). "Adhesion assembly, disassembly and turnover in migrating cells -- over and over and over again." Nat Cell Biol **4**(4): E97-100.
Wolven, A. K., L. D. Belmont, et al. (2000). "In vivo importance of actin nucleotide exchange catalyzed by profilin." J Cell Biol **150**(4): 895-904.
Wood, I. S. and P. Trayhurn (2003). "Glucose transporters (GLUT and SGLT): expanded families of sugar transport proteins." Br J Nutr **89**(1): 3-9.
Worthylake, R. A., S. Lemoine, et al. (2001). "RhoA is required for monocyte tail retraction during transendothelial migration." J Cell Biol **154**(1): 147-60.
Wright, S. D., J. I. Weitz, et al. (1988). "Complement receptor type three (CD11b/CD18) of human polymorphonuclear leukocytes recognizes fibrinogen." Proc Natl Acad Sci U S A **85**(20): 7734-8.
Wyss, M. and R. Kaddurah-Daouk (2000). "Creatine and creatinine metabolism." Physiol Rev **80**(3): 1107-213.
Yamamichi, H., S. Kasakura, et al. (2001). "Creatine kinase gene mutation in a patient with muscle creatine kinase deficiency." Clin Chem **47**(11): 1967-73.
Yamoah, E. N., E. A. Lumpkin, et al. (1998). "Plasma membrane Ca2+-ATPase extrudes Ca2+ from hair cell stereocilia." J Neurosci **18**(2): 610-24.
Yarmola, E. G. and M. R. Bubb (2004). "Effects of profilin and thymosin beta4 on the critical concentration of actin demonstrated in vitro and in cell extracts with a novel direct assay." J Biol Chem **279**(32): 33519-27.
Zhang, H., J. S. Berg, et al. (2004). "Myosin-X provides a motor-based link between integrins and the cytoskeleton." Nat Cell Biol **6**(6): 523-31.
Zheng, L., R. G. Roeder, et al. (2003). "S phase activation of the histone H2B promoter by OCA-S, a coactivator complex that contains GAPDH as a key component." Cell **114**(2): 255-66.

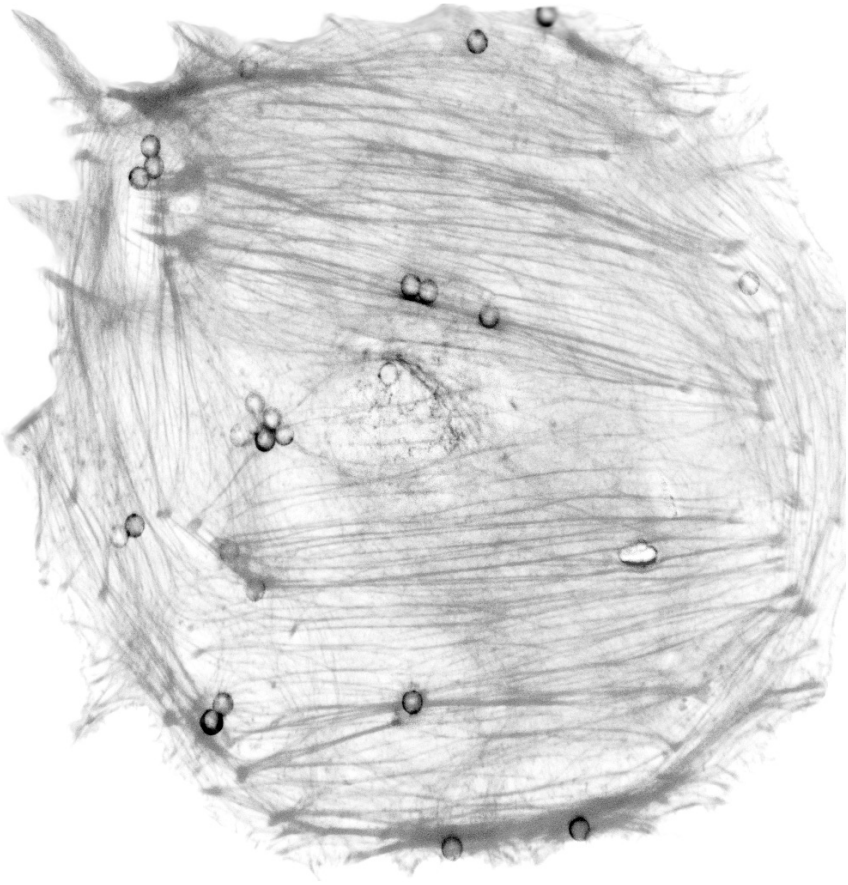

Chapter - 2 -

Creatine Kinase–mediated ATP supply fuels actin-based events in phagocytosis

Jan W. P. Kuiper, Helma Pluk, Frank Oerlemans, Frank N. van Leeuwen, Frank de Lange, Jack Fransen and Bé Wieringa

PLoS Biology, 2008, Vol. 6, No. 3, e51

Abstract

Phagocytosis requires locally-coordinated cytoskeletal rearrangements driven by actin polymerization and myosin motor activity. How this actomyosin dynamics is dependent upon systems that provide access to ATP at phagosome microdomains has not been determined. Here we analyzed the role of brain-type creatine kinase (CK-B), an enzyme involved in high-energy phosphoryl transfer. We demonstrate that endogenous CK-B in macrophages is mobilized from the cytosolic pool and co-accumulates with F-actin at nascent phagosomes. Live cell imaging with XFP-tagged CK-B and β-actin revealed the transient and specific nature of this partitioning process. Overexpression of a catalytic dead CK-B or CK-specific cyclocreatine inhibition caused a significant reduction of actin accumulation in the phagocytic cup area, and reduced complement-receptor mediated but not Fc-γR mediated ingestion capacity of macrophages. Finally, we found that inhibition of CK-B affected phagocytosis already at the stage of particle adhesion, most likely via effects on actin polymerization behavior. We propose that CK-B activity in macrophages contributes to complement-induced F-actin assembly events in early phagocytosis by providing local ATP supply.

Introduction

Dynamic reorganization and stabilization of the actin cytoskeleton and membrane-shape alterations of cells are intimately and reciprocally coupled events that are essential for a variety of distinct cell functions such as adhesion, motility, cytokinesis and endocytosis (Pollard and Borisy 2003). One of the processes that is critically dependent on proper regulation of actin polymerization is phagocytosis, essential for food intake in lower eukaryotes or the elimination of invading microbial pathogens and scavenging of dead cells in higher multicellular eukaryotes (Aderem and Underhill 1999). Engulfment of a phagocytic target is a spatially confined process, which is initiated at the cell membrane by recognition of the molecular structure at the surface of the phagocytic targets by dedicated receptors, such as Fc-gamma receptors (Fc-γRs), lectins or the complement receptor (CR3, Mac-1) (Gessner, Heiken et al. 1998; Ehlers 2000; Linehan, Martinez-Pomares et al. 2000). After binding of the target receptors cluster, become activated, and trigger actin-dependent cytoskeletal changes via the activation of small Rho GTPases and concomitant induction of specific protein kinase signaling cascades (Aderem and Underhill 1999; Stuart and Ezekowitz 2005). In Fc-γR mediated phagocytosis signals are mediated through Rac and Cdc42, whereas CR3-regulated phagocytosis of complement-opsonized targets requires only RhoA activation (Caron and Hall 1998). These pathways ultimately converge and lead to the induction of Arp2/3 mediated actin polymerization, which is considered the main driving force for the formation of circular pseudopod protrusions (i.e. a "phagocytic cup") around the target (May, Caron et al. 2000). Once the wrapping in cellular membrane protrusions is complete, a contractile force is generated to engulf the particle or dead cell completely and guide the contents of the vesicle into the endocytotic pathway for degradation (Vieira, Botelho et al. 2002).

All events during early phagocytosis, including ruffle formation, membrane delivery, closure of the phagocytic cup and short-range movement of newly formed vesicles through the cellular cortex, depend on actin polymerization and myosin motor proteins. In turn, for proper regulation of polymerization of G-actin into F-actin, which involves filament nucleation and extension, a spatially confined supply of

ATP for the loading of actin subunits is required (Wolven, Belmont et al. 2000; Dayel, Holleran et al. 2001; Jahraus, Egeberg et al. 2001). Theoretical models predict that ATP primarily promotes an "adjusted fit" of incoming monomers to the end of the actin filaments and multiple studies agree that the ATP/ADP loading state of actin and related Arp2/3 proteins determine filament assembly or branching behavior (Pollard and Borisy 2003; Becker 2006; Kovar 2006). Moreover, during filament severing or turnover, energy is used when ATP is hydrolyzed when still bound to F-actin, and P_i is released. Next, ADP-actin dissociates and free G-actin monomers can be subsequently reloaded with 'new' ATP. ATP- or ADP-loaded actin monomers are both competent for polymerization, but the nature of the bound nucleotide differentially modulates the kinetics of the association and dissociation at the pointed or barbed ends of filaments. Also the "storage" of G-actin monomers into thymosin or profilin-sequestered pools is dependent on nucleotide loading state and hence, the energy state of the cell (Goldschmidt-Clermont, Furman et al. 1992; Wolven, Belmont et al. 2000). Active recruitment of G-actin and F-actin dynamics thus consumes ATP in several steps and the active cell-shape remodeling needed for particle ingestion renders phagocytosis a process with a very high local requirement for high-energy phosphoryl (~P) groups.

In fact the energy dependence of phagocytosis is made even more prominent, because ATP is also necessary to sustain the activity of several non-muscle myosin ATPases, which help in actin and membrane recruitment, and provide motor activity around the phagocytic cup (Allen and Aderem 1995; Swanson, Johnson et al. 1999). For example, myosin-II activity is implicated in phagocytic cup formation and squeezing (Olazabal, Caron et al. 2002; Araki, Hatae et al. 2003), whereas myosins-X and VII may have roles in pseudopod extension and phagosome internalization (Swanson, Johnson et al. 1999; Tuxworth, Weber et al. 2001; Cox, Berg et al. 2002; Olazabal, Caron et al. 2002). By forming an ATP drain for these many actomyosin-based micromechanical events, phagocytosis may thus pose a formidable challenge to cellular energy homeostasis. Indeed, metabolic studies report increased energy turnover during phagocytosis (Guminska, Ptak et al. 1975; Loike, Kozler et al. 1979).

Creatine Kinase (CK) mediated phosphotransfer plays an important role in local delivery and cellular compartmentation of ATP and transport from glycolytic or

mitochondrial production sites (Wyss and Kaddurah-Daouk 2000; Dzeja and Terzic 2003). The CK reaction buffers ATP and ADP levels by the reversible transfer of high-energy phosphoryl onto creatine (Cr) ($MgATP^{2-} + Cr \leftrightarrow MgADP^{-} + PCr^{2-} + H^{+}$) (Wallimann, Wyss et al. 1992). In muscle, localized delivery of ATP by the muscle-type creatine kinase (CK-M) isoform is clearly of importance for sustenance of acto-myosin ATPase activity involved in myofibrillar sliding activity during repeated high-speed contraction (van Deursen, Heerschap et al. 1993). In brain, we (Jost, Van Der Zee et al. 2002) have obtained evidence that lack of brain-type CK (CK-B) activity affects synaptic coupling efficiency, a process for which active actin remodeling is essential (Bernstein and Bamburg 2003). By analogy we hypothesized that the functional coupling between actin-based cytoskeletal dynamics and CK-mediated ATP compartmentalization and supply could be more general, and might be of importance for shape changes and dynamics of non-muscle or non-neuronal cells as well. Here we confirm this view and report on the role of the CK-PCr system in the dynamics of phagocytosis. Interestingly, Loike *et al.* have found that brain type CK-B is expressed in macrophages and that phosphocreatine (PCr) levels decrease during phagocytosis (Loike, Kozler et al. 1979). Our data suggest that the metabolic ATP-supply activity of CK-B is of local importance and facilitates specific phagocytosis steps via effects on actin-based events early in the binding-ingestion process.

Results

Endogenous CK-B translocates to phagocytic cups in microglia and macrophages

Phagocytic cup formation is characterized by a localized expansion of the plasmalemmal membrane, coupled to highly active remodeling and myosin-based contraction of the actin cytoskeleton. We studied the possible fate and role of endogenous CK-B in this process, in primary microglia and peritoneal macrophages after induction of phagocytosis with non-opsonized zymosan. Macrophages and microglia (Kreutzberg 1996; Aderem and Underhill 1999) are cells of the immune system that are very active in ruffle extension and uptake of extracellular particles. Although it has been reported that primary macrophages express CK-B (Loike,

Kozler et al. 1984), no data are available on the enzyme's behavior under conditions of active phagocytosis. **Figures 1A, E** show that a fraction of CK-B always remained diffusely distributed throughout the cytosol, as in non-phagocytosing cells, but that a substantial portion of CK-B accumulated around the engulfed zymosan particles at nascent phagosomes. This accumulation did not occur exactly simultaneously in all cells as phagocytosis was not initiated fully synchronously throughout the culture, but at later time points the concentrated staining dissipated (not shown), indicating that CK-B associated only transiently with phagosome structures.

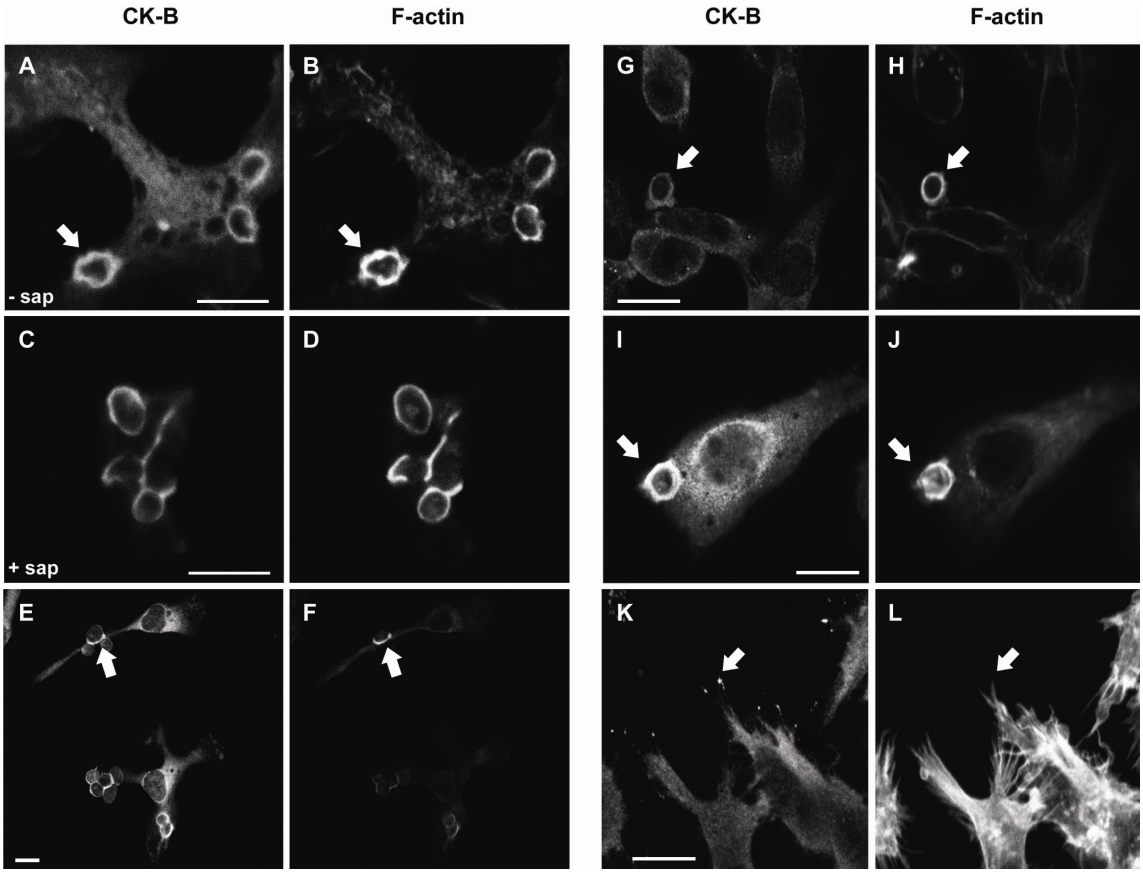

Figure 1. *Cytosolic CK-B accumulates in the phagocytic cup area of macrophages.* (A-J) Uptake of zymosan in primary microglia (A-D), primary peritoneal macrophages (E-F), and RAW 264.7 macrophages (G-J). Fixation followed by (immuno)staining with CK-B antibodies (A, C, E, G, I, K) or phalloidin (B, D, F, H, J, L) reveals the co-accumulation of CK-B and F-actin at the phagocytic cup (arrows). (C-D) Saponin extraction of phagocytosing microglia prior to fixation and CK-B or actin staining (I-L) RAW 264.7 macrophages overexpressing mouse CK-B. Note that CK-B shows additional pronounced spot-like accumulation at the distal tips of filopodia (arrows, K-L). Bar, 10 µm.

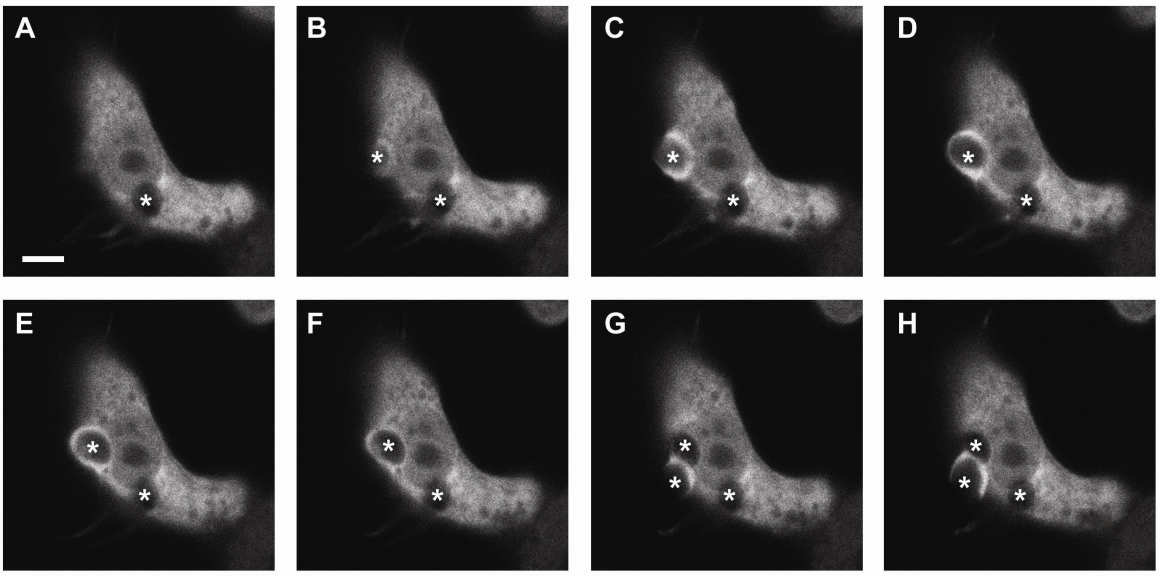

Figure 2. *Transient recruitment of EYFP-tagged CK-B.* (A-H) Time-lapse microscopy of zymosan uptake in RAW 264.7 cells transiently transfected with EYFP-tagged CK-B. Eight subsequent images captured at 6 sec intervals over a 48 sec recording period are shown. Asterisks indicate zymosan particles binding at the cellular membrane, during the process of engulfment and after internalization. Bar, 5 µm.

Phalloidin staining demonstrated an almost complete overlap with CK-B encircling the zymosan particles in the phagosome (**Figures 1B, F**). To assess if CK-B is actually locally bound within the cup area, microglia were permeabilized with saponin before fixation to remove most of the unbound cytosolic protein. Strikingly, a fraction of endogenous CK-B remained associated with the actin-rich area (**Figures 1C, D**). These data indicate that part of the CK-B molecules in the endogenous pool partition into sites of active F-actin remodeling.

To further verify the general validity of this picture we analyzed the behavior of endogenous or exogenously transfected CK-B in the murine macrophage cell line, RAW 264.7. As anticipated, also in this cell we observed a uniform cytosolic distribution of endogenous CK-B and co-accumulation with F-actin at nascent phagosomes (**Figures 1G, H**). To compensate for the rather weak endogenous CK-B staining in RAW 264.7 cells, we also produced pools of cells with a higher CK-B steady-state level by transduction with retroviral vectors to enhance immunofluorescent detection. Again, prominent accumulation of CK-B together with

F-actin appeared in the phagosome (**Figures 1H, J**). Notably, in RAW 264.7 cells with an overall high global CK-B level, we noticed CK-B accumulation at the distal tips of filopodia (**Figures 1K, L**). This phenomenon has been observed for a number of other proteins involved in cytoskeletal rearrangement, dynamic adhesion, and phagocytosis, including myosin-X, myosin-VII and vasodilator-stimulated phosphoprotein (VASP) (Castellano, Le Clainche et al. 2001; Tuxworth, Weber et al. 2001; Cox, Berg et al. 2002).

CK-B is transiently recruited to the phagocytic cup

As CK-B's role might involve the delicate interplay between compartmentalized energy supply and local molecular dynamics in the cell cortex area, we monitored the profile and timing of CK-B recruitment at the phagosome in more detail. To obtain dynamic information we transiently expressed EYFP-tagged CK-B (via N-terminal fusion) in RAW 264.7 cells, and applied live cell microscopy imaging after induction of phagocytosis. Earlier work showed that N-terminal tagging of CK-B does not affect its enzymatic or structural properties (Koretsky and Traxler 1989); (data not shown). In the first (**Figure 2A**) of 8 sequential frames of a movie (video **S1** is available at http://biology.plosjournals.org/archive/1545-7885/6/3/supinfo/10.1371_journal.pbio. 0060051.sv001.mov) of typical CK-B behavior in an active macrophage, one particle is already being internalized (indicated by an asterisk), but at that point in time EYFP-CK-B appears non-partitioned, and is still diffusely distributed throughout the cytoplasm. In subsequent frames (**Figures 2B-F**) a clear CK-B accumulation in the phagocytic cup is observed, dissipation of which occurs when the particle is fully internalized (**Figure 2G**). A second phagocytic event with recruitment is initiated in the same cell at a later time point (**Figures 2G-H**). In control cells expressing non-fused EYFP never any significant accumulation at the site of zymosan ingestion was seen. A relatively straightforward interpretation of these observations would be that the spatially confined recruitment of CK-B serves phagocytic cup formation and/or closure, presumably via local delivery of ATP.

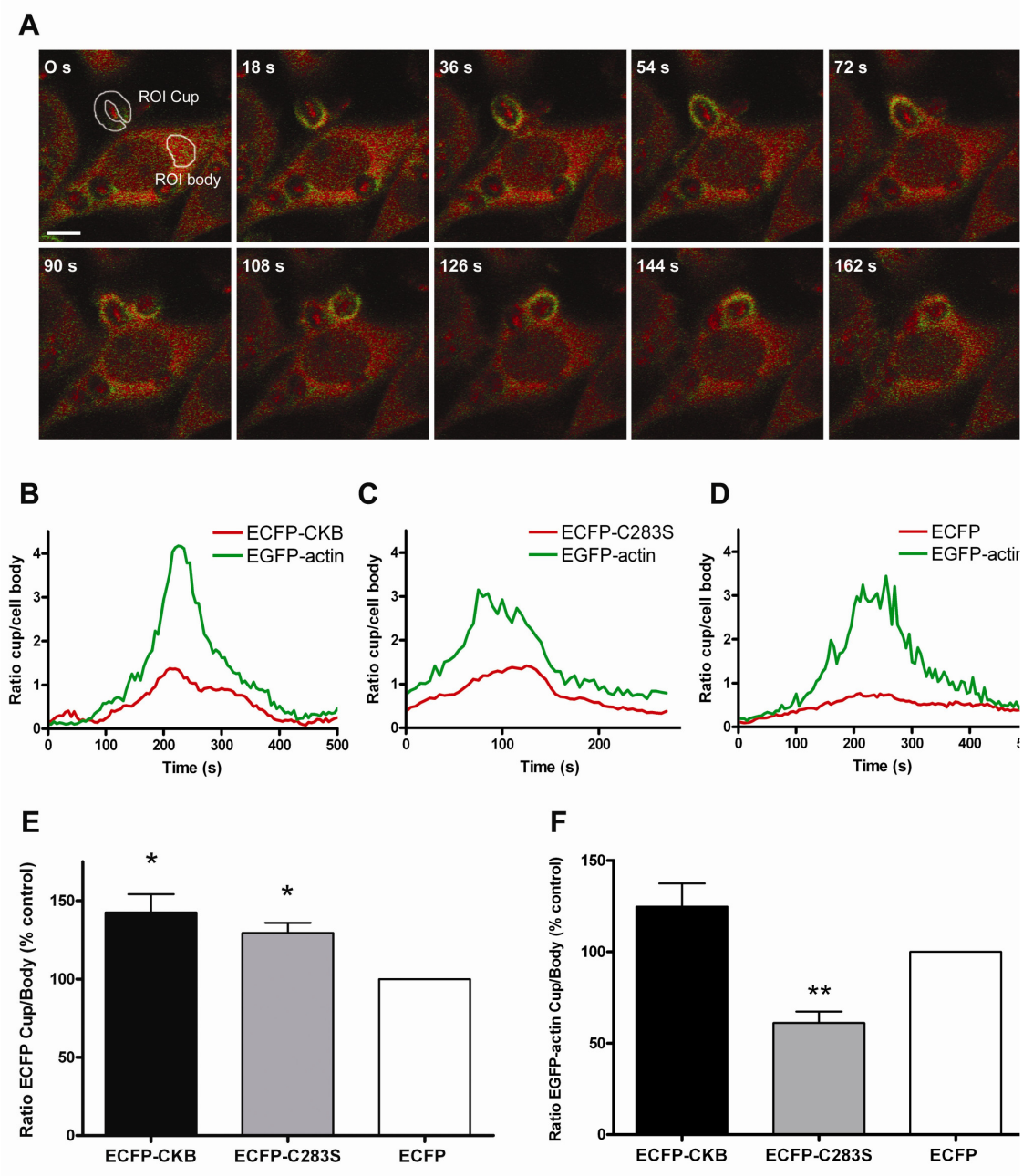

Figure 3. *CK-B_{C283S} decreases actin accumulation in phagocytic cups.* (A) Time-lapse images of a cell co-expressing EGFP-actin and ECFP-CK-B in the process of internalizing a zymosan particle, demonstrating the simultaneous accumulating signals from ECFP-CK-B (red) and EGFP-actin (green). Representative regions of interest (ROIs) are being shown for the phagocytic cup (ROI cup) and the cytosol (ROI body). Bar, 5 µm. (B-D) Signal intensities in the phagocytic cup and cell body were analyzed in cells co-expressing EGFP-actin and ECFP-CK-B, ECFP-CK-B_{C283S} or ECFP. The average pixel intensities in the ROIs were determined and the cup/body ratios for EGFP-actin (green) and ECFP-CK-B, ECFP-CK-B_{C283S} or ECFP (red) plotted against time. (E) Average maximal cup/body ratios for 10-16 events in cells expressing ECFP-CK-B, ECFP-CK-B_{C283S} and ECFP. (F) Average maximal EGFP-actin cup/body ratios in the same cells as in (E). Bars depict mean value with error bars representing the SEM. Number of events analyzed: n = 16 for ECFP-CK-B; n = 10 for ECFP-CK-B_{C283S} and n = 13 for ECFP. **, $p<0.005$, *, $p<0.01$.

Inhibition of CK-B diminishes actin accumulation in the phagocytic cup

A hallmark of phagosome formation is the rapid polymerization of F-actin, which drives the membrane extension around the target. Also actomyosin-motor sliding is intimately coupled to this process (Swanson, Johnson et al. 1999; Tuxworth, Weber et al. 2001; Cox, Berg et al. 2002; Olazabal, Caron et al. 2002). To study if these processes are indeed among the ones served by local CK-B activity we compared zymosan-driven phagocytosis in RAW 264.7 cells that were stably co-expressing EGFP-tagged β-actin and either ECFP alone, ECFP-tagged CK-B or a mutant CK-$B_{(C283S)}$. This latter CK-variant acts as a dominant-negative enzyme, occurring as a normal dimer with only 4% residual kinase activity (Hornemann, Rutishauser et al. 2000). Parallel spectral monitoring of fluorescence intensities enabled us to follow simultaneously the dynamic behavior of actin and CK-B variants, or the ECFP control, after induction of zymosan-driven phagocytosis (**Figure 3A**). Plotting of local signal intensities in relation to the global intensities in the cell body, which remained constant and were comparable for all cells examined (data not shown), showed that recruitment of ECFP-tagged CK-B and CK-$B_{(C283S)}$ occurred in nearly identical spatio-temporal overlap with EGFP-actin recruitment in all cases examined (**Figures 3B-C**; 10-16 individual events analyzed).

As anticipated, the average maximal cup/body signal ratio for ECFP-CK-B and ECFP- CK-$B_{(C283S)}$ (142% ± 47% and 129% ± 21% , respectively) was significantly higher ($p<0.005$) than that for ECFP alone (100%; **Figure 3E**). Thus, mobilization of CK-B protein to the phagosome area does not appear to be dependent on CK enzymatic activity. All cells examined displayed a clear accumulation of actin in the cup during a typical phagocytic event as defined by an increasing cup-to-body ratio of the EGFP signal ($EGFP_{Cup}/EGFP_{Body} > 1$) (**Figures 3B-D**). Strikingly, this accumulation differed significantly between cells expressing ECFP-CK-B or ECFP-CK-B_{C283S} (**Figure 3F**) and was for the ECFP- CK-$B_{(C283S)}$ cell line markedly decreased (61% ± 18%) compared to ECFP cells ($p<0.005$). Cells in an independently generated pool harboring the ECFP-tagged CK-$B_{(C283S)}$ exhibited a similar decrement, demonstrating that the observed decrease was not cell line or pool specific (data not shown). In ECFP-CK-B cells the green actin signal reached a

slightly higher maximal cup/body ratio of 117 % ± 51% than in ECFP-control cells (100%). This difference was not significant, however, and we therefore consider it result of experimental variation.

To establish whether effects of absence/presence of active CK-B affected the temporal profile of actin recruitment, we also compared the timing of actin mobilization between different movies of different cell transfectants. No significant

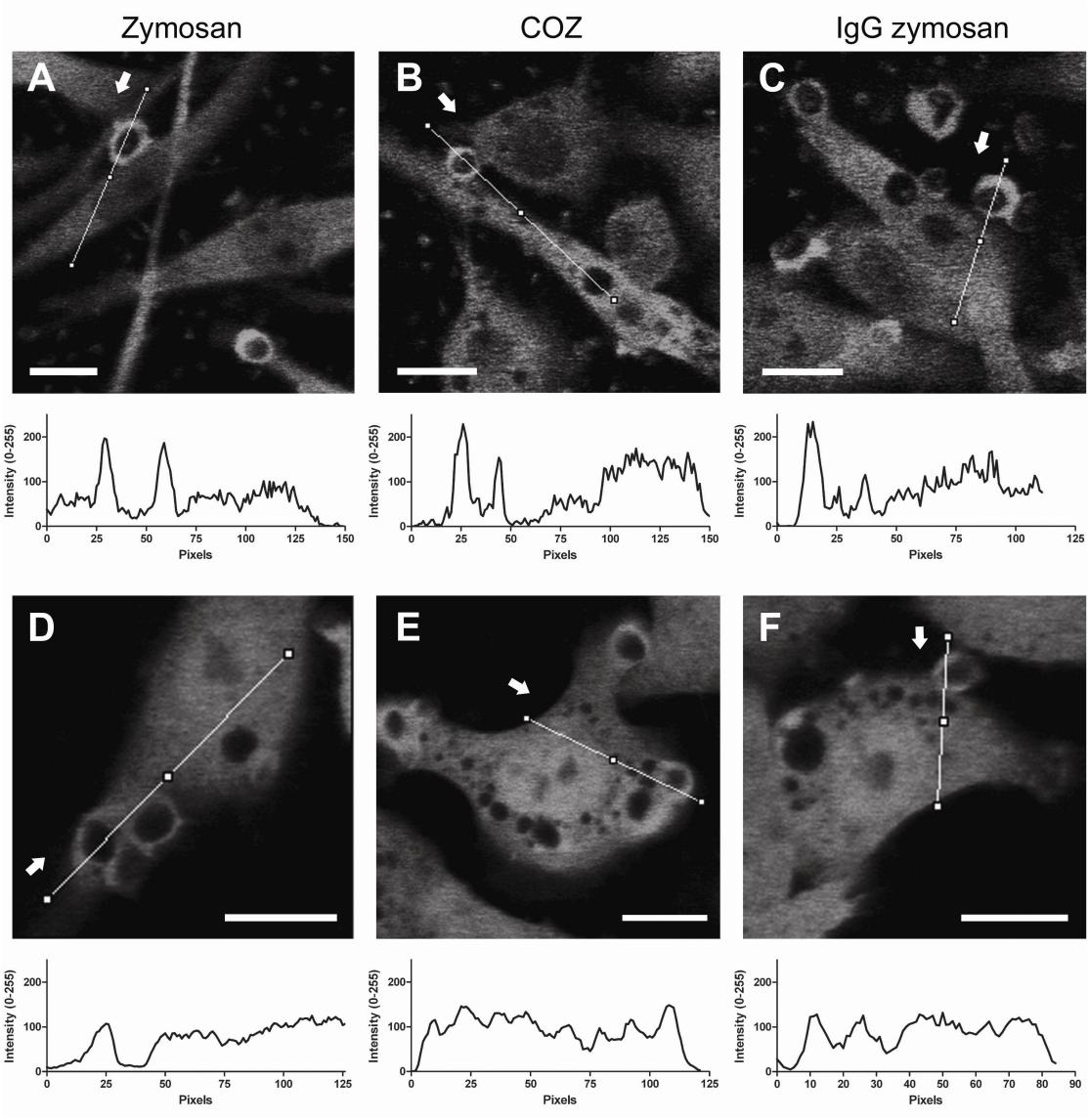

Figure 4. *Dynamic redistribution of EYFP tagged CK-B during phagocytosis.* (A-F) Time-lapse microscopy of zymosan (A, D), COZ (B, E) or IgG-opsonized zymosan (C, F) uptake in RAW 264.7 cells stably transfected with EYFP-CK-B (A-C) or EYFP (D-F). Photos represent a single frame at the peak of accumulation from a time-lapse recording; arrows mark the start of the corresponding line plot visualizing accumulation of signal in the cup. Bar, 10 µm.

differences were found. These results demonstrate that local presence of metabolically active CK-B alters the magnitude but not the timing of actin mobilization at the phagosome.

CK-B accumulates independent of type of opsonization

The molecular structure at the surface of the phagocytic target determines which receptor types become ligand-bound and activated. Subsequently, receptor-specific downstream signaling events, such as alternative use of small Rho GTPases and kinases, orchestrate the outcome of the phagocytic process (Allen and Aderem 1996; Caron and Hall 1998; Olazabal, Caron et al. 2002). To test whether CK-B recruitment is a default response or determined by the surface properties of the target, we repeated our time-lapse experiments with cells that were challenged with native zymosan (**Figure 4A**), or zymosan opsonized with either complement (**Figure 4B**; COZ) or IgG (**Figure 4C**). To avoid that effects of other properties of the target such as rigidity and geometry would influence the outcome of our study (Beningo and Wang 2002; Champion and Mitragotri 2006), we deliberately chose to change only the type of coat, not the particle type (i.e. zymosan) in these experiments. Line-plots of pixel intensities across the phagocytic cup and other areas of the cell body revealed that EYFP-CK-B recruitment occurred independently of the type of opsonization. Montages of control cells with untagged EYFP did not reveal any specific mobilization into or around phagocytic cups (**Figures 4D-F**). These data are consistent with the idea that spatially confined presence of CK-B in the cup area is interlinked with general steps in phagocytic cup formation and/or closure.

Cyclocreatine inhibits phagocytosis of zymosan and COZ

Based on this premise we wondered if the CK-driven ATP–PCr exchange reaction could be directly or indirectly coupled to the process of particle ingestion. Initially, we chose a pharmacological approach to modulate activity of the entire cellular pool of CK, applying Cr as a stimulating substrate or cyclocreatine (cCr) as a reversible inhibitor of the CK reaction. RAW 264.7 cells were preincubated with 5 mM cCr or Cr prior to the phagocytosis assay and then cells were challenged with differentially

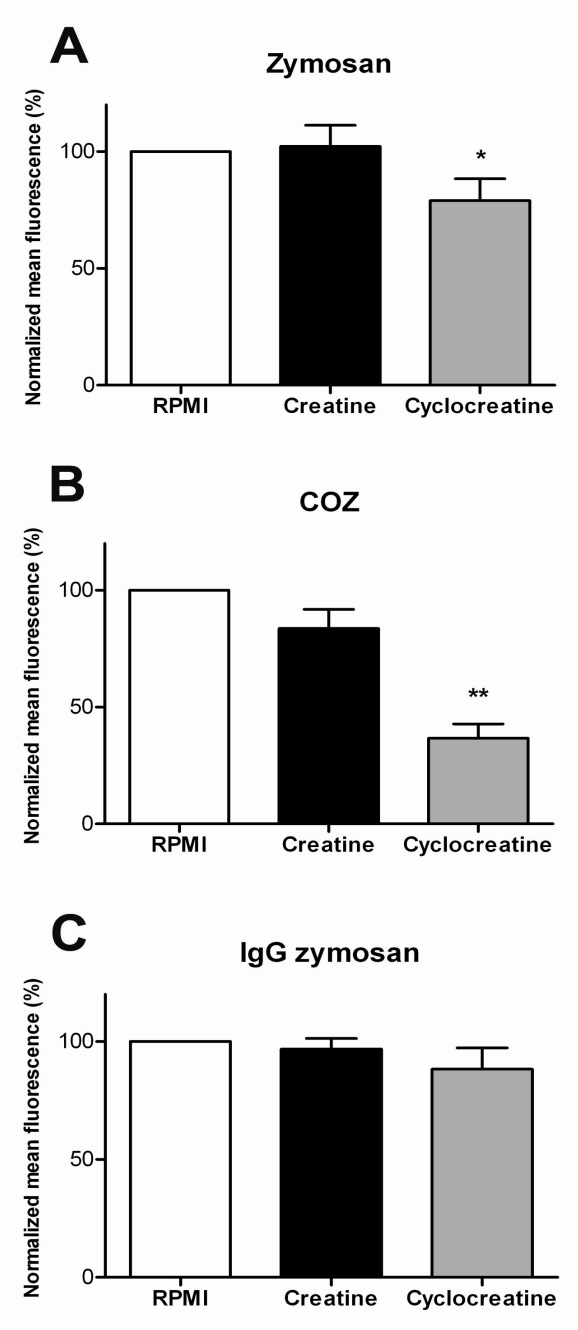

Figure 5. *Cyclocreatine inhibits phagocytosis.* (A-D) Fluorescent particle uptake capacity quantified by FACS in RAW 264.7 cells pre-incubated with 5 mM creatine, 5 mM cyclocreatine or normal growth medium. (A) Zymosan, (B) COZ, (C) IgG-opsonized zymosan. Bars represent averages of 3-4 experiments performed in duplicate (+/- SD). *, $p<0.03$; **, $p< 0.005$.

opsonized and fluorescently labeled phagocytic targets. After 30 minutes, phagocytic activity was quantified by determining the mean fluorescence intensity of ingested particles in the different cells by FACS analysis. In **Figure 5** data are shown that are normalized to values for non-treated cells. Phagocytosis of non-opsonized zymosan was slightly affected by cCr treatment, yielding an efficiency value of 79% ± 9% ($p < 0.05$), whereas Cr supply had no significant effect (102% ± 9%) (**Figure 5A**). Interestingly, cCr inhibition decreased phagocytosis of COZ to a much lower level, 37% ± 6% ($p < 0.005$) of that of non-treated cells, whereas Cr addition had no significant effect (value 84% ± 8%) (**Figure 5B**). In contrast, Cr and cCr addition had no significant effect on phagocytosis of IgG opsonized zymosan, with 97% ± 5% and 88% ± 9% for Cr and cCr treated cells, respectively (**Figure 5C**). In order to verify that this difference was indeed due to differential effects on CR3 and Fc-γR receptor-mediated activities and cannot be attributed to interference with other pathways, we performed receptor-blocking expe-

riments. Capture-uptake of the two different types of opsonized zymosan appeared indeed specific for the anticipated receptors (**Figure S2).** To study this point further, we also tested phagocytic activity on complement- and IgG-opsonized polystyrene beads, which lack obvious surface ligands such as mannose or β-glucan groups, and therefore form "clean" targets. Interestingly, uptake of complement opsonized beads was again inhibited by cyclocreatine (56 ± 4% of control), whereas IgG-mediated phagocytosis remained unaffected (95 ± 2% of control; **Figure S3**).

Thus, although CK mobilization is seemingly a default event in all types of phagocytosis (**Figure 4**), it may only selectively contribute to the efficiency of phagocytic ingestion of non-opsonized or complement-opsonized particles (**Figures 5** and **S3**). A similar situation was recently reported for the cytoskeletal actin-binding protein talin, whose functional role in phagocytic uptake appeared selectively coupled to complement receptor 3 (CR3), but which accumulates in phagosomes formed around IgG- and C3-opsonized particles (Shin, Streijger et al. 2007).

RAW 264.7 macrophages expressing CK-B$_{(C283S)}$ exhibit impaired phagocytosis

To address CK-B's specific role in phagocytic activity in another manner we also compared effects of expression of the CK-B$_{(C283S)}$ mutant and that of CK-B. To obtain comparable levels of expression of these proteins across all individual cells in and between cell populations, transduction with retroviral vectors encoding CK-B, the CK-B$_{(C283S)}$ mutant, or EYFP was used (resulting cell pools are hereafter referred to as RAW-CK-B, RAW-CK-B$_{(C283S)}$ and RAW-EYFP cells, respectively). Two independent cell pools were established for each construct, to rule out potential integration-site dependent effects and/or effects of overgrowth of specific cell clones. Western blotting was performed to assess expression levels in our stable cell lines (**Figure 6A**). The levels of the exogenously expressed wt or mutant CK-B protein in the RAW-CK-B or RAW-CK-B$_{(C283S)}$ cell pools amounted to roughly ten times more than the endogenous CK-B level in these cells. The total enzymatic phosphoryl transfer activity had increased accordingly, and approximated a 10-fold higher steady-state level in both RAW-CK-B cell populations relative to the reference RAW 264.7 cell pool (**Figure 6B**). As anticipated, the total CK-activity of the control

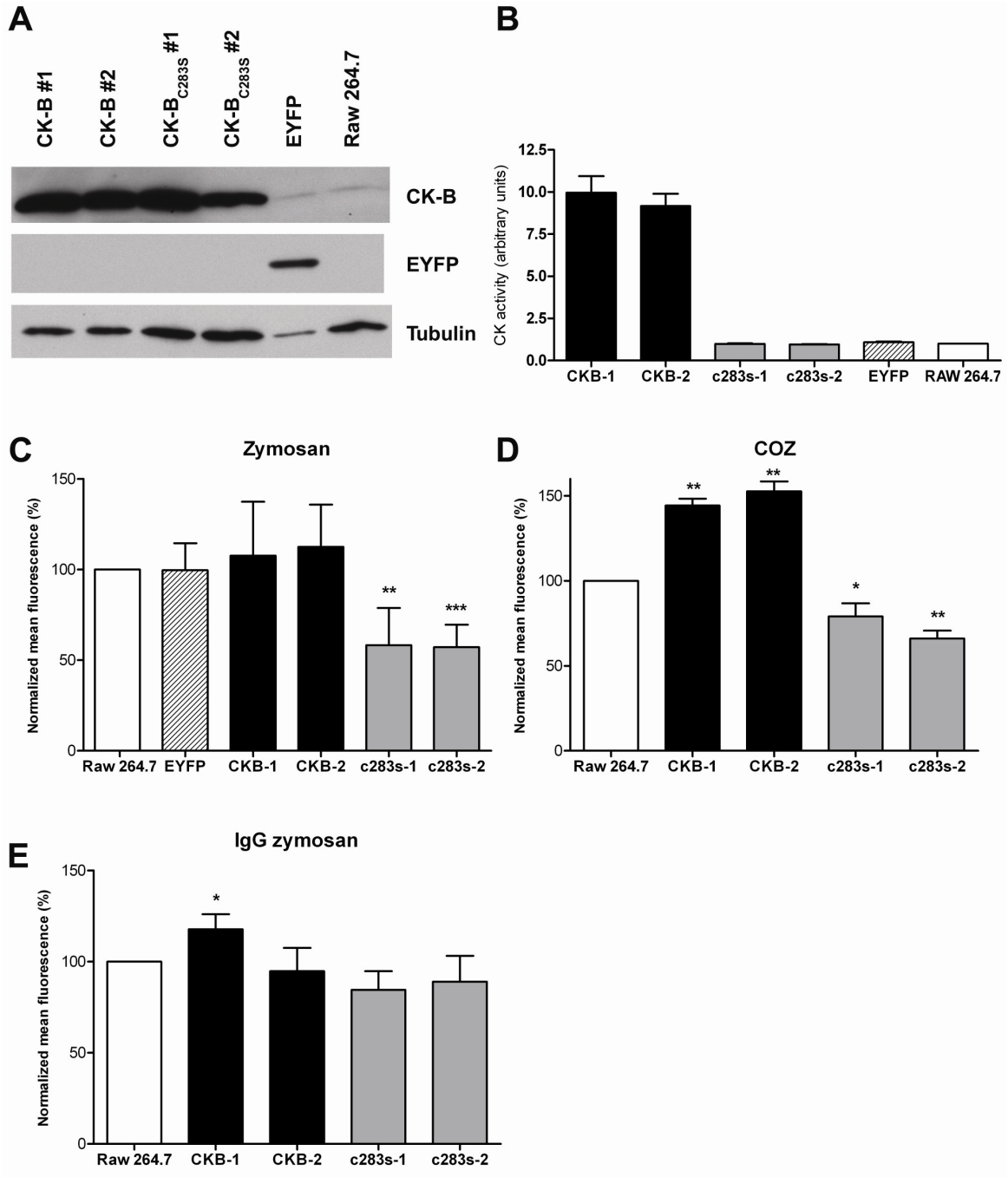

Figure 6. *CK-B and CK-B_{C283S} influence phagocytosis.* (A) Western blot analysis of RAW 264.7 cells stably expressing CK-B or CK-B_{C283S}. Two individual retrovirally transduced populations were maintained (CK-B #1 and CK-B #2, CK-B_{C283S} #1 and CK-B_{C283S} #2). RAW 264.7 cells expressing EYFP and non-infected cells were used as control. (B) Creatine kinase (CK) enzymatic activity of depicted cell lysates. (C-E) Fluorescent particle uptake capacity quantified by FACS in cell lines incubated with zymosan (C), COZ (D) or IgG zymosan (E). Bars represent the average of 3-4 experiments (+/- SD). *, $p<0.05$;**, $p<0.005$; ***, $p<0.0005$.

line expressing EYFP matched that of the endogenous activity in non-transduced control cells. Also both pools of RAW-CK-B$_{(C283S)}$ mutant cells exhibited levels of CK activity that were identical to endogenous levels. Clearly, the residual activity for the mutant CK-B$_{(C283S)}$ is very low, and therefore no appreciable increase in CK activity was noticeable despite the almost 10-fold increase in protein level.

Assessment of phagocytic capacity with fluorescently labeled zymosan and COZ confirmed that neither the retroviral infection nor the subsequent antibiotic selection procedure had affected phagocytic capacity, since RAW-EYFP cells and non-infected cells behaved identically (**Figure 6C**). Expression of CK-B$_{(C283S)}$, however, resulted in a considerable drop in phagocytosis efficiency. Uptake of non-opsonized zymosan was at 58 ± 21 % and 57 ± 12 % (** $p<0.005$) for both RAW-CK-B$_{(C283S)}$#1 and RAW-CK-B$_{(C283S)}$#2, respectively, relative to non-transduced or EYFP expressing cells. We observed that overexpression of CK-B had no stimulating effect and did not significantly alter phagocytosis of zymosan (108 ± 30% and 113 ± 23% for the two independent cell lines). In contrast, in the case of complement-mediated (COZ) phagocytosis, both RAW-CK-B cell pools did perform significantly better than controls (144 ± 4% and 153 ± 6%, ** $p < 0.005$) (**Figure 6D**). Conversely, the cell lines expressing CK-B$_{C283S}$ were also significantly impaired in the uptake of COZ (79 ± 8% and 66 ± 5%, * $p < 0.05$). Thus, expression of CK-B$_{(C283S)}$ impaired phagocytosis of both zymosan and COZ, whereas overexpression of wildtype CK-B stimulated only the phagocytosis of COZ. Importantly, expression of CK-B$_{(C283S)}$ did also not influence IgG mediated phagocytosis (**Figure 6E**; efficiency of 85 ± 10% and 89 ± 14%, for both lines), in line with our results with pharmacological inhibition. Unfortunately, our findings of effects of overexpression of wt CK-B on IgG mediated phagocytosis were inconclusive. One cell line displayed a moderate increase in phagocytotic efficiency (118 ± 8%; * $p<0.05$), whereas the other did not differ significantly from the control (95 ± 13%). Although identical cell pools were used for the experiments shown in **Figures 6C-E,** the experiments presented in **Figure 6E** were performed with cells at a higher passage number. We therefore may have to attribute the borderline stimulation to a CK-B-unrelated effect.

Because total cellular CK activity was identical between the parental RAW264.7 line and RAW-CK-B$_{(C283S)}$ and in addition, CK-B$_{(C283S)}$ is recruited in a similar fashion as wildtype CK-B (**Figure 3**), our findings suggest that the mutant protein competes with endogenous CK-B and thereby lowers the concentration of locally active CK-B molecules at crucial sites in the cell cortical area.

RAW 264.7 macrophages expressing CK-B$_{(C283S)}$ exhibit impaired adhesion and internalization of COZ

Phagocytosis occurs through a series of consecutive steps that ultimately lead to the engulfment of a particle. Probing for adhesion of coat molecules, and the actual binding of the phagocytic target to specific receptors on the protruding cell surface constitutes one of the first steps in this process. In order to specify which specific phase of thphagocytic process is linked to CK-B, we subjected the wild type CK-B or CK-B$_{(C283S)}$ cell pools to a particle adhesion assay, using COZ particles as the phagocytic targets with most discriminative effects (**Figure 7**). Quantification of the total number of particles per cell (inside + outside) in images of the cell lines with adherent and already internalized particles (**Figures 7A-C**; n = 3 experiments) demonstrated that an average of 1.3 ± 0.7 of COZ particles associated with RAW-CK-B$_{(C283S)}$ cells, significant less than with control cells which have 2.1 ± 0.7 particles/cell ($p < 0.001$). Interestingly, RAW-CK-B cells bound significant higher numbers of particles than control cells (2.8 ± 0.7 particles/cell; $p < 0.005$). Calculation of the percentage of external COZ particles revealed that control cells have 17 ± 10% of particles attached that are not yet (fully) internalized. Overexpression of CK-B did not affect this percentage (14 ± 9% external). With RAW-CK-B$_{(C283S)}$ cells a significantly higher percentage of particles remained external (27 ± 18% ; $p < 0.02$). Inhibition of CK-B thus apparently affects both the initial sampling of COZ particles from the added pool as well as well as the process of their internalization.

CK-B facilitates actin polymerization

Recently, it has been demonstrated that cells actively probe the extracelullar matrix for adhesion sites by clustering integrins in "sticky fingers" at the leading edge of cells. Actin polymerization has an active role in this process (Galbraith, Yamada et al. 2007). Since extension-retraction of filopodial tentacles that determine the efficiency of particle uptake in phagocytosis is also based on F-actin in combination with myosin-V, -VII and -X activities (Kress, Stelzer et al. 2007) we decided to study if the role of F-actin in adhesion of COZ and IgG-opsonized zymosan (**Figure 5B-C** and **6D-E**) in RAW 264.7 cells could be different, and correlated with the differential effects of CK-B. Therefore, adhesion experiments with COZ and IgG-opsonized zymosan particles in the presence of low concentrations of the actin polymerization inhibitor cytochalasin D were performed (**Figure 8A-B**). Interestingly, treatment with

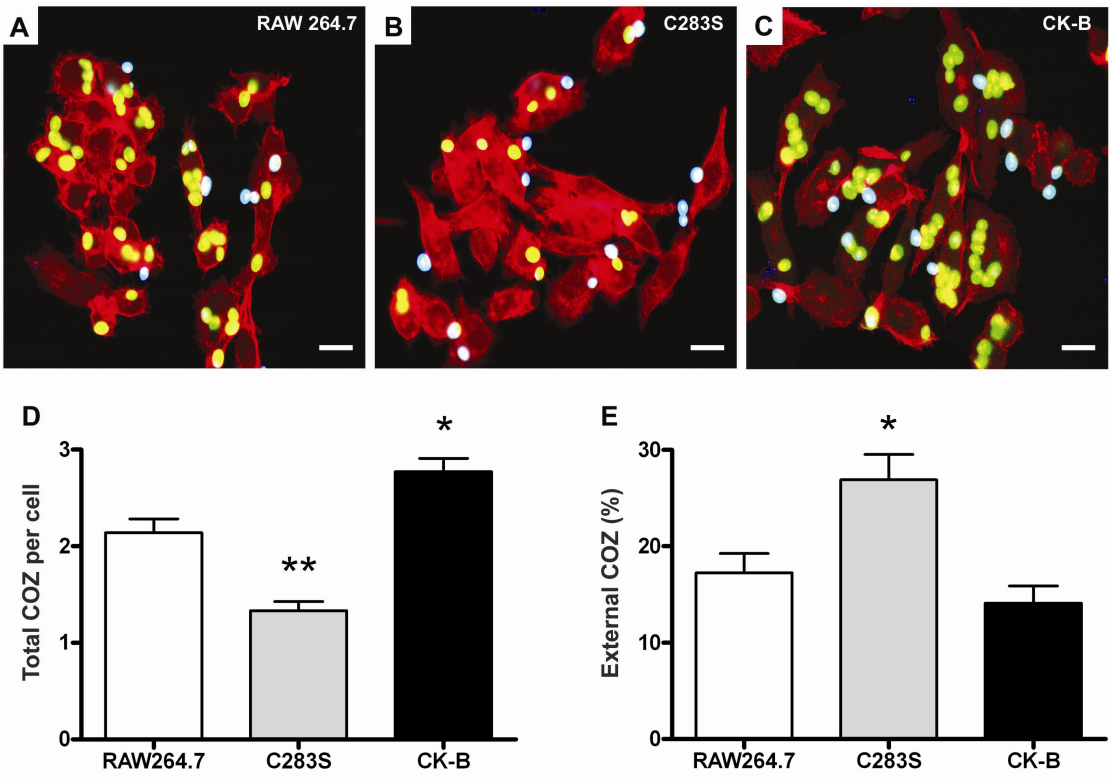

Figure 7. *CK-B is involved in the initial steps of phagocytosis.* (A-C) Adhesion and uptake of FITC-labeled COZ particles in RAW 264.7 cells (A) and RAW 264.7 cells expressing CK-B_{C283S} (B) or CK-B (C). Internalized particles appear green (or yellow, when co-localizing with F-actin) and external particles appear cyan. Bar, 10 µm. (D) Averages of total numbers of particles associated per cell (inside + outside) (+/- SEM). *, $p<0.005$; **, $p<0.001$. (E) Percentage particles attached to the cell, but not yet engulfed (+/- SEM). *, $p<0.05$.

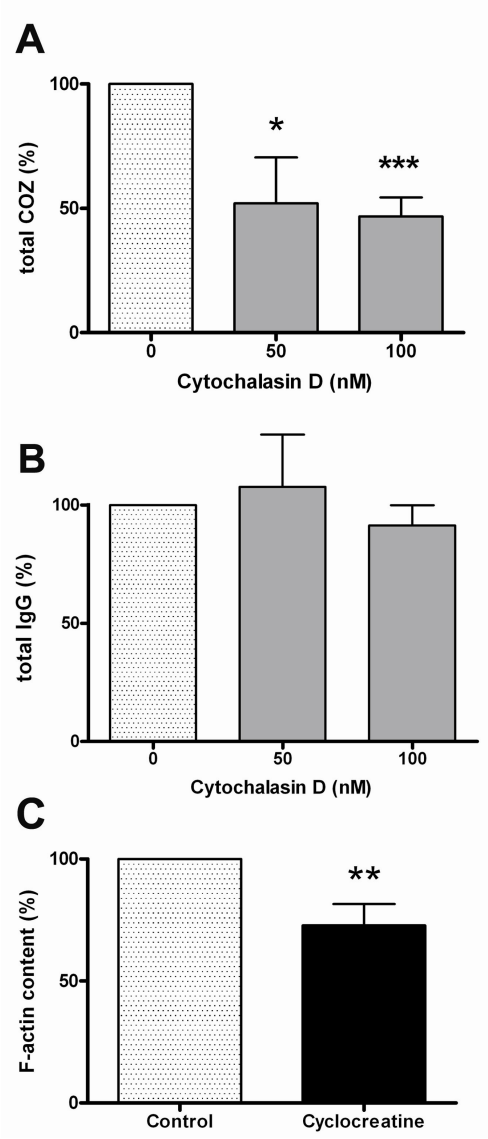

Figure 8. *Coupling between CK-B activity, actin polymerization state and phagocytosis.* Adhesion assays were performed with RAW 264.7 cells, pre-treated with cytochalasine D (50 or 100 nM), and COZ (A) or IgG-opsonized zymosan (B). The total number of particles (adherent and internalized) was determined and normalized to non-treated cells (averages of 3-4 experiments +/- SD). (C) Raw 264.7 cells were treated with 5 mM cyclocreatine prior to F-actin quantification using fluorescently labeled phalloidin (averages of 4 experiments +/- SD). *, $p<0.05$; **, $p<0.01$; ***, $p<0.001$.

50 nM or 100 nM cytochalasin D decreased adhesion of COZ dramatically (52 ± 18%; $p<0.05$ and 47 ± 8%; $p<0.001$, respectively; n=4; **Figure 8A**) while adhesion of IgG-opsonized zymosan was not significantly affected (108 ± 22% and 91 ± 9% for 50 nM and 100 nM CD, respectively; n=3; **Figure 8B**). We consider this evidence for a different role of F-actin in complement and IgG-mediated adhesion.

To further address if this discriminative coupling could indeed be linked to CK-B's role in providing adequate ATP supply for F-actin formation (Loisel, Boujemaa et al. 1999; Pantaloni, Le Clainche et al. 2001), RAW 264.7 cells were treated with cyclocreatine and the F-actin content was determined. Fluorescent phalloidin staining in combination with FACS analysis revealed that in cyclocreatine treated cells the global F-actin content significantly decreased to 73 ± 9% ($p<0.01$, n=4) of non-treated control cells (**Figure 8C**). Thus, inhibition of CK-B mediated activity indeed affects the formation of F-actin in RAW 264.7 cells. This is in agreement with our finding that actin recruitment to

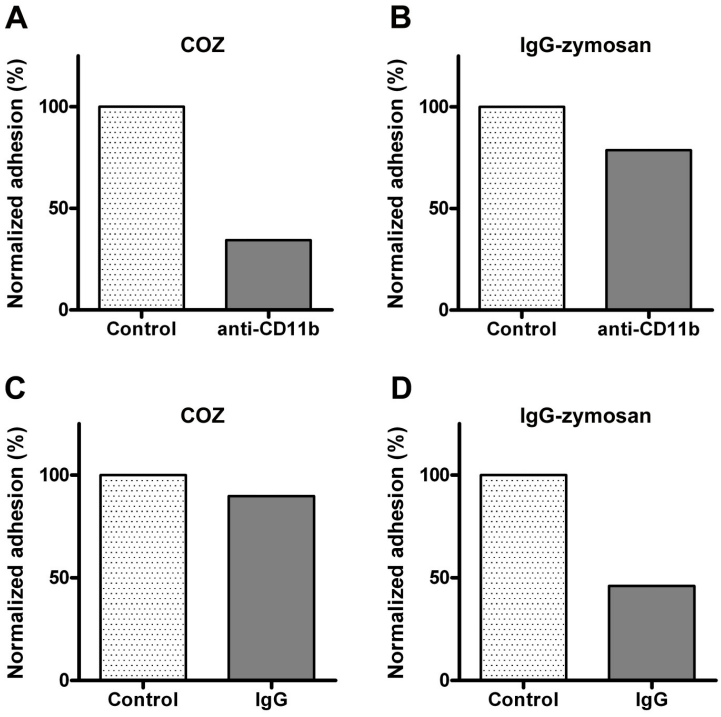

Figure S2. *Determination of receptors used in uptake of phagocytic particles.* (A-D) The receptors on RAW 264.7 cells involved in binding of differentially opsonized zymosan particles were determined in the presence of a CR3 blocking monoclonal antibody (M1/70, anti-CD11b) (A-B) or human IgG (3 mg/ml) (C-D). Bar diagrams represent the percentage particles (internalized and bound) of COZ (A) and IgG-zymosan (B) normalized to the control.

phagocytic cups is also diminished when CK-B is inhibited (**Figure 3F**). The question whether there is also a reciprocal relationship, whether the local F-actin state contributes to CK-B recruitment to the phagocytic cup, appeared more difficult to answer. Until now, we were unable to detect a direct binding between actin and CK-B in pull down experiments (data not shown). Furthermore, FRAP experiments revealed that the motility of YFP-actin and CFP-CK-B in cup areas differed during the phagocytic process (**Figure S4**), arguing against single association between actin and CK-B. Involvement of transient "kiss-and-run" type of interactions cannot be excluded, however. Combined, our data suggest that the activities of CK-B that we have described are likely to occur via ATP-supply effects on local F-actin polymerization capacity, which in turn affects CR3 mediated adhesion and internalization.

Discussion

Phagocytosis requires a rapid and spatially confined reorganization of the actin cytoskeleton. The underlying molecular processes, such as actin polymerization and

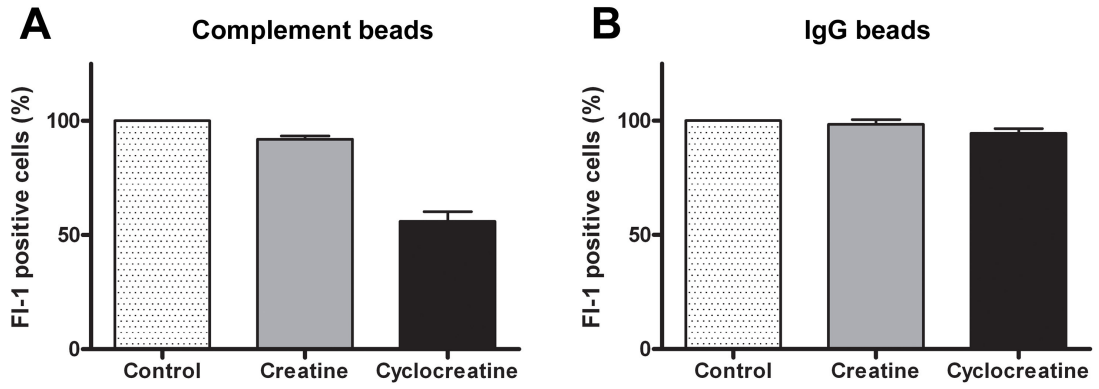

Figure S3. *Phagocytosis of complement and IgG-coated polystyrene beads.* (A-B) Uptake capacity for fluorescent polystyrene beads in RAW 264.7 cells pre-incubated with 5 mM creatine, 5 mM cyclocreatine or normal growth medium was quantified by FACS. (A) Complement coated 3-µm polystyrene beads, (B) IgG-coated 3-µm polystyrene beads. Bars represent averages of Fl-1 positive cells of 2 experiments performed in triplicate.

acto-myosin force generation, generate a sudden and localized demand for cellular ATP (Guminska, Ptak et al. 1975; Loike, Kozler et al. 1979). To reciprocate this challenge, sites of ATP production should be coupled tightly to sites of ATP consumption. From studies in cell and animal models, we know that CK isozymes are particularly well equipped for this role, as they provide the cell with a fast ATP regeneration and delivery system that can adequately provide high-energy phosphoryl groups to cellular locales with high energy turnover. Here, we established a tight functional and spatial link between the CK system and the actin-based cytoskeletal machinery in macrophages during phagocytosis. A similar relationship was found for the muscle isoform of CK, CK-M, which associates with the M- and I-bands of skeletal muscle and fuels local ATP consuming processes, including acto-myosin contraction and calcium pumping (Wallimann, Wyss et al. 1992; Steeghs, Benders et al. 1997). Importantly, CK-M's role in these physiological processes is supportive, not absolutely vital (van Deursen, Heerschap et al. 1993; Steeghs, Benders et al. 1997), just as we report here for CK-B's role in phagocytosis. For CK-M, the molecular nature of events that support its role has been unraveled to some extent. E.g., we know that interaction of CK-M with the sarcomeric M-band is mediated via

conserved lysine residues. In addition, particular amino acid segments in CK-M enable the protein to bind indirectly to the I-band via the glycolytic enzymes phosphofructokinase (PFK) and aldolase, which have actin-binding properties (Kraft, Hornemann et al. 2000). Interestingly, glycolytic enzymes are also known to be recruited to phagosomes (Garin, Diez et al. 2001; Campanella, Chu et al. 2005), so there may be parallel mechanisms. Unfortunately, to explain CK-B dynamics, it is not possible to use simple analogy since the lysine residues involved in CK-M M-band interaction are not conserved in CK-B (Hornemann, Kempa et al. 2003) and direct sequence comparison is not yielding clear clues for other binding modes – for example to glycolytic enzymes. Several mechanisms could therefore be involved in the recruitment of CK-B. One model would be the transient availability of CK-B binding sites at the nascent phagosome by modification of local proteins or presence of CK-B interacting proteins. Based on its co-localization with CK-B, we tested whether actin could be a candidate for such scaffolding, but pull-down assays and FRAP experiments did not reveal a tight interaction. Also yeast-2-hybrid assays did not disclose any CK-B-to-actin binding opportunities (data not shown). As another possibility, CK-B binding characteristics could also be transiently modified at the enzyme itself, possibly by (enzymatic) events located at the forming cup. Indeed, CK-B is prone to covalent modifications such as phosphorylation (Chida, Kasahara et al. 1990), oxidation (Aksenov, Aksenova et al. 2000), methylation (Iwabata, Yoshida et al. 2005) or ubiquination (Zhao, Yan et al. 2007). Simple presence of substrate may also determine binding ability, as recently shown for CK-M (Zurmanova, Difato et al. 2007). Further studies are necessary to discriminate between all these possibilities.

Because phagocytosis is a metabolically demanding process, CK-B recruitment to phagocytic cups could serve to promote or safeguard local events or – reciprocally – shield the rest of the cell from excessive local energy demand. To distinguish between these mechanistic models and elucidate CK-B global and local physiological role(s) in macrophages more precisely will be technically challenging because of the confined character of the events. This, therefore, also remains a topic for future study. Of particular importance was our finding that displacement of endogenous CK-B by ECFP-CK-B$_{(C283S)}$ during phagocytosis, reduced the local accumulation of EGFP-actin in the phagocytic cup area. The observation that inhibition of CK-B

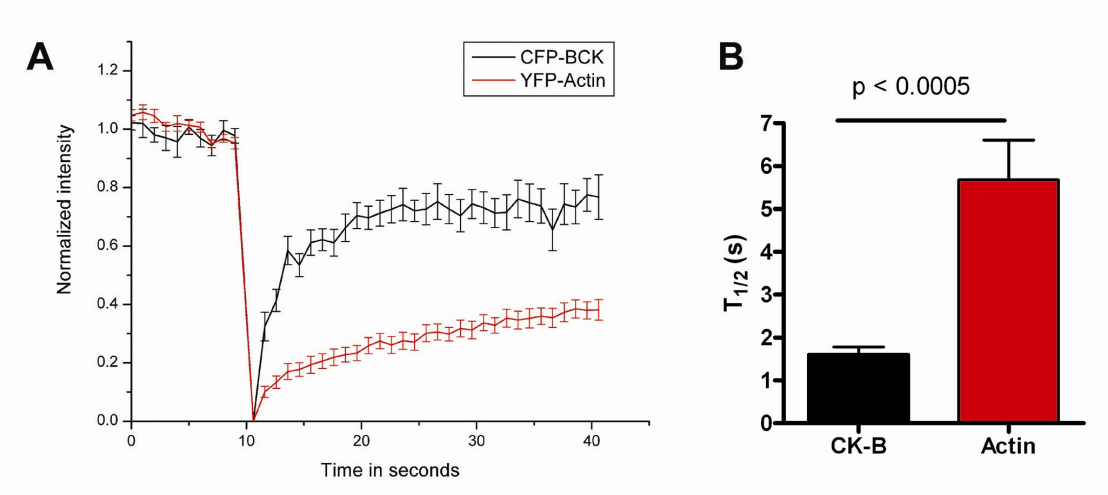

Figure S4. *Determination of the mobility of CK-B and actin in the phagocytic cup.* (A) Average (n=14) of normalized bleach and recovery curves of RAW264.7 cells stably expressing ECFP-CK-B and EYFP-actin. Fluorescence of CFP and YFP in the phagocytic cup was bleached by scanning a square region covering approximately half the cup area 20 times at high laser power. (B) T1/2 of recovery (in sec) of ECFP-CK-B and EYFP-actin in the phagocytic cup as determined from the individual recovery curves.

activity impairs global F-actin polymerization in RAW 264.7 cells was equally revealing. Normally, actin polymerization requires the incorporation of ATP-actin at the barbed end of actin filaments. During filament elongation ATP is hydrolyzed and ADP-actin is being released at the pointed end. Thus, constant reloading of actin with ATP is required for the continuation of the polymerization cycle (Loisel, Boujemaa et al. 1999; Wolven, Belmont et al. 2000; Pantaloni, Le Clainche et al. 2001). We propose here, that CK-B could specifically enhance this process by regenerating ATP at sites of active actin remodeling.

In addition to the polymerization reaction, actin nucleation and branching play an important role. The Arp2/3 complex, together with the Wiskott-Aldrich syndrome (adapter) protein, WASP (May, Caron et al. 2000) and the motor proteins myosin I (Evangelista, Klebl et al. 2000; Lee, Bezanilla et al. 2000) and myosin II (Olazabal, Caron et al. 2002) help to guide these processes during shaping of the cup of nascent phagosomes. Recently, also the involvement of the formin mDia has been implicated in phagocytosis of COZ. Inhibition of mDia results in decreased F-actin recruitment at the phagocytic cup and induces a concomitant decrease in efficiency of CR3, but

not Fc-γR, mediated phagocytosis (Colucci-Guyon, Niedergang et al. 2005). Formins promote actin polymerization by increasing polymerization associated ATP hydrolysis up to fifteen times via profilin (Romero, Le Clainche et al. 2004). Finally, regulation of cell structure via RhoA activation or AMP-activated kinase involvement is also directly energy-dependent (Mahajan, Pai et al. 2000; Lee, Koh et al. 2007). Thus, different types of actin regulatory processes form local and temporal energy drains, which may need compensation by CK-B mediated ATP regeneration.

Various associated myosin-motor mechanisms involved in formation of the specialized structures at the phagosome may also be CK-B dependent, because motor activity of myosins is controlled by ATP/ADP ratio. In *Dictyostelium*, myosin VII was found to be important for initial adhesion in phagocytosis (Tuxworth, Weber et al. 2001). In addition, another closely related myosin, myosin X, was implicated in adhesion and phagocytosis (Cox, Berg et al. 2002; Zhang, Berg et al. 2004). However, at this point we need more mechanistic information about how ATP fuelling separately serves actin and myosin activities in the phagocytic cup before we can analyse CK-B's presumed role(s) in detail further.

Intriguingly, Olazabal and co-workers have reported that inhibition of myosin II decreased actin recruitment in phagocytic cups during CR3 mediated phagocytosis, but not Fc-γR mediated events (Olazabal, Caron et al. 2002). Our results regarding differences in ingestion capacity for COZ or IgG-coated zymosan and beads after genetic blocking or pharmacological inhibition of CK activity fit with a model in which ATP-driven actomyosin activities differentially contribute to discrete phagocytic processes. Only phagocytosis of COZ and zymosan was significantly affected under conditions where CK activity was lowered, Fc-γR-mediated activity was not significantly affected by cyclocreatine or dominant-negative CK inhibition. Of note, phagocytosis of COZ is mainly but not exclusively mediated by complement molecules present on COZ. Also, sugar residues which are present on (non-)opsonized zymosan facilitate recognition by lectin domains in CR3 (Thornton, Vetvicka et al. 1996; Xia, Vetvicka et al. 1999; Le Cabec, Carreno et al. 2002) or alternative phagocytic receptors like dectin-1 (Brown, Taylor et al. 2002).

Based on our findings and these background notions regarding differences in pathways involved in cup formation in complement or IgG-modes of phagocytosis

(Caron and Hall 1998; Olazabal, Caron et al. 2002; Hoppe and Swanson 2004; Colucci-Guyon, Niedergang et al. 2005), it is tempting to speculate that CK-B enhances phagocytosis by modulating specific processes up- or downstream of CR3. It may be important to note that differences in the actin levels in the phagocytic cup, as seen between active ECFP-CK-B and mutant ECFP-CK-B$_{(C283S)}$ expressing cells, correlated better with the fraction of cells participating in phagocytosis than with the number of fully ingested particles per cell. The observation of the apparent delayed internalization of COZ particles in the RAW-CK-B$_{(C283S)}$ line (Figure 7E) suggests that after early binding requirements have been fulfilled CK-B also promotes transition to the next phases of phagocytosis. Therefore, we propose that the CK-B mediated modulation of actin polymerization is particularly relevant during early CR3-mediated phagocytosis, for example by increasing the number of successful probing attempts for particle binding. Our data also suggest that endogenous levels of resident CK-B molecules are largely sufficient to saturate these requirements for zymosan and COZ phagocytosis.

Complement receptor 3, is also known as CD11b/CD18 or αMβ2 integrin. Because actin polymerization is pivotal in early adhesion events mediated by integrins (Galbraith, Yamada et al. 2007), a picture emerges in which actin behavior determines the efficiency by which CR3s can bind their target. Actin behavior may be less central for IgG-mediated binding events. Our finding that low concentrations of the actin polymerization inhibitor, cytochalasin D, reduced binding of complement opsonized particles more than IgG-opsonized particles is consistent with such a model.

In conclusion, we have demonstrated that CK-B enhances phagocytosis of zymosan and COZ, likely via a specific synergistic role in mechanistic events involved in actin polymerization behavior. Although our data indicate that the enzyme's metabolic role is dominant, we cannot completely rule out a structural role of CK-B in phagocytosis at this point. Taken together with the finding that CK-B$_{(C283S)}$ was able to inhibit phagocytosis without decreasing the total CK activity, our data suggest that CK-B acts to steer the delicate local balance in ATP/ADP ratio, during formation of the phagocytic cup, around the time that pseudopod-filopodium extensions or CR3-mediated adhesions are formed. As we do see CK-B in filopodia and phagocytic cups in our RAW cells (Figures 1G-L and 4) but also observed CK-B

accumulation in dynamic actin structures of other cell types during adhesion to substratum, spreading and crawling, (e.g. in neurons and astrocytes; unpublished results) this raises the exciting possibility that CK-B facilitates rapid cytoskeletal dynamics in a broad range of specialized events that occur during tissue development and disease, including dendritic spine generation in brain (Carlisle and Kennedy 2005), formation of immune-synapses or protrusion dynamics for cancer cell invasion.

Methods

Cell culture

Resident peritoneal macrophages were isolated from adult (10-20 week old) mice of mixed genetic background (C57BL/6 x 129Ola). After sacrificing the mice by cervical dislocation, cells were harvested by rinsing the peritoneum twice with 5 ml ice-cold HBSS. Collected macrophages were cultured for 24 hours in RPMI supplemented with 10% fetal calf serum (FCS), glutamine (0.3 g/l), sodium pyruvate (0.11 g/l) and gentamycin (0.05 mg/ml). Primary microglia were collected from neocortices of newborn mice as described (Hassan, Rifat et al. 1991).

RAW 264.7 murine macrophages were maintained in RPMI 1640 (Gibco) containing 10% FCS, glutamine (0.3 g/l), sodium pyruvate (0.11 g/l) and gentamycin (0.05 mg/ml).

Plasmid and retroviral expression vectors

CK-B cDNA was amplified by PCR from DNA from mouse clone EST AW551905 using a complementary 5' primer 5'-TATACTCGAGCCATGCCCTTCTCCAC CAGGC-3' containing the start-codon of CK-B and a XhoI restriction site. The 3' primer was a 20-mer poly-dT primer, also containing a XhoI restriction site. The obtained PCR product (the entire CK-B ORF and 3' UTR) was subsequently cloned in XhoI-opened pEYFP-C1 (Clontech). For construction of pSG8puro-CK-B, the CK-B ORF was amplified by PCR from EST AA102913 using 5'-GCGGAATTCATGCCCTTCTCCAACAGC-3' and 5'-CGCCTCGAGTCACTTCT GGGCCGGC-3' as primers. The ORF was then cloned into the EcoRI and XhoI

sites of pSG8puro (de Bruin, Oerlemans et al. 2004). Expression vector pSG8puro-ECFP-CK-B was constructed by first subcloning the CK-B open reading frame in (EcoRI/SalI) pECFP-C2 (Clontech) after which the ECFP-CK-B fusion was excised with NheI and DraI and subsequently blunt-ended with T4 DNA polymerase. The recipient vector pSG8puro was cut with EcoRI and XhoI, blunt-ended with T4 DNA polymerase and 5'-terminal phosphate groups were removed by shrimp alkaline phosphatase (Roche) according to the manufacturer's protocols. The pSG8puro-ECFP control plasmid was generated by excising the CK-B ORF from pSG8puro-ECFP-CK-B with SacI and KpnI, followed by filling in the ends of the vector with T4 polymerase and subsequent religation of the vector. To generate a vector for expression of catalytically inactive CK-B, cysteine-283 was replaced by a serine using the site-directed mutagenesis kit and protocol (QuikChange Site-Directed Mutagenesis kit, Stratagene) with the oligos 5'-CTACATCCTCA CAAGCCCATCCAACCTG-3' and 5'-CAGGTTGGATGGGCTTGTGAGGA TGTAG-3' and pSG8puro-CK-B or pECFP-C2-CK-B as template DNA. The sequences of all constructs were verified by sequencing. Retroviral expression constructs were created by insertion of the ORF's of CK-B, CK-B$_{(C283S)}$ and EYFP into retroviral vector DNA pLZRS-IRES-zeo (Michiels, van der Kammen et al. 2000), giving rise to pLZRS-CK-B, pLZRS-CK-B$_{(C283S)}$ and pLZRS-EYFP, respectively.

Transfection and retroviral transduction

Transient transfections of RAW 264.7 cells with pEYFP-based plasmid DNAs were performed using Lipofectamine 2000 (Invitrogen) according to manufacturer's protocol. RAW 264.7 cells stably expressing EGFP-tagged ß-actin were generated by transfecting RAW 264.7 cells with pCMV-EGFP-β-actin, followed by neomycine selection. A population of cells with intermediate expression levels was obtained by FACS selection. To generate cells co-expressing EGFP-actin and ECFP-tagged CK-B or CK-B$_{(C283S)}$, pSG8puro constructs were linearized with restriction enzyme PvuI and transfected into EGFP-actin RAW 264.7 cells using Lipofectamine 2000. Clones with stably integrated vector DNA were selected by the ability to grow in medium

with puromycine (5 μg/ml). RAW 264.7 cell lines expressing wildtype murine CK-B, catalytically inactive CK-$B_{(C283S)}$ or EYFP were created by retroviral transduction, following procedures as described (Michiels, van der Kammen et al. 2000). In short, pLZRS retroviral vector constructs were transfected into the ecotrophic packaging cell line, Phoenix ΦNX-A (Kinsella and Nolan 1996; Michiels, van der Kammen et al. 2000) using Lipofectamine 2000 (Invitrogen). Viral supernatants (2 ml from 35 mm dish) were harvested after 48 hours and added to RAW 264.7 cells grown in 35 mm dishes (Costar). After 24 hours the virus containing medium was replaced and after another 24 hours selection for stably transduced cells was initiated by adding Zeocin (0.5 mg/ml).

Phagocytic targets and phagocytosis uptake assay

Unlabeled zymosan particles (dead yeast particles; Sigma) were suspended in PBS and briefly dispersed by sonification. For fluorescent labeling, zymosan particles (10 mg) were incubated for 2 hours at room temperature in sodium carbonate buffer (0.1 M, pH 9.6) with fluorescein isothiocyanate (FITC) or tetramethylrhodamine isothiocyanate (TRITC) at a final concentration of 0.5 mg/ml. After extensive washing the labeled zymosan was collected by centrifugation, resuspended into single particles by sonification in PBS and stored in aliquots at -80°C. Complement opsonization was performed as described (Hed and Stendahl 1982). Cells were activated with 200 nM phorbol 12-myristate 13-acetate (PMA) 15 minutes prior to phagocytosis of complement-opsonized zymosan (COZ). IgG opsonized zymosan was prepared using zymosan A BioParticles® opsonizing reagent from Invitrogen, according to manufacturer's protocol.

IgG coated 3-μm fluorescent polystyrene beads (Polysciences) were prepared as described (Kress, Stelzer et al. 2007). Complement coated polystyrene beads were prepared in a similar fashion. Briefly, carboxylated 3-μm fluorescent polystyrene beads (Fluoresbrite® Yellow Green Carboxylate Microspheres, Polysciences) were incubated with mouse IgM (Sigma) in MES buffer (pH 6.7). After incubation with EDAC (Sigma) beads were washed three times with PBS, freshly isolated mouse serum was added and beads were incubated for 30 min at 37°C. After washing with

1% Triton X-100 in 10 mM Tris pH 9.4 and PBS, the beads were stored at 4°C in PBS with 0.03% fish skin gelatin and 2 mM sodium azide. Before use, beads were washed three times with PBS to remove the azide.

To determine phagocytic uptake efficiency, fluorescently labeled zymosan or coated polystyrene beads suspended in RPMI without phenol red were added to $1x10^5$ RAW 264.7 cells at a ratio of 10 particles per cell. After incubating 30 minutes at 37°C, the cells were washed 3 times with PBS. Subsequently, the cells were incubated with lyticase (100U/ml, Sigma) in PBS for 10 minutes at room temperature to remove extracellular zymosan. After rigorous trypsinization, the cells were diluted in RPMI containing 10% FCS and spun down. Cell pellets were resuspended in PBS + 1% paraformaldehyde and samples were microscopically analyzed to confirm removal of extracelullar particles. For quantification of phagocytosis, $1x10^4$ cells per sample were analyzed on a Becton-Dickinson FACScan flow cytometer. Mean fluorescence was calculated for 3 to 4 experiments performed in duplo.

Indirect immunofluorescence

Cells grown on glass coverslips were fixed with 2% paraformaldehyde in PHEM buffer (25 mM HEPES, 10 mM EGTA, 60 mM PIPES, 2 mM $MgCl_2$, pH 6.9), permeabilized with 0.1% Triton X-100 and incubated 20 min in PBS containing 4% bovine serum albumine (BSA). Primary antibodies used were polyclonal anti-CKB (1:2000) and monoclonal anti-CKB 21E10 (1:2000). Primary antibodies were detected by goat-anti-rabbit IgG or goat-anti-mouse IgG conjugated to Alexa Fluor 488 or Alexa Fluor 568 (Molecular Probes). Images were taken sequentially for each wavelength with a Biorad MRC1024 confocal microscope using an oil immersion 60x, 1.4 NA objective using the Lasersharp software (Biorad, version 4.2). In the case of saponin-extraction, cells were permeabilized with 0.05 % saponin in PBS for 1 minute prior to fixation to remove cytosolic protein.

Live cell imaging and FRAP

Stably transfected RAW 264.7 cells expressing EYFP-CK-B or EYFP were cultured for 24 hours on glass bottomed Willco dishes (GWSt-3522) prior to live imaging. 30

minutes before each experiment, the culture medium was replaced by RPMI without phenol red (Gibco) containing 10 mM HEPES and 10% FCS. For dual imaging, RAW 264.7 cells stably expressing GFP-actin and ECFP constructs were cultured as described for the single transfectants. A Zeiss LSM510meta confocal laser-scanning microscope was used, equipped with a temperature controlled CO_2 incubator (type S) and sample stage. For recording we used a PlanApochromatic 63x, 1.4 NA oil immersion DIC lens (Carl Zeiss GmbH, Jena, Germany) to obtain optical slices of approximately 2.5 μm. To obtain the EGFP and ECFP signals, spectral recordings were taken with the meta-detector and separated using the linear unmixing option embedded in the Zeiss laser scanning microscope software (LSM 510 META version 3.2 SP2). Image acquisition was started after addition of zymosan particles.
For analysis of double transfected cells, regions of interest (ROIs) were placed around phagocytic cups and a portion of the cytosol next to the nucleus (also with embedded software). Accumulation of fluorescence in the phagocytic cup was calculated from the ratio between cup and cytosol. Alternatively, line plots of still images at the peak of accumulation were generated with ImageJ (National Institutes of Health, Bethesda, MD) software to determine accumulation of fluorescence in phagocytic cups of cells containing only EGFP-tagged constructs.

To study the relative mobilities of CK-B and actin in the phagocytotic cup we stably transfected RAW264.7 cells with ECFP-CK-B and EYFP-ß-actin. CFP and YFP images were collected sequentially. CFP was excited at 458 nm at moderate laser power, and emission was detected using a 470–500 nm bandpass filter and YFP was excited at 514 nm at moderate laser power, and emission was detected using a 560-nm longpass filter. After 10 images CFP and YFP fluorescence in the phagocytic cup were bleached by scanning a square region covering approximately half the cup area 20 times at high laser power. After photobleaching, recovery was monitored for 30 sec. The recovery curves were normalized by calculating $I_{norm} = (I - I_{bg})/(I_{pre} - I_{bg})$, where I_{pre}, is the fluorescent intensity before the bleach and I_{bg} the background intensity, and the T1/2 of recovery was determined.

Immunoblotting

Cells were scraped on ice in lysis buffer (12.5 mM Na_2HPO_4, 2.8 mM KH_2PO_4, 0.05% Triton X-100, 0.3 mM DTT) containing protease inhibitor cocktail (Roche) and incubated on ice for 20 min. Cell lysates were separated on a 10% SDS-PAGE gel, and electrotransferred to a nitrocellulose membrane. Subsequently, membranes were blocked with PBS containing 5% skim milk, and incubated with anti-CK-B (21E10, diluted 1:2000) for 1 hr. Secondary horse radish peroxidase (HRP) conjugated goat-anti-mouse IgG (diluted 1:10^4, Jackson Immunoresearch) was used in combination with the HRP substrate Lumi-Light (Roche) for detection of protein bands.

CK-activity assay

CK-activity was determined by enzyme-coupled reactions. Briefly, cell lysates were prepared as described (see immunoblotting) and protein content was determined. Lysates with equal protein content were serially diluted in PBS in a 96-wells plate (Corning). Then 100 µl assay mix, consisting of bis-Tris acetate buffer (0.1 M, pH 6.9), hexokinase (1 u/ml), glucose-6-phosphate dehydrogenase (0.8 u/ml), phosphocreatine (15 mM), glucose (2 mM), ADP (2 mM), NADP (2 mM), $MgCl_2$ (10 mM) and 10 µm bis(adenosine-5')-pentaphosphate (Ap5A), was added. Upon addition of 10% vol/vol Wst-1 reagent (Roche), CK-mediated formazan generation was measured every minute on a BioRad 3550 micro-plate reader at 450 nm. CK-activity was expressed in arbitrary units.

Adhesion assay

Cells were cultured on coverslips in 24-wells plates (1x10^5 per well) overnight. In some experiments cells were pre-treated (30 min) with 50 and 100 nM Cytochalasin D (Sigma). After PMA stimulation (200 nM, 15 min) and three subsequent PBS washes with serum-free RPMI, FITC-labeled COZ particles were added (10 per cell) to the cells for 30 minutes at 37°C. Cells were washed 2 times with PBS to remove non-bound particles upon fixation (30 minutes at room temperature) with PHEM buffer containing 2% paraformaldehyde and 0.5% glutaraldehyde. Subsequently, the

coverslips were washed with PBS, incubated in PBS/glycine/BSA for 20 minutes and external zymosan was stained with anti-zymosan IgG (1:500, Molecular Probes) followed by permeabilization (3 minutes 0.1% Triton X-100 in PBS) and incubation with secondary Alexa 660 conjugated goat-anti-rabbit IgG (1:300, Molecular Probes). Cells were counterstained with Alexa 568 conjugated phalloidin. In three independent experiments 9 random fields were imaged for each cell line with a Biorad MRC1024 confocal microscope using an oil immersion 60x objective. The total number of particles and the number of external adherent particles per cell were calculated.

For assessment of receptor-blocking effects, coverslips with cells were placed on parafilm (cells facing up) and incubations took place with smaller volumes. Involvement of CR3 was tested by pre-treating cells with either 100 μl RPMI containing 20 μg/ml human IgG (control) or M1/70 (anti-CR3; culture-supernatant, 1:25). COZ and IgG-opsonized zymosan were incubated for 30 minutes at 37°C in 200 μl RPMI containing either human IgG (20 μg/ml) or M1/70. Cells were subsequently washed and fixed as described. The number of particles (bound and internalized) was determined and normalized to the control. To block Fc-γRs human IgG (3 mg/ml) was added to the coverslips (30 min pre-incubation and during adhesion). BSA (3 mg/ml) served as control.

F-actin quantification

F-actin quantification was performed essentially as described (Geneste, Copeland et al. 2002). Briefly, RAW 264.7 cells were grown on non-tissue culture treated petri-dishes and incubated for 2 hours in presence or absence of 5 mM cyclocreatine prior to harvesting by scraping in PBS containing BSA (1%) and EDTA (5 mM). Subsequently, cells were washed once with RPMI and fixed with 4% paraformaldehyde in PHEM buffer. Small aliquots were permeabilized (PBS containing 0.1 % Triton X-100 and 2.5% BSA) and stained with Alexa 660 conjugated to phalloidin (Molecular Probes). Mean fluorescence (Fl-4) was determined by FACS (FacsCalibur, Becton Dickinson).

Acknowledgements

This work was supported by NWO ZON-MW Program grant 901-01-191 and by a KWF Kankerbestrijding grant from the Dutch Cancer Society (to B.W.). We thank Roger Sutmuller and Alessandra Cambi for their help with the FACS analysis, Annemiek van Spriel for generously providing the CD11b antibody (M1/70), Eik Hoffmann (EMBL Heidelberg) for advice on polystyrene bead coating, and Huib Croes for help with the microscopy and imaging facilities and our colleagues in the Central Animal Facility for their advice with animal care.

References

Aderem, A. and D. M. Underhill (1999). "Mechanisms of phagocytosis in macrophages." Annu Rev Immunol **17**: 593-623.

Aksenov, M., M. Aksenova, et al. (2000). "Oxidative modification of creatine kinase BB in Alzheimer's disease brain." J Neurochem **74**(6): 2520-7.

Allen, L. A. and A. Aderem (1996). "Molecular definition of distinct cytoskeletal structures involved in complement- and Fc receptor-mediated phagocytosis in macrophages." J Exp Med **184**(2): 627-37.

Allen, L. H. and A. Aderem (1995). "A role for MARCKS, the alpha isozyme of protein kinase C and myosin I in zymosan phagocytosis by macrophages." J Exp Med **182**(3): 829-40.

Araki, N., T. Hatae, et al. (2003). "Phosphoinositide-3-kinase-independent contractile activities associated with Fcgamma-receptor-mediated phagocytosis and macropinocytosis in macrophages." J Cell Sci **116**(Pt 2): 247-57.

Becker, E. W. (2006). "The roles of ATP in the dynamics of the actin filaments of the cytoskeleton." Biol Chem **387**(4): 401-6.

Beningo, K. A. and Y. L. Wang (2002). "Fc-receptor-mediated phagocytosis is regulated by mechanical properties of the target." J Cell Sci **115**(Pt 4): 849-56.

Bernstein, B. W. and J. R. Bamburg (2003). "Actin-ATP hydrolysis is a major energy drain for neurons." J Neurosci **23**(1): 1-6.

Brown, G. D., P. R. Taylor, et al. (2002). "Dectin-1 is a major beta-glucan receptor on macrophages." J Exp Med **196**(3): 407-12.

Campanella, M. E., H. Chu, et al. (2005). "Assembly and regulation of a glycolytic enzyme complex on the human erythrocyte membrane." Proc Natl Acad Sci U S A **102**(7): 2402-7.

Carlisle, H. J. and M. B. Kennedy (2005). "Spine architecture and synaptic plasticity." Trends Neurosci **28**(4): 182-7.

Caron, E. and A. Hall (1998). "Identification of two distinct mechanisms of phagocytosis controlled by different Rho GTPases." Science **282**(5394): 1717-21.

Castellano, F., C. Le Clainche, et al. (2001). "A WASp-VASP complex regulates actin polymerization at the plasma membrane." Embo J **20**(20): 5603-14.

Champion, J. A. and S. Mitragotri (2006). "Role of target geometry in phagocytosis." Proc Natl Acad Sci U S A **103**(13): 4930-4.

Chida, K., K. Kasahara, et al. (1990). "Purification and identification of creatine phosphokinase B as a substrate of protein kinase C in mouse skin in vivo." Biochem Biophys Res Commun **173**(1): 351-7.

Colucci-Guyon, E., F. Niedergang, et al. (2005). "A role for mammalian diaphanous-related formins in complement receptor (CR3)-mediated phagocytosis in macrophages." Curr Biol **15**(22): 2007-12.

Cox, D., J. S. Berg, et al. (2002). "Myosin X is a downstream effector of PI(3)K during phagocytosis." Nat Cell Biol **4**(7): 469-77.

Dayel, M. J., E. A. Holleran, et al. (2001). "Arp2/3 complex requires hydrolyzable ATP for nucleation of new actin filaments." Proc Natl Acad Sci U S A **98**(26): 14871-6.

de Bruin, W., F. Oerlemans, et al. (2004). "Adenylate kinase I does not affect cellular growth characteristics under normal and metabolic stress conditions." Exp Cell Res **297**(1): 97-107.
Dzeja, P. P. and A. Terzic (2003). "Phosphotransfer networks and cellular energetics." J Exp Biol **206**(Pt 12): 2039-47.
Ehlers, M. R. (2000). "CR3: a general purpose adhesion-recognition receptor essential for innate immunity." Microbes Infect **2**(3): 289-94.
Evangelista, M., B. M. Klebl, et al. (2000). "A role for myosin-I in actin assembly through interactions with Vrp1p, Bee1p, and the Arp2/3 complex." J Cell Biol **148**(2): 353-62.
Galbraith, C. G., K. M. Yamada, et al. (2007). "Polymerizing actin fibers position integrins primed to probe for adhesion sites." Science **315**(5814): 992-5.
Garin, J., R. Diez, et al. (2001). "The phagosome proteome: insight into phagosome functions." J Cell Biol **152**(1): 165-80.
Geneste, O., J. W. Copeland, et al. (2002). "LIM kinase and Diaphanous cooperate to regulate serum response factor and actin dynamics." J Cell Biol **157**(5): 831-8.
Gessner, J. E., H. Heiken, et al. (1998). "The IgG Fc receptor family." Ann Hematol **76**(6): 231-48.
Goldschmidt-Clermont, P. J., M. I. Furman, et al. (1992). "The control of actin nucleotide exchange by thymosin beta 4 and profilin. A potential regulatory mechanism for actin polymerization in cells." Mol Biol Cell **3**(9): 1015-24.
Guminska, M., W. Ptak, et al. (1975). "Macrophage metabolism during phagocytosis and digestion of normal and IgG antibody-coated sheep erythrocytes." Enzyme **19**(1): 24-37.
Hassan, N. F., S. Rifat, et al. (1991). "Isolation and flow cytometric characterization of newborn mouse brain-derived microglia maintained in vitro." J Leukoc Biol **50**(1): 86-92.
Hed, J. and O. Stendahl (1982). "Differences in the ingestion mechanisms of IgG and C3b particles in phagocytosis by neutrophils." Immunology **45**(4): 727-36.
Hoppe, A. D. and J. A. Swanson (2004). "Cdc42, Rac1, and Rac2 display distinct patterns of activation during phagocytosis." Mol Biol Cell **15**(8): 3509-19.
Hornemann, T., S. Kempa, et al. (2003). "Muscle-type creatine kinase interacts with central domains of the M-band proteins myomesin and M-protein." J Mol Biol **332**(4): 877-87.
Hornemann, T., D. Rutishauser, et al. (2000). "Why is creatine kinase a dimer? Evidence for cooperativity between the two subunits." Biochim Biophys Acta **1480**(1-2): 365-73.
Iwabata, H., M. Yoshida, et al. (2005). "Proteomic analysis of organ-specific post-translational lysine-acetylation and -methylation in mice by use of anti-acetyllysine and -methyllysine mouse monoclonal antibodies." Proteomics **5**(18): 4653-64.
Jahraus, A., M. Egeberg, et al. (2001). "ATP-dependent membrane assembly of F-actin facilitates membrane fusion." Mol Biol Cell **12**(1): 155-70.
Jost, C. R., C. E. Van Der Zee, et al. (2002). "Creatine kinase B-driven energy transfer in the brain is important for habituation and spatial learning behaviour, mossy fibre field size and determination of seizure susceptibility." Eur J Neurosci **15**(10): 1692-706.
Kinsella, T. M. and G. P. Nolan (1996). "Episomal vectors rapidly and stably produce high-titer recombinant retrovirus." Hum Gene Ther **7**(12): 1405-13.
Koretsky, A. P. and B. A. Traxler (1989). "The B isozyme of creatine kinase is active as a fusion protein in Escherichia coli: in vivo detection by 31P NMR." FEBS Lett **243**(1): 8-12.
Kovar, D. R. (2006). "Arp2/3 ATP hydrolysis: to branch or to debranch?" Nat Cell Biol **8**(8): 783-5.
Kraft, T., T. Hornemann, et al. (2000). "Coupling of creatine kinase to glycolytic enzymes at the sarcomeric I-band of skeletal muscle: a biochemical study in situ." J Muscle Res Cell Motil **21**(7): 691-703.
Kress, H., E. H. Stelzer, et al. (2007). "Filopodia act as phagocytic tentacles and pull with discrete steps and a load-dependent velocity." Proc Natl Acad Sci U S A **104**(28): 11633-8.
Kreutzberg, G. W. (1996). "Microglia: a sensor for pathological events in the CNS." Trends Neurosci **19**(8): 312-8.
Le Cabec, V., S. Carreno, et al. (2002). "Complement receptor 3 (CD11b/CD18) mediates type I and type II phagocytosis during nonopsonic and opsonic phagocytosis, respectively." J Immunol **169**(4): 2003-9.
Lee, J. H., H. Koh, et al. (2007). "Energy-dependent regulation of cell structure by AMP-activated protein kinase." Nature **447**(7147): 1017-20.
Lee, W. L., M. Bezanilla, et al. (2000). "Fission yeast myosin-I, Myo1p, stimulates actin assembly by Arp2/3 complex and shares functions with WASp." J Cell Biol **151**(4): 789-800.

Linehan, S. A., L. Martinez-Pomares, et al. (2000). "Macrophage lectins in host defence." Microbes Infect **2**(3): 279-88.
Loike, J. D., V. F. Kozler, et al. (1979). "Increased ATP and creatine phosphate turnover in phagocytosing mouse peritoneal macrophages." J Biol Chem **254**(19): 9558-64.
Loike, J. D., V. F. Kozler, et al. (1984). "Creatine kinase expression and creatine phosphate accumulation are developmentally regulated during differentiation of mouse and human monocytes." J Exp Med **159**(3): 746-57.
Loisel, T. P., R. Boujemaa, et al. (1999). "Reconstitution of actin-based motility of Listeria and Shigella using pure proteins." Nature **401**(6753): 613-6.
Mahajan, V. B., K. S. Pai, et al. (2000). "Creatine kinase, an ATP-generating enzyme, is required for thrombin receptor signaling to the cytoskeleton." Proc Natl Acad Sci U S A **97**(22): 12062-7.
May, R. C., E. Caron, et al. (2000). "Involvement of the Arp2/3 complex in phagocytosis mediated by FcgammaR or CR3." Nat Cell Biol **2**(4): 246-8.
Michiels, F., R. A. van der Kammen, et al. (2000). "Expression of Rho GTPases using retroviral vectors." Methods Enzymol **325**: 295-302.
Olazabal, I. M., E. Caron, et al. (2002). "Rho-kinase and myosin-II control phagocytic cup formation during CR, but not FcgammaR, phagocytosis." Curr Biol **12**(16): 1413-18.
Pantaloni, D., C. Le Clainche, et al. (2001). "Mechanism of actin-based motility." Science **292**(5521): 1502-6.
Pollard, T. D. and G. G. Borisy (2003). "Cellular motility driven by assembly and disassembly of actin filaments." Cell **112**(4): 453-65.
Romero, S., C. Le Clainche, et al. (2004). "Formin is a processive motor that requires profilin to accelerate actin assembly and associated ATP hydrolysis." Cell **119**(3): 419-29.
Shin, J. B., F. Streijger, et al. (2007). "Hair bundles are specialized for ATP delivery via creatine kinase." Neuron **53**(3): 371-86.
Steeghs, K., A. Benders, et al. (1997). "Altered Ca2+ responses in muscles with combined mitochondrial and cytosolic creatine kinase deficiencies." Cell **89**(1): 93-103.
Stuart, L. M. and R. A. Ezekowitz (2005). "Phagocytosis: elegant complexity." Immunity **22**(5): 539-50.
Swanson, J. A., M. T. Johnson, et al. (1999). "A contractile activity that closes phagosomes in macrophages." J Cell Sci **112 (Pt 3)**: 307-16.
Thornton, B. P., V. Vetvicka, et al. (1996). "Analysis of the sugar specificity and molecular location of the beta-glucan-binding lectin site of complement receptor type 3 (CD11b/CD18)." J Immunol **156**(3): 1235-46.
Tuxworth, R. I., I. Weber, et al. (2001). "A role for myosin VII in dynamic cell adhesion." Curr Biol **11**(5): 318-29.
van Deursen, J., A. Heerschap, et al. (1993). "Skeletal muscles of mice deficient in muscle creatine kinase lack burst activity." Cell **74**(4): 621-31.
Vieira, O. V., R. J. Botelho, et al. (2002). "Phagosome maturation: aging gracefully." Biochem J **366**(Pt 3): 689-704.
Wallimann, T., M. Wyss, et al. (1992). "Intracellular compartmentation, structure and function of creatine kinase isoenzymes in tissues with high and fluctuating energy demands: the 'phosphocreatine circuit' for cellular energy homeostasis." Biochem J **281 (Pt 1)**: 21-40.
Wolven, A. K., L. D. Belmont, et al. (2000). "In vivo importance of actin nucleotide exchange catalyzed by profilin." J Cell Biol **150**(4): 895-904.
Wyss, M. and R. Kaddurah-Daouk (2000). "Creatine and creatinine metabolism." Physiol Rev **80**(3): 1107-213.
Xia, Y., V. Vetvicka, et al. (1999). "The beta-glucan-binding lectin site of mouse CR3 (CD11b/CD18) and its function in generating a primed state of the receptor that mediates cytotoxic activation in response to iC3b-opsonized target cells." J Immunol **162**(4): 2281-90.
Zhang, H., J. S. Berg, et al. (2004). "Myosin-X provides a motor-based link between integrins and the cytoskeleton." Nat Cell Biol **6**(6): 523-31.
Zhao, T. J., Y. B. Yan, et al. (2007). "The generation of the oxidized form of creatine kinase is a negative regulation on muscle creatine kinase." J Biol Chem **282**(16): 12022-9.
Zurmanova, J., F. Difato, et al. (2007). "Creatine kinase binds more firmly to the M-band of rabbit skeletal muscle myofibrils in the presence of its substrates." Mol Cell Biochem **305**(1-2): 55-61.

Chapter - 3 -

Local ATP generation by brain-type Creatine Kinase (CK-B) facilitates cell spreading and migration

Jan W.P. Kuiper, Remco van Horssen, Frank Oerlemans, Wilma Peters, Michiel van Dommelen, Mariska M. te Lindert, Timo L.M. ten Hagen, Loes van de Pasch, Edwin Janssen, Jack Fransen and Bé Wieringa

Manuscript Submitted

Abstract

Creatine Kinases (CK) catalyze the reversible transfer of high-energy phosphate groups between ATP and phosphocreatine, thereby playing a storage and distribution role in cellular energetics. Brain-type CK (CK-B) deficiency is coupled to loss of function in neural cell circuits, altered bone-remodeling by osteoclasts and complement-mediated phagocytotic activity of macrophages, processes sharing dependency on actomyosin dynamics.

Here, we provide evidence for direct coupling between CK-B and actomyosin activities in cortical microdomains of astrocytes and fibroblasts during spreading and migration. CK-B transiently accumulates in membrane ruffles and ablation of CK-B activity affects spreading and migration performance. Complementation experiments in CK-B-deficient fibroblasts, using new strategies to force protein relocalization from cytosol to cortical sites at membranes, confirmed the contribution of compartmentalized CK-B to cell morphogenetic dynamics. Our results provide evidence that local cytoskeletal dynamics is coupled to on-site availability of ATP generated by CK-B.

Introduction

Distinctly different processes like protrusion and retraction of narrow surface projections by astrocytes, development of invadopodia by malignant cancer cells, pathogen binding and formation of phagocytic cups by macrophages, and the generation of protrusive structures at leading edges of migrating or extending cells share that they are driven by extensive local remodeling of the actin cytoskeleton (Friedl and Wolf 2003; Swanson 2008). Central to the cytoskeletal dynamics in these protrusive structures, commonly involving formation of lamellipodia or filopodia, is the highly regulated actin cytoskeleton assembly, controlled by a dynamic balance between the addition of ATP-bound G-actin to the plus (i.e. "barbed") end of a filament, the dissociation of ADP-actin from the minus end of the polymer, and the retrograde flow of the actin filament bundle (Pollard and Borisy 2003; Le Clainche and Carlier 2008; Mattila and Lappalainen 2008). In this process there is tight coupling to the intrinsic ATP hydrolysis capacity of individual actin subunits in the F-actin filament. Ultimately, the dynamic sheet and finger-like shape alterations that are characteristic for lamellipodial and filopodial protrusions are determined by branching, cross-linking and bundling of the linear actin filaments. The tight spatial and temporal control of the formation and dissipation of these higher-order structures involves a broad set of actin-binding proteins, like filamins, Arp2/3, cofilin, profilin and capping proteins, all regulating specific steps of actin dynamics (dos Remedios, Chhabra et al. 2003; Mattila and Lappalainen 2008). In concert with this actin machinery, molecular motor proteins like the non-muscle myosin-II and -X generate the periodically contractile force and provide the cargo-transport role that is important for fate specification of lamellipodia and filopodia during cell migration and adhesion (Giannone, Dubin-Thaler et al. 2004; Zhang, Berg et al. 2004).

For the dynamic polymerization and filament-bundling of the actin cytoskeleton and for the control of movement and force generation by associated non-muscle myosin ATPases (Pollard and Borisy 2003; Schliwa and Woehlke 2003; Zhang, Berg et al. 2004) appropriate spatiotemporal regulation of ATP supply is needed (Huang, Minamide et al. 2008). Indeed, the weight of evidence in various studies now argues in favor of a model in which up to 50% of cellular energy

expenditure via ATP hydrolysis is required for actomyosin dynamics in cell types with a constantly changing morphology, like neurons, astrocytes and immune cells (Bernstein and Bamburg 2003; Hertz, Peng et al. 2007).

The intensively fluctuating rate of ATP turnover in mammalian cells with a high energy demand requires a robust system for supply, storage and distribution of energy in the form of high-energy phosphate compounds (Ames 2000; Dzeja, Terzic et al. 2004). Besides by direct generation of ATP via glycolytic kinases, or OXPHOS activity in the mitochondrial network, cells also fulfill this need via adenylate kinase (AK)-catalyzed phosphotransfer between the γ and β phosphate groups of ATP and ADP, or by creatine kinase (CK)-catalyzed phosphotransfer between phosphocreatine and ATP (Wallimann, Wyss et al. 1992; Dzeja, Terzic et al. 2004). CK and AK circuits demonstrate both redundancy and specialization in their ATP generating functions (Janssen, Terzic et al. 2003; Dzeja, Terzic et al. 2004; Ventura-Clapier, Kaasik et al. 2004).

As shown by experiments in muscle tissue of AK-knockout mouse models, AK activity has an important role in the control of energetic economy (Janssen, Dzeja et al. 2000), and recently we found that local AK1 expression facilitates motility of fibroblasts (van Horssen, Janssen et al. 2008). Muscle-type CKs (CK-M) have an important role in the control of contractile burst activity via maintenance of optimal local ATP/ADP ratios close to myosin ATPases in the contractile apparatus or by providing Ca^{2+}-ATPases preferential access to ATP for calcium sequestration (Steeghs, Benders et al. 1997; de Groof, Fransen et al. 2002). Another CK, the brain-type isoform (CK-B, expressed in a range of cell types), may have similar roles in fueling of ATP-dependent cytoskeletal processes in non-muscle cells like oligodendrocytes, astrocytes, macrophages, osteoclasts and tumor cells (Mulvaney, Stracke et al. 1998; Jost, Van Der Zee et al. 2002; Chang, Ha et al. 2008; Kuiper, Pluk et al. 2008). Functionally, CK-B is connected to spatial memory acquisition and behavior, development of the hippocampus (Jost, Van Der Zee et al. 2002), functioning of hair bundle cells in the auditory system (Shin, Streijger et al. 2007), phagocytosis (Kuiper, Pluk et al. 2008) and bone resorption (Chang, Ha et al. 2008). Despite extensive studies, the exact mechanisms by which CK-B activity controls these processes are still incompletely understood. A role in direct coupling of ATP

supply to actin-myosin dynamics is by far the most likely mechanism since cytoskeletal activity is central to all processes named above.

Here, we provide evidence for a direct mechanistic connection between CK-B mediated phosphotransfer activity and local actin remodeling during cell migration and morphological changes. We show that the subcellular distribution of CK-B partially overlaps with that of dynamic actin in protrusion-active cortical areas of astrocytes and fibroblasts, but not with static F-actin of stress fibers in these cells. CK-B activity in astrocytes and fibroblasts directly facilitates actomyosin-driven motility, as demonstrated by cell spreading and migration assays. Additionally, by using deliberate positional swapping of CK-B from a cytosolic to membrane-bound location, we show that spatial confinement of CK-B activity controls local actin dynamics and therewith determines morphology and migration behavior.

Results

CK-B expression in cultured primary astrocytes

Within the brain, CK-B is expressed at high levels in astrocytes (Jost, Van Der Zee et al. 2002; Tachikawa, Fukaya et al. 2004), which -in the *in vivo* context- are cells with highly dynamic surface extensions. We applied Western blot analysis to confirm that CK-B protein expression is also high in cultured primary astrocytes, *in vitro*. As anticipated, astrocytes derived from wild type (WT) mice gave a prominent signal, while control astrocytes derived from CK-B deficient mice (Jost, Van Der Zee et al. 2002) displayed no CK-B expression (**Figure 1a**). Immunostaining of CK-B in astrocytes revealed a diffuse cytoplasmic staining in most cells and strikingly, a number of cells displayed CK-B accumulation in peripheral patches. A magnification of the relevant cell area shows that these partially co-localize with phalloidin-stained actin. Interestingly, no overlap in localization was observed between the more prominent static actin stress-fibers and CK-B (**Figures 1b and c**).

CK-B co-localizes with cortical actin and facilitates spreading of astrocytes

To study the possible coupling between CK-B accumulation and local actin dynamics in more detail, we analyzed astrocyte spreading in presence and absence of cytochalasin D, an inhibitor of actin polymerization. We took cell spreading as this is

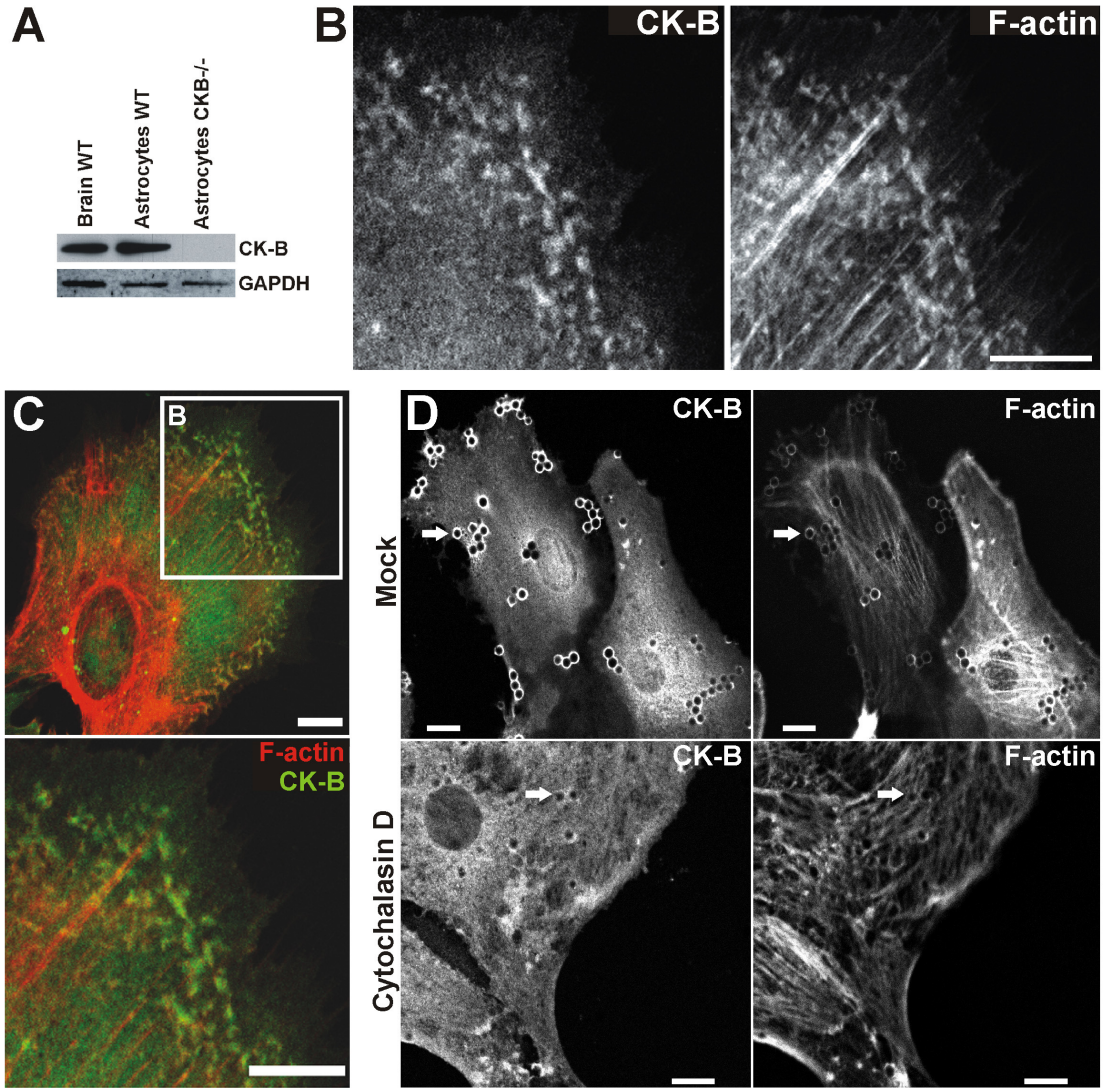

Figure 1. *CK-B localization in cultured astrocytes is F-actin dependent.*
(**A**) WT Brain tissue, cultured WT and CK-B knockout (CK-B-/-) astrocytes were analyzed for endogenous CK-B expression by Western blotting. GAPDH re-probing was used as protein loading control. (**B**) Astrocytes co-stained for CK-B and F-actin. CK-B expression is cytosolic and additionally observed in peripheral patches that also stain positive for F-actin. (**C**) Merge images of panel B revealed partial co-localization of CK-B and F-actin in peripheral patches but not in stress fibers. Bar, 10 μm. (**D**) WT astrocytes exposed to FN-coated latex beads were stained for CK-B and F-actin. Both CK-B and F-actin accumulated around the beads (arrows). Cytochalasin D (10 μM) treated wild type astrocytes (lower panels) lack accumulation of CK-B and F-actin around FN-beads (arrows). Bar, 10 μm.

a process that is partially analogous to cell migration and dependent on actomyosin dynamics (Cramer and Mitchison 1995; Mooney, Langer et al. 1995). During spreading, broad lamellipodial sheets and thin protrusions are formed, which are

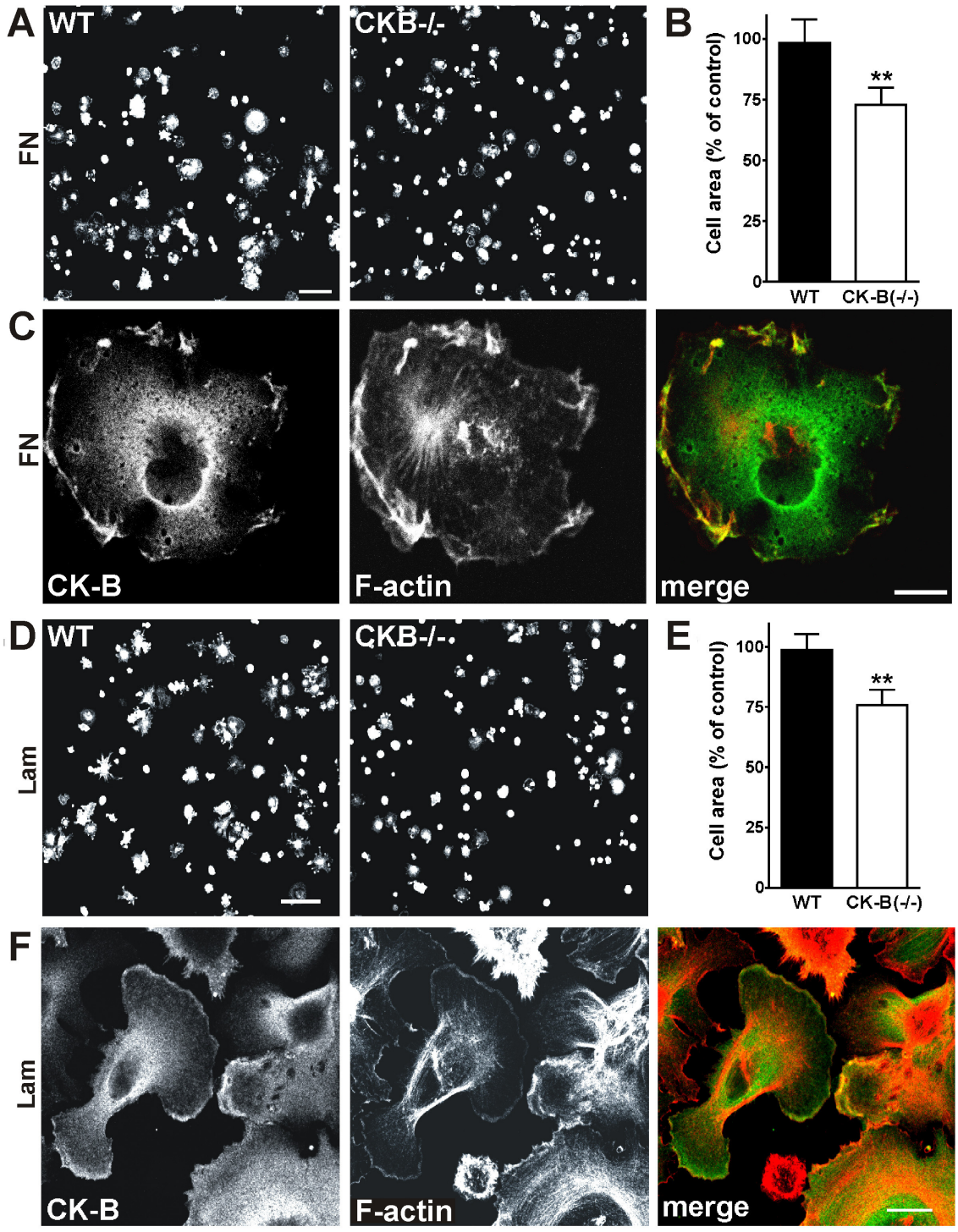

integrin- and receptor-rich and serve to "probe" the surrounding matrix and promote cell adhesion. Because cytochalasin D prevented astrocyte attachment in the conventional assay we used an approach by which fibronectin (FN)-coated beads were applied onto astrocytes as an "inverted adherence" assay (Cougoule, Wiedemann et al. 2004). In mock treated cells, CK-B and F-actin accumulated

Figure 2. *CK-B-/- astrocytes spread slower than wild type astrocytes.*
(**A**) Astrocytes derived from WT and CK-B(-/-) mice were compared in quantitative cell spreading assays. Cells were seeded on FN and 30 min after seeding the cells were fixed and stained for F-actin. Bar, 100 μm. (**B**) Quantification of astrocyte spreading on FN represented as a percentage of the control (see Materials and methods for details). (**C**) Astrocytes spreading on FN co-stained for CK-B and F-actin. CK-B is distributed throughout the cytoplasm and accumulation is seen at membrane ruffles. Co-localization with cortical F-actin is shown in the merged image. Bar, 10 μm. (**D**) Quantitative cell spreading assay using WT and CK-B-/- astrocytes. Cells were seeded on Laminin (Lam) and 30 min after seeding the cells were fixed and stained for F-actin. Bar, 100 μm (**E**) Quantification of astrocyte spreading on Lam showing decreased spreading capacities of CK-B-/- cells. (**F**) Astrocytes spreading on Lam co-stained for CK-B and F-actin. CK-B accumulation is seen at membrane ruffles. Co-localization with cortical F-actin is shown in the merged image. Bar, 10 μm

together at sites where FN-beads bound the cell membrane. In contrast, accumulation of F-actin and CK-B around beads was virtually absent in cells treated with cytochalasin D (**Figure 1d**) confirming the coupling between local CK-B accumulation and local actin dynamics.

To study the functional contribution of CK-B to astrocyte spreading, we performed cell spreading assays using WT and CK-B deficient (-/-) astrocytes. As shown in **Figure 2**, CK-B deficient cells consistently spreaded slower than their WT counterparts on both FN and laminin (Lam) although morphological appearances differed on both substrates. Under the experimental conditions used, the average area occupied by CK-B deficient cells was 27% smaller on FN and 24% smaller on Lam compared to WT cells (**Figures 2b and 2e** respectively; $p<0.005$; $N=3$). Intriguingly, in most cells, a fraction of CK-B and F-actin jointly accumulated to ruffles at the periphery in actively spreading cells, i.e. in areas where actin-based structures are most dynamic (**Figures 2c and 2f**). It is of note, that for both matrixes we never observed co-localization of CK-B with actin stress fibers. We consider these data in support of a link between actin polymerisation dynamics and recruitment of CK-B activity in sub-cortical microdomains of astrocytes during spreading.

CK-B enhances migration of astrocytes

Since spreading and migration events have analogous protrusive processes in

common, we wondered whether astrocyte migration was also affected by absence or presence of CK-B. Using the barrier migration assay (van Horssen, Galjart et al. 2006) we showed that WT-astrocytes migrated along FN matrices fairly efficiently (481 ± 15 μm distance covered in 48 hr; **Figure 3a** and Video 1) but that astrocytes without CK-B migrated at 46% lower rate (252 ± 22 μm distance covered in 48 hr, open bars in **Figure 3b**, $p<0.0001$). Moreover, migration distances of WT-astrocytes decreased to similar levels as observed for knockout cells, when cells were treated with the specific CK-inhibitor cyclocreatine (closed bars in **Figure 3b**, $p<0.0001$). We conclude that the difference in migration capacity is most likely directly attributable to the metabolic role of CK-B, i.e. its ATP generating capacity. Morphologically we did not observe major differences between migrating WT and CK-B deficient astrocytes.

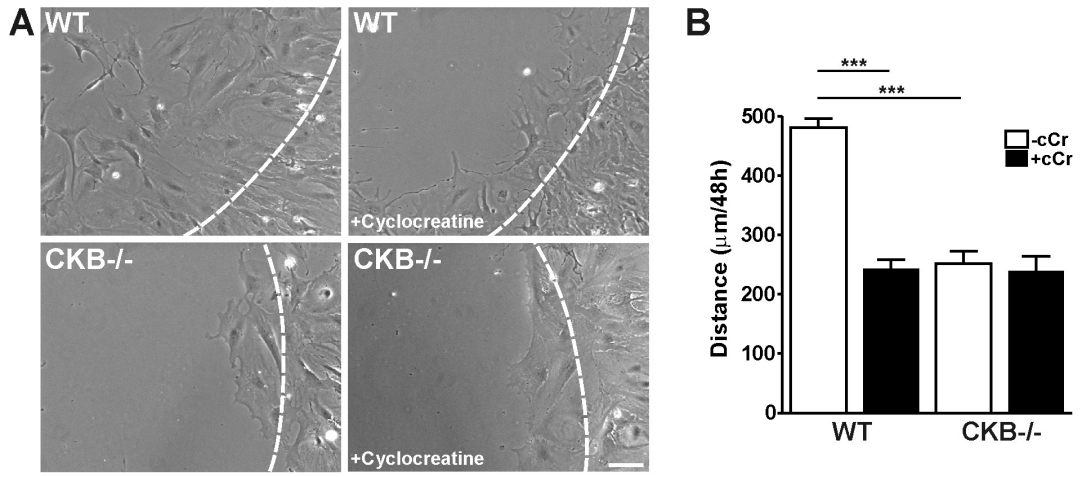

Figure 3. *Astrocyte migration is dependent on presence and activity of CK-B.*
(**A**) Migration assays of WT and CK-B-/- astrocytes with and without cyclocreatine (5 mM) treatment. Representative images of migrating cells after 24 h, obtained from migration movies (Video 1). Dashed lines indicate migration front at 0 h. Bar, 100 μm. (**B**) Average migration distances of astrocytes migrating along laminin (10 μg/ml). Note that both CK-B presence and activity are required for migration, *** $p<0.001$.

Subcellular targeting of CK-B affects migration and morphology in MEFs

Cell shape changes require highly coordinated activities of actin machinery that is localized (close) to the plasma membrane (Mattila and Lappalainen 2008). We designed a new experimental setting to test whether the observed recruitment of CK-

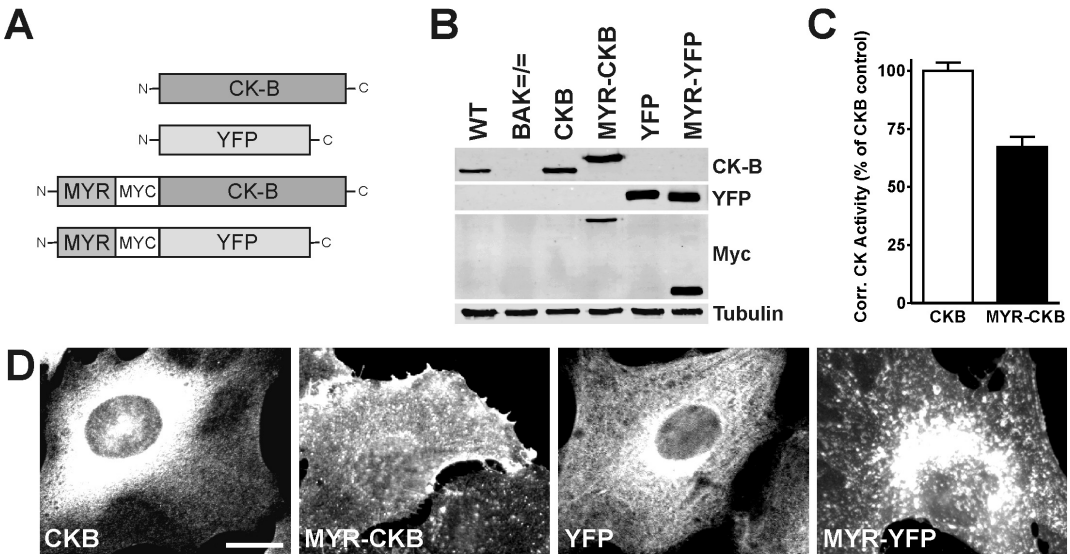

Figure 4. *Generation of membrane-targeted CK-B expressing MEFs.*
(**A**) Constructs used to complement MEF-BAK=/= cells with CK-B and membrane-targeted CK-B (MYR-CKB) and their corresponding YFP controls (not drawn to scale). (**B**) Western blot analysis of complemented MEF-BAK=/= cell lines. CK-B is seen in WT and (MYR)-CKB complemented cells, YFP in YFP complemented cells, Myc in membrane-targeted CK-B and YFP, Tubulin was used as protein loading control. (**C**) CK-activity in whole cell lysates corrected for CK-B protein expression. Coupling of MYR-domain to CK-B renders the enzyme less active (approximately 70% of native CK-B). (**D**) Distribution of (targeted) CK-B and YFP in the generated cell lines. CK-B and YFP show a rather homogeneous cytoplasmic distribution while MYR-CKB and MYR-YFP expressing cells showed staining of organellar and plasma membranes. Bar, 10 µm.

B from the general cytosolic pool and concentration of its activity at cortical regions would serve ATP-dependent reactions directed to this machinery. Since primary astrocytes have a limited life-span and are inherently difficult to work with in permanent transfection protocols, we decided to use a complementation strategy in mouse embryonic fibroblasts (MEFs) to investigate the coupling between CK-B mediated phosphotransfer and regional cytoskeletal remodeling in greater detail.

We chose to work in MEFs derived from CK-B/AK1 double knockout mice (MEF-BAK=/=). Activity of the ATP-generating enzyme AK1, which is expressed in MEF cells, is also linked to control of cell migration (van Horssen, Janssen et al. 2008) and partly interchangeable with CK activity for offering fuel-demanding systems access to ATP (Dzeja, Terzic et al. 2004). Removal of both enzymes therefore gave us the opportunity to study effects of redistribution of enzymatic

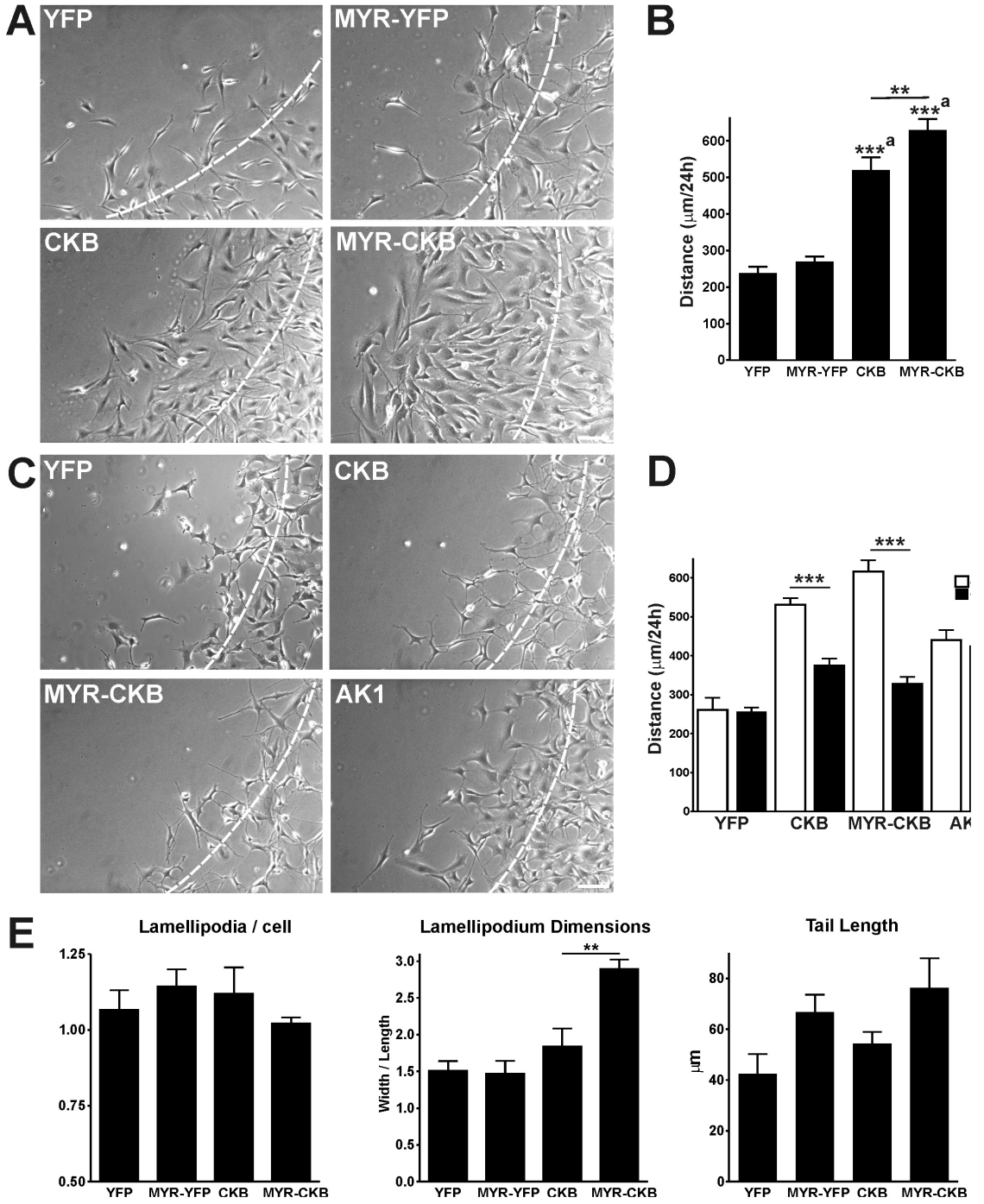

ATP/ADP exchange capacity without background effects. Re-expression of CK-B in MEF-BAK=/= cells was accomplished by retroviral infection. Cells were generated that express either cytosolic native CK-B or CK-B fused to a myristoylation (MYR)-tag, which provides a membrane-anchor function and (partly) redirects the enzyme to cellular membranes, thus enforcing accumulation of enzyme activity close to the sites with high cortical cytoskeletal plasticity. Control cell lines were generated by

Figure 5. *CK-B expression and localization increases fibroblast migration*
(**A**) Morphology of migrating MEFs. Pictures of migrating cells after 24 h obtained from migration movies (Video 2). Dashed lines indicate migration front at 0 h. Bar, 100 μm.
(**B**) Quantification of migration distances. MEF-CKB and MEF-MYR-CKB cells have higher migration capacities compared to the YFP-controls. Membrane targeting of CK-B further induces cell migration. Average migration distances in 24 h are shown, CK-B and MYR-CK-B compared to matched YFP controls, *** $p<0.001$, ** $p<0.01$. (**C**) Morphology of migrating MEFs with cyclocreatine (cCr, 5 mM) treatment. Pictures of migrating cells after 24 h obtained from migration movies (Video 3). Dashed lines indicate migration front at 0 h. Bar, 100 μm. (**D**) Migration distances after 24 h of MEFs migrating along FN with (closed bars) and without (open bars) cyclocreatine (cCr, 5 μM). MEF-CKB and MEF-MYR-CKB cells respond to cCr treatment while MEF-YFP and MEF-AK1 (van Horssen, Janssen et al. 2008) controls do not. *** $p<0.001$ compared to non-treated cells. (**E**) Quantification of migration morphology. The number of lamellipodia per cell, lamellipodium dimensions and tail length were measured from migration movies. No differences were found for the YFP-complemented cells (open bars), MYR-CKB complemented cells showed an increased lamellipodium width/length ratio compared to CK-B complemented cells (closed bars, ** $p<0.01$). Measurements explanation and zoom-in images are depicted in Fig. S2.

introduction of YFP variants (**Figure 4a**). Expression levels of native CK-B and MYR-CKB were comparable between the two complemented cell lines and 2-3 times higher than that of endogenous CK-B in WT MEFs (**Figure 4b**). Importantly, CK activity in cells complemented with MYR-CKB was about 30% lower than that in cells complemented with CK-B (normalized for CK-B expression levels; **Figure 4c**). This finding can be most easily explained by the observation that CKs expressed as N-terminal fusion proteins with β-galactosidase, GST or other peptide tags generally have a somewhat lower specific enzymatic activity (data not shown). Staining with CK-B specific antibodies or direct visualization of YFP fluorescence revealed a diffuse cytosolic distribution for CK-B and YFP in the MEF-CKB and MEF-YFP cell pools, as anticipated. Analysis of MYR-CKB and MYR-YFP cell lines confirmed that a significant part of CK-B and YFP protein was located at plasma and organellar membranes (**Figure 4d**).

Migration analysis (presented in **Figure 5a** (left panels) and **Figure 5b**) showed that re-expression of CK-B doubled the fibroblast migration capacity as compared to YFP-complemented controls (513 ± 23 vs. 246 ± 33 μm; $p<0.0001$).

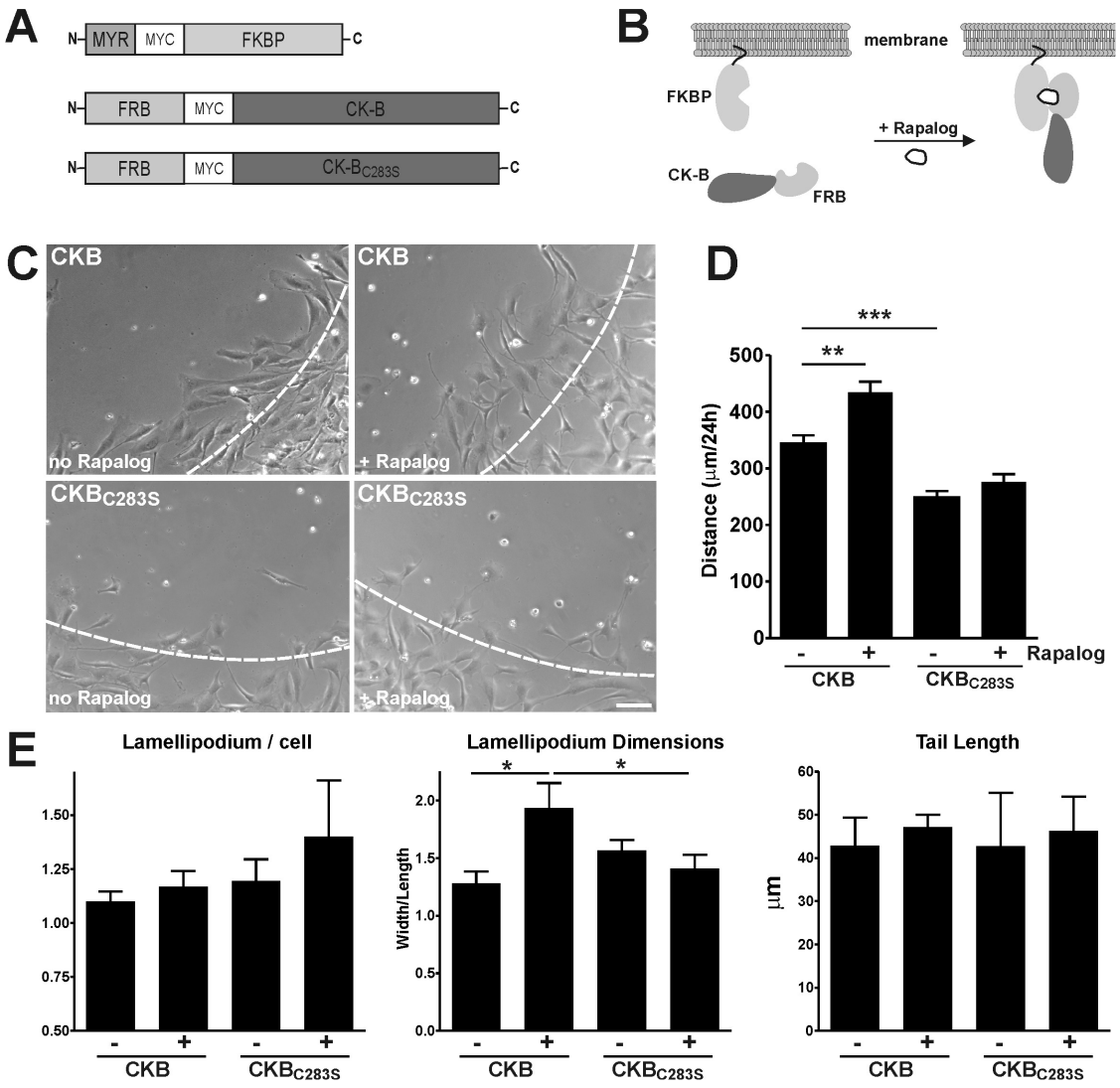

Figure 6. *Rapalog-induced translocation of CK-B to membranes induced migration*

(**A**) Constructs used to target CK-B, CK-B$_{C283S}$ to cellular membranes. Vector inserts are not drawn to scale. (**B**) Scheme of heterodimerization of the MYR-FKBP fragment with FRB-CKB on cellular membranes upon Rapalog addition. (**C**) Migration morphology of MEFs after 24 hr in absence or presence of Rapalog (Video 4). Dashed lines indicate migration front at 0 h. Bar, 100 µm. (**D**) Quantification of migration distances of MEF-MYR-FKBP complemented with FRB-CKB or FRB-CKB$_{C283S}$ with and without Rapalog-treatment. Rapalog-induced translocation of FRB-CKB, in contrast to FRB-CKB$_{C283S}$, enhanced cell migration. *** $p<0.001$, ** $p<0.01$. (**E**) Quantification of migration morphology. The number of lamellipodia per cell, lamellipodium dimensions and tail length were measured from migration movies. Lamellipodium dimensions for FRB-CKB with Rapalog-treatment was significantly changed. * $p<0.05$. See Fig. S4B for corresponding enlarged images of the migration front.

This result corroborates the astrocyte migration data and underscores that our findings on CK-B effects can be extrapolated to other cell types. Interestingly, anchoring of CK-B to membranes (MYR-CKB), thereby mimicking the change in distribution that occurs naturally in motile cells with CK-B, had a clear stimulatory effect on motility (**Figures 5a and 5b**, Video 2). Migration distances in MYR-CKB cells were increased by a factor 2.4 (623 ± 28 vs 262 ± 21 μm, $p<0.0001$) when compared to control MYR-YFP cells and also significantly enhanced compared to cells with non-tagged CK-B (21 %, $p=0.0042$). As indicated above, this latter effect could be even underestimated, because overall enzymatic activity in cells with MYR-CKB was 30% lower than in cells with native CK-B. Enzymatic activity of CK-B was indispensable since cyclocreatine completely blocked the gain in migration capacity in both CK-B expressing cell pools (**Figures 5c and 5d**, Video 3) without overt effects on viability or proliferation rate (**Figure S1**). It is of note here that the directionality of cell movements, being the ratio of the direct distance from start to end point to the total migrated distance, was similar for all tested cell lines (data not shown). Thus, migratory capacity is increased without changing the type of cell movement. Additionally, we observed that the morphological appearance of migrating MEF-MYR-CKB differed from that of MEF-CKB, and displayed a more flat morphology with broad lamellipodia. Quantification of the lamellipodium dimensions (width/length of lamellipodium including lamella, measured in μm after 24 h or migration, see **Figure S2**) revealed that lamellipodia in migrating MYR-CKB cells

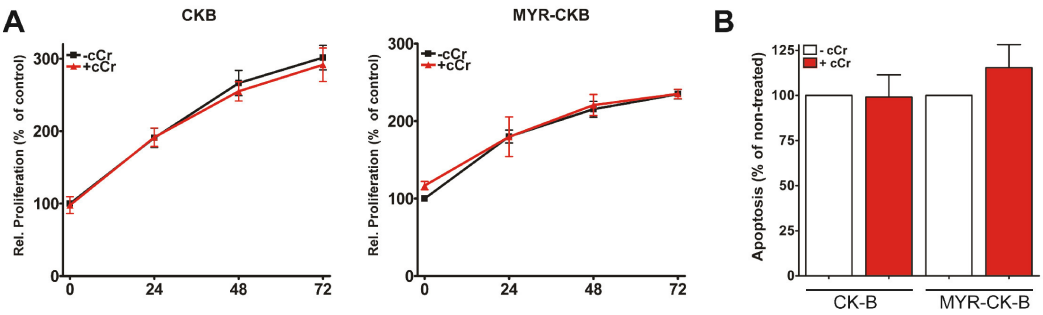

Figure S1. *Cyclocreatine does not alter proliferation and apoptosis*

(**A**) Proliferation of MEF-CKB (left) and MEF-MYR-CKB (right) cells with (red) and without (black) cCr (5 mM). Relative proliferation rates, taking non-treated cells as control, are shown of three independent experiments. (**B**) Apoptosis of MEF-CKB and MEF-MYR-CKB cells cultured without (open bars) and with (red bars) cCr (5 mM). Non-treated cells were set as 100% to compare cCr effect.

were broader, but not longer (ratio = 2.9 ± 0.2, p=0.0017), compared to dimensions in cells with native CK-B, YFP or MYR-YFP (ratios of 1.8 ± 0.3, 1.5 ± 0.1, 1.5 ± 0.2, respectively; See **Figure 5e** for quantification and **Figure S2** for high magnification images of migration fronts). In contrast, the number of lamellipodia per cell and the tail length of migrating cells appeared unaffected by the presence or specific localization of CK-B. To determine if any of the observed functional consequences of altered ATP supply capacity are also associated with matrix adhesion and extension as seen in spreading astrocytes, we performed spreading assays with the MEF lines (**Figure S3**). We observed no change in spreading capacity in MEFs with native CK-B, but MEFs with MYR-anchored CK-B covered a 25% larger area than MEFs without CK-B or with native CK-B under the experimental conditions used, confirming the importance for local CK-B in actin-dependent cell processes.

Inducible translocation of CK-B to membranes: motility and morphological analyses

Finally, we sought to uncouple effects of enzyme location from effects of enzyme level and activity in an independent approach. We reasoned that analyzing effects of manipulation of the intracellular spatial distribution of CK-B within the same cell would provide the most effective strategy. Therefore, we used the rapamycin dimerizer system (Castellano, Montcourrier et al. 1999) and engineered pools of MEF-BAK=/= cells with the constructs for inducible targeting of CK-B that are shown in **Figure 6a and 6b**. One vector was designed for expression of FK506-binding protein (FKBP) with a MYR-anchor for targeting to membranes (MYR-FKBP). Other vectors were destined for expression of active CK-B or CK-B_{C283S}, a catalytic-dead protein, both with N-terminal extensions consisting of the FK506-Rapamycin Binding (FRB) domain. Upon addition of Rapalog (rapamycin analog AP21967), inducible translocation of a significant fraction of cytosolic distributed CK-B and CK-B_{C283S} to membranes occurred, as verified by immunofluorescent staining (**Figure S4a**). Results of analysis of migration capacity of different MEFs in the presence and absence of Rapalog are shown in **Figure 6c** and Video 4. Quantification of video data showed that cells expressing native CK-B migrated significantly faster than cells expressing the enzymatically inactive CK-B_{C283S}, independent of Rapalog-mediated induction.

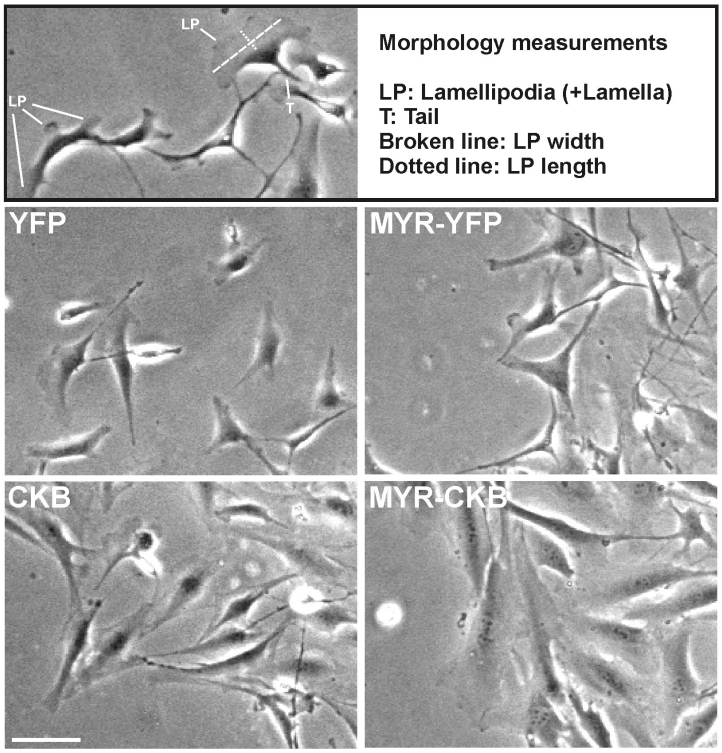

Figure S2. *Morphology measurements of migrating MEFs.*
Top panel shows the way of analysis of migration morphology. The number of lamellipodia per cell, the lamellipodium dimensions (width and length measured with cell body as reference, lamellipodium includes lamella-region) and tail length was measured. Lower panels show high magnification images of migration fronts of complemented MEFs and correspond to Fig. 5A. Bar, 50 µm.

Secondly, when Rapalog was added during migration of cells with enzymatically active CK-B to redirect (part of) CK-B to membranes, distances increased from 344 ± 15 to 434 ± 19 µm over the period measured (3 independent experiments, p=0.0021). Addition of Rapalog did not alter locomotion of CK-B$_{C283S}$ expressing cells (**Figure 6d**). Together, these results indicate that covalent or interactive fusion of CK-B with FRB or FRB-FKBP does not impede CK-B intrinsic capacity to promote cell migration, and corroborate our finding that cell cortical presence of functional activity and not the mere structural presence of CK-B protein is essential (**Figure 5**). Since we noted earlier that permanent targeting of CK-B to membranes changed the lamellipodium dimensions in MEFs, we also assessed whether morphological changes would be inducible with Rapalog-treatment (**Figure 6e and Figure S4b**). Rapalog addition to CK-B MEFs caused a significant increase in the ratio of lamellipodium dimensions to 1.9 ± 0.2, compared to 1.3 ± 0.1 in non-treated cells (p=0.0219). Importantly, Rapalog did not show this effect in MEFs expressing CK-B$_{C283S}$, demonstrating that this effect solely depended on relocalisation of the

enzymatic activity of CK-B and was not caused by non-specific effects of CK-B binding or the Rapalog treatment itself.

Discussion

Actin-driven processes need considerable amounts of ATP to facilitate cytoskeletal dynamics. ATP exchange and hydrolysis is thereby critically involved in the process of actin treadmilling, controlled by recycling of G-actin and the stability of F-actin (Le Clainche and Carlier 2008) and is also important for the activity of many actin-associated proteins. In the present study, we investigated the contribution of local ATP generation by CK-B to actomyosin dynamics by measuring spreading and motility of astrocytes and MEFs. Straightforward immunofluoresence and Western blot assays demonstrated that cultured astrocytes from mouse brain express high levels of CK-B, which corroborates findings with immunostaining and in-situ hybridization on whole mouse brain that appeared in other reports (Sistermans, de Kok et al. 1995; Jost, Van Der Zee et al. 2002). Furthermore, it was demonstrated that astrocytes can synthesize creatine endogenously suggesting that a functional CK phosphoryl-transfer system is present in these cells (Dringen, Verleysdonk et al. 1998; Braissant, Henry et al. 2001). Recently, an emerging role of astrocytes as active modulators of synaptic transmission has been acknowledged. In this process, which depends on the intimate physical interactions between astrocytes and neurons, local actin-driven dynamics of astrocytic protrusions play an organizing and maintaining role (Hirrlinger, Hulsmann et al. 2004; Haber, Zhou et al. 2006). Based on this knowledge, we propose that astrocytes use a significant amount of their ATP for cytoskeletal remodeling, comparable to the ATP need for actomyosin activity in neurons (Bernstein and Bamburg 2003) .

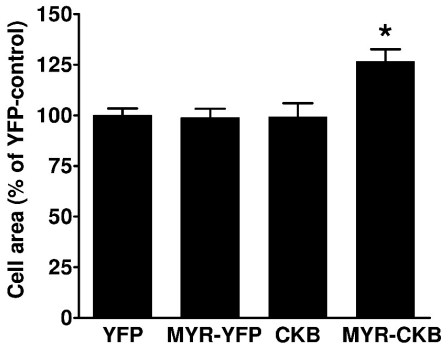

Figure S3. *MEF-MYR-CKB cells spread out faster than MEF-CKB cells.*
Quantification of MEF spreading on FN for 30 min, showing that expression of MYR-CK-B facilitates cell spreading.
* $p<0.05$.

Besides astrocytes, we also used mouse embryonic fibroblasts (MEFs) as archetypal motile cells for study of the localized role of CK-B in cell dynamics. Our data on recruitment of CK-B from the cytosolic pool and it's transient co-accumulation in areas with cortical F-actin but not with the less dynamic F-actin in stress fibers in both cell types support the idea that CK-B activity is generally most needed at sites where the actin cytoskeleton is highly dynamic. This idea was already proposed for the accumulation of CK-B in nascent phagosomes as well (Kuiper, Pluk et al. 2008). Interesting parallels can also be drawn to the fate of the muscle specific isoform of CK, CK-M, which is strategically localized in the M-band of myofibrils to support localized myosin ATPase activity (Wallimann and Eppenberger 1985), or is recruited to the I-band by binding to the glycolytic enzymes phosphofructokinase and aldolase (Kraft, Hornemann et al. 2000). CK-B lacks essential lysine residues that are required for CK-M accumulation at the M-band (Hornemann, Kempa et al. 2003), but in view of its high homology with CK-M, it is temping to speculate that other mechanisms for recruitment may be shared between the two enzymes. Especially, the possible interaction with glycolytic enzymes capable of binding to F-actin should be studied further as several of these enzymes are enriched in lamellipodia (Beckner, Chen et al. 2005) and other types of dynamic cell structures (de Hoog, Foster et al. 2004). We know already that CK-B and CK-M have an interchangeable character with respect to recruitment in the phagocytic cup of macrophages (data not shown), but the precise mechanistic link between protrusion formation and CK recruitment remains to be elucidated.

The direct functional link between CK-B activity and cell shape changes was clarified by our cell spreading and migration assays, in which ablation of CK-B slowed down these processes in both astrocytes and MEFs. Overall, findings between astrocytes and MEFs were comparable, only CK-B effects on spreading were not reproduced in MEF tests. Cell spreading is a complex process consisting of substrate adherence and passive-descent events, later followed by active probing of the cellular environment (Cuvelier, Thery et al. 2007). These later events in spreading may be more reliant on infrastructural organization within the cell and be cell-type dependent. The observed discrepancies between the roles of soluble and anchored CK-B in spreading of astrocytes and MEFs may therefore be explained by

differences in the relative importance of CK-mediated ATP supply during the early and late phases, and be not easily comparable between cell types.

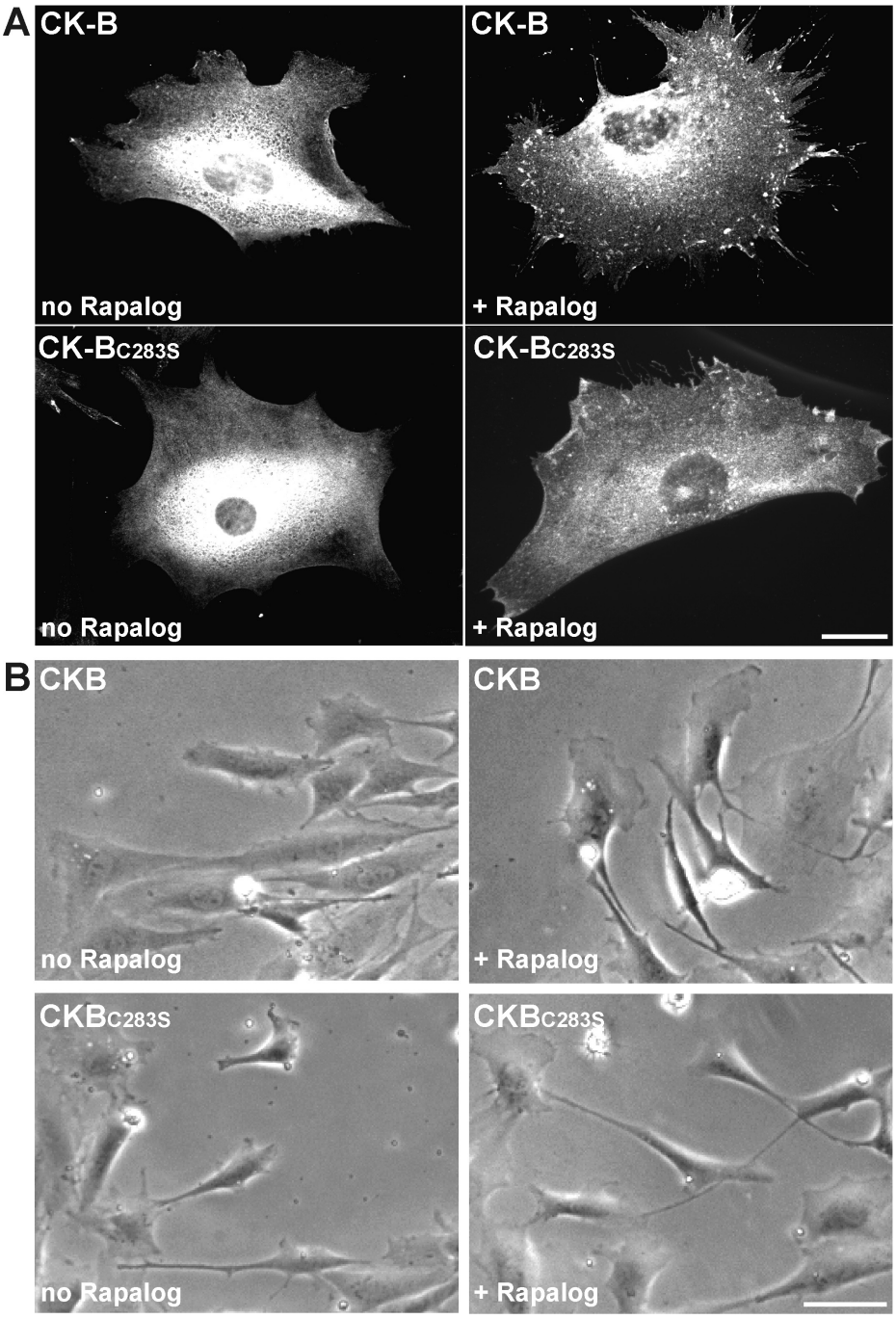

Figure S4. *Rapalog-induced membrane localization of CK-B and CK-B$_{C238S}$ in MEFs.*
(**A**) MEF-BAK=/= cells stably expressing MYR-FKBP were retrovirally transduced with FRB-CK-B (upper panels) or CK-B$_{C283S}$ (lower panels) and stained for CK-B. Rapalog treatment (100 nM, 1h, left panels) resulted in translocation of (a fraction of) CK-B and CK-B$_{C283S}$ to cellular membranes. Bar, 10 µm (**B**) High magnification images of migration fronts of are shown, corresponding to Fig. 6C. CK-B (upper panels) and CK-B$_{C238S}$ (lower panels) without (left) and with (right) Rapalog treatment. Measurements were the same as shown in Fig. S2. Bar, 50 µm.

Importantly, the experiments with pharmacological inhibition with cyclocreatine or substitution of native CK-B by the catalytically dead CK-B$_{C283S}$ in the positional swapping/tagging experiments demonstrated that the contribution of CK-B to enhanced cell migration capacity did not depend merely on its structural interference, but that its catalytic ATP-generating activity is required.

We propose that cells use CK-B to balance ATP/ADP ratios and buffer temporary demands for ATP in specialized structures with highly dynamic actin, such as lamellipodia and filopodia, to sustain optimal migration rates. The early observation that cyclocreatine was able to inhibit motility in tumor cells (Mulvaney, Stracke et al. 1998) and the long known importance of ATP for actin polymerization and myosin force generation (Pollard and Borisy 2003; Giannone, Dubin-Thaler et al. 2004) support this model.

One most conspicuous finding in our studies was that manipulation of CK-B location had an effect on both migratory capacity and lamellipodial morphology in MEFs. Interestingly, targeting CK-B to membranes changed the lamellipodial dimensions. Formation of lamellipodia is largely dependent on branched actin polymerization at the cell's periphery, which requires the availability of free ATP-loaded actin monomers (Pollard and Borisy 2003; Le Clainche and Carlier 2008). The process of re-loading of G-actin with ATP and incorporation of actin monomers at linear-barbed or branched-ends of polymeric filaments could be the decisive step that takes advantage of local ATP generated by CK-B. Our experimental verification of this obviously speculative model showed that CK-B with a membrane anchor could indeed facilitate lamellipodia formation and stimulated cell migration. Interestingly, expression of native cytosolic CK-B had an effect on migratory capacity but did not enhance lamellipodium formation proper. This suggests that other (ATP dependent) migration promoting processes, which are morphologically more difficult to delineate and therefore association with local CK-B recruitment goes undetected, may also be fuelled by CK-B. Although speculative, actin mediated adhesion (Galbraith, Yamada et al. 2007) or myosin force generation (Giannone, Dubin-Thaler et al. 2004; Gupton and Waterman-Storer 2006) may be examples of such directly served processes. Earlier it has been suggested that CK-B may provide bursts of site-specific high-energy phosphate for signal transduction involved in cytoskeletal reorganisation

(Mahajan, Pai et al. 2000). In this latter process association of CK-B to the C-tail of protease activated receptor-1 (PAR-1) is involved. Whether similar stimulating activities of CK-B at other cellular locations would also require regional accumulation of enzyme is completely unknown.

By using the Rapalog heterodimerizer system, we were able to manipulate the localization of CK-B without altering the total cellular levels of CK-B, thus excluding effects of variation in activity levels or in genetic or metabolic background between cells in our pool. As rapamycin is reported to inhibit F-actin reorganization (Liu, Chen et al. 2008), we verified that Rapalog (a chemically modified derivative of rapamycin) itself did not influence cell motility (data not shown). We feel that our observations with this system, i.e. the finding that migratory capacity and cell morphology are truly directly responsive to the localization of CK-B, underscore the importance that site-specific availability of ATP has for local cytoskeletal dynamics. Besides CK-B, also other enzymes have been reported to act as local distributors of ATP at actin-rich structures. For example, translocation of adenylate kinase (AK1) to focal contacts sites in MEFs induced migratory capacity of these cells (van Horssen, Janssen et al. 2008). Other regulators of nucleoside-triphosphates levels (NTPs), such as nm23-H2 and arginine kinase, translocate to actin-rich cellular protrusions and lamellipodia and regulate their dynamics (Wang, Esbensen et al. 1998; Fournier, Dupe-Manet et al. 2002). As yet other examples, glycolytic enzymes form complexes that partition at specific subcellular locations such as pseudopodia (Beckner, Chen et al. 2005), actin filaments (Schmitz and Bereiter-Hahn 2002) and phagosomes (Garin, Diez et al. 2001) and may have an energy supply role there. In Drosophila flight muscle, glycolytic multienzyme complexes provide myosin ATPases with preferential access to ATP when brought in close vicinity by physical protein-protein interactions (Wojtas, Slepecky et al. 1997). Different cells may therefore use different systems to fulfill the ATP needs of active actomyosin.

In summary, data presented here demonstrate that cytoskeletal dynamics involved in cell extension and motility are dependent on the enzymatic activity of CK-B. Our findings suggest that locally generated ATP is an important regulator for actin-behavior in subcellular compartments and that CK-B is a controlling enzyme in the inhomogeneity and compartmentalization of ATP availability. This model also

provides a plausible explanation for our earlier findings on synaptic function and development of neural cell networks in CK-B knockout mice (Jost, Van Der Zee et al. 2002), on epithelial hair cell function in the inner ear of (Shin, Streijger et al. 2007), and on impairment of bone remodeling activity of osteoclasts (Chang, Ha et al. 2008) of these mice. In an analogous study we recently showed that CK-B fuels local actin dynamics in phagocytosis (Kuiper, Pluk et al. 2008). All processes mentioned have in common that they are dependent on the functional integrity and timely control of actin filament nucleation, elongation and associated motor protein activity in cell cortical areas that forms ruffles or membrane tubulation areas. More research is required to investigate whether the precise mechanistic events that connect CK-B mediated ATP supply with actin in this axis are shared between different CK-expressing cell types.

Materials and methods

Cell culture

Primary cultures of astrocytes were established from embryonic wild type (C57BL/6 x 129Ola) or CK-B deficient mice (Jost, Van Der Zee et al. 2002) at embryonic day 17 (E17) as described (Hoop de, Meyn et al. 1998), verified for astrocyte isolation by immunofluorescence staining for the astrocyte marker glial fibrillary acid protein (GFAP) and cultured for 2-3 weeks in Dulbecco's Modified Eagle Medium (DMEM, Gibco) supplemented with 4 mM glutamine, 2 mM sodium pyruvate, 10% Fetal Calf Serum (FCS) and 0.5 mg/ml gentamycin. Mouse embryonic fibroblasts (MEFs) and Phoenix (HEK293) packaging cells were maintained in the same medium without gentamycin. MEFs were derived from wild type (C57BL/6 x 129Ola) or CK-B/AK1 double knock-out mice. To generate CK-B/AK1 double knock out (BAK=/=) mice, CK-B deficient mice (Jost, Van Der Zee et al. 2002) were mated with Adenylate Kinase-1 (AK1) deficient mice (Janssen, Dzeja et al. 2000). Mice were genotyped and lack of CK-B and AK1 was confirmed by Western blot and zymogram analysis. MEFs derived from the double knock out (MEF-BAK=/=) were immortalized using established techniques (Rittling 1996) and used for retroviral complementation studies.

Retroviral constructs and transfections

cDNA encoding CK-B, myristoylation tagged CK-B (MYR-CK-B) and their YFP controls were cloned into the EcoR1/Xho1 sites of the retroviral transfection vector pLZRS-IRES-Zeo (Michiels, van der Kammen et al. 2000). The MYR-localization tag was introduced 5'-upstream of the myc-tagged CK-B and YFP by PCR using primers containing BamHI sites to amplify a 50 bp MYR-domain segment from AK1β cDNA (Collavin, Lazarevic et al. 1999). Natural start codons in the CK-B and YFP ORF were substituted by alanine codons to ensure the use of the ATP start codon of the MYR-domain. Inducible translocation of CK-B to membranes was studied using the ARGENT Regulated Heterodimerization Kit (ARIAD Pharmaceuticals), based on the rapamycin-induced heterodimerization of FKBP- and FRB-tagged proteins. The FKBP fragment (316 bp) from the pC4EN-F1 plasmid (ARIAD) was PCR-amplified, provided with EcoRI/XhoI sites, and cloned into the pLZRS-IRES-Zeo behind the MYR-myc sequence to generate the targeting construct. Subsequently, a 276 bp FRB fragment was PCR-amplified from plasmid pC4-RhE (ARIAD) with primers containing BamHI/BglII sites and cloned into the BamHI site upstream of the myc-tagged CK-B or CK-B_{C283S} (catalytic death mutant) sequence in vector pLZRS-IRES-Zeo. Constructs and targeting principle are depicted in **Figure 6a** and 6B, respectively. Mixed pools of MEF-BAK=/= cells that co-expressed proteins with FKBP or FRB moieties were generated by sequential retroviral transduction. To generate retrovirus, Phoenix cells grown on poly-L-lysine (10 μg/ml) coated 6-wells plates were transfected with retroviral pLZRS constructs (5 μg) using Lipofectamine 2000 (10 μl, Invitrogen) diluted in Optimem (Gibco) according to the manufacturers protocol. Viral medium was harvested, polybrene (5 μg/ml) was added, filtered and used to infect MEF-BAK=/= cells grown to 40% confluence. After 24 h, medium was replaced by medium containing zeocin (450 μg/ml) and cells were cultured under selection for at least two weeks. Cells were analyzed for protein expression by western blotting and immunofluorescence.

Western blotting

Astrocyte cell lysates were prepared in lysisbuffer (12.5 mM Na_2HPO_4, 2.8 mM KH_2PO_4, 0.05% Triton X-100, 0.3 mM DTT) containing protease inhibitor cocktail

(Roche). After incubation on ice (20 min) the cell lysates were centrifuged for 10 min at 13000 rpm and supernatants were collected. MEFs were lysed directly in sample buffer or in NP-40 Buffer (50 mM Tris-HCl, pH 7.5, 100 mM NaCl, 5 mM $MgCl_2$, 1% NP-40, 1 mM PMSF and 1x protease inhibitor cocktail) and protein content was determined using the Bradford method. Samples were resolved by 10% SDS-PAGE and blotted onto nitrocellulose membranes. Subsequently, the membranes were blocked with PBS containing 5% non-fat milk, blots were probed with anti-CK-B (21E10, 1:2000) (Sistermans, de Kok et al. 1995), polyclonal anti-CK-B, 1:2000 (de Kok, Geurds et al. 1995), anti-myc (1:100, Developmental Studies Hybridoma Bank, University of Iowa), anti-YFP, 1:3000 (Cuppen, Wijers et al. 1999), anti-GAPDH (1:3000, Trevigen) and anti-Tubulin (1:2000, Developmental Studies Hybridoma Bank, University of Iowa) for 1 hr at RT or overnight at 4ºC. Antibodies were detected with HRP-conjugated goat-anti-mouse IgG (1:10000, Jackson ImmunoResearch) and the signal was developed with the HRP substrate Lumi-Light system (Roche). Alternatively, blots were incubated with goat-anti-mouse IRDye800 (Rockland) and goat-anti-mouse Alexa680 (Molecular Probes) simultaneously and signals were detected using the Odyssey Imaging System (LI-COR Biosciences).

Immunofluorescence

Cells were grown on glass cover slips, washed twice in PBS and fixed with 2% paraformaldehyde in PHEM buffer (25 mM HEPES, 10 mM EGTA, 60 mM PIPES, 2 mM $MgCl_2$, pH 6.9). Subsequently, cells were permeabilized with 0.1% Triton X-100 or 0.1% saponin and incubated for 20 min in PBS containing 1% bovine serum albumin (BSA). Incubation with primary and secondary antibodies was done for 1 h and in between incubations the cells were washes thrice with PBS. Primary antibodies used: polyclonal anti-GFAP (1:500, DAKO), monoclonal anti-CK-B (21E10, 1:2000) and polyclonal anti-CK-B (1:2000). Secondary goat-anti-mouse and goat-anti-rabbit conjugated to Alexa 488 or Alexa 568 (1:500, Molecular Probes). F-actin was visualized by phalloidin conjugated to Alexa 660 or TexasRed (Molecular Probes). Samples were dehydrated in 70% and 100% ethanol, air dried and mounted onto microscope slides using mowiol. Samples were analyzed on a Biorad MRC1024 laser scanning confocal microscope using an oil immersion 60x objective or on an

Axiovert 35M fluorescence microscope using 63x and 100x oil immersion objectives (Carl Zeiss).

Cell spreading assay

Cover slips were coated with laminin (40 μg/ml) or fibronectin (50 μg/ml) for 2 hours at 37ºC. Cells were collected by centrifugation, washed in DMEM/1% BSA, fatty acid free and incubated in DMEM/1% BSA for 20 minutes at 37 ºC before seeding onto coated cover slips. After 30 minutes spreading on coated cover slips, cells were washed once with PBS and fixed in 2% paraformaldehyde. Cells were permeabilized and stained for CK-B and TexasRed conjugated phalloidin (Molecular Probes). For every cover slip 5 to 9 random fields were imaged with a Biorad Confocal Microscope MRC1024 using a 10x objective. The total surface occupied by cells was determined by ImageJ software (http://rsb.info.nih.gov/ij) and divided by the number of cells to calculate the area per cell. Five random fields were analyzed in each of 3 independent experiments. For every experiment the ratio between knockout and wild type was calculated (wildtype set at 100%).

Cell migration assays and time-lapse microscopy

Barrier migration assays were performed as described previously (van Horssen, Galjart et al. 2006). Briefly, a coverslip was placed in an Attofluor incubation chamber (Molecular Probes) which was subsequently sterilized and coated with fibronectin. In this set up a removable, sterile circular migration barrier was placed creating a two compartment culture chamber which prevents cell growth into the middle of the coated cover slip. Cells were seeded around this barrier and grown until confluence. Subsequently, the migration barrier was removed and cells were washed twice before being incubated with the appropriate medium. MEFs were starved 4-24 h in DMEM containing 0,2% FCS and 5 mg/ml fatty-acid free BSA before bFGF (200 ng/ml, Peprotech) was added to stimulate migration. Astrocytes were analyzed in standard culture medium without starvation. Time-lapse imaging of migrating cells was done for 24 h in a Microscope Stage Incubator (Oko-Lab, Italy), ensuring proper culture conditions, using a Nikon DiaPhot equipped with a Hamamatsu C8484-05G digital camera. Images were taken every 10 min using TimeLapse Software (Oko-

Lab), version 2.7 with a 10X objective. Using time-lapse movies, cells were tracked taking nuclei as reference. For each treatment at least 8 migrating cells of 3 or 4 independent migration assays were analyzed. After cell division one of the daughter cells was followed. The total track distance (T) and the direct distance from start to end point (D) were measured. Measurements were done using Metamorph 6.2 software (Universal Imaging Corporation).

Adhesion of fibronectin-coated beads to astrocytes

Polystyrene latex beads (3 μm, Sigma) were sonificated and coated by incubation in carbonate buffer (pH 9.6) with fibronectin (100 μg/ml) for 2 hours. The beads were washed twice in PBS and resuspended in serum free DMEM containing cytochalasin D (10 μm, Sigma) or DMSO as control before seeding onto cultured astrocytes. After incubation with FN-beads for 30 min at 37 ºC/5% CO_2, cells were fixed and immunostained for CK-B and F-actin as described above.

Proliferation and apoptosis assays

Proliferation rates and apoptosis of cyclocreatine-treated and control cells were determined using the WST-1 proliferation assay (Roche) and the Apo-ONE Homogeneous Caspase 3/7 Assay (Promega) according to manufacturers' protocols. MEFs were seeded at 5000 and 10000 cells per well for proliferation and apoptosis assays respectively. Proliferation was measured for time points op to 72 h. Apoptosis was measured in semi-confluent MEFs treated with cyclocreatine (5 mM, Sigma) for 24 h, staurosporin (0.5 μM, Sigma) was used as positive control.

CK activity assay

CK activity was determined by enzyme coupled reactions using the Liquid NAC activated UV test (Human GmbH, Germany) according to manufactures' protocol. Cell lysates were prepared in NP-40 lysis buffer (50 mM Tris-HCL pH 7.5, 100 mM NaCl, 5 mM $MgCl_2$, 1% NP-40, 1 mM PMSF, 1x protease inhibitor cocktail). Activity was normalized to CK-B content by performing quantitative western blotting in the same samples.

Rapalog-induced membrane-targeting of CK-B

Translocation of CK-B from the cytosolic pool to cellular membranes within the same cell was done using the dimerization strategy based on the heterodimeration of FKBP and FRB protein domains by Rapalog (Castellano, Montcourrier et al. 1999). MEF-BAK=/=, stably transfected with MYR-FKBP and non-transfected MEF-BAK=/= cells (control), were retrovirally transduced with FRB-CK-B or FRB-CK-B_{C283S} and directly (passage 2-8) used for further analysis. Rapalog-treated (200 nM, ARIAD) and untreated cells were analyzed for subcellular positioning of CK-B or CK-B_{C283S} and cell migration was monitored.

Statistics

Data are presented as mean ± SEM of at least three independent experiments. Groups were compared with Student's t-test for single values, one-sample t-test for relative values and with Ratio t-test for ratio-values and considered significant different when $p<0.05$.

Legends for online supplemental videos

Videos are available at: http://www.ncmls.eu/celbio

Video 1. *CK-B mediates astrocyte migration.*

WT (upper panels) and CK-B-/- (lower panels) astrocytes migrating along laminin for 48 h. Migration assays were performed without (left panels) and with (right panels) cyclocreatine treatment. Both CK-B knockout and inhibition strongly decreased migratory behavior of astrocytes. Video corresponds with Figure 3a. Time-lapse phase-contrast microscopy was performed taking an image every 10 min. Display rate is 10 frames/s.

Video 2. *CK-B expression and localization affects MEF migration.*

YFP/MYR-YFP complemented (upper panels) and CK-B/MYR-CKB complemented MEFs migration along FN for 24 h. Migration assays of non-targeted (left panels) and membrane-targeted (right panels) cells showed that CK-B induced migration and additionally that MEF-MYR-CKB were the most motile. Video

corresponds with Figure 5a. Time-lapse phase-contrast microscopy was performed taking an image every 10 min. Display rate is 10 frames/s.

Video 3. *Cyclocreatine selectively inhibits CK-B-induced migration.*
MEF-YFP, MEF-CKB, MEF-MYR-CKB and MEK-AK1 cells were followed during migration along FN. In contrast to YFP and AK1 complemented MEFs, MEF-CKB and MEF-MYR-CKB migration was inhibited by cCr and an strong morphological effect was observed. Video corresponds with Figure 5c. Time-lapse phase-contrast microscopy was performed taking an image every 10 min. Display rate is 10 frames/s.

Video 4. *Repositioning of CK-B to cellular membranes induces migration.*
MEF-MYR-FKBP cells transfected with FRB-CKB (upper panels) or FRB-CKB_{C283s} (lower panels) and allowed to migrate along FN without (left panels) and with Rapalog (right panels). CK-B complemented and additionally its targeting to membranes induced migration compared to the mutant CK-BC_{283s}. Video corresponds to Figure 6c. Time-lapse phase-contrast microscopy was performed taking an image every 10 min. Display rate is 10 frames/s.

Acknowledgements
We thank Marieke Willemse and Rinske van de Vorstenbosch for experimental assistance, Helma Pluk and Ad de Groof for useful discussions and Huib Croes for help with microscopy experiments. This work was supported by NWO ZON-MW Program grant 901-01-191 and by a KWF Kankerbestrijding grant from the Dutch Cancer Society.

References

Ames, A. r. (2000). "CNS energy metabolism as related to function." Brain Res Brain Res Rev 34(1-2): 42-68.

Beckner, M. E., X. Chen, et al. (2005). "Proteomic characterization of harvested pseudopodia with differential gel electrophoresis and specific antibodies." Lab Invest 85(3): 316-27.

Bernstein, B. W. and J. R. Bamburg (2003). "Actin-ATP hydrolysis is a major energy drain for neurons." J Neurosci 23(1): 1-6.

Braissant, O., H. Henry, et al. (2001). "Endogenous synthesis and transport of creatine in the rat brain: an in situ hybridization study." Brain Res Mol Brain Res 86(1-2): 193-201.

Castellano, F., P. Montcourrier, et al. (1999). "Inducible recruitment of Cdc42 or WASP to a cell-surface receptor triggers actin polymerization and filopodium formation." Curr Biol 9(7): 351-60.

Chang, E. J., J. Ha, et al. (2008). "Brain-type creatine kinase has a crucial role in osteoclast-mediated bone resorption." Nat Med.

Collavin, L., D. Lazarevic, et al. (1999). "wt p53 dependent expression of a membrane-associated isoform of adenylate kinase." Oncogene 18(43): 5879-88.

Cougoule, C., A. Wiedemann, et al. (2004). "Phagocytosis, an alternative model system for the study of cell adhesion." Semin Cell Dev Biol 15(6): 679-89.

Cramer, L. P. and T. J. Mitchison (1995). "Myosin is involved in postmitotic cell spreading." J Cell Biol 131(1): 179-89.

Cuppen, E., M. Wijers, et al. (1999). "A FERM domain governs apical confinement of PTP-BL in epithelial cells." J Cell Sci 112 (Pt 19): 3299-308.

Cuvelier, D., M. Thery, et al. (2007). "The universal dynamics of cell spreading." Curr Biol 17(8): 694-9.

de Groof, A. J., J. A. Fransen, et al. (2002). "The creatine kinase system is essential for optimal refill of the sarcoplasmic reticulum Ca2+ store in skeletal muscle." J Biol Chem 277(7): 5275-84.

de Hoog, C. L., L. J. Foster, et al. (2004). "RNA and RNA binding proteins participate in early stages of cell spreading through spreading initiation centers." Cell 117(5): 649-62.

de Kok, Y. J., M. P. Geurds, et al. (1995). "Production of native creatine kinase B in insect cells using a baculovirus expression vector." Mol Cell Biochem 143(1): 59-65.

dos Remedios, C. G., D. Chhabra, et al. (2003). "Actin binding proteins: regulation of cytoskeletal microfilaments." Physiol Rev 83(2): 433-73.

Dringen, R., S. Verleysdonk, et al. (1998). "Metabolism of glycine in primary astroglial cells: synthesis of creatine, serine, and glutathione." J Neurochem 70(2): 835-40.

Dzeja, P. P., A. Terzic, et al. (2004). "Phosphotransfer dynamics in skeletal muscle from creatine kinase gene-deleted mice." Mol Cell Biochem 256-257(1-2): 13-27.

Fournier, H. N., S. Dupe-Manet, et al. (2002). "Integrin cytoplasmic domain-associated protein 1alpha (ICAP-1alpha) interacts directly with the metastasis suppressor nm23-H2, and both proteins are targeted to newly formed cell adhesion sites upon integrin engagement." J Biol Chem 277(23): 20895-902.

Friedl, P. and K. Wolf (2003). "Tumour-cell invasion and migration: diversity and escape mechanisms." Nat Rev Cancer 3(5): 362-74.

Galbraith, C. G., K. M. Yamada, et al. (2007). "Polymerizing actin fibers position integrins primed to probe for adhesion sites." Science 315(5814): 992-5.

Garin, J., R. Diez, et al. (2001). "The phagosome proteome: insight into phagosome functions." J Cell Biol 152(1): 165-80.

Giannone, G., B. J. Dubin-Thaler, et al. (2004). "Periodic lamellipodial contractions correlate with rearward actin waves." Cell 116(3): 431-43.

Gupton, S. L. and C. M. Waterman-Storer (2006). "Spatiotemporal feedback between actomyosin and focal-adhesion systems optimizes rapid cell migration." Cell 125(7): 1361-74.

Haber, M., L. Zhou, et al. (2006). "Cooperative astrocyte and dendritic spine dynamics at hippocampal excitatory synapses." J Neurosci 26(35): 8881-91.

Hertz, L., L. Peng, et al. (2007). "Energy metabolism in astrocytes: high rate of oxidative metabolism and spatiotemporal dependence on glycolysis/glycogenolysis." J Cereb Blood Flow Metab 27(2): 219-49.

Hirrlinger, J., S. Hulsmann, et al. (2004). "Astroglial processes show spontaneous motility at active synaptic terminals in situ." Eur J Neurosci 20(8): 2235-9.
Hoop de, M. J., L. Meyn, et al. (1998). Culturing hippocampal neurons and astrocytes from fetal rodent brain. Cell Biology: a laboratory handbook. J. E. Celis. San Diego, Academic Press. 1: 154-163.
Hornemann, T., S. Kempa, et al. (2003). "Muscle-type creatine kinase interacts with central domains of the M-band proteins myomesin and M-protein." J Mol Biol 332(4): 877-87.
Huang, T. Y., L. S. Minamide, et al. (2008). "Chronophin mediates an ATP-sensing mechanism for cofilin dephosphorylation and neuronal cofilin-actin rod formation." Dev Cell 15(5): 691-703.
Janssen, E., P. P. Dzeja, et al. (2000). "Adenylate kinase 1 gene deletion disrupts muscle energetic economy despite metabolic rearrangement." Embo J 19(23): 6371-81.
Janssen, E., A. Terzic, et al. (2003). "Impaired intracellular energetic communication in muscles from creatine kinase and adenylate kinase (M-CK/AK1) double knock-out mice." J Biol Chem 278(33): 30441-9.
Jost, C. R., C. E. Van Der Zee, et al. (2002). "Creatine kinase B-driven energy transfer in the brain is important for habituation and spatial learning behaviour, mossy fibre field size and determination of seizure susceptibility." Eur J Neurosci 15(10): 1692-706.
Kraft, T., T. Hornemann, et al. (2000). "Coupling of creatine kinase to glycolytic enzymes at the sarcomeric I-band of skeletal muscle: a biochemical study in situ." J Muscle Res Cell Motil 21(7): 691-703.
Kuiper, J. W., H. Pluk, et al. (2008). "Creatine Kinase-Mediated ATP Supply Fuels Actin-Based Events in Phagocytosis." PLoS Biol 6(3): e51.
Le Clainche, C. and M. F. Carlier (2008). "Regulation of actin assembly associated with protrusion and adhesion in cell migration." Physiol Rev 88(2): 489-513.
Liu, L., L. Chen, et al. (2008). "Rapamycin inhibits F-actin reorganization and phosphorylation of focal adhesion proteins." Oncogene 27(37): 4998-5010.
Mahajan, V. B., K. S. Pai, et al. (2000). "Creatine kinase, an ATP-generating enzyme, is required for thrombin receptor signaling to the cytoskeleton." Proc Natl Acad Sci U S A 97(22): 12062-7.
Mattila, P. K. and P. Lappalainen (2008). "Filopodia: molecular architecture and cellular functions." Nat Rev Mol Cell Biol 9(6): 446-54.
Michiels, F., R. A. van der Kammen, et al. (2000). "Expression of Rho GTPases using retroviral vectors." Methods Enzymol 325: 295-302.
Mooney, D. J., R. Langer, et al. (1995). "Cytoskeletal filament assembly and the control of cell spreading and function by extracellular matrix." J Cell Sci 108 (Pt 6): 2311-20.
Mulvaney, P. T., M. L. Stracke, et al. (1998). "Cyclocreatine inhibits stimulated motility in tumor cells possessing creatine kinase." Int J Cancer 78(1): 46-52.
Pollard, T. D. and G. G. Borisy (2003). "Cellular motility driven by assembly and disassembly of actin filaments." Cell 112(4): 453-65.
Rittling, S. R. (1996). "Clonal nature of spontaneously immortalized 3T3 cells." Exp Cell Res 229(1): 7-13.
Schliwa, M. and G. Woehlke (2003). "Molecular motors." Nature 422(6933): 759-65.
Schmitz, H. D. and J. Bereiter-Hahn (2002). "Glyceraldehyde-3-phosphate dehydrogenase associates with actin filaments in serum deprived NIH 3T3 cells only." Cell Biol Int 26(2): 155-64.
Shin, J. B., F. Streijger, et al. (2007). "Hair bundles are specialized for ATP delivery via creatine kinase." Neuron 53(3): 371-86.
Sistermans, E. A., Y. J. de Kok, et al. (1995). "Tissue- and cell-specific distribution of creatine kinase B: a new and highly specific monoclonal antibody for use in immunohistochemistry." Cell Tissue Res 280(2): 435-46.
Steeghs, K., A. Benders, et al. (1997). "Altered Ca2+ responses in muscles with combined mitochondrial and cytosolic creatine kinase deficiencies." Cell 89(1): 93-103.
Swanson, J. A. (2008). "Shaping cups into phagosomes and macropinosomes." Nat Rev Mol Cell Biol 9(8): 639-49.
Tachikawa, M., M. Fukaya, et al. (2004). "Distinct cellular expressions of creatine synthetic enzyme GAMT and creatine kinases uCK-Mi and CK-B suggest a novel neuron-glial relationship for brain energy homeostasis." Eur J Neurosci 20(1): 144-60.

van Horssen, R., N. Galjart, et al. (2006). "Differential effects of matrix and growth factors on endothelial and fibroblast motility: application of a modified cell migration assay." J Cell Biochem 99(6): 1536-52.
van Horssen, R., E. Janssen, et al. (2008). "Modulation of cell motility by spatial repositioning of enzymatic ATP/ADP exchange capacity." J Biol Chem.
Ventura-Clapier, R., A. Kaasik, et al. (2004). "Structural and functional adaptations of striated muscles to CK deficiency." Mol Cell Biochem 256-257(1-2): 29-41.
Wallimann, T. and H. M. Eppenberger (1985). "Localization and function of M-line-bound creatine kinase. M-band model and creatine phosphate shuttle." Cell Muscle Motil 6: 239-85.
Wallimann, T., M. Wyss, et al. (1992). "Intracellular compartmentation, structure and function of creatine kinase isoenzymes in tissues with high and fluctuating energy demands: the 'phosphocreatine circuit' for cellular energy homeostasis." Biochem J 281 (Pt 1): 21-40.
Wang, Y. E., P. Esbensen, et al. (1998). "Arginine kinase expression and localization in growth cone migration." J Neurosci 18(3): 987-98.
Wojtas, K., N. Slepecky, et al. (1997). "Flight muscle function in Drosophila requires colocalization of glycolytic enzymes." Mol Biol Cell 8(9): 1665-75.
Zhang, H., J. S. Berg, et al. (2004). "Myosin-X provides a motor-based link between integrins and the cytoskeleton." Nat Cell Biol 6(6): 523-31.

Chapter - 4 -

Creatine kinase B deficient neurons exhibit an increased fraction of motile mitochondria

Jan W.P. Kuiper, Frank T.J.J. Oerlemans, Jack A.M. Fransen and Bé Wieringa

BMC Neuroscience, 2008, 9:73

Abstract

Neurons require an elaborate system of intracellular transport to distribute cargo throughout axonal and dendritic projections. Active anterograde and retrograde transport of mitochondria serves in local energy distribution, but at the same time also requires input of ATP. Here we studied whether brain-type creatine kinase (CK-B), a key enzyme for high-energy phosphoryl transfer between ATP and CrP in brain, has an intermediary role in the reciprocal coordination between mitochondrial motility and energy distribution. Therefore, we analysed the impact of brain-type creatine kinase (CK-B) deficiency on transport activity and velocity of mitochondria in primary murine neurons and made a comparison to the fate of amyloid precursor protein (APP) cargo in these cells, using live cell imaging.

Comparison of average and maximum transport velocities and global transport activity showed that CK-B deficiency had no effect on speed of movement of mitochondria or APP cargo, but that the fraction of motile mitochondria was significantly increased by 36% in neurons derived from CK-B knockout mice. The percentage of motile APP vesicles was not altered.

CK-B activity does not directly couple to motor protein activity but cells without the enzyme increase the number of motile mitochondria, possibly as an adaptational strategy aimed to enhance mitochondrial distribution versatility in order to compensate for loss of efficiency in the cellular network for ATP distribution.

Introduction

Neurons, by virtue of their unique architecture, have developed specific transport systems to regulate anterograde and retrograde flow of macromolecules, vesicles or organelles between the cell body and distal regions in the axon and dendrites. To maintain efficiency and directionality in the bidirectional flow of these cellular constituents strict control over movement of cargo by motor proteins on cytoskeletal elements such as microtubules, intermediate filaments, and actin, is needed (Goldstein and Yang 2000; Brown 2003; Chen and Chan 2006). One of the basic elements in this control is adequate fuelling with ATP, the major carrier of cellular energy. Homeostasis of global and compartmentalized ATP levels, i.e. regulation of production, distribution, and consumption of intracellular ATP, is controlled by an elaborate metabolic network, which varies with cell type. In neurons this circuit involves both cytosolic-glycolytic and oxidative mitochondrial production pathways and a high level of ATP consumption for fuelling of acto-myosin dynamics, ion transporters, and neurotransmitter cycling activity in the synapse (Lim, Hall et al. 1983; Lipton and Robacker 1983; Bernstein and Bamburg 2003). Neurons use glucose from the circulation as the main carbohydrate source for ATP production, but – depending on specific physiological conditions - a fair percentage of their energy may also be derived from lactate, which they exchange with astrocytes (Ames 2000; Pellerin and Magistretti 2004), or from ketone bodies imported from circulation. Because of the highly branched morphology of neurons, sites of energy consumption are usually spatially separated from sites of energy generation in this cell type. Since diffusion of ATP might usually be too slow to achieve optimal supply of high-energy phosphoryl groups (~P), neurons have developed more efficient mechanisms for transport and distribution of ~P. One way to minimize the diffusion distance of ATP and regulating natural inhomogeneity in ATPs intracellular distribution is by redirecting mitochondria to sites were ATP demand is high, e.g. in the vicinity of synapses (Verstreken, Ly et al. 2005). This requires active mitochondrial transport, which is mainly driven by members of the kinesin and dynein superfamilies of microtubule directed motor proteins such as KIF1Bα and

KIF5 (Nangaku, Sato-Yoshitake et al. 1994; Tanaka, Kanai et al. 1998), although, actin guided motility may also be involved (Morris and Hollenbeck 1995; Sturmer, Baumann et al. 1995; Vale 2003).

An alternative strategy to optimize spatial energy transfer within cells is to relay high-energy phosphoryl groups (~P) by enzymatic transfer systems, such as the creatine kinase (CK) family of isozymes (Dzeja and Terzic 2003). These enzymes buffer ATP and ADP levels by the reversible transfer of ~P onto creatine (Cr) ($MgATP^{2-}$ + Cr ↔ $MgADP^{-}$ + CrP^{2-} + H^{+}) (Wallimann and Hemmer 1994; Dzeja and Terzic 2003). Indeed, CKs are mainly expressed in tissues with high energy-turnover and sudden rises in energy demand, such as muscle and brain (van Deursen, Heerschap et al. 1993; Jost, Van Der Zee et al. 2002). Ubiquitous mitochondrial CK (UbCKmit) and cytosolic brain-type CK (CK-B) are the two predominant isoforms in brain (Jost, Van Der Zee et al. 2002; Tachikawa, Fukaya et al. 2004) and broadly distributed throughout neurons (moderate-low expression) and glial cells (high expression in astrocytes and microglia) across different brain areas. The CK system provides cells with both a temporal and spatial energy buffer (Wallimann and Hemmer 1994; Dzeja and Terzic 2003). During transient rises in energy consumption, the CrP pool is addressed by CK to provide the cell with ATP (van Deursen, Heerschap et al. 1993; Steeghs, Benders et al. 1997). In addition, CK isozymes connect spatially separated subcellular locales of ATP generation and ATP hydrolysis (Saks, Khuchua et al. 1994; Dzeja, Bortolon et al. 2002)

We have demonstrated that genetic ablation of CK-B in mice causes changes in behavior, diminished performance in spatial learning tasks and delayed development of pentylenetetrazole-induced seizures (Jost, Van Der Zee et al. 2002). Furthermore, the intra- and infrapyramidal mossy fiber areas in CK-B-/- mice appeared increased. We explained these features by diminished synaptic plasticity or compensatory adaptation with altered neuronal outgrowth during development.

Here we investigated whether compromised intracellular energy transport could underlie the diminished synaptic plasticity or altered morphology (in analogy to (Wong, Setou et al. 2002; Guillaud, Setou et al. 2003; Yuen, Jiang et al. 2005)).

Intracellular transport in neurons is comprised of membranous organelles and cytoplasmic proteins (or protein complexes) that are conveyed from the cell body to

the synapse, and vice versa, by either fast or slow axonal transport (Brown 2003). In general, movement of organelles is mediated by fast axonal transport, whereas cytosolic and cytoskeletal proteins move at a slower pace. This difference in velocity is attributed to the duty ratio of the motor proteins involved in both types of transport (Shah and Cleveland 2002; Brown 2003).

CK-B was identified in slow component B (SCb) which, together with slow component A (SCa), make up the branch of slow axonal transport (Brady and Lasek 1981). However, it is not known if CK-B facilitates this particular type of axonal transport, or that it is merely transported as inert cargo to subcellular destinations where it is needed. To address the question whether CK-B enzymatically contributes to axonal transport in more detail, we compared cultured primary hippocampal neurons derived from CK-B knockout and wildtype mice and monitored the fate of YFP tagged amyloid precursor protein (APP) as a representative component in fast transport. This type of transport correlates with a high duty ratio of motor proteins and with high ATPase activity. In addition, we analysed mitochondrial dynamics. Our results suggest that CK-B does not influence the velocity of intracellular transport of APP or mitochondria in neurons. Rather, cells deficient in CK-B display show a conspicuous alteration in magnitude of transport, concomitant with an increase in the fraction of motile mitochondria.

Results

Distribution of CK-B in primary neurons

To assess effects of CK-B efficiency in primary neurons, we used a co-culture system of hippocampus-derived neurons on a monolayer of primary astrocytes (see material and methods). Neuronal expression of CK-B has been demonstrated in several organisms, but not much is known about its subcellular localization (Friedman and Roberts 1994; Hemmer, Zanolla et al. 1994).

Immunolocalization on murine hippocampal neurons of different age with an isoform-specific antibody (Sistermans, de Kok et al. 1995) showed that CK-B was evenly distributed throughout the entire cell body, and rarely detected in the nucleus.

Figure 1 displays confocal images of hippocampal neurons, which were cultured for 1, 3 or 6 days *in vitro* (**Figure 1a,b** and **c**, respectively). No obvious changes were observed in either the intensity or localization of CK-B during the 6-day culture period. Neurons derived from CK-B knockout mice did not display any positive immunostaining with our antibody, demonstrating specificity of our assay (data not shown). In addition to localization studies, we also performed zymogram analysis on cultured primary neurons to assess enzymatic activity. As expected, CK-B catalytic activity was present in wildtype cells, but was completely absent in CK-B knockout cells (**Figure 1d**).

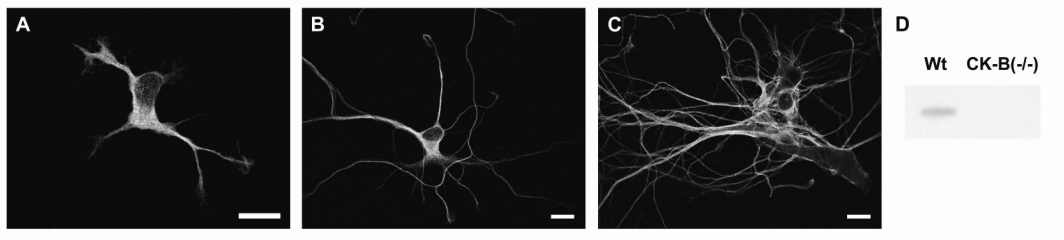

Figure 1. Primary neurons derived from wildtype mice were co-cultured with astrocytes for 1, 3 and 6 days. Subsequently, the cells were fixed and immunostained with an isoform specific monoclonal antibody against CK-B (21E10). Confocal images display the subcellular distribution of CK-B after A) 1 day, B) 3 days and C) 6 days. Image bars represent 10 µm. D) Lysates were prepared from wildtype and CK-B deficient neurons (7 div) and zymogram analysis was applied to determine enzymatic CK activity.

APP-transport in CK-B deficient neurons

To investigate a possible role for CK-B in axonal transport, we focused on the amyloid precursor protein (APP). APP is a membrane spanning type-1 protein which is conveyed from the cell body to the synapse by fast axonal transport (Koo, Sisodia et al. 1990; Kaether, Skehel et al. 2000; Kamal, Stokin et al. 2000). The kinesin KIF-I was identified as the tubulin directed motor protein responsible for APP transport (Kamal, Stokin et al. 2000) and real time live imaging revealed that APP fused to Yellow Fluorescent Protein (YFP) is transported over long distances with speeds up to 9 µm/s (Kaether, Skehel et al. 2000). To maintain this dynamics a continuously high supply of ATP is needed for motor protein functioning. To test whether CK-B

mediated ~P transfer has a role in safeguarding this process, we compared the appearance and movements of APP containing vesicles in wildtype and CK-B knockout neurons after transfection with YFP-tagged APP. In **Figure 2a** we show 5 successive frames of a time-lapse registration of a cell with APP-YFP. Careful analysis demonstrated that APP was transported in elongated tubular vesicles, confirming earlier observations by Kaether *et al.* (Kaether, Skehel et al. 2000). Vesicle appearance did not overtly differ between wildtype and CK-B knockout cells. For further comparison, 45 and 53 APP-YFP containing vesicles from wildtype and knockout cells, respectively, were tracked and their average velocities calculated. **Figure 2b** shows that the distribution of velocities was similar for both types of cells.

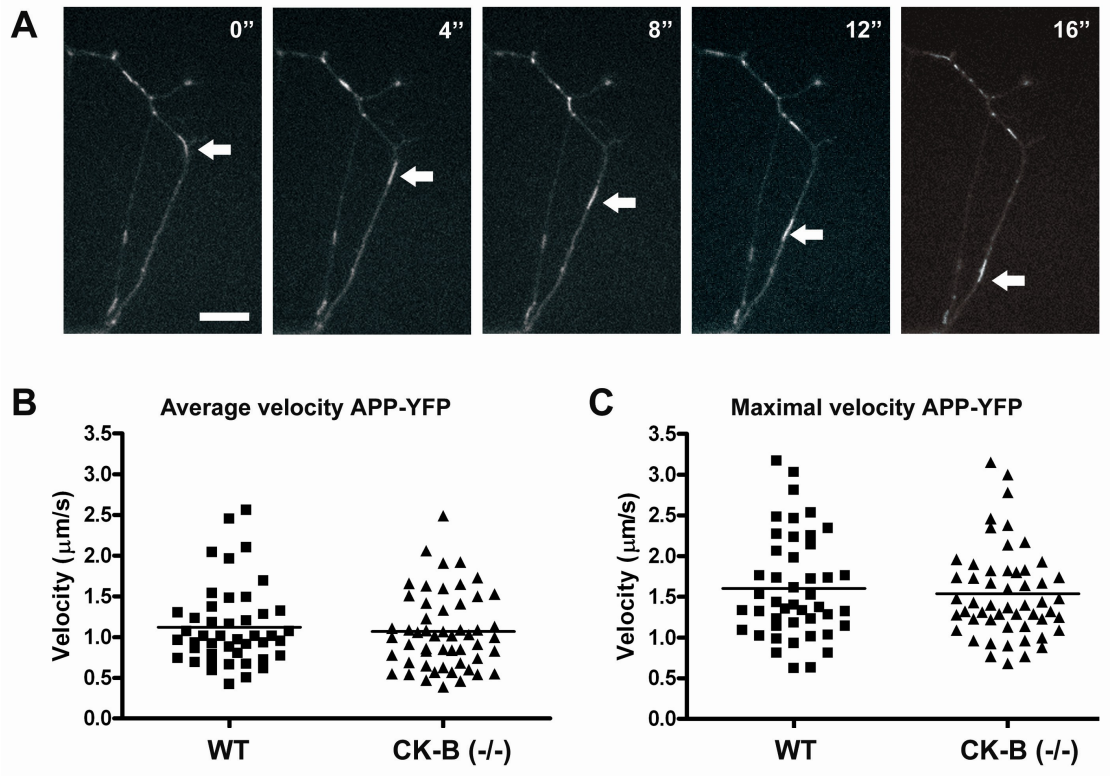

Figure 2. 7-day-old CK-B deficient and wildtype neurons were transfected with plasmid DNA encoding APP-YFP. After 24 hours cells were subjected to live imaging at 37□C and 5% CO2. Panel A shows 5 successive captures of a transfected neuron. An APP-YFP-containing vesicle, which traverses the neuron, is marked by arrows. The bar represents 10 µm. B) The average velocity of APP-YFP positive vesicles in both wildtype and CK-B deficient neurons was calculated and plotted in the diagram. For wildtype and CK-B (-/-) cells 45 vesicles and 53 vesicles were tracked, respectively. C) Maximum velocities for individual particles of wildtype and CK-B knockout cells were also plotted.

On average, APP-YFP vesicles moved at 1.12 ± 0.49 and 1.07 ± 0.47 μm/s for wildtype and CK-B knockout, respectively. Because vesicles sometimes changed their speed during time-lapse recording, we also calculated the maximum velocity for each vesicle during one recording. In **Figure 2c** these maximum values are displayed. Maximal velocities found were comparable, with 1.60 ± 0.62 μm/s for APP-YFP vesicles in wildtype cells and 1.54 ± 0.55 μm/s for CK-B knockout cells. Also no difference was found in the distribution of maximal velocities. Both knockout and wildtype vesicles reach maximal velocities up to 3 μm/s. It may be of note here, that this is 3 times slower than the maximum and 4 times slower than the average velocities of APP reported in rat primary neurons (Kaether, Skehel et al. 2000).

Mitochondrial transport in CK-B deficient neurons

Mitochondrial transport and repositioning is an important mechanism for neurons to comply with alterations in local energy demand. Fission, fusion and intracellular motility are essential processes involved in the regulation of subcellular distribution of mitochondria. It is therefore not surprising that many neurodegenerative diseases are associated with perturbations of these processes (Chan 2006; Chen and Chan 2006). To investigate if CK-B coordinates the fueling role and transport fate of mitochondria, we compared the dynamic behavior of mitochondria between primary hippocampal neurons from wildtype and CK-B knockout mice. Staining with rhodamine 123 to visualize mitochondria and time-lapse recording and subsequent image analysis were used to determine the average mitochondrial velocity (**Figure 3a**). Mitochondria included in the analysis traveled a minimum of 3 frames and were tracked till they stopped or reversed direction. Mitochondria from wildtype cells traveled at an average velocity of 0.59 ± 0.26 μm/s, which was almost identical to CK-B knockout cells (0.57 ± 0.24 μm/s). Furthermore, frequency histogram analysis revealed no differences in the distribution of average mitochondrial velocity (**Figure 3b**), suggesting that there is also no subset of mitochondrial movements that is affected by CK-B deficiency. Because a single mitochondrion could vary its speed during the cause of one movement, we also calculated the maximum speed for every mitochondrion during its recording period. The bar-diagram in **Figure 3c** displays

the average of maximal reached speeds of all tracked mitochondria in wildtype (1.13 ± 0.43 μm/s) and CK-B deficient cells (1.07 ± 0.38 μm/s). A frequency distribution diagram of maximal speeds also revealed no significant differences in maximal velocities of mitochondria between knockout and wildtype cells (**Figure 3d**).

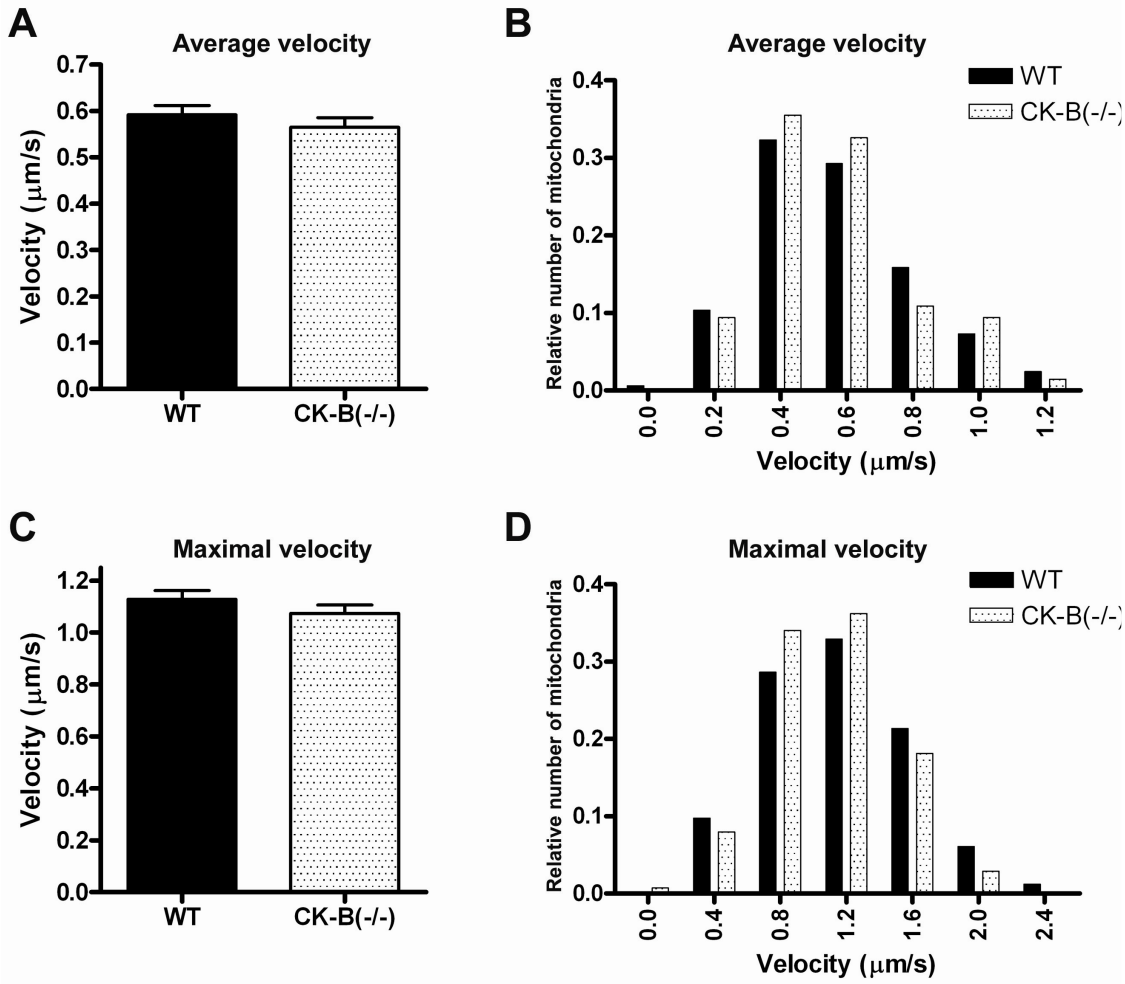

Figure 3. Mitochondria of 7-day-old CK-B deficient and wildtype neurons were stained with rhodamine 123. Live imaging was applied to track these mitochondria. Average velocities were determined for mitochondria of wildtype cells (164 mitochondria) and CK-B deficient cells (138 mitochondria). The bar diagrams in panel A, display average velocities with error bars representing the standard deviation (SD). Panel B shows the distribution of mitochondrial velocities. Maximum velocities for individual tracked mitochondria were also determined and the average of these are presented in panel C. Error bars represent SD. D) The distribution of maximal velocities of individual mitochondria are shown for wildtype and CK-B knockout neurons.

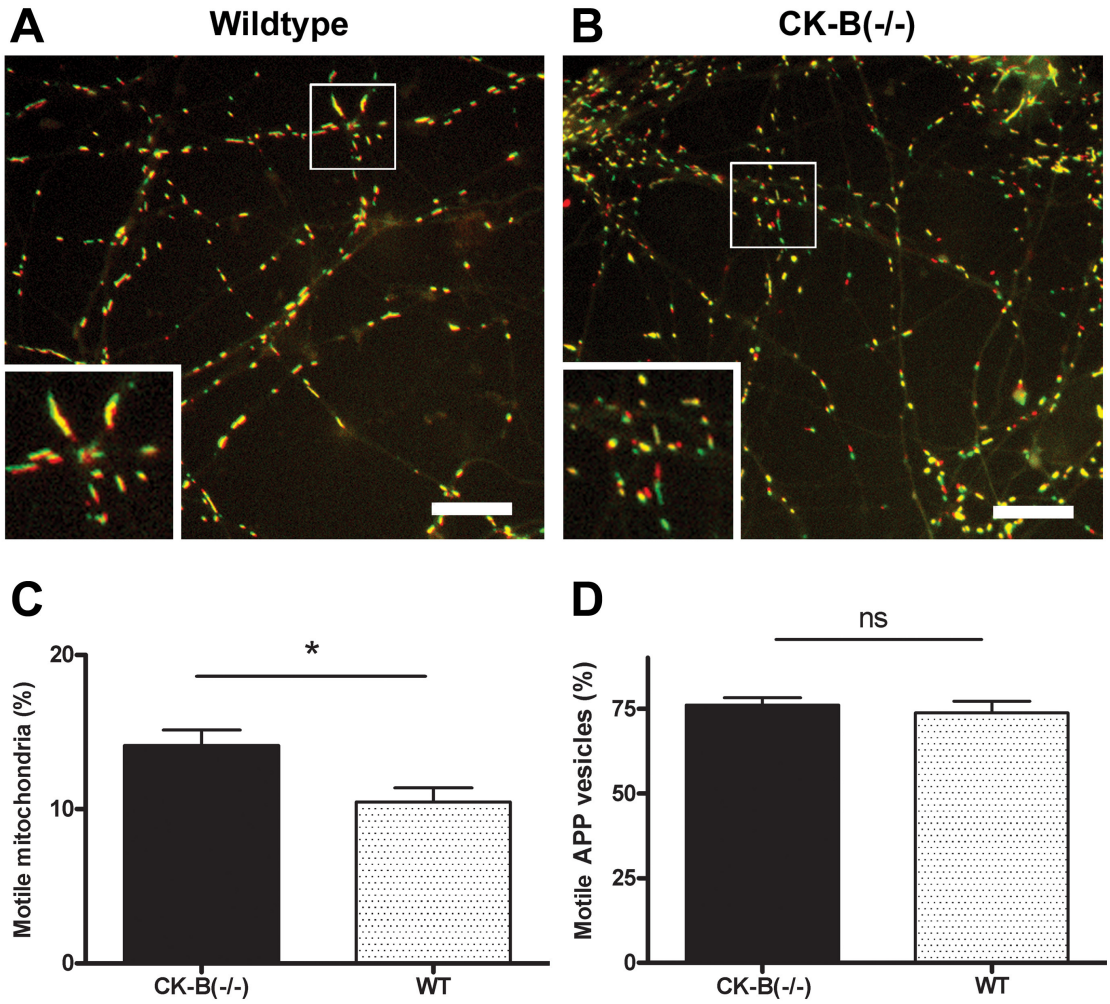

Figure 4. The percentage of motile mitochondria in wildtype and CK-B knockout neurons was determined. The first (red) frame and the 100th frame (green) of a movie were merged. Yellow mitochondria are non-motile mitochondria. Panel A) 1st and 100th frames of a movie of mitochondria in a wildtype neuron after merging. Panel B) displays the CK-B knockout equivalent. For wildtype (n=12) and CK-B knockout (n=15) movies were analyzed using the stack difference method (see methods). The percentage of motile mitochondria is presented in the scatter dot plot in panel C ($p<0.05$). The percentage of motile YFP-APP particles in wildtype and CK-B knockout neurons was determined by analyzing 2 sets of merged frames from every movie (see also figure 5). Panel D shows the average percentages (WT: 74%; CK-B: 76%; $p=0.57$) of motile YFP-APP vesicles (error bars represent SEM). n=22 for WT and n=14 for CK-B(-/-). Bars represent 10 µm.

Since CK-B deficiency had no impact on the average and maximal velocities by which mitochondria travel in neurites, we wondered if lack of CK-B mediated ~P transfer could elicit more subtle effects and have impact on the rate of engagement in intracellular transport or affect the process of anchorage of mitochondria, two types

of events which are also believed to be regulated by local energy demand (Morris and Hollenbeck 1993; Li, Okamoto et al. 2004). To answer this question, we analysed whether the fraction of mitochondria that was rendered motile might be affected by CK-B deficiency (**Figure 4**). Image stack difference analysis was applied to estimate the percentage of mitochondria that moved during the time of one recording (3 minutes). For wildtype cells 10.5 ± 3.2 % of mitochondria were motile at any moment during the course of one recording. Surprisingly, CK-B deficient cells showed a significant increase of 35% ($p < 0.05$) in motile mitochondria (14.1 ± 3.8%). The dot plot in **figure 4c** also clearly shows the shift towards more motile mitochondria in CK-B deficient cells. To validate this conclusion, we also applied a method with manual counting (see Additional file 1). Importantly, the outcome of this analysis was almost identical (37% increase in the fraction of motile mitochondria in CK-B deficient neurons), although absolute percentages of motile mitochondria were lower with this method (5.9 % ± 2.2 % for wildtype and 8.1 ± 2.0 % for CK-B(-/-); $p < 0.0005$) (**Figure 5**)**.** When this same image analysis methodology was applied to YFP-APP vesicles, no significant effect of absence or presence of CK-B was found (**Figure 4d**).

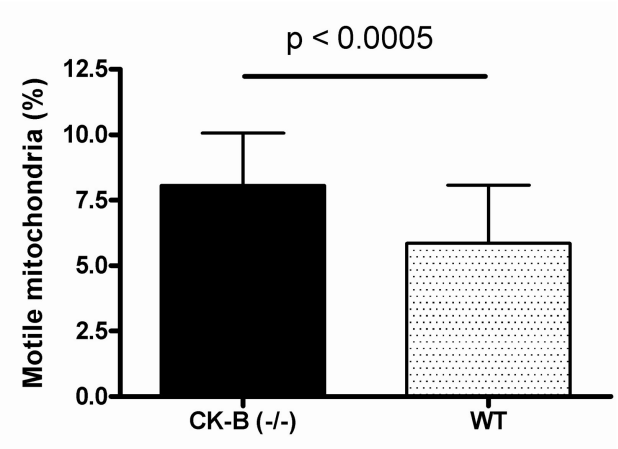

Figure 5. The percentage of motile mitochondria in wildtype and CK-B knockout neurons was determined by manually analyzing 2 sets of merged frames (n=24 for WT and n=30 for CK-B(-/-)) from every movie. The bar diagram depicts the average percentage of motile mitochondria (error bars represent the SD).

In conclusion, CK-B is not influencing the speed of intracellular transport of APP or mitochondria once this transport is initiated, however, in cells that lack CK-B a larger fraction of mitochondria is recruited into the actual motile pool.

Discussion

ATP generation and distribution is essential for the highly compartmentalized eukaryotic cell. Especially in neurons with their extended axonal and dendritic networks, it is important to modulate fuelling logistics. Spatially confined cellular processes like synapse functioning require local supply of energy. In order to fuel these functions optimally, they are coupled to sites of energy production. The CK system provides cells with a temporal and spatial ATP buffer to connect local energy consumption with sites of energy production (Tombes and Shapiro 1985; Friedman and Roberts 1994; Wallimann and Hemmer 1994). Other phosphotransfer enzymes, like adenylate kinases and nucleoside diphosphate kinases are also active in neurons, and serve in the global network that distributes ATP throughout the cell. In addition, neurons have the capacity to relocate their energy production machinery to specialized subcellular sites to help in local ATP generation. Partitioning of glycolytic enzymes on cortical actin or membrane-near sites can provide local energy to membrane pumps by functional coupling (Glitsch and Tappe 1993; Xu, Zweier et al. 1995), whereas oxidative generated ATP can be generated locally, by recruiting mitochondria to sites of high ATP consumption such as synapses and dendritic spines (Li, Okamoto et al. 2004; Hollenbeck and Saxton 2005; Verstreken, Ly et al. 2005).

We focused on the question whether CK-B facilitates efficient axonal transport by comparing transport of APP and mitochondria in primary murine neurons derived from CK-B deficient and proficient mice.

Active transport of cargo in neurons is achieved by a wide variety of motor proteins, which are guided by the infrastructure of the cellular cytoskeleton (Vale 2003). These cargos can travel along actin filaments or microtubules either by plus end or minus end directed trafficing, thus facilitating both anterograde and retrograde axonal transport. Both types of cytoskeletal structures have their own assortment of motor proteins, which can be divided in actin-guided myosins (Sellers 2000) and microtubule-guided kinesins and dyneins (Goldstein and Yang 2000). A common denominator for myosins, dyneins and kinesins is that they require ATP hydrolysis to exert their function.

Fast axonal transport of membranous organelles and membrane proteins depends on highly processive motor activity and, consequently, a steady and adequate ATP/ADP ratio for optimal fuelling of motor proteins. Our data show that the actual speed of fast axonal transport of APP-YFP is not affected by CK-B deficiency. Although the maximum and average velocities observed are lower than reported for rat neurons (Kaether, Skehel et al. 2000), this may be a mouse related feature and no differences between wildtype cells and CK-B deficient cells were found. In addition, mitochondrial transport velocities were not affected in CK-B knockout cells. Mitochondria are subject to saltatory movement, which involves cycles of anterograde and retrograde transport driven by kinesins and dyneins, respectively (Hollenbeck and Saxton 2005). Because axons and dendrites in 7-day-old cultures of primary neurons are totally intertwined, we were unable to distinguish between axonal/dendritic or anterograde/retrograde transport. Therefore, and also because other groups have reported that mitochondrial velocity and the rate of anterograde and retrograde transport are highly similar in axons and dendrites of hippocampal neurons (Overly, Rieff et al. 1996; Ligon and Steward 2000), we decided not to discriminate between CK-B effects further. At this point, we thus consider it unlikely - but can also not fully exclude - that CK-B deficiency affects the ratio of anterograde/retrograde transport of mitochondria.

We hypothesized that CK-B deficiency would bring about an altered capacity to distribute intracellular ATP, and create abnormal inhomogeneity in local ATP. Because neurons rearrange their mitochondria according to local ATP needs (Hollenbeck and Saxton 2005; Verstreken, Ly et al. 2005), altered local ATP distribution may determine altered mitochondrial motility. The fact that no differences in either mitochondrial or YFP-APP velocities in combined anterograde/retrograde transport were found is therefore an interesting finding in its own right. Possibly, flexibility in the energetic network, with higher ~P flux through adenylate kinase (AK) or glycolytic enzymes helps to compensate the loss of CK-B (de Groof, Oerlemans et al. 2001; de Groof, Smeets et al. 2001; Janssen, de Groof et al. 2003), or – alternatively – mitochondria produce are still able to produce enough ATP to sustain their own transport.

Indeed, our findings suggest that initiation or abrogation of transport may be steps in the process that are more crucially dependent on cell energy state. Quantification of the fraction of mobile mitochondria revealed that CK-B deficient neurons contain on average 36% more mitochondria in the motile fraction. The metabolic factors that modulate and mobilize mitochondrial motility are largely unknown. Local ATP depletion, or locally elevated H+ and ADP levels caused by CK absence, could serve as a direct or indirect signal to attract mitochondria, or arrest nearby motor activity, arresting mitochondria while passing the "fuel-arid" area (Hollenbeck 1996; Terada, Kinjo et al. 2000; Hollenbeck and Saxton 2005; Mironov 2007). A combination of mechanistic events is also possible. In addition, secondary effects like inadequate Ca2+ handling, due to CK-B deficiency (Steeghs, Benders et al. 1997; de Groof, Fransen et al. 2002), could act in signalling pathways for mitochondrial motility and/or docking (Yi, Weaver et al. 2004). For neurons, it has been found that local neuronal growth factor (NGF) application triggers mitochondrial recruitment through PI3K. Moreover, an intact F-actin cytoskeleton is required (Chada and Hollenbeck 2003; Chada and Hollenbeck 2004), which is organized by the action of formins and RhoA (Minin, Kulik et al. 2006). Interestingly, we recently found that CK-B increases the F-actin content in phagosomes (Kuiper, Pluk et al. 2008). Although the underlying molecular mechanisms of this effect on F-actin are yet unclear, it is tempting to speculate that CK-B deficiency in neurons could induce less efficient actin accumulation at sites of mitochondrial arrest. Indeed, a prominent role for actin-state in mitochondrial movement has been proposed (Boldogh and Pon 2007). Future research might help to discriminate between these different putative mechanisms.

Methods

Isolation and culture of primary neurons

The generation of CK-B knockout mice and the study of genotype-phenotype relationships of these animals in comparison to wildtype controls has been described in detail elsewhere (also (Jost, Van Der Zee et al. 2002; Streijger, In 't Zandt et al. 2007)). Primary cultures of mouse hippocampal neurons were established using a

modified protocol (Hoop de, Meyn et al. 1998). In short, brains were isolated from CK-B(-/-) (Jost, Van Der Zee et al. 2002) fetuses (E16.5) or fetuses of mixed background (C57BL/6 x 129Ola). Meninges were removed and hippocampi were separated from the hemispheres. Hippocampi were incubated for 20 minutes at 37°C in Hanks' Balanced Saline Solution (HBSS, Gibco) containing 0.05 % trypsin, 1 mM EDTA and 20 mM HEPES (pH 7.35) and subsequently dissociated by pipetting and seeded onto 24 mm coverslips. Cells were allowed to attach for 3-4 hours in Neurobasal medium (Gibco), after which they were placed inverted on a layer of primary astrocytes (also see (Hoop de, Meyn et al. 1998)). The co-culture was maintained in Neurobasal medium containing 1x B27 supplement (Gibco), 0.5 mM glutamine and 0.05 mg/ml gentamycin (= NBM+).

Creatine kinase activity (zymogram)

Cultured primary neurons (5 days *in vitro*) were lysed in buffer containing 12.6 mM Na_2HPO_4, 2.8 mM KH_2PO_4, 0.05 % Triton-x-100 and 0.3 mM DTT. Zymogram analysis was performed as described (Steeghs, Benders et al. 1997) and, zymograms were subsequently developed using the colorimetric detection kit from Sigma Diagnostics (procedure number 715-EP).

Indirect immunofluorescence

Neurons (3-7 days *in vitro*) grown on glass coverslips were fixed with 2% paraformaldehyde in PHEM buffer (25 mM HEPES, 10 mM EGTA, 60 mM PIPES, 2 mM $MgCl_2$, pH 6.9), permeabilized with 0.1% Triton X-100 and incubated 20 min in PBS containing 4% bovine serum albumine (BSA). CK-B was detected by subsequent incubation of monoclonal 21E10 (1:2000) (Sistermans, de Kok et al. 1995) and goat-anti-mouse IgG conjugated to Alexa Fluor 488 (Molecular Probes). Images were taken with a Biorad MRC1024 confocal microscope using an oil immersion 60x objective.

Transfection and rhodamine 123 labeling of neurons

Neurons (7 days *in vitro*) grown in glass bottomed 35 mm Willco dishes (GWSt-3522) were transfected using Nupherin-neuron (Biomol) transfection reagent in combination with Lipofectamine (Invitrogen). Per dish 0.5 μg pcDNA3-APP-YFP (kind gift from Carlos Dotti (Kaether, Skehel et al. 2000)) and 2.5 μl Nupherin were premixed in phenol red free Neurobasal medium and incubated for 10 minutes. An equal volume of phenol red free NBM with 1 μl Lipofectamine was added and after 30 minutes this mix was added to the neurons. After 2 hours the medium was replaced by NBM+ medium and neurons were cultured for 24 hours prior imaging. For tracking mitochondria cells were loaded with rhodamine 123 (10 μM) for 1 minute in NBM+ w/o phenol red.

Live imaging and image analysis

Cells cultured on Willco dishes were imaged on an inverted microscope (Axiovert 200 M; Zeiss, Jena, Germany) equipped with a temperature controlled CO_2 incubator (type S) and sample stage, and using a PlanApochromatic 63x 1.4 oil immersion Plan NeoFluar DIC lens (Carl Zeiss GmbH, Jena, Germany). Rhodamine 123 was excited using a monochromator (Polychrome IV; TILL Photonics, Gräfelfing, Germany) set at 488 nm. Images were recorded with the appropriate filter set (Omega Optical, Brattleboro, VT, USA) on a CoolSNAP HQ monochrome charge-coupled device (CCD) camera (Roper Scientific, Vianen, The Netherlands). All hardware was controlled with Metafluor 6 software (Molecular Devices Corp., Downingtown, PA, USA). For particle (i.e. APP-cargo vesicles or mitochondria) tracing, sequential images were taken every 2 seconds to obtain image stacks of 100 images each. Particles were tracked using Metamorph 6 software (Molecular Devices Corp., Downingtown, PA, USA) software by marking them manually in subsequent frames (only particles that moved at least in 3 subsequent frames were tracked). The velocity per particle-vesicle was calculated by dividing the travelled distance by time. Additionally, for each moving particle the maximal velocity (during two subsequent frames) was determined. The number of analysed particles is mentioned in the text or legends.

To estimate the percentage moving mitochondria the same dataset as mentioned above was analyzed with ImageJ software version 1.34s (U. S. National Institutes of Health, Bethesda, Maryland, USA, http://rsb.info.nih.gov/ij/). The original image stacks were converted to binary stacks by manually applying a threshold, according to the quality of each individual stack. The total number of mitochondria in the stack was counted using the particle count function (5 < mitochondria <50 pixels). To distinguish between moving and stationary mitochondria, every frame "n" was compared to an earlier frame "n-3" ("stackdifference" option from the ImageJ kymograph plugin, EMBL, Heidelberg, Germany). The resulting stack of images contains motile mitochondria, which were counted. Numbers obtained were divided by two to compensate for double counting of both "old and new" mitochondrial positions in "difference-stack" images. Finally, percentages of motile mitochondria in the stacks were calculated.

Manual particle tracking

An alternative approach to determine the percentage motile mitochondria and YFP-APP vesicles was applied in the figure shown in Additional file 2. For this analysis, 2 x 2 frames (frames 37 and 40; frames 87 and 90) from every movie were merged (using pseudo-colours red and green). From the resulting images we manually counted the red and green (old and new position of) particles and divided them by 2 (gives the number of particles that moved). Stationary particles appear as yellow in the merged images. Percentages were calculated by dividing the number of motile mitochondria (or YFP-APP-vesicles) by the total number of mitochondria (or YFP-APP-vesicles).

Acknowledgements

This work was supported by NWO ZON-MW Program grant 901-01-191 and partly by grants KUN 2002-1763 and KUN 2004-3125 from the Dutch Cancer Society (Nederlandse Kankerbestrijding NKB/KWF to B.W.).

References

Ames, A., 3rd (2000). "CNS energy metabolism as related to function." Brain Res Brain Res Rev **34**(1-2): 42-68.

Bernstein, B. W. and J. R. Bamburg (2003). "Actin-ATP hydrolysis is a major energy drain for neurons." J Neurosci **23**(1): 1-6.

Boldogh, I. R. and L. A. Pon (2007). "Mitochondria on the move." Trends Cell Biol **17**(10): 502-10.

Brady, S. T. and R. J. Lasek (1981). "Nerve-specific enolase and creatine phosphokinase in axonal transport: soluble proteins and the axoplasmic matrix." Cell **23**(2): 515-23.

Brown, A. (2003). "Axonal transport of membranous and nonmembranous cargoes: a unified perspective." J Cell Biol **160**(6): 817-21.

Chada, S. R. and P. J. Hollenbeck (2003). "Mitochondrial movement and positioning in axons: the role of growth factor signaling." J Exp Biol **206**(Pt 12): 1985-92.

Chada, S. R. and P. J. Hollenbeck (2004). "Nerve growth factor signaling regulates motility and docking of axonal mitochondria." Curr Biol **14**(14): 1272-6.

Chan, D. C. (2006). "Mitochondria: dynamic organelles in disease, aging, and development." Cell **125**(7): 1241-52.

Chen, H. and D. C. Chan (2006). "Critical dependence of neurons on mitochondrial dynamics." Curr Opin Cell Biol **18**(4): 453-9.

de Groof, A. J., J. A. Fransen, et al. (2002). "The creatine kinase system is essential for optimal refill of the sarcoplasmic reticulum Ca2+ store in skeletal muscle." J Biol Chem **277**(7): 5275-84.

de Groof, A. J., F. T. Oerlemans, et al. (2001). "Changes in glycolytic network and mitochondrial design in creatine kinase-deficient muscles." Muscle Nerve **24**(9): 1188-96.

de Groof, A. J., B. Smeets, et al. (2001). "Changes in mRNA expression profile underlie phenotypic adaptations in creatine kinase-deficient muscles." FEBS Lett **506**(1): 73-8.

Dzeja, P. P., R. Bortolon, et al. (2002). "Energetic communication between mitochondria and nucleus directed by catalyzed phosphotransfer." Proc Natl Acad Sci U S A **99**(15): 10156-61.

Dzeja, P. P. and A. Terzic (2003). "Phosphotransfer networks and cellular energetics." J Exp Biol **206**(Pt 12): 2039-47.

Friedman, D. L. and R. Roberts (1994). "Compartmentation of brain-type creatine kinase and ubiquitous mitochondrial creatine kinase in neurons: evidence for a creatine phosphate energy shuttle in adult rat brain." J Comp Neurol **343**(3): 500-11.

Glitsch, H. G. and A. Tappe (1993). "The Na+/K+ pump of cardiac Purkinje cells is preferentially fuelled by glycolytic ATP production." Pflugers Arch **422**(4): 380-5.

Goldstein, L. S. and Z. Yang (2000). "Microtubule-based transport systems in neurons: the roles of kinesins and dyneins." Annu Rev Neurosci **23**: 39-71.

Guillaud, L., M. Setou, et al. (2003). "KIF17 dynamics and regulation of NR2B trafficking in hippocampal neurons." J Neurosci **23**(1): 131-40.

Hemmer, W., E. Zanolla, et al. (1994). "Creatine kinase isoenzymes in chicken cerebellum: specific localization of brain-type creatine kinase in Bergmann glial cells and muscle-type creatine kinase in Purkinje neurons." Eur J Neurosci **6**(4): 538-49.

Hollenbeck, P. J. (1996). "The pattern and mechanism of mitochondrial transport in axons." Front Biosci **1**: d91-102.

Hollenbeck, P. J. and W. M. Saxton (2005). "The axonal transport of mitochondria." J Cell Sci **118**(Pt 23): 5411-9.

Hoop de, M. J., L. Meyn, et al. (1998). Culturing hippocampal neurons and astrocytes from fetal rodent brain. Cell Biology: a laboratory handbook. J. E. Celis. San Diego, Academic Press. **1:** 154-163.

Janssen, E., A. de Groof, et al. (2003). "Adenylate kinase 1 deficiency induces molecular and structural adaptations to support muscle energy metabolism." J Biol Chem **278**(15): 12937-45.

Jost, C. R., C. E. Van Der Zee, et al. (2002). "Creatine kinase B-driven energy transfer in the brain is important for habituation and spatial learning behaviour, mossy fibre field size and determination of seizure susceptibility." Eur J Neurosci **15**(10): 1692-706.

Kaether, C., P. Skehel, et al. (2000). "Axonal membrane proteins are transported in distinct carriers: a two-color video microscopy study in cultured hippocampal neurons." Mol Biol Cell **11**(4): 1213-24.

Kamal, A., G. B. Stokin, et al. (2000). "Axonal transport of amyloid precursor protein is mediated by direct binding to the kinesin light chain subunit of kinesin-I." Neuron **28**(2): 449-59.
Koo, E. H., S. S. Sisodia, et al. (1990). "Precursor of amyloid protein in Alzheimer disease undergoes fast anterograde axonal transport." Proc Natl Acad Sci U S A **87**(4): 1561-5.
Kuiper, J. W., H. Pluk, et al. (2008). "Creatine Kinase-Mediated ATP Supply Fuels Actin-Based Events in Phagocytosis." PLoS Biol **6**(3): e51.
Li, Z., K. Okamoto, et al. (2004). "The importance of dendritic mitochondria in the morphogenesis and plasticity of spines and synapses." Cell **119**(6): 873-87.
Ligon, L. A. and O. Steward (2000). "Movement of mitochondria in the axons and dendrites of cultured hippocampal neurons." J Comp Neurol **427**(3): 340-50.
Lim, L., C. Hall, et al. (1983). "Neurone-specific enolase and creatine phosphokinase are protein components of rat brain synaptic plasma membranes." J Neurochem **41**(4): 1177-82.
Lipton, P. and K. Robacker (1983). "Glycolysis and brain function: [K+]o stimulation of protein synthesis and K+ uptake require glycolysis." Fed Proc **42**(12): 2875-80.
Minin, A. A., A. V. Kulik, et al. (2006). "Regulation of mitochondria distribution by RhoA and formins." J Cell Sci **119**(Pt 4): 659-70.
Mironov, S. L. (2007). "ADP regulates movements of mitochondria in neurons." Biophys J **92**(8): 2944-52.
Morris, R. L. and P. J. Hollenbeck (1993). "The regulation of bidirectional mitochondrial transport is coordinated with axonal outgrowth." J Cell Sci **104 (Pt 3)**: 917-27.
Morris, R. L. and P. J. Hollenbeck (1995). "Axonal transport of mitochondria along microtubules and F-actin in living vertebrate neurons." J Cell Biol **131**(5): 1315-26.
Nangaku, M., R. Sato-Yoshitake, et al. (1994). "KIF1B, a novel microtubule plus end-directed monomeric motor protein for transport of mitochondria." Cell **79**(7): 1209-20.
Overly, C. C., H. I. Rieff, et al. (1996). "Organelle motility and metabolism in axons vs dendrites of cultured hippocampal neurons." J Cell Sci **109 (Pt 5)**: 971-80.
Pellerin, L. and P. J. Magistretti (2004). "Neuroenergetics: calling upon astrocytes to satisfy hungry neurons." Neuroscientist **10**(1): 53-62.
Saks, V. A., Z. A. Khuchua, et al. (1994). "Metabolic compartmentation and substrate channelling in muscle cells. Role of coupled creatine kinases in in vivo regulation of cellular respiration--a synthesis." Mol Cell Biochem **133-134**: 155-92.
Sellers, J. R. (2000). "Myosins: a diverse superfamily." Biochim Biophys Acta **1496**(1): 3-22.
Shah, J. V. and D. W. Cleveland (2002). "Slow axonal transport: fast motors in the slow lane." Curr Opin Cell Biol **14**(1): 58-62.
Sistermans, E. A., Y. J. de Kok, et al. (1995). "Tissue- and cell-specific distribution of creatine kinase B: a new and highly specific monoclonal antibody for use in immunohistochemistry." Cell Tissue Res **280**(2): 435-46.
Steeghs, K., A. Benders, et al. (1997). "Altered Ca2+ responses in muscles with combined mitochondrial and cytosolic creatine kinase deficiencies." Cell **89**(1): 93-103.
Streijger, F., H. J. In 't Zandt, et al. (2007). Developmental and functional consequences of disturbed energetic communication in brain of creatine kinase-deficient mice: Understanding CK's role in the fuelling of behavior and learning. Molecular system bioenergetics. V. A. Saks. Weinheim, Wiley-VCH Verlag GmbH & Co. KGaA**:** 339-366.
Sturmer, K., O. Baumann, et al. (1995). "Actin-dependent light-induced translocation of mitochondria and ER cisternae in the photoreceptor cells of the locust Schistocerca gregaria." J Cell Sci **108 (Pt 6)**: 2273-83.
Tachikawa, M., M. Fukaya, et al. (2004). "Distinct cellular expressions of creatine synthetic enzyme GAMT and creatine kinases uCK-Mi and CK-B suggest a novel neuron-glial relationship for brain energy homeostasis." Eur J Neurosci **20**(1): 144-60.
Tanaka, Y., Y. Kanai, et al. (1998). "Targeted disruption of mouse conventional kinesin heavy chain, kif5B, results in abnormal perinuclear clustering of mitochondria." Cell **93**(7): 1147-58.
Terada, S., M. Kinjo, et al. (2000). "Oligomeric tubulin in large transporting complex is transported via kinesin in squid giant axons." Cell **103**(1): 141-55.
Tombes, R. M. and B. M. Shapiro (1985). "Metabolite channeling: a phosphorylcreatine shuttle to mediate high energy phosphate transport between sperm mitochondrion and tail." Cell **41**(1): 325-34.
Vale, R. D. (2003). "The molecular motor toolbox for intracellular transport." Cell **112**(4): 467-80.
van Deursen, J., A. Heerschap, et al. (1993). "Skeletal muscles of mice deficient in muscle creatine kinase lack burst activity." Cell **74**(4): 621-31.

Verstreken, P., C. V. Ly, et al. (2005). "Synaptic mitochondria are critical for mobilization of reserve pool vesicles at Drosophila neuromuscular junctions." Neuron **47**(3): 365-78.
Wallimann, T. and W. Hemmer (1994). "Creatine kinase in non-muscle tissues and cells." Mol Cell Biochem **133-134**: 193-220.
Wong, R. W., M. Setou, et al. (2002). "Overexpression of motor protein KIF17 enhances spatial and working memory in transgenic mice." Proc Natl Acad Sci U S A **99**(22): 14500-5.
Xu, K. Y., J. L. Zweier, et al. (1995). "Functional coupling between glycolysis and sarcoplasmic reticulum Ca2+ transport." Circ Res **77**(1): 88-97.
Yi, M., D. Weaver, et al. (2004). "Control of mitochondrial motility and distribution by the calcium signal: a homeostatic circuit." J Cell Biol **167**(4): 661-72.
Yuen, E. Y., Q. Jiang, et al. (2005). "Microtubule regulation of N-methyl-D-aspartate receptor channels in neurons." J Biol Chem **280**(33): 29420-7.

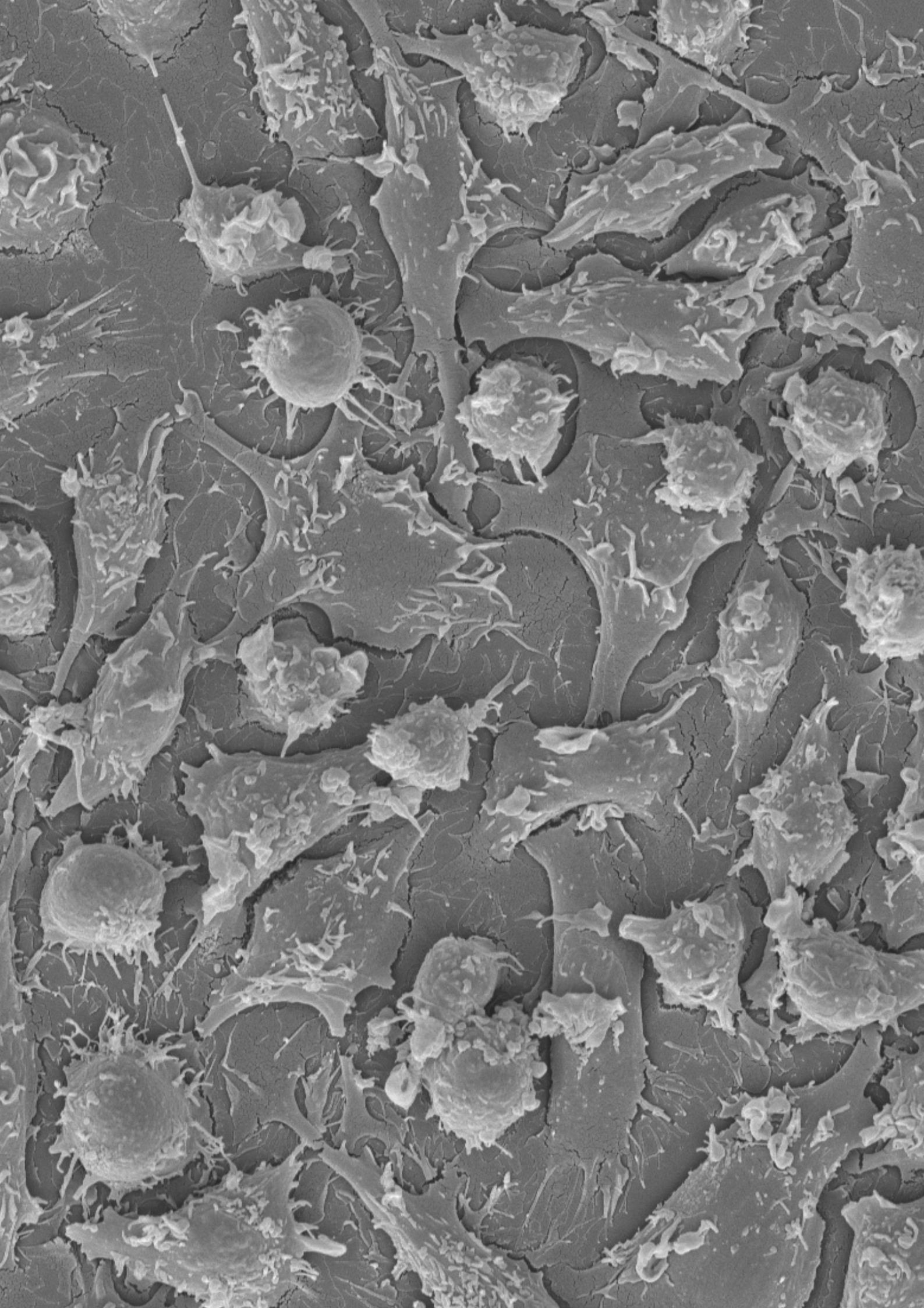

Chapter - 5 -

Creatine kinase B facilitates cell spreading: Study in an astroglial cell line derived from brain of CK-B -/- mouse

Jan W.P. Kuiper, Frank Oerlemans and Bé Wieringa

Abstract

Brain function poses a high demand on cellular energy, which is reciprocated by an elaborate and highly plastic network of metabolic supply pathways in both neurons and astrocytes. By catalyzing the distribution and buffering of adenosine triphosphate (ATP), the universal energy carrier, brain-type creatine kinase (CK-B) is thought to play a central role in this energetics network To examine this role in specific brain functions in more detail, dedicated neural cell models are indispensable.

Here we report on the derivation of conditionally immortalized cells of the astroglial and neuronal lineages from brains of CK-B deficient mice carrying the H-2K^b-tsA58 gene for thermolabile SV40 large T antigen (tsA58). Several cell lines that displayed astrocytic and/or neuronal differentiation characteristics with GFAP or β-III-tubulin positivity were obtained and one model with astrocyte-like characteristics was used for complementation-transfection to reintroduce CK-B function. Cell-spreading assays demonstrated the facilitating role of enzymatically active CK-B in cytoskeletal remodeling, an actomyosin-based process, which is particularly important during brain development and spine remodeling. Our findings confirm other findings of our group regarding the ATP supply role of CK-B (Kuiper, Pluk et al. 2008) and establish the new cell models as useful tools for further study of CK-B's role in actomyosin-dynamics in neuron-glial communication.

Introduction

Efficient neuronal functioning depends on adequate provision of cellular energy in the form of adenosine triphosphate (ATP) to fuel ion pumps for electrogenic activity, neurotransmitter recycling and cytoskeletal remodeling (Ames 2000; Hertz and Dienel 2002; Bernstein and Bamburg 2003) Metabolic breakdown of glucose by glycolysis and mitochondrial oxidative phosphorylation is the main pathway that drives the production of ATP in neurons. In addition, intercellular exchange of metabolites between neurons and astrocytes contribute to the elaborate metabolic energy network in brain (Magistretti 2006). Because neurons exhibit transient patterns of elevated activity in ion homeostasis and spine remodeling, their ATP requirements will transiently peak. Likewise, the transport role, modulation of impulse transmission and cell shape transitions of astrocytes are energy-requiring processes (Hirrlinger, Hulsmann et al. 2004; Hertz, Peng et al. 2007). Strikingly, in mammals the period of highest brain-energy demand generally coincides with the neonatal period of most intense brain growth and development, i.e. the period when neurons and astrocytes undergo most profound morphological changes (Boero, Qin et al. 2003; Shen, Willis et al. 2003; Erecinska, Cherian et al. 2004).

Vast and sudden rises in local energy demand in brain cells can be reciprocated by the activity of phosphotransfer systems, including the circuits in which members of the family of creatine kinase isozymes (CKs) are active. CKs catalyze the transfer of high-energy phosphoryl groups (~P) from ATP to creatine and vice versa ($MgATP^{2-} + Cr \leftrightarrow MgADP^{-} + PCr^{2-} + H^{+}$), thereby providing cells with optimal distribution and buffering of energy (Wallimann and Hemmer 1994; Dzeja and Terzic 2003). Two isoforms of CK are expressed in brain. Ubiquitously expressed mitochondrial CK (UbCKmit) is mainly expressed in neurons, whereas cytosolic brain-type CK (CK-B) is the dominant isoform in astrocytes among glial populations and in inhibitory neurons (Jost, Van Der Zee et al. 2002; Tachikawa, Fukaya et al. 2004). Our lab has created gene knockout models for both CK isoforms. Phenotypical analysis of mice deficient for the mitochondrial isoform in brain, UbCKmit, revealed a mild phenotype including slower spatial learning acquisition and diminished open field habituation (Steeghs, Oerlemans et al. 1995;

Streijger, Jost et al. 2004). In contrast, ablation of CK-B induced more overt changes in behavior, diminished performance in spatial learning tasks and delayed development of pentylenetetrazole-induced seizures, as well as an increased intra- and infrapyramidal mossy fibre area (Jost, Van Der Zee et al. 2002). In addition, mice deficient for both brain isoforms had a reduced body weight, problems with thermogenesis and a diminished acoustic startle reflex (Streijger, Oerlemans et al. 2005; Streijger F 2007), later attributed to problems in hair cell mechanotransduction (Shin, Streijger et al. 2007). To gain a deeper molecular understanding of the processes that require CK mediated ATP supply in brain, study at the cellular level is required.

Although primary cells isolated from tissues from transgenic animals are in routine use they have major disadvantages. Their limited life span in culture makes experiments requiring long-term culturing or further genetic manipulation virtually impossible. In addition, genetic background variation between animals often is a potential pitfall when comparing cells derived from wild type and transgenic animals. Cell lines on the other hand, have the advantage of unlimited availability, cellular homogeneity and relatively easy manipulation. However, use of cells from transgenic animals that have emerged as a result of spontaneous uncontrolled (oncogenic) transformation *in vivo* or *in vitro* should be avoided because events could be involved that affect normal physiological processes and permanently alter the cellular phenotype.

A particular elegant strategy to circumvent these types of problems and obtain conditionally immortalized cell types from transgenic mice with a controlled genetic background was developed by Jat et al. (Jat, Noble et al. 1991). The strategy is based on crossbreeding of transgenic (e.g. knockout) mice of interest with H-2K^{b}-tsA58 mice, bearing a transgene that encodes the thermo-labile simian virus 40 (SV40) large T antigen (TsA58 protein) under transcriptional control of the ubiquitously active major histocompatibility complex H-2Kb promoter (H-2K^{b}) (Jat, Noble et al. 1991). TsA58 is functionally active at 33°C and intervenes with the p53/Rb pathway (Bryan and Reddel 1994; Pipas and Levine 2001; Ahuja, Saenz-Robles et al. 2005), but its immortalization potential vanishes at temperatures above 37°C due to protein instability (Jat and Sharp 1989). In this study we report on the use of this system for

the generation of conditionally immortalized astrocytic/neuronal cell lines that lack the CK-B gene. Profiling of expression of neuronal and astrocytic markers following terminal differentiation at non-permissive temperature (39°C) was used to phenotype the different cell lines, and characterize their differentiation potential. One cell line that expressed glial fibrillary acid protein (GFAP) was used for transfection studies with an expression cassette to reintroduce CK-B activity. A clear facilitating role of CK-B emerged when cell-spreading performance was compared between complemented and non-complemented cells, corroborating earlier findings on the facilitating role of local ATP delivery by CK-B in actomyosin-based cytoskeletal dynamics (Kuiper, Pluk et al. 2008). Pharmacological inhibition experiments helped to demonstrate that the ability of CK-B to promote spreading activity requires the protein's enzymatic activity. Our findings illustrate the potential usefulness of conditionally immortalized cells from mouse brain with CK-B deficiency as models for study of the relationship between energy transfer pathways and the complex processes of cell dynamics.

Results

Generation and analysis of conditionally immortalized brain-derived cells

To obtain CK-B deficient neuronal/astrocytic cell lines, homozygous H-2K^b-tsA58 transgenic mice (Jat, Noble et al. 1991) were interbred with CK-B(-/-) mice (Jost, Van Der Zee et al. 2002), yielding a F1 generation that was heterozygous for CK-B and the H-2K^b-tsA58 transgene cassette. Mice deficient for CK-B and harboring at least one copy of the H-2K^b-tsA58 cassette were selected from F2-generation litters by PCR screening (data not shown) and used for further breeding. Brain cells of embryonic F3 mice (E16.5) were isolated and cultured at 33°C with mouse recombinant γ-interferon (10 U/ml) for several passages, as described in methods. The cells were maintained as a mixed population and their differentiation fate was assessed by determining the expression of the neuronal marker β-III-tubulin and the astrocytic marker glial fibrillary acid protein (GFAP), using an indirect immunofluorescence assay (**Figure 1**). Cell differentiation was induced by replacing

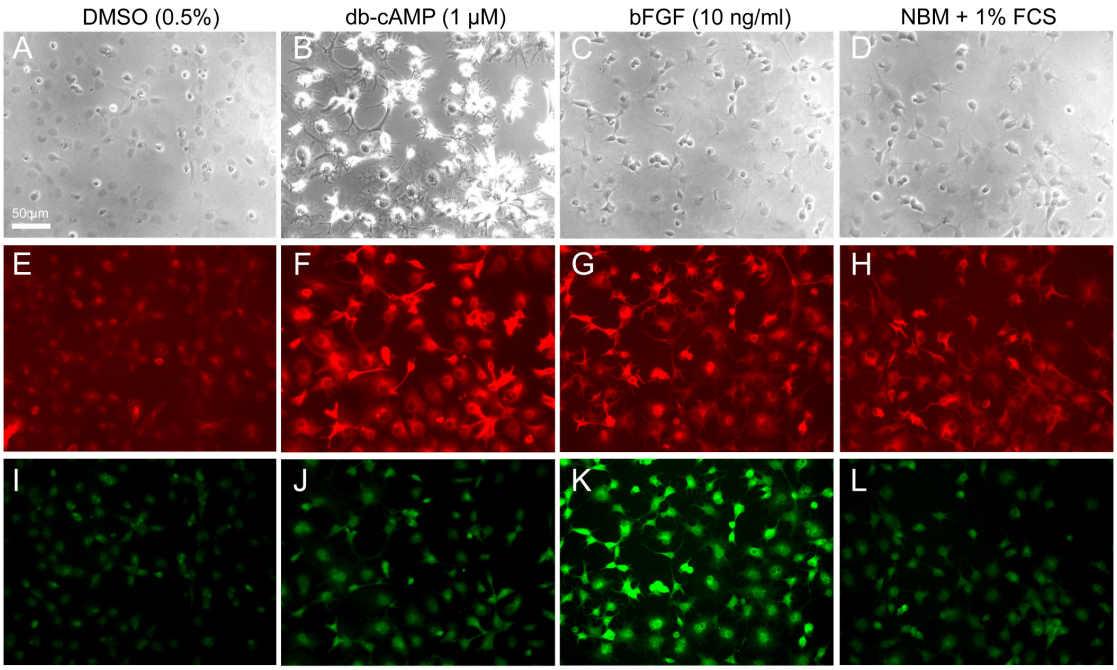

Figure 1. *Effect of differentiation factors on conditionally immortalized cells.*
Conditionally immortalized CK-B(-/-) cells were grown on poly-lysine coated cover slips for 24 hours in DMEM with 10% FCS at 33°C. Medium was replaced by DMEM without FCS, supplemented with: DMSO 0.5% (A,E,I), db-cAMP 1 µM (B,F,J), bFGF 10 ng/ml (C,G,K), NBM + 1% FCS (D,H,L). After 48 hours of incubation at 39°C, the cells were fixed and processed for immunofluorescent detection of β-III-tubulin by use of β-III-tubulin MoAb and secondary goat-anti-mouse IgG conjugated to Alexa 568 (E-H), or GFAP by use of polyclonal anti-GFAP and secondary goat-anti-rabbit IgG conjugated to Alexa 488 (I-L). DIC images are shown in panels A-D. The bar indicates 50 µm.

the medium (DMEM + 10% FCS) with serum-free DMEM supplemented with the differentiation factors DMSO (0.5%; **Figure 1a, e, i**), dibutyryl cyclic adenosine monophosphate (db-cAMP, 1 µM; **Figure 1b ,f, j**) or basic fibroblast growth factor (bFGF, 10 ng/ml; **Figure 1c, g, k**). In addition, the switch towards differentiation was initiated using Neurobasal medium containing 1% fetal calf serum (NBM/FCS) (**Figure 1d, h, l**). Cells were subsequently cultured for 48 hours at 39°C in the absence of γ-interferon, but in the presence of the differentiation factors.

Strikingly, up to 50% of db-cAMP treated cells expressed high levels of β-III-tubulin (**Figure 1f**). In addition, the majority of db-cAMP treated cells rounded up and formed extensive protrusions (**Figure 1b**), reminiscent of a neuronal morphology. In contrast, bFGF induced neuronal differentiation in only a minor fraction of cells in

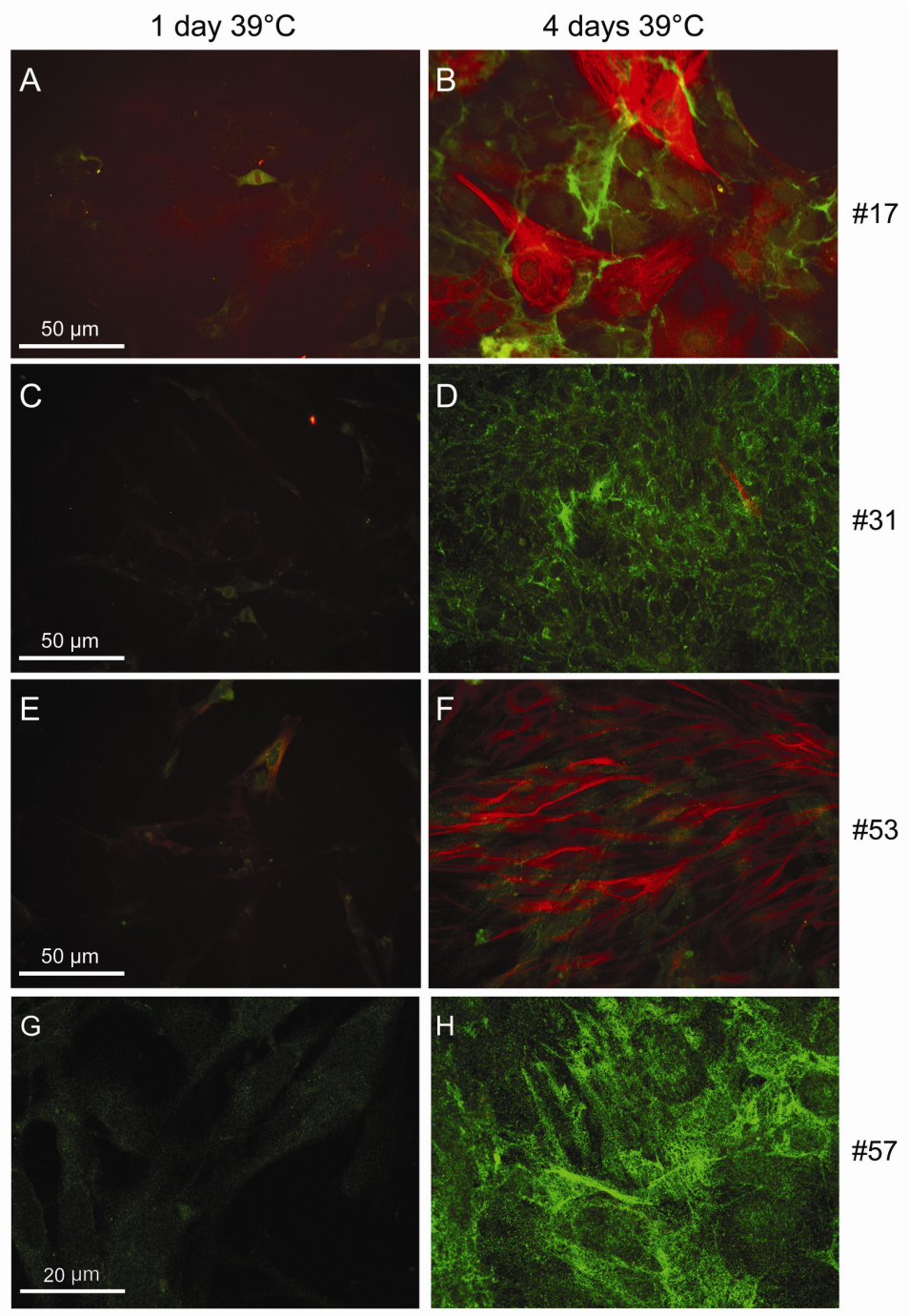

Figure 2. *Intrinsic differentiation potential of derived immortalized cell lines.*
Conditionally immortalized CK-B(-/-) cell lines #17 (A and B), #31 (C and D), #53 (E and F) and #57 (G and H) were grown on poly-lysine coated cover slips in DMEM with 10% FCS at 39°C. After one day (A,C,E,G) cells were fixed and processed for immunofluorescent staining with anti-β-III-tubulin antibodies followed by secondary goat-anti-mouse IgG conjugated to Alexa 568, or with anti-GFAP antibodies followed by secondary goat-anti-rabbit IgG conjugated to Alexa 488. Alternatively, cells were fixed and processed for immunofluorescent staining after 4 days (B,D,F,H).

the population (**Figure 1g**) with a somewhat higher percentage of β-III-tubulin positive cells than in the populations that received DMSO (**Figure 1e**) or NBM/FCS (**Figure 1h**) treatment. Conversely, presence of bFGF induced astrocytic differentiation in the majority of cells, as deduced from GFAP positivity after 48 hours in more than 90% of the cells in the population (**Figure 1k**). Indeed, bFGF (also named FGF-2) is known as a cell survival factor and endows neural progenitors with the ability to undergo astroglial differentiation. bFGF is also a regulator of GFAP expression (Reuss, Dono et al. 2003). These results demonstrate that a significant fraction of immortalized CK-B-/- brain cells retained (to some extent) their capacity to undergo neural differentiation, and that the neuron versus astroglial fate-specification can be modulated to some extend by the growth conditions used.

Derivation of clonal cell lines

In order to render individual neural cells suitable for study of CK-B function, clonal cell lines were established for CK-B complementation studies. Limited dilution procedures were applied to obtain single cell cultures in 96-wells culture plates (see methods). These cells were grown for multiple passages under permissive conditions (33°C with γ-interferon) to establish clonal cell lines. In total 72 clonal lines were derived of which 24 were tested for their intrinsic differentiation capacity (again assessed by GFAP and β-III-tubulin expression) by culturing them under non-permissive conditions without specific differentiation factors (4 days at 39°C without γ-interferon). Of these, 4 lines expressed GFAP, β-III-tubulin or both differentiation markers. **Figure 2** shows four selected cell lines, #17, #31, #53 and #57, at the start (day 1) and end (after 4 days) of the differentiation period, after staining for β-III-tubulin (in red) and GFAP (in green). All four lines exhibited an increase of marker expression over the 4-day period (compare **Figure 2a, c, e, g** with **2b, d, f, h**). Interestingly, neuronal/astroglial cell fate decisions under non-permissive conditions appeared mutual exclusive, resulting in lines with solely β-III-tubulin expressing cells, lines with only GFAP expressing cells, or lines consisting of mixed population of either β-III-tubulin expressing or GFAP expressing cells. Upon differentiation cell line #57 adopted an astrocytic fate with clear GFAP expression (**Figure 2h**), whereas cell line #53 expressed solely β-III-tubulin (**Figure 2f)**, suggestive of a neuronal

phenotype. In contrast, differentiated cells derived from cell line #17 displayed strong expression of both β-III-tubulin as well as GFAP after differentiation, however, never coinciding within the same cell (**Figure 2b**). These data suggest that the four lines chosen consist of neural progenitor cells at different phases of fate specification, with an intrinsic capacity to express either neuronal or astrocytic markers under non-permissive conditions.

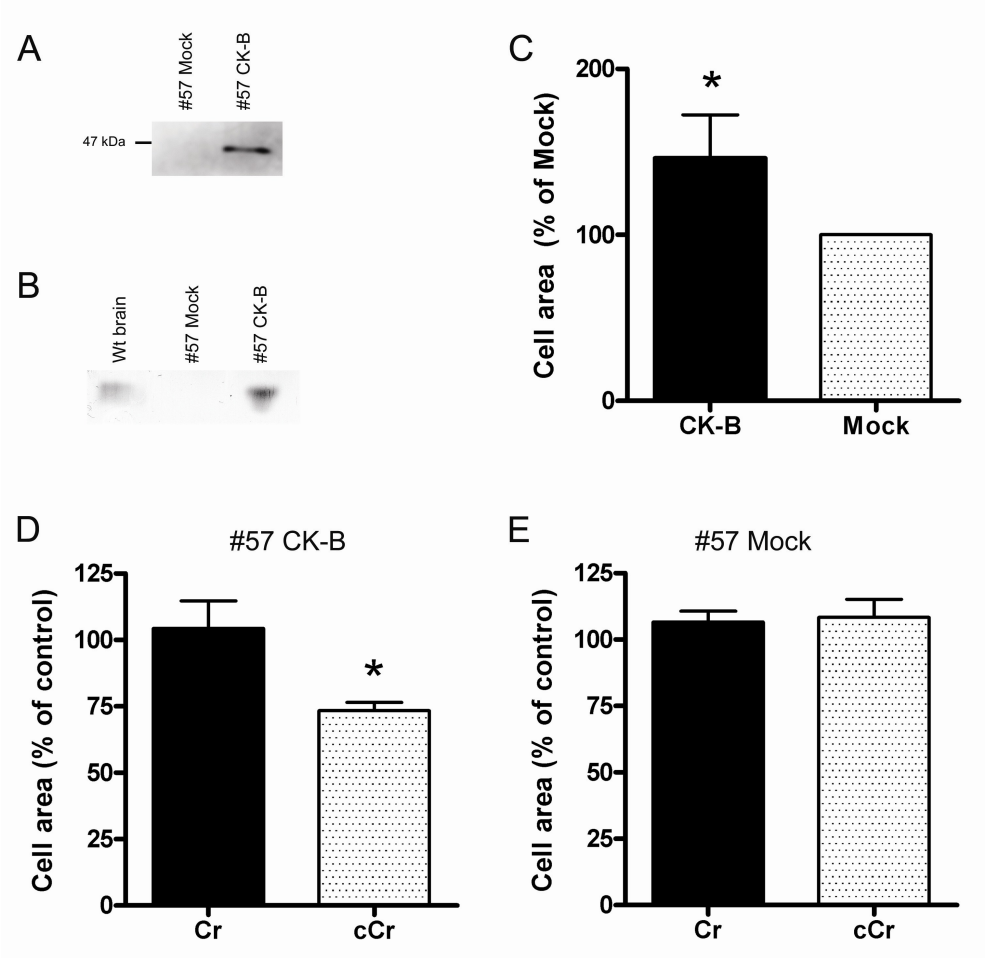

Figure 3. *Effect of CK-B on cell spreading in an immortalized glial cell line.*
Expression of CK-B in transfected cell lines #57-CK-B and #57-mock was detected by analysis of protein in cell lysates by Western blotting using the CK-B-specific moAb 21E10 (Sistermans et al., 1995) (A) or by staining for enzymatic CK-B activity on zymogram (B). Wild type brain lysate was used as a positive control for determination of CK-B enzymatic activity. Cell spreading assays were performed with #57-CK-B and #57-CK-mock cell lines (C). The average cell area after spreading was quantified and the ratio between #57-CK-B and #57-CK-mock was determined (mock set at 100%; n=6 and $p<0.05$; error bars represent SE). Cell spreading assays were repeated in the absence (control) and presence of 5 mM creatine (Cr) or 5 mM cyclocreatine (cCr) for both the #57-CK-B (D) and #57-mock (E). Bar diagrams represent the average cell area as a ratio compared with non-treated cells (n=3 and $p<0.02$; error bars represent SE).

Functional analysis of a clonal brain derived cell line

In adult brain, CK-B is most abundantly expressed in cells of the astroglial cell lineage (Manos and Bryan 1993; Jost, Van Der Zee et al. 2002; Tachikawa, Fukaya et al. 2004). Therefore, we chose line #57, which preferentially adapts an astroglial fate, as a candidate cell model for study of CK-B function. Previously, we had attributed a functional role in cell adherence-spreading to CK-B (see chapter 3), and spreading activity was therefore chosen as a relatively simple test criterion for assessing line #57's potential as a faithful reporter of CK-B function. To initiate these studies, cell line #57 was stably transfected with an expression vector encoding native mouse CK-B or the empty vector as a mock control. After puromycine selection several clonal cell lines were sub-cultured and analyzed for CK-B expression. Two cell lines, one expressing CK-B and one mock control, were ultimately chosen and CK-B expression was determined by Western blotting (**Figure 3a**). In addition, CK-B enzymatic activity was visualized by zymogram analysis (**Figure 3b**). As anticipated, CK-B complemented (#57-CK-B) cells expressed CK-B with the expected size of the native protein, ~ 43 kDa, whereas mock-treated (#57-mock) cells were completely devoid of CK-B. These results were in agreement with the enzymatic analysis, in which CK-B activity was detected in #57-CK-B, but not in #57-mock (Figure 3b). A wild-type mouse brain lysate served as a positive control for CK-B enzymatic activity.

Both #57-CK-B and #57-mock cells were subjected to a spreading assay (see methods) and the average cell area occupied after 30 min of adherence was determined. For every independent experiment (n=6) the ratio in spreading areas between #57-CK-B and #57-mock was calculated (with mock set at 100%). Average cell areas of #57-CK-B after spreading were 146% ($p<0.05$, SE: 26%) compared to the mock transfected cells (**Figure 3c**). Thus, re-expression of CK-B in CK-B deficient #57 cells promotes cell spreading. To assess if this increase in cell spreading related to mere presence of the CK protein or depended on its enzymatic activity, #57-CK-B and #57-mock cells were pre-incubated with either creatine or a specific pharmacological inhibitor of CK, cyclocreatine, before and during cell spreading. Values obtained for both cell lines were normalized for non-treated cells. Creatine

treatment did not have any promoting effect on cell spreading in either CK-B complemented or mock-treated cells (**Figure 3d, e**). In contrast, the inhibitor cyclocreatine decreased the average cell area after spreading with 27 ± 6% ($p<0.02$, n=3) compared to non-treated CK-B expressing cells, demonstrating that enzymatic activity of CK-B is required (**Figure 3d**). Of note, cyclocreatine had no effect on mock transfected cells (**Figure 3e**). When combined, these data demonstrate that presence of CK-B facilitates cell spreading in the immortalized cell line #57, apparently via events for which the enzymatic phosphoryl-transfer activity of CK-B is needed.

Discussion

Conditional immortalization of cells with a thermolabile mutant of the SV40 large T antigen, tsA58, causes cells to divide at the permissive temperature, but differentiation is restored/continued at the non-permissive temperature (Noble, Groves et al. 1995). Indeed, also brain derived immortalized cells retain their capacity to undergo neuronal/astroglial fate specification during differentiation upon loss of SV40Tag (Renfranz, Cunningham et al. 1991). By crossbreeding H-2K^b-tsA58 mice with CK-B(-/-) mice we aimed to isolate conditionally immortalized cells from brain that are deficient for CK-B, but otherwise still capable to establish the fully intact metabolism and cellular infrastructure that is normally found in neural cells. Our ultimate goal was to use these cells as models for revealing any differences from absence-presence of CK-B, as a further attempt to have a better understanding of the physiological significance of CK-B mediated ATP supply in individual cells of the brain. Initial differentiation experiments demonstrated that the neural cell-specification program in our cells was still intact, and that cells isolated could adapt neuronal or astroglial fate, as judged by expression of the markers β-III-tubulin and GFAP. Interestingly, db-cAMP induced profound β-III-tubulin expression combined with neuronal phenotypic aspects like the formation of cell protrusions and a rounded cell body. This is in accordance with literature, implicating cAMP and the PKA pathway in neuronal differentiation (Suon, Jin et al. 2004; Kim, Choi et al. 2005). Addition of bFGF as a differentiating factor had as main effect that it

increased the number of GFAP positive cells, possibly by regulating GFAP expression and astrocytic maturation as was found for endogenous bFGF in mouse models (Reuss, Dono et al. 2003).

An interesting observation is that cell fate specification in some of the clonal cell lines obtained by limited dilution was apparently already established, and resulted in intrinsic "fixed" preference for either the astrocytic or the neuronal developmental choice upon a switch towards non-permissive conditions. As an example, lines #31 and #53 demonstrated a clear preference for astrocytic and neuronal development, respectively. Since in these experiments we added no differentiation factors and differentiation was induced solely by cultivation at the non-permissive temperature we have to assume that these cells have an intrinsically poised state, with commitment towards a specific differentiation program. Among the cells in our mixed populations also cells with a more uncommitted progenitor phenotype may occur. Further analysis of differentiation markers, and their induction under different specific differentiation protocols, will be necessary to characterize the full spectrum of developmental properties of each cell line.

The cell spreading studies in the CK-B deficient cell line, #57, demonstrates that the "impaired spreading" phenotype could be rescued by reintroducing CK-B. In addition, pharmacological inhibition of CK in the CK-B complemented cells decreased cell spreading, whereas mock-transfected cells were not affected by this treatment. This clearly demonstrates the requirement for CK-B's ATP regenerating capacity as opposed to a more structural/scaffolding role for CK-B. The observation that creatine supplementation did not promote (or decrease) cell spreading is in accordance with data that shows no effect of creatine on phagocytosis (Kuiper, Pluk et al. 2008). Alternatively, immortalized #57 cells may be able to synthesize creatine endogenously, as was found for astrocytes (Dringen, Verleysdonk et al. 1998; Tachikawa, Fukaya et al. 2004). Clearly, any synthetic capacity would render creatine supplementation redundant, but whether this explains our findings is matter for future study.

Actin-driven morphological changes in astrocytes are important for astrocyte-neuron communication and modulate synapse formation (Hirrlinger, Hulsmann et al. 2004; Oliet, Piet et al. 2004). ATP-driven actin polymerization is a major player in

facilitating dynamic cell behavior (Kirschner 1980; Pollard and Borisy 2003) and is recognized as a major energy drain in neurons (Bernstein and Bamburg 2003). Since, cell spreading also requires extensive remodeling of the actin cytoskeleton to facilitate adhesion and morphological changes, it is widely used as an *in vitro* readout for actin dynamics. Our finding that CK-B promotes cell spreading corroborates recent data showing that CK-B is involved in actin-dynamics during phagocytosis (Kuiper, Pluk et al. 2008) and cell migration and spreading in primary astrocytes and fibroblasts (Chapter 3), and thus emphasizes the value of conditionally immortalized CK-B deficient cells for physiological studies on CK-B functioning in brain.

Acknowledgements

This work was supported by grants KUN 2002-1763 and KUN 2004-3125 from the Dutch Cancer Society (Nederlandse Kankerbestrijding NKB/KWF) to B.W.

Methods

Animals

Transgenic H-2K^b-tsA58 mice (immorto-mice) were purchased at Charles River Laboratories Inc. (Wilmington, MA). Crossbreeding CK-B(-/-) mice (Jost, Van Der Zee et al. 2002) and immorto-mice gave rise to a heterozygous F1 generation with a tsA58(+/-)/CK-B(+/-) genotype. Back-crossing the F1 animals with CK-B(-/-) partners yielded homozygous CK-B knockout mice carrying one H-2K^b-tsA58 transgene (confirmed by PCR genotyping).

Derivation of neuronal/astrocytic cell lines

Embryos (E16.5) resulting from intercross mating of tsA58(+/-)/CK-B(-/-) mice were used for isolating neocortical cells (Hoop de, Meyn et al. 1998). In short, meninges were removed and cerebri were trypsinized followed by trituration to obtain a single-cell suspension. Subsequently, the cells were cultured at the permissive temperature (33°C) in Dulbecco's Modified Eagle's Medium (DMEM), supplemented with 4 mM glutamine, 2 mM sodium pyruvate, 10% Fetal Calf Serum (FCS), 0.5

mg/ml gentamycin and mouse recombinant interferon-γ (10 units/ml). After 8 passages the resulting cells were either kept as a mixed population or serially diluted in 96 wells plates to obtain clonal cell lines. Differentiation of cell lines was performed as mentioned in the text.

CK-B(-/-) #57 cell lines

A GFAP-expressing (see results) clonal line, #57, was established by serial dilution and absence of CK-B expression was confirmed by Western blotting. For construction of the expression vector pSG8-puro-CK-B, the mouse CK-B ORF was amplified by PCR from EST AA102913 using a forward 5'-GCGGAATTCA TGCCCTTCTCCAACAGC-3' primer and a reverse 5'-CGCCTCGAGTCAC TTCTGGGCCGGC-3' primer. The obtained ORF-containing fragment was then cloned as insert between the EcoRI and XhoI sites into the eukaryotic expression vector pSG8-puro (de Bruin, Oerlemans et al. 2004) to generate CK-B expression vector pSG8-puro-CK-B. Subsequently, cells (10 cm dish; 80% confluent) were stably transfected with this expression vector or with vector alone (20 μg) using Lipofectamine 2000 according to the manufacturer's protocols. Clonal cell lines were established by selection on puromycine containing medium (5 μg/ml) followed by pipette picking of resistant colonies.

Immunofluorescence assay

Cells grown under permissive or non-permissive conditions on glass cover slips were fixed with 2% paraformaldehyde in PHEM buffer (25 mM HEPES, 10 mM EGTA, 60 mM PIPES, 2 mM $MgCl_2$, pH 6.9), subsequently permeabilized with 0.1% Triton X-100, and incubated for 20 min in PBS containing 4% bovine serum albumine (BSA). Primary antibodies against GFAP (diluted 1:400, rabbit polyclonal, DAKO) and β-(III)-tubulin (diluted 1:200, mouse monoclonal) were applied first (1 hr), followed by secondary goat-anti-mouse and goat-anti-rabbit conjugated to Alexa 488 or Alexa 568 (1 hr; diluted 1:300, Molecular Probes). Cells were visualized using a Leica DMRA Fluorescence microscope with COHU CCD camera and QFluoro 1.2 software.

Cell spreading assay

Cells were trypsinized, collected by centrifugation, washed in DMEM/1% BSA and incubated in DMEM/1% BSA for 20 minutes at 37°C before seeding onto glass cover slips in 12-well plates (1 ml/well). In some experiments (see text) cells were pre-incubated with cyclocreatine (cCr) or creatine (Cr; 2 hr, 5 mM). Cells were allowed to adhere and spread for a 30 minutes period in DMEM/1% BSA (+ Cr/cCr were mentioned) at 37°C. Then, cells attached to the cover slips were washed once with PBS, fixed in 2% paraformaldehyde in PHEM buffer for 15 minutes, permeabilized with Triton X-100 (0.1%) and stained with TexasRed conjugated phalloidin (diluted 1:200, Molecular Probes). For every coverslip 5 to 9 random fields were imaged with a Biorad Confocal Microscope MRC1024 using a 10x objective. The total surface occupied by cells was determined by ImageJ software and divided by the number of cells to calculate the area per cell. Five random fields were analyzed in each of three experiments. For every experiment the ratio between knockout and wild type astrocytes was calculated (wild type set at 100%) and significance was determined by using a one-sample t-test (expected value: 100%).

References

Ahuja, D., M. T. Saenz-Robles, et al. (2005). "SV40 large T antigen targets multiple cellular pathways to elicit cellular transformation." Oncogene **24**(52): 7729-45.

Ames, A., 3rd (2000). "CNS energy metabolism as related to function." Brain Res Brain Res Rev **34**(1-2): 42-68.

Bernstein, B. W. and J. R. Bamburg (2003). "Actin-ATP hydrolysis is a major energy drain for neurons." J Neurosci **23**(1): 1-6.

Boero, J., W. Qin, et al. (2003). "Restricted neuronal expression of ubiquitous mitochondrial creatine kinase: changing patterns in development and with increased activity." Mol Cell Biochem **244**(1-2): 69-76.

Bryan, T. M. and R. R. Reddel (1994). "SV40-induced immortalization of human cells." Crit Rev Oncog **5**(4): 331-57.

de Bruin, W., F. Oerlemans, et al. (2004). "Adenylate kinase I does not affect cellular growth characteristics under normal and metabolic stress conditions." Exp Cell Res **297**(1): 97-107.

Dringen, R., S. Verleysdonk, et al. (1998). "Metabolism of glycine in primary astroglial cells: synthesis of creatine, serine, and glutathione." J Neurochem **70**(2): 835-40.

Dzeja, P. P. and A. Terzic (2003). "Phosphotransfer networks and cellular energetics." J Exp Biol **206**(Pt 12): 2039-47.

Erecinska, M., S. Cherian, et al. (2004). "Energy metabolism in mammalian brain during development." Prog Neurobiol **73**(6): 397-445.

Hertz, L. and G. A. Dienel (2002). "Energy metabolism in the brain." Int Rev Neurobiol **51**: 1-102.

Hertz, L., L. Peng, et al. (2007). "Energy metabolism in astrocytes: high rate of oxidative metabolism and spatiotemporal dependence on glycolysis/glycogenolysis." J Cereb Blood Flow Metab **27**(2): 219-49.

Hirrlinger, J., S. Hulsmann, et al. (2004). "Astroglial processes show spontaneous motility at active synaptic terminals in situ." Eur J Neurosci **20**(8): 2235-9.

Hoop de, M. J., L. Meyn, et al. (1998). Culturing hippocampal neurons and astrocytes from fetal rodent brain. Cell Biology: a laboratory handbook. J. E. Celis. San Diego, Academic Press. **1:** 154-163.

Jat, P. S., M. D. Noble, et al. (1991). "Direct derivation of conditionally immortal cell lines from an H-2Kb-tsA58 transgenic mouse." Proc Natl Acad Sci U S A **88**(12): 5096-100.

Jat, P. S. and P. A. Sharp (1989). "Cell lines established by a temperature-sensitive simian virus 40 large-T-antigen gene are growth restricted at the nonpermissive temperature." Mol Cell Biol **9**(4): 1672-81.

Jost, C. R., C. E. Van Der Zee, et al. (2002). "Creatine kinase B-driven energy transfer in the brain is important for habituation and spatial learning behaviour, mossy fibre field size and determination of seizure susceptibility." Eur J Neurosci **15**(10): 1692-706.

Kim, S. S., J. M. Choi, et al. (2005). "cAMP induces neuronal differentiation of mesenchymal stem cells via activation of extracellular signal-regulated kinase/MAPK." Neuroreport **16**(12): 1357-61.

Kirschner, M. W. (1980). "Implications of treadmilling for the stability and polarity of actin and tubulin polymers in vivo." J Cell Biol **86**(1): 330-4.

Kuiper, J. W., H. Pluk, et al. (2008). "Creatine kinase-mediated ATP supply fuels actin-based events in phagocytosis." PLoS Biol **6**(3): e51.

Magistretti, P. J. (2006). "Neuron-glia metabolic coupling and plasticity." J Exp Biol **209**(Pt 12): 2304-11.

Manos, P. and G. K. Bryan (1993). "Cellular and subcellular compartmentation of creatine kinase in brain." Dev Neurosci **15**(3-5): 271-9.

Noble, M., A. K. Groves, et al. (1995). "The H-2KbtsA58 transgenic mouse: a new tool for the rapid generation of novel cell lines." Transgenic Res **4**(4): 215-25.

Oliet, S. H., R. Piet, et al. (2004). "Glial modulation of synaptic transmission: Insights from the supraoptic nucleus of the hypothalamus." Glia **47**(3): 258-67.

Pipas, J. M. and A. J. Levine (2001). "Role of T antigen interactions with p53 in tumorigenesis." Semin Cancer Biol **11**(1): 23-30.

Pollard, T. D. and G. G. Borisy (2003). "Cellular motility driven by assembly and disassembly of actin filaments." Cell **112**(4): 453-65.

Renfranz, P. J., M. G. Cunningham, et al. (1991). "Region-specific differentiation of the hippocampal stem cell line HiB5 upon implantation into the developing mammalian brain." Cell **66**(4): 713-29.

Reuss, B., R. Dono, et al. (2003). "Functions of fibroblast growth factor (FGF)-2 and FGF-5 in astroglial differentiation and blood-brain barrier permeability: evidence from mouse mutants." J Neurosci **23**(16): 6404-12.

Shen, W., D. Willis, et al. (2003). "Expression of creatine kinase isoenzyme genes during postnatal development of rat brain cerebrum: evidence for posttranscriptional regulation." Dev Neurosci **25**(6): 421-35.

Shin, J. B., F. Streijger, et al. (2007). "Hair bundles are specialized for ATP delivery via creatine kinase." Neuron **53**(3): 371-86.

Steeghs, K., F. Oerlemans, et al. (1995). "Mice deficient in ubiquitous mitochondrial creatine kinase are viable and fertile." Biochim Biophys Acta **1230**(3): 130-8.

Streijger F, I. t. Z. H., Renema WKJ, Oerlemans F, Heerschap A, Kuiper J, Pluk H, Jost CR, Van der Zee CEEM, Wieringa B (2007). "Developmental and functional consequences of disturbed energetic communication in brain of creatine kinase deficient mice: Understanding CK's role in fueling of behavior and learning." (Valdur Saks, Wiley-VCH Verlag GmbH & Co).

Streijger, F., C. R. Jost, et al. (2004). "Mice lacking the UbCKmit isoform of creatine kinase reveal slower spatial learning acquisition, diminished exploration and habituation, and reduced acoustic startle reflex responses." Mol Cell Biochem **256-257**(1-2): 305-18.

Streijger, F., F. Oerlemans, et al. (2005). "Structural and behavioural consequences of double deficiency for creatine kinases BCK and UbCKmit." Behav Brain Res **157**(2): 219-34.

Suon, S., H. Jin, et al. (2004). "Transient differentiation of adult human bone marrow cells into neuron-like cells in culture: development of morphological and biochemical traits is mediated by different molecular mechanisms." Stem Cells Dev **13**(6): 625-35.

Tachikawa, M., M. Fukaya, et al. (2004). "Distinct cellular expressions of creatine synthetic enzyme GAMT and creatine kinases uCK-Mi and CK-B suggest a novel neuron-glial relationship for brain energy homeostasis." Eur J Neurosci **20**(1): 144-60.

Wallimann, T. and W. Hemmer (1994). "Creatine kinase in non-muscle tissues and cells." Mol Cell Biochem **133-134**: 193-220.

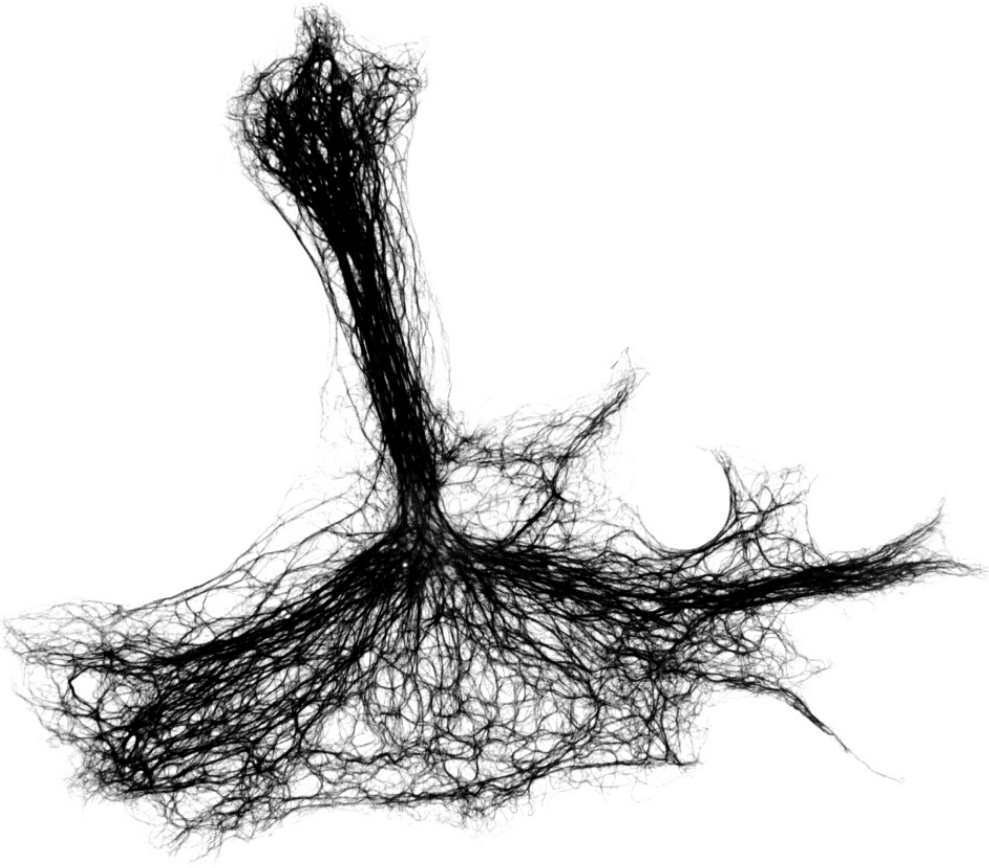

Chapter - 6 -

General Discussion

General Discussion

Every living cell has to maintain a balance between ATP expenditure and ATP generation to support essential processes, such as production and modification of macromolecules, generation and preservation of electrochemical gradients and cellular motility. However, it is still unknown how cells exactly match intermittent energy requirements with an adequate production of ATP and whether cells control their ATP fluxes by "demand- or supply-management". In principle, generation of ATP by OXPHOS is strongly dependent on the availability of ADP (Kunz, Bohnensack et al. 1981) and therefore, excessive hydrolysis of ATP (increasing ADP) stimulates OXPHOS. In addition to this simplified "demand-driven" mechanism, ATP production is regulated by "supply-driven" factors such as, oxygen availability, free calcium concentration and the presence of ATP buffering systems (Kunz 2001; Dzeja and Terzic 2003).

The creatine kinase (CK) system plays a central role in buffering ATP/ADP levels in cells with fluctuating energy demands. Moreover, the inhomogenity of ATP levels due to spatially and temporally separated consumption and production is thought to be bridged by the CK reaction (Bessman and Carpenter 1985; Dzeja and Terzic 2003). Therefore, to elaborate on the role of CK in global and regional buffering of ATP/ADP levels it is important to consider the cellular distribution of CK isoforms in cells. Although many studies investigated functional aspects of the CK-system in muscle tissue, relatively few reports provide insight in the role of CKs in non-muscle cells. In this thesis the brain-type CK isozyme (CK-B) was studied in the context of cellular processes occurring in astrocytes, neurons and macrophages.

The main finding of this Ph.D. study is that CK-B exhibits a non-homogenous distribution during active remodeling of the actin cytoskeleton. Furthermore, we demonstrate that this compartmentalization of CK-B, by virtue of its effects on local enzymatic ~P exchange capacity, facilitates processes such as cell spreading, migration and morphology.

These findings form a firm basis for future work, wherein more study will be required to address the question whether the dynamic partitioning of CK activity also leads to concordant variations in local ATP/ADP concentration(s).

CK-B recruitment to subcellular sites involved in actin remodeling

Our studies in macrophages and microglia demonstrated that the evenly smooth cytosolic distribution of CK-B was altered during local actin remodeling in phagocytosis, cell migration and cell spreading (Chapter 2 and 3). During formation of the phagocytic cup, CK-B co-accumulated with dynamic F-actin in nascent phagosomes. In a similar fashion CK-B was partitioned at actin-rich ruffles of fibroblasts and astrocytes during cell spreading and migration. Interestingly, CK-B was never found to be associated with the more static F-actin in stress fibers. This suggests an indirect binding of CK-B to F-actin, since associated proteins differ between stress fibers and F-actin structures found in membrane ruffles (Fukui, Lynch et al. 1989; Borowsky and Hynes 1998). A model in which CK-B and actin are functionally but not structurally associated is also consistent with findings from pull-down assays, yeast-2-hybrid and FRAP experiments that did not demonstrate an obvious interaction between actin and CK-B (Chapter 2 and unpublished data). However, fast "kiss-and-run"-type of interactions between CK-B and actin or actin-binding proteins cannot be excluded at this stage.

Another explanation for our findings is that partner proteins, though exhibiting a spatial and temporal distribution pattern similar to actin, mediate binding and accumulation of CK-B. Complement mediated phagocytosis, cell motility and cell spreading depend on integrin-mediated adhesion. During adhesion, integrin outside-inside signaling triggers the recruitment of focal adhesion proteins including vinculin, talin and alpha-actinin (Allen and Aderem 1996; Swanson and Hoppe 2004). In addition to proteins of the actin polymerization machinery, several myosins and small GTPases, do accumulate in those dynamic structures (Diakonova, Bokoch et al. 2002; Hoppe and Swanson 2004). It is possible that CK-B is recruited through binding of one of these focal adhesion or actin-associated proteins. Interesting parallels could occur here with the recruitment of the nucleoside diphosphate kinase NM23-H1, which associates with β1-integrins via the adapter protein ICAP-1α (Fournier, Dupe-Manet et al. 2002). Engagement of β1-integrins with their respective ligands, thereby mobilizes NM23-H1 into local adhesion sites via binding to ICAP-1α. Here, its ~P transfer capabilities could affect cell motility and adhesion (Fournier,

Albiges-Rizo et al. 2003). An analogous mechanism could be envisaged for CK-B, but until now, no obvious binding domains have been identified in CK-B, except for its own homodimerization domain (Eder, Schlattner et al. 1999). However, proteins have been found to interact with CK-B, including Golgi matrix protein 130 (GM130) (Burklen, Hirschy et al. 2007), metallothionein-3 (Lahti, Hoekman et al. 2005), the SOCS box-containing protein Asb-9 (Debrincat, Zhang et al. 2007), K^+-Cl^- co-transporter 2 (KCC2) (Inoue, Ueno et al. 2004) and the thrombin receptor, PAR-1 (Mahajan, Pai et al. 2000). Unfortunately, none of these proteins are known to actin interactors or focal adhesion components.

Another possibility is that CK-B interacts with a protein that is constitutively present at these specific sites, but only creates a temporal docking place during actin remodeling. Reversible post-translational modifications, such as phosphorylation, methylation (Clarke and Tamanoi 2004), oxidation (van den Berk, Landi et al. 2005), arginylation (Decca, Carpio et al. 2007) or sumoylation (Wasiak, Zunino et al. 2007) could provide the structural requirements for such a docking site.

Alternatively, CK-B itself is modified to facilitate binding to an existing docking site. Indeed, CK-B is prone to covalent modifications such as (auto)phosphorylation (Hemmer, Furter-Graves et al. 1995; Reiss, Hermon et al. 1996), oxidation (Aksenov, Aksenova et al. 2000) and methylation (Iwabata, Yoshida et al. 2005) and ubiquitin modification (Debrincat, Zhang et al. 2007) . Phosphorylation of CK-B by protein kinase C (PKC) forms an attractive possibility, since PKC signaling is prominently involved in phagocytosis (Allen and Aderem 1995; Larsen, Ueyama et al. 2002) and other cytoskeletal remodeling processes, such as formation of cell protrusions (Frank, Hatfield et al. 1998), cell spreading (Disatnik, Boutet et al. 2002) and generation of dendritic spines (Calabrese and Halpain 2005).

Moreover, several studies suggest that CK-B is indeed a target for PKC phosphorylation (Chida, Kasahara et al. 1990; Chida, Tsunenaga et al. 1990; Reiss, Hermon et al. 1996). In an attempt to identify potential phosphorylation sites involved in localization, we changed 6 potential phosphorylation sites by site-directed mutagenesis (S128A, S129A, S163A, T180A, T262A, Y82F) based on software-based phosphorylation prediction and accessibility in the 3D structure of CK-B (Blom, Gammeltoft et al. 1999; Eder, Schlattner et al. 1999). Unfortunately, none of these

mutations abolished recruitment of CK-B to phagosomes or affected phagocytosis efficiency (unpublished results). Clearly, the limited number of mutations tested does not exclude a role of phosphorylation yet, and therefore, more research addressing this issue is needed, but concomitantly, our attention should also be directed more intensively to possible effects of other types of modification.

CK-B and GTPase signaling

Chapters 2 and 3 demonstrated that the presence of CK-B at sites of extensive actin remodeling was important for cell adhesion, cell migration and complement mediated phagocytosis. Displacement of endogenous CK-B in macrophages by catalytically inactive CK-B$_{(C283S)}$ inhibited complement mediated phagocytosis, demonstrating that local presence of active CK-B is the key parameter. Our findings also show that a mere structural role of CK-B in cell shape dynamics is unlikely. Pharmacological inhibition studies confirm this point. Moreover, specific targeting of CK-B to membranes increased cell migration and lamellipodium formation. One important remaining question is what the ATP-consuming molecules are that are dependent on CK-B mediated phosphotransfer during actin remodeling? A number of clues come from the phagocytosis experiments that demonstrated that CK-B only contributed to complement-mediated phagocytosis, but not IgG-mediated phagocytosis. At first glance this was a puzzling observation since both types of phagocytosis require actin remodeling and moreover, CK-B recruitment was observed in both types of events. However, this finding might be better explained if we consider that unique molecular pathways, such as small GTPase and kinase signaling, differ dramatically between these types of phagocytosis (Allen and Aderem 1996; Caron and Hall 1998). While IgG mediated phagocytosis requires activity of Rac and Cdc42, complement mediated phagocytosis utilizes RhoA and Rap1 (Caron and Hall 1998; Caron, Self et al. 2000). CK-B could differentially regulate RhoA and/or Rap1 by providing a privileged supply of GTP (e.g. by converting ATP to GTP through NDPK). Intriguingly, RhoA activity is more sensitive to ATP depletion, than Rac and Cdc42 (Hallett, Dagher et al. 2003). Because the concentration of GTP under ATP depleted conditions was almost 100 times higher (~17 μM) than the affinity constant of RhoA

(K_D~0.2 μM), the authors consider a direct effect of ATP depletion on RhoA activity unlikely (Hallett, Dagher et al. 2003). However, the possibility remains that subcellular levels of GTP and GDP differ from global levels. Affinity for GTP is similar for all three Rho GTPases, which makes specific regulation by local [GTP] only difficult to imagine, but not impossible if seen in combination with a distinct intracellular distribution of these proteins. Instead, the authors favor another model and suggest that ATP depletion affects the activity of GAPs and/or GEFs that subsequently modulate Rho GTPase activity. The fact that inhibition of CK-B decreased complement-mediated phagocytosis could point to a decreased GEF (or increased GAP) activity towards RhoA. Interestingly, Mahajan *et al.* reported that PAR-1 and CK-B interact and modulate RhoA effects (Mahajan, Pai et al. 2000) during thrombin signaling. However, no mechanism was uncovered that could explain how CK-B's enzymatic activity is linked with RhoA activity. Clearly, more research is necessary to clarify if – and how - CK-B is involved in regulating GTP status of small Rho GTPases during actin-based processes.

CK-B and myosin

During phagocytosis, cell spreading and migration several myosins are required for force generation, e.g. to promote closure of the phagocytic cup and retraction of the rear end of the cell (Kolega 2006; Giannone, Dubin-Thaler et al. 2007; Koestler, Auinger et al. 2008). CK-B can contribute to these processes by providing preferential access to ATP for myosins and decreasing concentrations of the inhibiting hydrolysis product, ADP.

Myosin-X is an non-convential myosin that associates with dynamic actin in lamellipodia and filopodia (Berg, Derfler et al. 2000) and is able to bind phosphatidylinositol (3,4,5)-trisphosphate (PIP_3) through its PH domains (Isakoff, Cardozo et al. 1998). The FERM domain of the protein is important for binding integrins and subsequently, position it at the tips of filopodia (Zhang, Berg et al. 2004). These properties make myosin-X a key-organizer of adhesion. Indeed, it was demonstrated that myosin-X facilitates integrin dependent elongation and adhesion of filopodia, as well as pseudopod extension during phagocytosis (Cox, Berg et al.

2002; Zhang, Berg et al. 2004). Strikingly, myosin-X and CK-B share a remarkably similar subcellular distribution: Both accumulate in membrane ruffles, lamellipodia and tips of filopodia. Moreover, CK-B is involved in integrin mediated adhesion events during complement-mediated phagocytosis, while myosin-X is able to bind NPL(Y/F) motifs found in β-integrins and mediates adhesion (Zhang, Berg et al. 2004). Therefore, myosin-X would be an interesting candidate to be (partially) dependent on CK-B mediated ATP supply.

Also another myosin, myosin-II, has been implicated in linking adhesion formation to protrusion of the leading edge during cell migration (Giannone, Dubin-Thaler et al. 2007), cell spreading (Betapudi, Licate et al. 2006) and complement mediated phagocytosis (Olazabal, Caron et al. 2002). Preliminary protein interaction studies with CK-B and CK-B fragments point at myosin-II regulatory light chain (MRLC) as a potential binding partner for CK-B (Helma Pluk, personal communication), suggesting that myosin-II could fueled by CK-B. In the near future, our group will devote more work to validate these findings and obtain a better understanding of the molecular and functional aspects of this CK-B v.s. myosin-II interaction.

Obviously, optimal local ATP/ADP ratios would also benefit any other/additional myosin ATPase isoforms involved in cell migration and phagocytosis. It is therefore clear that it will surely become a technically enormously challenging task to discriminate between all the possible roles that CK-B mediated ~P relay could have in the control of different myosin isoforms in living cells.

CK-B and actin polymerization

Central to actin remodeling is the continuous polymerization and depolymerization of actin filaments, called treadmilling. Although monomers can be added to both the barbed and the pointed end of filaments, barbed-end polymerization is promoted by its lower on-rate constant for ATP-actin (Pollard and Cooper 1986). Addition of ATP-actin at the barbed end of actin-filaments, followed by hydrolysis of bound ATP and subsequent release of actin monomers and P_i, therefore requires a constant supply of ATP (Wolven, Belmont et al. 2000; Pollard and Borisy 2003). Besides the

intrinsic polymerization properties of actin, a plethora of actin-associated proteins modulate its dynamic properties. Depolymerization kinetics are controlled by accessory proteins, such as gelsolin ADF and cofilin (Hotulainen, Paunola et al. 2005; Larson, Arnaudeau et al. 2005). Thymosins and profilins sequester actin monomers and thereby alter the effective concentrations of free G-actin, whereby profilin also catalyzes nucleotide exchange (Selden, Kinosian et al. 1999; Wolven, Belmont et al. 2000; Pollard and Borisy 2003). Interestingly, the sequestering properties of these proteins depend on the bound nucleotide of actin (Atkinson, Hosford et al. 2004). Therefore, the process of actin polymerization cannot be seen outside the context of its complex regulation, but the importance of the basic relevance of various ATP-driven reactions in this whole process is clear. Recently, this was experimentally demonstrated by a study estimating that actin-polymerization accounts for up to 50% of total ATP hydrolysis in brain (Bernstein and Bamburg 2003).

As shown in this thesis study, and in work of others elsewhere, actin polymerization in cells is tightly regulated in a spatial and temporal manner during cell migration and phagocytosis. To explain the here-identified role of CK-B on actin behavior several models are possible. The simplest model would be that CK-B provides ATP to sustain a constant pool of ATP-actin, necessary for optimal polymerization (Selden, Kinosian et al. 1999; Wolven, Belmont et al. 2000; Pollard and Borisy 2003; Atkinson, Hosford et al. 2004). More complex mechanisms may also be involved, as actin depolymerization may also indirectly rely on ATP-supply. Because CK isozymes are implicated in calcium handling by fueling calcium pumps (de Groof, Fransen et al. 2002; Shin, Streijger et al. 2007), it is possible that CK-B regulates F-actin levels by modulating local calcium levels. Gelsolin is an actin capping and severing protein which activity depends on intracellular calcium. Decreasing intracellular calcium levels will inactivate its depolymerization ability and thereby increase F-actin levels (Larson, Arnaudeau et al. 2005). Intriguingly, bioinformatic analysis disclosed an evolutionary conserved co-expression profile of CK-B and gelsolin (Helma Pluk, personal communication), which could predict a functional relationship (van Noort, Snel et al. 2003). The central role of gelsolin in various processes involving actin-remodeling, such as phagocytosis and cell motility,

mark it as an interesting partner for functional interaction (Silacci, Mazzolai et al. 2004).

In addition to decreases in F-actin we also observed defects in the adhesive properties of cells that lack CK-B activity. Wildtype astrocytes performed better in cell spreading assays than CK-B (-/-) astrocytes, suggesting altered adhesion properties and/or faster extension of lamellipodia. Inhibition of CK-B's enzymatic activity also caused defective integrin-mediated adhesion of particles to macrophages. Adhesive properties of integrins are regulated by extracellular signals (outside-in) and intracellular signals (inside-out). Outside-in signals are mediated after binding of specific ligands, whereas inside-out signals involve (small GTPase) signaling events (Caron, Self et al. 2000; Carman and Springer 2003). Recently, actin polymerization was identified as a major factor in integrin probing (Galbraith, Yamada et al. 2007), which facilitates adhesion. Accordingly, our studies indicate that only integrin-mediated adhesion required actin polymerization, whereas IgG-mediated adhesion was not diminished by low doses of an actin polymerization inhibitor. Strikingly, a recent study confirmed this observation and proposes a cell ruffle-mediated capture mechanism for the uptake of complement coated particles, which is driven by cytoskeletal forces (Patel and Harrison 2008). Therefore, we propose that CK-B mediated regulation of F-actin levels may be crucial for integrin mediated adhesion events. If this proposal holds, this raises the interesting question if such cooperation is equally effective for all integrin-mediated processes, or rather is integrin-type and cell type dependent.

CK-B knockout mouse

Animal models provide ideal opportunities to answer such questions in the integral physiological context. Genetic engineering of mice provides a powerful tool to remove (knock-out), alter or add genes (knock-in) in order to unravel their functions during development, normal physiology and pathology (Cohen-Tannoudji and Babinet 1998). Using this approach, our group ablated all four genes encoding CK subunits in individual mouse models and studied the phenotypic consequences of deficiency (van Deursen, Heerschap et al. 1993; Steeghs, Oerlemans et al. 1995;

Steeghs, Heerschap et al. 1997; Jost, Van Der Zee et al. 2002). Deletion of the muscle-specific isoforms of CK revealed phenotypical changes, including lack of burst activity (van Deursen, Heerschap et al. 1993) and changes in calcium handling (Steeghs, Benders et al. 1997; de Groof, Fransen et al. 2002). Also, metabolic adaptations were observed, including increases in mitochondrial volume and glycolytic potential (van Deursen, Heerschap et al. 1993; Steeghs, Benders et al. 1997; de Groof, Oerlemans et al. 2001).

Since the non-muscle isoforms of CK, CK-B and ubCKmit, are highly expressed in brain, it was not surprising that ablation of these isoforms in mice revealed concordantly phenotypic changes, such as behavioral changes and altered brain morphology (Jost, Van Der Zee et al. 2002; Streijger, Oerlemans et al. 2005). These studies learned us that also animal model studies do not offer the final answer, and therefore reversion of studies to the cellular level was still necessary to understand the molecular mechanisms involved in the different problems seen in these mice. By combining earlier findings and findings presented here in this thesis we can now propose a clearer picture on the proposed coupling between CK-B and the complex actin-based processes that play a key role in brain development and physiology, e.g. axon guidance (Nakamoto, Kain et al. 2004), synaptic plasticity (Shi and Ethell 2006) and dendritic spine remodeling or astrocyte end-feet dynamics (Hirrlinger, Hulsmann et al. 2004; Hertz, Peng et al. 2007). One intriguing circumstantial finding came from the observation that the complement pathway is implicated in synapse elimination (Stevens, Allen et al. 2007). We placed CK-B in the same pathway, by finding that CK-B facilitates complement-mediated phagocytosis (Chapter 2). Therefore, it is tempting to speculate that disturbances of actin-based events in CK-B knockout mice, possible those involved in cell pruning, could lead to some of the observed phenotypic changes, such as deteriorated spatial learning or aberrant morphology of intra-infra pyramidal fibers (Jost, Van Der Zee et al. 2002).

Concluding remarks

The main objective of this thesis was to identify specific cellular processes that require CK-B to maintain a favorable ATP/ADP ratio. In the different chapters I

provide congruent evidence, demonstrating that CK-B plays a key-role in actin-based processes during phagocytosis, adhesion and cell migration, processes that are of importance in pathological situations, such as infection and cancer. The next challenge in further work will be the dissection of the molecular effectors that benefit from CK-mediated ATP generation in different cell types, in healthy and diseased tissues. Identification of molecular interactions of CK-B with potential effectors and/or functional protein complexes could reveal some clues, but these studies will be difficult due to the very dynamic and transient nature of these interactions. Undoubtedly, new technology will also be required in order to address the (subcellular) modulation of metabolite distribution by CK-B in the living cell during the aforementioned processes. For this purpose, the development of ATP sensors could provide a valuable tool (Shih, Gryczynski et al. 2000; Iino, Murakami et al. 2005; Willemse, Janssen et al. 2007). Finally, it is also important to take into account indirect ATP-modulated factors that alter the actin cytoskeleton, such as calcium- and metabolic signaling (e.g. AMPK signaling) (Ponticos, Lu et al. 1998; Lee, Koh et al. 2007).

In conclusion, the studies presented in this thesis offer new insights and perspectives in understanding how metabolism and actin-based processes are spatially and temporally interlinked, under normal physiological conditions and under pathological circumstances.

References

Aksenov, M., M. Aksenova, et al. (2000). "Oxidative modification of creatine kinase BB in Alzheimer's disease brain." J Neurochem **74**(6): 2520-7.

Allen, L. A. and A. Aderem (1996). "Molecular definition of distinct cytoskeletal structures involved in complement- and Fc receptor-mediated phagocytosis in macrophages." J Exp Med **184**(2): 627-37.

Allen, L. H. and A. Aderem (1995). "A role for MARCKS, the alpha isozyme of protein kinase C and myosin I in zymosan phagocytosis by macrophages." J Exp Med **182**(3): 829-40.

Atkinson, S. J., M. A. Hosford, et al. (2004). "Mechanism of actin polymerization in cellular ATP depletion." J Biol Chem **279**(7): 5194-9.

Berg, J. S., B. H. Derfler, et al. (2000). "Myosin-X, a novel myosin with pleckstrin homology domains, associates with regions of dynamic actin." J Cell Sci **113 Pt 19**: 3439-51.

Bernstein, B. W. and J. R. Bamburg (2003). "Actin-ATP hydrolysis is a major energy drain for neurons." J Neurosci **23**(1): 1-6.

Bessman, S. P. and C. L. Carpenter (1985). "The creatine-creatine phosphate energy shuttle." Annu Rev Biochem **54**: 831-62.

Betapudi, V., L. S. Licate, et al. (2006). "Distinct roles of nonmuscle myosin II isoforms in the regulation of MDA-MB-231 breast cancer cell spreading and migration." Cancer Res **66**(9): 4725-33.

Blom, N., S. Gammeltoft, et al. (1999). "Sequence and structure-based prediction of eukaryotic protein phosphorylation sites." J Mol Biol **294**(5): 1351-62.

Borowsky, M. L. and R. O. Hynes (1998). "Layilin, a novel talin-binding transmembrane protein homologous with C-type lectins, is localized in membrane ruffles." J Cell Biol **143**(2): 429-42.

Burklen, T. S., A. Hirschy, et al. (2007). "Brain-type creatine kinase BB-CK interacts with the Golgi Matrix Protein GM130 in early prophase." Mol Cell Biochem **297**(1-2): 53-64.

Calabrese, B. and S. Halpain (2005). "Essential role for the PKC target MARCKS in maintaining dendritic spine morphology." Neuron **48**(1): 77-90.

Carman, C. V. and T. A. Springer (2003). "Integrin avidity regulation: are changes in affinity and conformation underemphasized?" Curr Opin Cell Biol **15**(5): 547-56.

Caron, E. and A. Hall (1998). "Identification of two distinct mechanisms of phagocytosis controlled by different Rho GTPases." Science **282**(5394): 1717-21.

Caron, E., A. J. Self, et al. (2000). "The GTPase Rap1 controls functional activation of macrophage integrin alphaMbeta2 by LPS and other inflammatory mediators." Curr Biol **10**(16): 974-8.

Chida, K., K. Kasahara, et al. (1990). "Purification and identification of creatine phosphokinase B as a substrate of protein kinase C in mouse skin in vivo." Biochem Biophys Res Commun **173**(1): 351-7.

Chida, K., M. Tsunenaga, et al. (1990). "Regulation of creatine phosphokinase B activity by protein kinase C." Biochem Biophys Res Commun **173**(1): 346-50.

Clarke, S. and F. Tamanoi (2004). "Fighting cancer by disrupting C-terminal methylation of signaling proteins." J Clin Invest **113**(4): 513-5.

Cohen-Tannoudji, M. and C. Babinet (1998). "Beyond 'knock-out' mice: new perspectives for the programmed modification of the mammalian genome." Mol Hum Reprod **4**(10): 929-38.

Cox, D., J. S. Berg, et al. (2002). "Myosin X is a downstream effector of PI(3)K during phagocytosis." Nat Cell Biol **4**(7): 469-77.

de Groof, A. J., J. A. Fransen, et al. (2002). "The creatine kinase system is essential for optimal refill of the sarcoplasmic reticulum Ca2+ store in skeletal muscle." J Biol Chem **277**(7): 5275-84.

de Groof, A. J., F. T. Oerlemans, et al. (2001). "Changes in glycolytic network and mitochondrial design in creatine kinase-deficient muscles." Muscle Nerve **24**(9): 1188-96.

Debrincat, M. A., J. G. Zhang, et al. (2007). "Ankyrin repeat and suppressors of cytokine signaling box protein asb-9 targets creatine kinase B for degradation." J Biol Chem **282**(7): 4728-37.

Decca, M. B., M. A. Carpio, et al. (2007). "Post-translational arginylation of calreticulin: a new isospecies of calreticulin component of stress granules." J Biol Chem **282**(11): 8237-45.

Diakonova, M., G. Bokoch, et al. (2002). "Dynamics of cytoskeletal proteins during Fcgamma receptor-mediated phagocytosis in macrophages." Mol Biol Cell **13**(2): 402-11.

Disatnik, M. H., S. C. Boutet, et al. (2002). "Sequential activation of individual PKC isozymes in integrin-mediated muscle cell spreading: a role for MARCKS in an integrin signaling pathway." J Cell Sci **115**(Pt 10): 2151-63.

Dzeja, P. P. and A. Terzic (2003). "Phosphotransfer networks and cellular energetics." J Exp Biol **206**(Pt 12): 2039-47.

Eder, M., U. Schlattner, et al. (1999). "Crystal structure of brain-type creatine kinase at 1.41 A resolution." Protein Sci **8**(11): 2258-69.

Fournier, H. N., C. Albiges-Rizo, et al. (2003). "New insights into Nm23 control of cell adhesion and migration." J Bioenerg Biomembr **35**(1): 81-7.

Fournier, H. N., S. Dupe-Manet, et al. (2002). "Integrin cytoplasmic domain-associated protein 1alpha (ICAP-1alpha) interacts directly with the metastasis suppressor nm23-H2, and both proteins are targeted to newly formed cell adhesion sites upon integrin engagement." J Biol Chem **277**(23): 20895-902.

Frank, S. R., J. C. Hatfield, et al. (1998). "Remodeling of the actin cytoskeleton is coordinately regulated by protein kinase C and the ADP-ribosylation factor nucleotide exchange factor ARNO." Mol Biol Cell **9**(11): 3133-46.

Fukui, Y., T. J. Lynch, et al. (1989). "Myosin I is located at the leading edges of locomoting Dictyostelium amoebae." Nature **341**(6240): 328-31.

Galbraith, C. G., K. M. Yamada, et al. (2007). "Polymerizing actin fibers position integrins primed to probe for adhesion sites." Science **315**(5814): 992-5.
Giannone, G., B. J. Dubin-Thaler, et al. (2007). "Lamellipodial actin mechanically links myosin activity with adhesion-site formation." Cell **128**(3): 561-75.
Hallett, M. A., P. C. Dagher, et al. (2003). "Rho GTPases show differential sensitivity to nucleotide triphosphate depletion in a model of ischemic cell injury." Am J Physiol Cell Physiol **285**(1): C129-38.
Hemmer, W., E. M. Furter-Graves, et al. (1995). "Autophosphorylation of creatine kinase: characterization and identification of a specifically phosphorylated peptide." Biochim Biophys Acta **1251**(2): 81-90.
Hertz, L., L. Peng, et al. (2007). "Energy metabolism in astrocytes: high rate of oxidative metabolism and spatiotemporal dependence on glycolysis/glycogenolysis." J Cereb Blood Flow Metab **27**(2): 219-49.
Hirrlinger, J., S. Hulsmann, et al. (2004). "Astroglial processes show spontaneous motility at active synaptic terminals in situ." Eur J Neurosci **20**(8): 2235-9.
Hoppe, A. D. and J. A. Swanson (2004). "Cdc42, Rac1, and Rac2 display distinct patterns of activation during phagocytosis." Mol Biol Cell **15**(8): 3509-19.
Hotulainen, P., E. Paunola, et al. (2005). "Actin-depolymerizing factor and cofilin-1 play overlapping roles in promoting rapid F-actin depolymerization in mammalian nonmuscle cells." Mol Biol Cell **16**(2): 649-64.
Iino, R., T. Murakami, et al. (2005). "Real-time monitoring of conformational dynamics of the epsilon subunit in F1-ATPase." J Biol Chem **280**(48): 40130-4.
Inoue, K., S. Ueno, et al. (2004). "Interaction of neuron-specific K+-Cl- cotransporter, KCC2, with brain-type creatine kinase." FEBS Lett **564**(1-2): 131-5.
Isakoff, S. J., T. Cardozo, et al. (1998). "Identification and analysis of PH domain-containing targets of phosphatidylinositol 3-kinase using a novel in vivo assay in yeast." Embo J **17**(18): 5374-87.
Iwabata, H., M. Yoshida, et al. (2005). "Proteomic analysis of organ-specific post-translational lysine-acetylation and -methylation in mice by use of anti-acetyllysine and -methyllysine mouse monoclonal antibodies." Proteomics **5**(18): 4653-64.
Jost, C. R., C. E. Van Der Zee, et al. (2002). "Creatine kinase B-driven energy transfer in the brain is important for habituation and spatial learning behaviour, mossy fibre field size and determination of seizure susceptibility." Eur J Neurosci **15**(10): 1692-706.
Koestler, S. A., S. Auinger, et al. (2008). "Differentially oriented populations of actin filaments generated in lamellipodia collaborate in pushing and pausing at the cell front." Nat Cell Biol **10**(3): 306-13.
Kolega, J. (2006). "The role of myosin II motor activity in distributing myosin asymmetrically and coupling protrusive activity to cell translocation." Mol Biol Cell **17**(10): 4435-45.
Kunz, W., R. Bohnensack, et al. (1981). "Relations between extramitochondrial and intramitochondrial adenine nucleotide systems." Arch Biochem Biophys **209**(1): 219-29.
Kunz, W. S. (2001). "Control of oxidative phosphorylation in skeletal muscle." Biochim Biophys Acta **1504**(1): 12-9.
Lahti, D. W., J. D. Hoekman, et al. (2005). "Identification of mouse brain proteins associated with isoform 3 of metallothionein." Protein Sci **14**(5): 1151-7.
Larsen, E. C., T. Ueyama, et al. (2002). "A role for PKC-epsilon in Fc gammaR-mediated phagocytosis by RAW 264.7 cells." J Cell Biol **159**(6): 939-44.
Larson, L., S. Arnaudeau, et al. (2005). "Gelsolin mediates calcium-dependent disassembly of Listeria actin tails." Proc Natl Acad Sci U S A **102**(6): 1921-6.
Lee, J. H., H. Koh, et al. (2007). "Energy-dependent regulation of cell structure by AMP-activated protein kinase." Nature **447**(7147): 1017-20.
Mahajan, V. B., K. S. Pai, et al. (2000). "Creatine kinase, an ATP-generating enzyme, is required for thrombin receptor signaling to the cytoskeleton." Proc Natl Acad Sci U S A **97**(22): 12062-7.
Nakamoto, T., K. H. Kain, et al. (2004). "Neurobiology: New connections between integrins and axon guidance." Curr Biol **14**(3): R121-3.
Olazabal, I. M., E. Caron, et al. (2002). "Rho-kinase and myosin-II control phagocytic cup formation during CR, but not FcgammaR, phagocytosis." Curr Biol **12**(16): 1413-18.
Patel, P. C. and R. E. Harrison (2008). "Membrane Ruffles Capture C3bi-opsonized Particles in Activated Macrophages." Mol Biol Cell.

Pollard, T. D. and G. G. Borisy (2003). "Cellular motility driven by assembly and disassembly of actin filaments." Cell **112**(4): 453-65.
Pollard, T. D. and J. A. Cooper (1986). "Actin and actin-binding proteins. A critical evaluation of mechanisms and functions." Annu Rev Biochem **55**: 987-1035.
Ponticos, M., Q. L. Lu, et al. (1998). "Dual regulation of the AMP-activated protein kinase provides a novel mechanism for the control of creatine kinase in skeletal muscle." Embo J **17**(6): 1688-99.
Reiss, N., J. Hermon, et al. (1996). "Interaction of purified protein kinase C with key proteins of energy metabolism and cellular motility." Biochem Mol Biol Int **38**(4): 711-9.
Selden, L. A., H. J. Kinosian, et al. (1999). "Impact of profilin on actin-bound nucleotide exchange and actin polymerization dynamics." Biochemistry **38**(9): 2769-78.
Shi, Y. and I. M. Ethell (2006). "Integrins control dendritic spine plasticity in hippocampal neurons through NMDA receptor and Ca2+/calmodulin-dependent protein kinase II-mediated actin reorganization." J Neurosci **26**(6): 1813-22.
Shih, W. M., Z. Gryczynski, et al. (2000). "A FRET-based sensor reveals large ATP hydrolysis-induced conformational changes and three distinct states of the molecular motor myosin." Cell **102**(5): 683-94.
Shin, J. B., F. Streijger, et al. (2007). "Hair bundles are specialized for ATP delivery via creatine kinase." Neuron **53**(3): 371-86.
Silacci, P., L. Mazzolai, et al. (2004). "Gelsolin superfamily proteins: key regulators of cellular functions." Cell Mol Life Sci **61**(19-20): 2614-23.
Steeghs, K., A. Benders, et al. (1997). "Altered Ca2+ responses in muscles with combined mitochondrial and cytosolic creatine kinase deficiencies." Cell **89**(1): 93-103.
Steeghs, K., A. Heerschap, et al. (1997). "Use of gene targeting for compromising energy homeostasis in neuro-muscular tissues: the role of sarcomeric mitochondrial creatine kinase." J Neurosci Methods **71**(1): 29-41.
Steeghs, K., F. Oerlemans, et al. (1995). "Mice deficient in ubiquitous mitochondrial creatine kinase are viable and fertile." Biochim Biophys Acta **1230**(3): 130-8.
Stevens, B., N. J. Allen, et al. (2007). "The classical complement cascade mediates CNS synapse elimination." Cell **131**(6): 1164-78.
Streijger, F., F. Oerlemans, et al. (2005). "Structural and behavioural consequences of double deficiency for creatine kinases BCK and UbCKmit." Behav Brain Res **157**(2): 219-34.
Swanson, J. A. and A. D. Hoppe (2004). "The coordination of signaling during Fc receptor-mediated phagocytosis." J Leukoc Biol **76**(6): 1093-103.
van den Berk, L. C., E. Landi, et al. (2005). "Redox-regulated affinity of the third PDZ domain in the phosphotyrosine phosphatase PTP-BL for cysteine-containing target peptides." Febs J **272**(13): 3306-16.
van Deursen, J., A. Heerschap, et al. (1993). "Skeletal muscles of mice deficient in muscle creatine kinase lack burst activity." Cell **74**(4): 621-31.
van Noort, V., B. Snel, et al. (2003). "Predicting gene function by conserved co-expression." Trends Genet **19**(5): 238-42.
Wasiak, S., R. Zunino, et al. (2007). "Bax/Bak promote sumoylation of DRP1 and its stable association with mitochondria during apoptotic cell death." J Cell Biol **177**(3): 439-50.
Willemse, M., E. Janssen, et al. (2007). "ATP and FRET--a cautionary note." Nat Biotechnol **25**(2): 170-2.
Wolven, A. K., L. D. Belmont, et al. (2000). "In vivo importance of actin nucleotide exchange catalyzed by profilin." J Cell Biol **150**(4): 895-904.
Zhang, H., J. S. Berg, et al. (2004). "Myosin-X provides a motor-based link between integrins and the cytoskeleton." Nat Cell Biol **6**(6): 523-31.

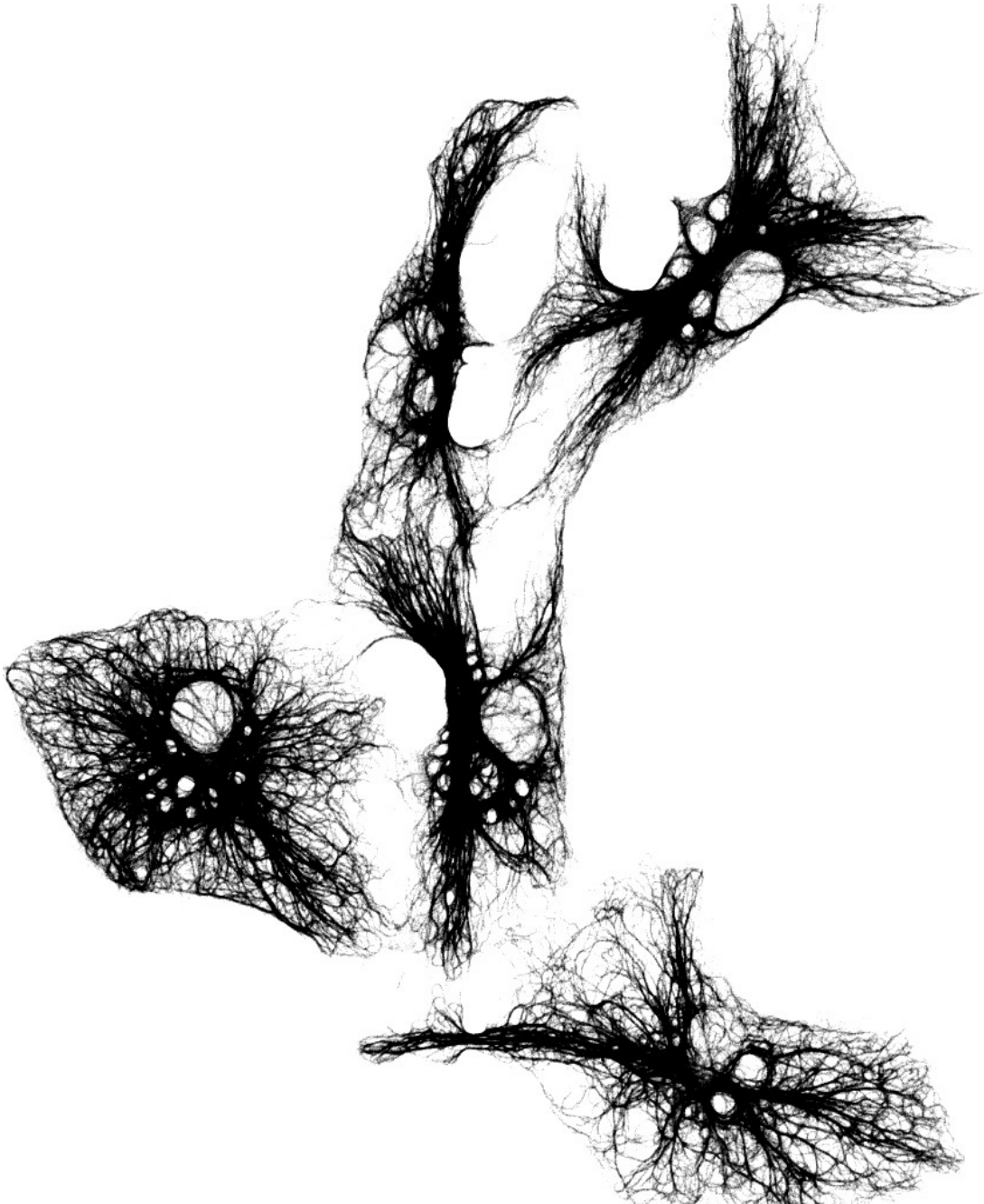

Summary / Samenvatting

Summary

Living cells perform a phenomenal number of functions, of which most are driven by hydrolysis of ATP. Under "normal" cellular conditions glycolysis and OXPHOS are able to preserve adequate levels of ATP and keep generation, distribution and consumption of ATP in balance. However, during periods of sudden rises in energy demand, the cellular availability of ATP could be potentially endangered. To prevent (local) ATP-depletion, cells developed several strategies to safeguard ATP levels and facilitate efficient distribution. The family of creatine kinase (CK) isoforms plays an important role in the temporal and spatial buffering of ATP in tissues with highly fluctuating energy demands, such as brain and muscle, by reversibly catalyzing the transfer of the high-energy phosphoryl (~P) of ATP onto creatine.

Although the role of CK isoforms in skeletal muscle has been studied extensively using mouse knockout models, the specific functions of non-muscle isoforms have remained elusive. Recently, mice lacking non-muscle isoforms (CK-B and UbCKmit) were analyzed at the physiological, histological and behavioral level, revealing aberrations in brain morphology, behavior and thermoregulation. In this dissertation the role of CK-B has been investigated at the cellular level by analyzing highly ATP-consuming processes in various cell types.

In chapter 2, the relation between CK-B and actin dynamics during phagocytosis was studied. Strikingly, CK-B, which is generally considered to be a cytosolic protein, accumulated transiently at the forming phagosome and at the tips of filopodia. Pharmacological inhibition of CK decreased phagocytic potential in a opsonin-dependent manner; CR3 mediated phagocytosis was reduced, whereas Fc-γR mediated phagocytosis remained unaffected. Dissection of the whole process into the discrete events of initial adhesion and subsequent engulfment, demonstrated that CK-B principally was involved in the initial adhesion of particles, which in turn was shown to be dependent on active actin polymerization. Remarkably, inhibition of CK-B reduced the F-actin content in macrophages, suggesting a mechanism in which CK-B facilitates actin-driven early adhesion events during phagocytosis.

In chapter 3 the identified link between actin dynamics and CK-B mediated ATP generation was investigated in the context of cell spreading and migration.

Astrocytes deficient for CK-B displayed diminished cell spreading kinetics compared to wildtype counterparts. In line with this finding, cell migration velocity was reduced when CK-B was lacking. The positive effect of CK-B on these actin-driven processes was found to be dependent on its ATP-generating capacity. In addition, transfection studies in mouse embryonic fibroblasts (MEFs) revealed that subcellular targeting of CK-B to areas involved in motility is also crucial. This corroborates our findings in macrophages and demonstrates that both enzymatic activity and subcellular targeting are important for the facilitating effect of CK-B on actin dynamics.

Chapter 4 reports studies in which the role of CK-B in intracellular transport of amyloid-precursor protein (APP) and mitochondria in primary neurons was investigated. Strikingly, no changes were found in the average and maximum velocities of mitochondria and APP in CK-B deficient neurons, although both types of transport rely heavily on ATP hydrolysis. Determination of the motile mitochondrial fraction revealed a small, but significant increase in motile mitochondria in CK-B deficient cells. It is tempting to speculate that potential shortages of local ATP due to CK-B ablation are counteracted by optimizing ATP distribution through motile mitochondria. However, more research will we needed to investigate this possibility.

The study presented in chapter 5 reports on the generation of a range of brain-derived, CK-B deficient cell lines. By cross-breeding CK-B deficient mice with "immorto-mice" the thermolabile SV40 large T antigen, tsA58, was introduced in the offspring. Derivation and subsequent analysis of conditionally immortalized cells yielded cell lines with various degrees of differentiation capacity towards the astrocytic and neuronal lineage. By re-expressing CK-B in one of the astrocytic cell lines, a cellular model system was obtained in which the function of CK-B can be studied in an otherwise "nomal" background. Cell spreading assays demonstrated that CK-B enhanced cell spreading kinetics in a cyclocreatine-inhibitable manner, which corroborates with the data obtained with primary astrocytes (Chapter 3) and thus, strengthens the usability of the cell line as a model system to study the role of CK-B.

The work presented in this thesis presents an important role for CK-B in facilitating actin dynamics during cell spreading, migration and phagocytosis.

Although it is unknown yet, how actin dynamics are controlled by CK-B's ATP generating capacity at the molecular level, the variety of actin-dependent cellular functions in different cell types predict a central role for the CK system in processes ranging from development to memory formation.

Samenvatting

De energie waarmee een levende cel zijn enorme diversiteit aan taken kan uitvoeren, wordt geleverd door de hydrolysering van ATP moleculen. Onder "normale" omstandigheden zijn glycolyse en oxidative fosforylering in staat om de productie, distributie en consumptie van ATP in balans te houden. Als cellulaire processen echter tijdelijk een sterk verhoogde vraag naar ATP hebben, kan de (lokale) beschikbaarheid van ATP potentieel in gevaar komen. Teneinde dit te voorkomen hebben cellen verschillende strategieën ontwikkeld om de concentratie en distributie van ATP te reguleren. Creatine kinase isovormen, behorend tot de familie van creatine kinases (CK), spelen een prominente rol in de temporele en spatiële buffering van ATP, door katalyse van de reversibele uitwisseling van een hoog energetisch fosfaat groep (~P) tussen ATP en creatine. Dit is met name belangrijk in in weefsels met sterk fluctuerende ATP behoeften, zoals hersenen en spieren.

De functie van CK in spieren is uitgebreid onderzocht in "knockout muizen", waarbij de CK spier-isovormen genetisch zijn uitgeschakeld. Over de functie van CK isovormen in andere weefsels en celtypen is echter aanzienlijk minder bekend. Recentelijk zijn "knock-out" muizen gecreëerd waarin deze "niet in spier voorkomende" isovormen, CK-B en UbCKmit, zijn uitgeschakeld. Fysiologische, histologische en etiologische analyses wezen uit dat brein-morfologie, gedrag en thermoregulatie in deze dieren afwijkingen vertonen. In dit proefschrift is onderzocht welke rol het cytosolische familielid CK-B speelt op cellulair niveau, waarbij gekeken is naar ATP-consumerende processen in verschillende celtypen.

In hoofdstuk 2 is de relatie tussen CK-B en actine-polymerisatie onderzocht tijdens fagocytose. Een opvallende observatie was dat CK-B, normaliter voorkomend als vrij diffundeerbaar cytosolisch eiwit, tijdens fagocytose accumuleerde in de nieuwgevormde fagosomen. Tevens hoopte CK-B zich op in de uiteinden van filopodia. Cyclocreatine, een farmacologische remmer van CK, kon fagocytose opsonisatie-afhankelijk remmen. Complement (CR3) gemediëerde fagocytose werd drastisch geremd door cyclocreatine, terwijl de efficiëntie van IgG-afhankelijke fagocytose onveranderd bleef. Door het fagocytische proces op te delen in een initiële adhesiefase en een daarop volgende internalisatiefase, bleek dat CK-B met

name betrokken was bij CR3-gemedieerde adhesie en dat dit proces op zijn beurt weer afhankelijk bleek te zijn van actieve actine polymerisatie. Opvallend ook, was dat remming van CK-B de totale hoeveelheid filamenteus actine (F-actine) in macrofagen verlaagde. Dit duidt op een mechanisme waarbij CK-B complement-afhankelijke adhesie reguleert door actine-polymerisatie te faciliteren.

In hoofdstuk 3 werd de link tussen CK-B en actine-polymerisatie verder onderzocht door te kijken naar cel-spreiding en cel-migratie. Dit zijn processen waarbij reorganisatie van het actine cytoskelet een centrale rol speelt. CK-B-deficiënte astrocyten bleken langzamer te spreiden dan wildtype astrocyten. Overeenkomstig met deze observatie bleek dat de migratiesnelheid aanzienlijk lager uitviel als astrocyten CK-B misten. Belangrijk is dat deze effecten volledig afhankelijk waren van de ATP-genererende activiteit van CK-B. Uit studies in fibroblasten werden deze resultaten bevestigd, en bleek ook dat de subcellulaire localisatie van CK-B belangrijk is voor de dynamiek van migratie en cel-morfologie, beide actine gemedieerde processen. De verkregen inzichten ondersteunen onze eerdere bevindingen in macrofagen en laten bovendien het primaire belang van CK-B's enzymatische activiteit zien.

In hoofdstuk 4 worden studies gepresenteerd waarin het effect van CK-B deficiëntie op intracellulair transport van amyloid precursor protein (APP) en mitochondria in primaire neuronen nader wordt onderzocht. Alhoewel transport van APP en mitochondria in neuronen sterk afhankelijk is van ATP, werden er door ons geen verschillen gevonden tussen in transportsnelheden in CK-B (-/-) en wildtype cellen. De fractie actief bewegende mitochondriën bleek echter significant groter te zijn in CK-B deficiënte neuronen. Het is verleidelijk om te speculeren dat CK-B deficiëntie lokale ATP tekorten veroorzaakt, en dat deze gecompenseerd worden door het verplaatsen van mitochondriën. Verder onderzoek moet echter uitwijzen of dit inderdaad het geval is.

In het vijfde hoofdstuk wordt beschreven hoe verschillende cellijnen werden afgeleid van hersenen van CK-B deficiënte muizen. Door CK-B "knockout" muizen te kruisen met "immorto-muizen", werd het thermolabiele SV40 Large-T antigen (tsA58) geïntroduceerd in het genoom van de nakomelingen. De conditioneel geïmmortaliseerde cellijnen die hiervan werden afgeleid vertoonden een

onderscheidbaar vermogen tot astrocytaire of neuronale differentiatie. Door CK-B te herintroduceren in een van de astrocytaire cellijnen, werd een cellulair model gecreëerd om de functie van CK-B te ontrafelen tegen een constante genetische achtergrond. Celspreidingsexperimenten lieten vervolgens zien dat introductie van CK-B spreiding versnelde. Dit effect werd echter teniet gedaan door additie van cyclocreatine, overeenkomstig met de resultaten in primaire astrocyten (hoofdstuk 3). Genoemde vinding benadrukt ons inziens nogmaals de bruikbaarheid van deze cellijn als cellulair modelsysteem.

Het in dit proefschrift beschreven werk laat zien dat CK-B een cruciale rol speelt in het faciliteren van actine remodellering tijdens celspreiding, migratie en fagocytose. Alhoewel nog onbekend is hoe CK-B's ATP-genererende vermogen het proces van actine polymerisatie precies beïnvloedt, voorspelt de grote variëteit aan door ons gevonden actine-afhankelijke cellulaire functies in verschillende celtypen dat er een centrale rol is weggelegd voor het CK-systeem in processen van embryonale ontwikkeling tot geheugenformatie.

List of abbreviations

ADP	Adenosine diphosphate
ADF	Actin depolymerizing factor
AGAT	L-arginine:glycine amidinotransferase
AK	Adenylate kinase
AMP	Adenosine monophosphate
AMPK	AMP-dependent kinase
ANT	adenine nucleotide translocase
Ap5A	P^1,P^5-Di(Adenosine-5')Pentaphosphate
APP	Amyloid precursor protein
ATP	Adenosine triphosphate
BAK(--/--)	Double CK-B/AK knockout
BCK	Brain-type creatine kinase
bFGF	Basic fibroblast growth factor
BSA	Bovine serum albumin
cCr	Cyclocreatine
cDNA	Copy DNA
CK	Creatine kinase
CK-B	Brain-type creatine kinase
CK-M	Muscle-type creatine kinase
CLSM	Confocal laser scanning microscopy
CoA	Coenzyme A
COZ	Complement opsonized zymosan
Cr	Creatine
CR3	Complement receptor 3
Cyto-D	Cytochalasin D
db-cAMP	Dibutyryl cyclic adenosine monophosphate
div	Days *in vitro*
DMEM	Dulbecco's Modified Eagle's Medium
DMSO	Dimethyl sulfoxide
DNA	Deoxyribonucleic acid
DTT	Dithiothreitol
EDTA	Ethylenediamine tetra-acetic acid
ECFP	Enhanced cyan fluorescent protein
EGFP	Enhanced green fluorescent protein
EST	Expressed sequence tag
EVH1	Ena-VASP homology domain 1
EYFP	Enhanced yellow fluorescent protein
FACS	Fluorescent-activated cell sorting
F-actin	Filamentous actin
FAD	Flavin adenine dinucleotide
$FADH_2$	Reduced flavin adenine dinucleotide
FcγR	Fragment-crystalizable gamma receptor (IgG receptor)
FCS	Fetal calf serum
FERM	band 4.1/ezrin/radixin/moesin (protein domain)
FKRB	FK506-binding protein
FN	Fibronectin
FITC	Fluorescein isothiocyanate
FRB	Rapamycin binding domain
G-actin	Globular actin
GAMT	S-adenosyl-L-methionine:N-guanidinoacetate methyltransferase
GAPDH	Glyceraldehyde-3-phosphate dehydrogenase
GDP	Guanosine diphosphate
GFAP	Glial fibrillary acidic protein
GTP	Guanosine triphosphate
HBSS	Hank's balanced salt solution

HEK 293	Human embryonic kidney cell line 293
HEPES	4-(2-Hydroxyethyl)piperazine-1-ethanesulfonic acid
IgG	Immunoglobulin G
ITAM	Tyrosine-based activation motif
IRES	Internal ribosome entry site
KWF/NKB	Koningin Wilhelmina Fonds / Nederlandse Kankerbestrijding
Lam	Laminin
MEF	Mouse embryonic fibroblast
Myr	Myristoylation
NAD	Nicotinamide adenine dinucleotide
NADH	Reduced nicotinamide adenine dinucleotide
NBM	Neurobasal medium
NBM+	Neurobasal medium + glutamine + gentamycin + B27 supplement
NDPK	Nucleoside diphosphate kinase
NWO	Nederlandse Organisatie voor Wetenschappelijk Onderzoek
O/N	Overnight
ORF	Open reading frame
OXPHOS	Oxidative phosphorylation
~P	High-energy phosphoryl
PAGE	Polyacrylamide gel electrophoresis
PBS	Phosphate buffered saline
PCr	Phophocreatine (Creatine-phosphate)
PCR	Polymerase chain reaction
PF	Paraformaldehyde
PFK	Phosphofructokinase
PHEM	Pipes/HEPES/EDTA/$MgCl_2$ (Buffer solution)
P_i	Inorganic phosphate
PIP	Phosphatidylinositol phosphate
PMA	Phorbol 12-myristate 13-acetate
PMF	Proton motive force
Puro	Puromycin
RNA	Ribonucleic acid
RPMI 1640	Roswell Park Memorial Institute culture medium 1640
ScCKmit	Sarcomeric mitochondrial creatine kinase
SV40	Simian virus 40
Rho123	Rhodamine 123
SDS	Sodium dodecyl sulphate
TCA	Tricarboxylic acid cycle
TRITC	Tetramethyl rhodamine iso-thiocyanate
tsA58	thermolabile SV40 large T antigen
UbCKmit	Ubiquitous mitochondrial creatine kinase
VCA	Verprolin-cofilin-acidic
WASP	Wiskott-Aldrich syndrome family protein
WH2	WASP-Homology 2
WT	Wild type
Zeo	Zeocine

Dankwoord

En dan opeens na al die jaren mag je de laatste bladzijden van je proefschrift schrijven: het dankwoord! Alhoewel dit op het eerste gezicht een relatief eenvoudige taak lijkt, realiseer ik me dat dit onderdeel van het proefschrift minutieus zal worden geanalyseerd door iedereen. Ik besef dan ook dat er een kans is dat ik iemand onbedoeld vergeet te bedanken. Echter, gezien de definitieve aard van een gedrukt proefschrift, biedt het dankwoord geen mogelijkheid voor revisie en zal iedereen zich tevreden moeten stellen met versie 1.0...

Allereerst mijn dank aan jou, Bé. Naast het feit dat ik altijd voor advies bij je terecht kon, wil ik je vooral ook bedanken voor de enorme vrijheid die ik genoten heb tijdens mijn promotieonderzoek. Je zult vast wel eens diep gezucht hebben als ik weer eens een nieuw "proefje" deed, terwijl er ook nog een proefschrift geschreven moest worden... Bedankt voor je geduld, visie en de altijd prettige samenwerking!

De CK/AKers van het eerste uur: Frank, jij hebt mij de fijne kneepjes van de weefselkweek bijgebracht; het opzetten van de neuronkweek is mede dankzij jouw inzet geslaagd. Bedankt voor je enthousiasme en gezelligheid! Edwin en Ad, tijdens mijn eerste rondleiding op het lab stelden jullie je voor als “de Mounties”. Deze eerste kennismaking maakte me duidelijk dat het met de werksfeer wel goed zat. Bedankt voor de dagelijkse dosis onzin, maar zeker ook voor de wetenschappelijke discussies. Wilma (14 mei 1968 – 22 november 2006), ik wil je toch op deze manier bedanken. Voor de gezelligheid, je bereidheid om de organisatie van “social events” op je te nemen en uiteraard voor je expertise: met de echt lastige kloneringen kon ik altijd bij jou terecht. Wieke, ook al voelt het al weer als lang geleden (en dat is het ook wel), we hebben veel gelachen in het lab. Bedankt voor de gezelligheid! Helma, ondanks, of mischien wel dankzij, onze zeer verschillende manier van werken konden we het goed met elkaar vinden. Ik heb veel van je nauwkeurige manier van experimenteren en organiseren geleerd: En ja, ik plan tegenwoordig ook al mijn proefjes in Excel! Bedankt voor de gezellige samenwerking! Ook wil ik de CK/AK-ers van het 2e uur bedanken voor hun bijdrage: Remco, onze joint-venture heeft een fraai resultaat opgeleverd; Marieke, Mariska en Michiel, bedankt voor jullie bijdrage aan de experimenten en goede labsfeer! Jack, alhoewel je misschien officieel geen

CK/AK-er bent, ben je nauw betrokken geweest bij de planning en uitvoering van een groot aantal experimenten; bedankt voor je input! Helaas is de macrofaag movie voorzien van smak-geluiden er nog niet van gekomen; wie weet ooit nog... En natuurlijk wil ik de nog niet genoemde (ex-)collega's van de afdeling bedanken voor hun hulp, discussies en gezelligheid tijdens mijn promotietijd: Frank de L., Hans (24 december 1944 – 12 november 2001), Huib, Ineke, Jan S., Klaas-Jan, Magda, Marcel, Marga, Marianne, Marion, Marloes, Mietske (en zo komen de mooie SEM foto's toch nog goed terecht !), Ralph, Renato, Rick, Rinske, Toine, Walther en Wiljan: bedankt !

Een prettige werkomgeving is een niet te onderschatten motivatie voor het volbrengen van een promotie. Naast de bereidheid om elkaar met raad en daad bij te staan, hebben ook de talloze (vrijdag-)borrels, filmavonden, lunches, labuitjes en de gedenkwaardige kerstdiners indirect bijgedragen aan de totstandkoming van dit boekje. Hiervoor is het natuurlijk wel noodzakelijk dat mensen bereid zijn om dit te organiseren: Susan, Lieke, Femke en Marieke, bedankt dat jullie vaak deze rol op je hebben genomen! Suus, Lieke, Femke, Marieke, Yvetje, Bas, Ed, Marco, René, Gerrit en Gönül, bedankt voor de leuke tijd! Onze vele (soms diepzinnige) gesprekken, etentjes en avondjes stappen in niet nader te noemen kroegen, zal ik niet vergeten. Hierbij wil ik ook "de buren" bedanken die ook vaak van de partij waren: de moldieren, de Boertjes en de TIL-lers (jullie hebben wellicht nu met een overschot aan FACS-buisjes te kampen). Bedankt voor jullie interesse en input, tijdens koffiepauzes, werkbesprekingen en borrels. Johannes, Rob, Theo, Klaas en Tom: bedankt voor de leuke en leerzame periode op de afdeling evolutionaire microbiologie.

During the last phase of thesis-writing I relocated (twice) to Ithaca to spend the summer with Lutz. This time probably would not have been that productive if I wouldn't have been offered my own work space in the Hairston lab. Nelson and Colleen: I really enjoyed my stays in Ithaca & Cornell, Thanks!

Zoals iemand ooit tegen me zei (Toine?) : Een gelukkig mens gaat 's morgens graag naar zijn werk, maar gaat 's avonds ook graag weer naar huis. Daarom wil ik mijn vrienden bedanken, gewoon omdat ze er simpelweg altijd voor me zijn. Stan en Gijs: bedankt dat jullie me bijstaan als paranimf.

En natuurlijk mijn ouders en zusje: pap, mam, Thea, jullie hebben me altijd onvoorwaardelijk gesteund in mijn keuzes. Bedankt dat jullie altijd voor me klaar staan! Schliesslich du Lutz; Danke das du immer da bist. Ich freue mich sehr auf unseres Kanada Abenteuer!

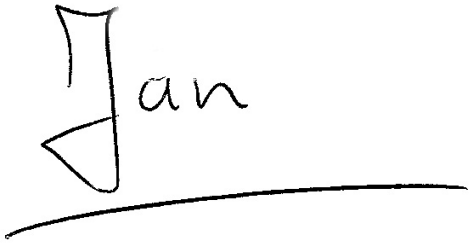

Jan Kuiper werd geboren op 21 Januari 1976 te Oldenzaal. In 1994 behaalde hij zijn VWO diploma aan het Thijcollege in Oldenzaal. In datzelfde jaar begon hij de studie (Medische) Biologie aan de Radboud Universiteit in Nijmegen. Tijdens de specialisatiefase voltooide hij een stage Moleculaire Biologie onder supervisie van prof. dr. Ir. H. Stunnenberg en dr. A. Braks. Een tweede stage werd verricht in het Peter Maccallum Cancer Institute in Melbourne (Australië) onder supervisie van prof. dr. B. Wieringa en dr. D. Dorow. Na het voltooien van zijn studie in 2000, was hij verbonden als junior onderzoeker (AIO) aan de afdeling Celbiologie (UMC Nijmegen) onder leiding van prof. dr. B. Wieringa. In het kader van zijn promotie verrichte hij onderzoek naar de functie van brain-type Creatine Kinase, een eiwit dat belangrijk is voor de energiehuishouding van verschillende celtypen. De resultaten van dit onderzoek staan beschreven in dit proefschrift. In de periode 2005-2007 was Jan tevens werkzaam bij de vakgroep Evolutionaire Microbiologie van dr. J. Hackstein, waar hij ondermeer onderzoek verrichtte naar "horizontal gene transfer" en anaeroob metabolisme in ciliaten.

Vanaf 2008 is Jan werkzaam als post-doctoraal onderzoeker in de "matrix dynamics group" aan de universiteit van Toronto (Canada), waar hij in samenwerking met prof. dr. M. Glogauer en prof. dr. S. Grinstein onderzoek verricht naar de differentiële functies van de GTPases Rac1 en Rac2 in immuuncellen.

Janssen, E., Kuiper, J., Hodgson, D., Zingman, L. V., Alekseev, A. E., Terzic, A. and Wieringa, B. (2004). "Two structurally distinct and spatially compartmentalized adenylate kinases are expressed from the AK1 gene in mouse brain." *Mol Cell Biochem* 256-257, 59-72.

Kuiper, J. W., Oerlemans, F. T., Fransen, J. A. and Wieringa, B. (2008). "Creatine kinase B deficient neurons exhibit an increased fraction of motile mitochondria." *BMC Neurosci* 9, 73.

Kuiper, J. W., Pluk, H., Oerlemans, F., van Leeuwen, F. N., de Lange, F., Fransen, J. and Wieringa, B. (2008). "Creatine kinase-mediated ATP supply fuels actin-based events in phagocytosis." *PLoS Biol* 6, e51.